



The
University
Of
Sheffield.

**THE DEVELOPMENT OF *IN VITRO* MODELS OF
HUMAN SALIVARY GLANDS**

ZULAIHA A RAHMAN

A thesis submitted in partial fulfilment of the requirements for the
degree of Doctor of Philosophy (Ph. D)

The University of Sheffield
Faculty of Medicine, Dentistry and Health
Department of Oral & Maxillofacial Pathology
School of Clinical Dentistry

December 2018

(This page is left blank intentionally)

Dedicated to:

My beloved parents A Rahman Eting & Che Jam Musa,
for raising me to believe that everything was possible

My caring husband Mohd Afizul,
for believing in me and making everything possible

My lovely son Zamil Afnan,
a strong smart wonderful magical boy

&

My cheeky daughter Hanan Aleesya,
her shining star of the morning.

ACKNOWLEDGEMENT

I owe my deepest gratitude to my beloved supervisor Dr Lynne Bingle, without her continuous optimism concerning this study, enthusiasm, encouragement and support this study would hardly have been completed. I would like to express my warmest gratitude to my co-supervisor Professor Colin Bingle, who has always been supportive and approachable. A special thank you to Dr Aileen Crawford for her support and word of wisdom in every aspect throughout my study years.

I was fortunate to be able to collaborate with Dr Frederik Claeysens and Dr Colin Sherborne, from Biomaterials and Tissue Engineering Group, Kroto Research Institute, for generating PolyHIPes scaffold. I am indebted to those who provide me technical assistance: David for teaching me on histology techniques, Mrs Fiona J Wright for processing my histological sample, Mrs Brenka McBabe for her guidance in molecular work, and Mr Jason Heath for helping me in culturing bacteria.

Special thanks to the lovely members of the Bingle group (Khondoker, Apoorva, Priyanka, Renata, Hannah, and Chloe) and everyone within the iBio Science group who have made this journey an extremely enjoyable experience. A big thank you to my Malaysian buddies in the department who always helpful and supportive when I was struggling with the experiment: Zaki, Zulfahmi and Amalina. You guys make me feels at home!

I would like to extend my gratitude to the Ministry of Higher Education Malaysia and Universiti Sains Islam Malaysia for the scholarship and giving me the opportunity to do the PhD.

And most importantly, a huge thank you to my loving family: Mom, for your prayers and encouragement for me to follow my dreams; my husband and kids for their unconditional love, sacrifice and inspiration; my sisters, nieces, nephews and in-law family for their continuous support and prayers for my success. I love you all!

ABSTRACT

Introduction: At present, due to the lack of good, representative, human models, it is not possible to fully investigate the development of a number of salivary gland disorders such as tumour development, Sjogren's syndrome or viral-associated infections. Radiotherapy for head and neck cancer, and chemotherapy for non-oral cancers, can also lead to salivary gland damage, reduced salivary flow, xerostomia and a worst-case scenario of severe, debilitating mucositis with potentially life-threatening systemic infections. An artificial salivary gland is a novel alternative treatment for patients who suffer from diseased or damaged glands and subsequent hyposalivation which often leads to untreatable and irreversible xerostomia. Salivary gland (SG) organoids developed from mice SG cells exhibit self-organizing properties with structural and functional properties closely resembling the native organ. Thus, organoid technology has potential as a model of human organ development, for the investigation of human pathologies *in vitro* and also for regenerative medicine.

Aims: To develop *in vitro* three-dimensional culture system of human salivary glands, to elucidate the pathogenesis of salivary gland disease and to further understand the development of salivary glands for regenerative studies.

Methods: Organoids were developed from biopsy samples of normal human sublingual gland tissue. Cells were isolated and cultured in extracellular matrices (Matrigel and/or Myogel), as well as on Polymerised High Internal Phase Emulsions (PolyHIPES) scaffolds. They were cultured either at an Air Liquid Interface (ALI) or were submerged in tissue culture medium (non-ALI) and Wnt-3A, R-spondin1, EGF, and FGF2 were added to supplement the medium. TGF β , BMP, and LIMK inhibitors were added to an enriched media for further differentiation studies. SG organoids were infected with *Staphylococcus aureus* in preliminary study of glandular infection. Haematoxylin and eosin stained sections of the cultures were used to visualise growth. RT-PCR, immunohistochemistry and immunofluorescence were used to determine the differential expression of cell specific markers.

Results: Overall, the data from this study indicate that salivary gland cells from single cell suspensions were able to proliferate and differentiate to form small structures resembling mini-glands (organoids) for up to 14-days in a defined culture system. Organoid structures developed when the cells were grown in Matrigel but this was less obvious when grown in Myogel. Compared to those grown at an ALI, non-ALI organoids were significantly fewer in number and smaller in size. Organoids cultured in Matrigel at ALI formed buds and branches, and expressed acinar cell-specific markers (amylase, AQP5 and MUC7), as well as staining positively for CK5. Inhibition of TGF β , BMP and LIMK signalling promoted cell proliferation and induced cell differentiation. Organoids cultured in the presence of the TGF β inhibitor, A8301, and in the presence of all three inhibitors, ALL-media, displayed distinct characteristics that closely mimicked native glands and expressed CK5, BPIFA2, AQP5, CK7 and E-cadherin, whilst those cultured in the presence of the BMP inhibitor, DMH1, demonstrated the growth of duct-like structures. α -AMY activity was significantly higher in SG organoids grown in the presence of the LIMK inhibitor, SR7826. Finally, cells grown in PolyHIPE scaffolds were able to form budding and branching structures more closely resembling human salivary glands

Conclusion: Our culture system enables the growth of human salivary gland organoids. This culture system can be used to study the initial stages of infectious disease and the pathogenesis of other salivary gland diseases. This study provides a competent *in vitro* culture system that can be used in further study on human SG development, pathophysiology as well as pioneering a novel pathway in salivary gland regeneration.

TABLE OF CONTENTS

ACKNOWLEDGEMENT	iv
ABSTRACT	v
TABLE OF CONTENTS	vii
LIST OF FIGURES	xii
LIST OF TABLES	xvi
LIST OF ABBREVIATIONS	xvii
CHAPTER 1: LITERATURE REVIEW	2
1.1 INTRODUCTION	2
1.2 SJÖGREN’S SYNDROME.....	3
1.3 SALIVARY GLANDS: NORMAL DEVELOPMENT	4
1.3.1 Anatomy of Salivary Glands	4
1.3.2 Histology of Salivary Glands.....	5
1.3.3 Embryology of Salivary Glands.....	7
1.3.4 Physiology of Salivary Glands	8
1.4 STEM CELLS	9
1.5 TISSUE ENGINEERING: GENERATING <i>IN VITRO</i> THREE-DIMENSIONAL (3D) MODELS OF HUMAN SALIVARY GLAND (hSG)	9
1.5 DEVELOPMENT OF <i>IN VITRO</i> 3D MODELS.....	11
1.5.1 Primary Human Salivary Glands.....	11
1.5.2 Basement Membrane	12
1.5.3 Culture Conditions	14
1.6 ORGANOID CULTURES	14
1.6.1 Defined Growth Factors.....	15
1.6.2 The Inhibitors in Enriched Media.....	17
1.7 CELL SPECIFIC MARKERS	20
1.8 TISSUE ENGINEERING SCAFFOLD: POLYMERISED HIGH INTERNAL PHASE EMULSION (POLYHIPE) SCAFFOLDS	24
1.9 ORGANOIDS AS MODEL FOR INFECTIOUS DISEASE: <i>STAPHYLOCOCCUS. AUREUS</i>	25
1.10 AIMS AND HYPOTHESIS.....	26
1.11 SIGNIFICANCE OF THIS STUDY	27
CHAPTER 2: GENERAL METHODOLOGY	30
2.1 MATERIALS.....	30

2.2	BASIC CELL CULTURE TECHNIQUE.....	30
2.2.1	Cell Culture/Thawing Cells.....	30
2.2.2	Culture and Passage Cells.....	30
2.2.3	Counting Cells.....	31
2.2.4	Freezing Cells.....	31
2.3	PREPARATION OF CELL CULTURE MEDIUM.....	31
2.4	REVERSE-TRANSCRIPTION POLYMERASE CHAIN REACTION.....	33
2.4.1	Sample Preparation.....	33
2.4.2	RNA Isolation.....	34
2.4.3	RNA Quantification using Nanodrop.....	34
2.4.4	Denaturing Formaldehyde Agarose Gel Electrophoresis.....	34
2.4.5	Reverse Transcription-Polymerase Chain Reaction (RT-PCR).....	35
2.5	HISTOLOGICAL ANALYSIS OF 3D MODEL.....	39
2.5.1	Fixing and Processing 3D Model.....	39
2.5.2	Sectioning Blocks of the 3D Model.....	40
2.5.3	Haematoxylin and Eosin (H&E) Staining.....	40
2.5.4	Immunohistochemistry.....	42
2.6	IMMUNOFLUORESCENCE STAINING.....	44
2.6.1	Sample preparation.....	44
2.6.2	Transwell Fixation.....	45
2.6.3	Immunostaining.....	46
2.7	CONFOCAL MICROSCOPY.....	46
CHAPTER 3: ESTABLISHMENT OF IN VITRO MODELS OF HUMAN SALIVARY GLAND.....		49
3.1	INTRODUCTION.....	49
3.2	AIMS.....	51
3.3	MATERIALS AND METHODS.....	52
3.3.1	Cell culture.....	52
3.3.2	Preparation of Extracellular Matrices (ECM).....	52
3.3.3	Coating Alvetex® Scaffold with ECM.....	52
3.3.4	Coating PET Transwells with ECM.....	53
3.3.5	Human Primary Cell Isolation.....	53
3.3.6	Cell Characterisation of HuSG From Explant Tissues.....	55
3.3.7	Culturing 3D <i>in vitro</i> Model.....	55
3.3.8	Analysis techniques.....	56

3.4	RESULTS.....	58
3.4.1	HTB41 Cell Line in 3D Culture Systems	58
3.4.2	Immunohistochemistry of HTB41 Cultures.....	62
3.4.3	Reverse Transcription Polymerase Chain Reaction (RT-PCR) of HTB41 cultures	68
3.4.4	Human Salivary Gland Tissue Isolation	70
3.4.5	Cell characterisation of HuSG from explant tissues by using cytopins.	75
3.4.6	3D <i>in Vitro</i> Models of Human Sublingual Glands.....	77
3.4.7	Reverse transcription polymerase chain reaction (RT-PCR) of HuSG cultures	80
3.5	DISCUSSION.....	82
3.5.1	HTB41 Cultured as 3D Model.....	82
3.5.2	Human Sublingual Gland as 3D Model	83
3.6	KEY EXPERIMENTAL CONCLUSIONS	86
CHAPTER 4: DEVELOPMENT OF ORGANOID MODELS OF HUMAN SALIVARY GLAND		89
4.1	INTRODUCTION.....	89
4.2	AIMS.....	90
4.3	MATERIALS AND METHODS	91
4.3.1	Cell culture	91
4.3.2	Media preparation for organoid models	91
4.3.3	Organoid models of human salivary glands.....	93
4.3.4	Organoid model analysis.....	93
4.3.5	Culture of Bacteria	96
4.3.6	Infection of SG Organoid Model with <i>S. Aureus</i>	98
4.4	RESULTS.....	98
4.4.1	Morphological analysis of SG organoids cultured in Matrigel.....	99
4.4.2	Expression of cell specific markers in SGs organoids cultured in Matrigel...	102
4.4.3	Localisation of epithelial markers in SG organoids cultured in Matrigel.....	103
4.4.4	Morphological analysis of SG organoids cultured in Myogel	106
4.4.5	Morphological analysis of SG cells cultured in combinations of Matrigel and Myogel	107
4.4.6	Expression of cell specific markers in SG organoid models cultured in Myogel with and without Matrigel.....	108
4.4.7	Infection of SG Organoid cultured in Matrigel with <i>S. aureus</i>	110
4.5	DISCUSSION.....	112

4.6	KEY EXPERIMENTAL CONCLUSIONS	116
CHAPTER 5: HUMAN SALIVARY GLAND ORGANOID MODELS CULTURED IN DIFFERENT MEDIA		
		118
5.1	INTRODUCTION	118
5.2	AIM.....	120
5.3	MATERIALS AND METHODS	120
5.3.1	Media preparation with differentiation factors in enriched media	120
5.3.2	Cell culture	121
5.3.3	AlamarBlue®	121
5.3.4	Amylase Activity Assay.....	121
5.3.5	Organoid model analysis.....	122
5.3.6	Statistical analysis	123
5.4	RESULTS.....	124
5.4.1	Viability and morphology of SG cells cultured in enriched media with differentiation factors.....	124
5.4.2	Morphological analysis of SGs organoids cultured in enriched media with differentiation inhibitors	127
5.4.3	RNA expression of cell specific markers in SG organoid models cultured in enriched media with differentiation inhibitors	132
5.4.4	Localisation of epithelial cell marker, CK5 and ductal cell marker, CK7 in SG organoid cultured in enriched media with differentiation factors.....	133
5.4.5	Localisation of acinar cell marker, BPIFA2 in SG organoid cultured in enriched media with differentiation factors.....	136
5.4.6	Localisation of the acinar cell marker, AQP5 in SG organoids cultured in enriched media with differentiation factors	138
5.4.7	Localisation of E-cadherin in SG organoid cultured in enriched media with differentiation factors.....	140
5.4.8	Amylase assay activity in SG organoids cultured in enriched media with differentiation factors.....	142
5.5	DISCUSSION.....	143
5.6	KEY EXPERIMENTAL CONCLUSIONS	147
CHAPTER 6: CULTURES ON POLYMERISED HIGH INTERNAL PHASE EMULSIONS (POLYHIPE) SCAFFOLD		
		150
6.1	INTRODUCTION	150
6.2	AIMS.....	151
6.3	MATERIALS AND METHODS	151

6.3.1	PolyHIPE scaffold	151
6.3.2	SG cells cultured on PolyHIPE scaffold.....	152
6.3.3	Immunofluorescent confocal microscopy of SG cells on PolyHIPE scaffolds	153
6.4	RESULTS.....	154
6.4.1	PolyHIPE scaffold	154
6.4.2	SG organoids cultured in enriched media on PolyHIPE scaffold (design A), seeded with a mixture of SG cells and Matrigel.	156
6.4.3	SG organoids cultured on PolyHIPE scaffold (design A), seeded with a mixture of SG cells and Matrigel, in different inhibitors media.....	159
6.4.4	SG organoids cultured on PolyHIPE scaffold (design B), coated with Matrigel before seeding SG cells	161
6.5	DISCUSSION.....	163
6.6	KEY EXPERIMENTAL CONCLUSIONS	165
CHAPTER 7: GENERAL DISCUSSION & CONCLUSION		168
7.1	GENERAL DISCUSSION.....	168
7.2	CONCLUSION.....	171
7.3	FUTURE STUDIES	172
REFERENCES.....		176
APPENDICES.....		187

LIST OF FIGURES

Figure 1.1	Schematic diagram shows component of cell types (serous and mucous acinar cells, duct cells and myoepithelial cells) of a salivary gland.....6
Figure 1.2	Schematic diagram shows stage of salivary gland development from prebud to terminal bud of mouse submandibular gland as a model.. 8
Figure 1.3	Schematic diagram show TGF β /BMP Signalling Pathway.....19
Figure 3.1	Overview of culturing 3D <i>in vitro</i> model of human salivary glands by using HTB-41 cells..... 57
Figure 3.2	Haematoxylin and eosin stained sections of 3D <i>in vitro</i> models of HTB41 cell line cultured on PET transwell with or without ECM coating, at ALI and non-ALI, under static or dynamic culture conditions at 14 days of culture show a number of different phenotypes present.....60
Figure 3.3	Haematoxylin and eosin stained sections of 3D <i>in vitro</i> models of HTB41 cell line cultured on Alvetex [®] scaffold with or without ECM coating, at ALI and non-ALI, under static or dynamic culture conditions at 14 days of culture show a number of different phenotypes present.61
Figure 3.4	Positive immunohistochemistry staining of 3D <i>in vitro</i> models of HTB41 cells. Amylase staining on collagen-coated inserts63
Figure 3.5	Positive immunohistochemistry staining of 3D <i>in vitro</i> models of HTB41 cells. cKIT on collagen-coated inserts.64
Figure 3.6	Positive immunohistochemistry staining of 3D <i>in vitro</i> models of HTB41 cells. cKIT on fibronectin-coated inserts.....65
Figure 3.7	Positive immunohistochemistry staining of 3D <i>in vitro</i> models of HTB41 cells. BPIFA2 on fibronectin-coated inserts66
Figure 3.8	Positive immunohistochemistry staining of 3D <i>in vitro</i> models of HTB41 cells. BPIFA2 on matrigel-coated insertd.....67
Figure 3.9	RT-PCR of HTB41 cultures at day 14 on four types of ECM (collagen, fibronectin, poly-L-lysine, matrigel) showing mRNA expression under different growth conditions.69

Figure 3.10	Normal human salivary gland tissue.	72
Figure 3.11	Phase-contrast pictures showing the typical appearance of primary human salivary gland cell cultures following 3 isolation methods. ...	73
Figure 3.12	Haematoxylin and eosin staining of an excised human sublingual gland, and single cells from explant culture using cytospin.....	74
Figure 3.13	Immunofluorescence microscopy of single cells from explant technique cultured in KGM media.	76
Figure 3.14	Haematoxylin and eosin stained sections of 3D <i>in vitro</i> models of human salivary gland cells cultured on PET transwell with or without ECM coating, at ALI and non-ALI, under static or dynamic culture conditions at 14 days of culture show a number of different phenotypes present..	78
Figure 3.15	Haematoxylin and eosin stained sections of 3D <i>in vitro</i> models of human salivary gland cells cultured on Alvetex scaffold with or without ECM coating, at ALI and non-ALI, under static or dynamic culture conditions at 14 days of culture show a number of different phenotypes present..	79
Figure 3.16	RT-PCR showed mRNA expression of human sublingual cell cultures at day 14 on four types of ECM (collagen, fibronectin, poly-L-lysine, matrigel) under different growth conditions.	81
Figure 4.1	Overview of developing an organoid model of human salivary glands by using SG cells.....	95
Figure 4.2	Organoid models of human salivary glands cultured at an ALI.	100
Figure 4.3	SG organoids cultured in Matrigel. Haematoxylin and eosin stained sections of SG organoids cultured in Matrigel at ALI (A) for up to 14-days were significantly larger than non-ALI (B) cultures.....	101
Figure 4.4	SG organoids cultured in Matrigel. Diameter of SG organoids (A), and number of SG organoids formed(B) cultured in Matrigel was compared between ALI and non-ALI cultures..	101
Figure 4.5	Expression of cell-type specific markers of SG organoids cultured in Matrigel.	102
Figure 4.6	Immunohistochemistry of SG organoids cultured in Matrigel.	104

Figure 4.7	Immunofluorescent confocal microscopy of SG organoids cultured in Matrigel.	105
Figure 4.8	Salivary gland cells cultured in Myogel.	106
Figure 4.9	Salivary gland cells cultured in a mixture of Matrigel and Myogel (1:1).	107
Figure 4.10	Expression of cell specific markers of SG cells cultured in Myogel with and without Matrigel.	109
Figure 4.11	SG Organoids as Model for Infectious Diseases: <i>S. Aureus</i>	111
Figure 5. 1	Cell viability analysis of SG cells cultured as monolayer in different inhibitor media.....	125
Figure 5. 2	Haematoxylin and eosin stained sections of SG cells cultured as monolayer in different inhibitor media.....	126
Figure 5. 3	SG organoids cultured in different inhibitor media.....	129
Figure 5. 4	SG organoids cultured in Matrigel at ALI in different inhibitor media.....	130
Figure 5. 5	Haematoxylin and eosin stained sections of SG organoids cultured in different inhibitor media.....	131
Figure 5. 6	Expression of cell specific markers of SG organoids cultured in different inhibitor media.....	132
Figure 5. 7	Localisation of ductal cell marker, CK7 in SG organoids cultured in different inhibitor media.....	135
Figure 5. 8	Localisation of acinar cell marker, BPIFA2 in SG organoids cultured in different inhibitor media.....	137
Figure 5. 9	Localisation of acinar cell marker, AQP5 of SG organoids cultured in different inhibitor media.....	139
Figure 5. 10	Localisation of cell-cell adhesion marker, E-cadherin in SG organoids cultured in different inhibitor media.....	141

Figure 5. 11	Amylase assay activity in SG organoid cultured in different inhibitors media.....	142
Figure 6. 1	SEM images of a PolyHIPE scaffold	154
Figure 6. 2	Laser cutting design of PolyHIPE scaffold.....	155
Figure 6. 3	SG organoid model cultured on PolyHIPE scaffold (design A) in enriched media.	157
Figure 6. 4	SG organoid model cultured on PolyHIPE scaffold (design A) in enriched media.	158
Figure 6. 5	SG organoid model cultured on PolyHIPE scaffold (design A) in different inhibitor media.	160
Figure 6. 6	SG organoid model cultured on PolyHIPE scaffold (design B) in different inhibitor media.	162

LIST OF TABLES

Table 2.1	HTB41 cell culture medium	32
Table 2.2	KGM medium	33
Table 2.3	Short processing run	40
Table 2.4	Haematoxylin and eosin staining procedure	41
Table 2.5	Primary antibodies, suppliers, dilutions, serum, and antigen retrieval. .	42
Table 2.6	Haematoxylin staining procedure.....	44
Table 2.7	Preparation of primary antibodies	45
Table 2.8	Preparation of secondary antibody.	45
Table 3.1	Optimised primer pairs of human salivary gland expressed genes.....	68
Table 5.1	Enriched media with differentiation factors.....	120

LIST OF ABBREVIATIONS

ABC	Avidin-biotin complex
ALI	Air liquid interface
AMY	Amylase
ANOVA	Analysis of variance
AQP	Aquaporin
BMP	Bone morphogenetic protein
BPIFA2	Bacterial permeability increasing fold-containing proteinA1
BSA	Bovine serum albumin
CK	Cytokeratin
DAB	3,3'-diaminobenzidine
DMSO	Dimethyl sulfoxide
DMEM	Dulbecco's modified Eagle's medium
ECM	Extracellular matrix
EDTA	Ethylenediaminetetraacetic acid
EGF	Epidermal growth factor
FBS	Foetal bovine serum
FGF	Fibroblast growth factor
HBBS	Hank's Balanced Salt solution
H&E	Haematoxylin and eosin
IFC	Immunofluorescence cytochemistry
IHC	Immunohistochemistry
h	hour
hpi	hours post infection
L	Litre
LIMK	LIM kinase
M	Molar
min	minute
mL	millilitre
mM	milli molar

MOI	Multiplicity of infection
MUC	Mucin
°C	degree Celsius
OD	Optical density
PBS	Phosphate buffered saline
PCR	Polymerase chain reaction
PDGF	Platelet-derived growth factor
RNA	Ribonucleic acid
ROCKi	Rho-kinase inhibitor
rpm	revolution per minute
RT	Reverse transcription
RT	Room temperature
RT-PCR	Endpoint reverse transcription PCR
<i>S. aureus</i>	<i>Staphylococcus aureus</i>
SEM	Standard Error Mean
SG	Salivary glands
TGF- β	Transforming growth factor- β
ZO-1	Zona occludens
v/v	volume per volume
w/v	weight per volume
α	alpha
α -SMA	Alpha-smooth muscle actin
β	beta
μ g	micro gram
μ L	micro litre

CHAPTER 1

Literature Review

CHAPTER 1: LITERATURE REVIEW

1.1 INTRODUCTION

Head and neck cancers are a heterogeneous group of malignancies with different aetiology and affecting various sites. In Europe, head and neck cancer accounts for around 4 percent of cancer incidence with approximately 140,000 Europeans developing head and neck cancer annually and 63,500 dying from the disease in 2012. There is a four times higher risk of men developing the disease than females (Gatta *et al.*, 2015) with tobacco and alcohol use being “traditional” risk factors and human papillomavirus (HPV) being the main risk factor associated with the recent increase in incidence. Other known risk factors include low intake of fruit and vegetables.

Salivary gland tumours are uncommon, with around 0.5% of the cancers diagnosed in the UK being of salivary gland origin (Cancer Research UK1). These tumours most commonly occur in the major glands, with mucoepidermoid carcinoma being the most prevalent tumour in both major and minor glands. The pathogenesis of tumour growth and development is still understudied, but there are associations with the presence of viral infections (Melnick, Deluca and Jaskoll, 2014).

The treatment of most patients with head and neck cancer, including salivary gland tumours, is radiation therapy. Radiotherapy for head and neck cancer always leads to irreversible damage to any salivary gland in the path of the radiation. This can result in a reduction in salivary flow, xerostomia (dry mouth), increased oral infection and can result in debilitating mucositis and/or systemic infection. Radiation-induced salivary hypofunction and associated pain can severely impair a patient’s quality of life and may lead to the patient refusing further treatment (Baum *et al.*, 2010). Therefore, the regeneration of salivary glands, which can be achieved by greater study of salivary gland development, may help such patients. The establishment of an *in vitro* model of salivary glands may provide a useful tool to investigate the regeneration of glands and also the pathogenesis of disease.

1.2 SJÖGREN'S SYNDROME

Sjögren's syndrome (SS) is a chronic autoimmune disease affecting exocrine glands. It is characterized by a lymphocytic infiltration of salivary glands and lacrimal glands, which results in loss of function and a subsequent reduction in salivary and lacrimal gland secretions (Bayetto and Logan, 2010). Clinically, the major feature of SS is the presence of dry mouth and eyes (Mavragani and Moutsopoulos, 2014). Accordingly, decreased salivary flow has many oral implications such as dental caries, microbial infections, swallowing and speech dysfunction, and can significantly, negatively impact quality of life.

The pathogenesis of SS is a multifactorial process resulting in destruction and dysfunction of the exocrine glands. It is thought to be initiated by environmental or exogenous factors which affect the salivary gland epithelial cells and stimulates the cells to activate T lymphocyte migration and lymphocytic infiltration of exogenous glands. This leads to overstimulation and production of immunoglobulins and autoantibodies. Subsequently, the tissue damage results in chronic inflammation of the tissue glands and loss of their normal function (Bayetto and Logan, 2010; Sipsas, Gamaletsou and Moutsopoulos, 2011).

There are a number of trigger factors that have been associated with the onset of SS. Genetic, environmental, hormonal and immunological factors are considered important in SS development. Sex hormones have been suggested to be involved in the destruction of exocrine glands. Taiym et al (2004) proposed that the difference in the ratio of oestrogen to androgen, or the decline of oestrogen levels during menopause, might be involved with the onset of SS (Taiym, Haghghat and Al-Hashimi, 2004). This is in agreement with the higher numbers of women reported with SS compared to men (Bayetto and Logan, 2010). Viral infections such as human T-cell Leukaemia virus-1 (HTLV-1), human immunodeficiency virus (HIV) and hepatitis C virus (HCV) can also trigger autoimmune reactions and have been associated with inflammation and damage to the salivary glands (Ramos-Casals, Muñoz and Zerón,

2008; Sipsas, Gamaletsou and Moutsopoulos, 2011). Bacterial infections, pathological injury and desiccating stress can also induce the development of autoimmune disease (Niederhorn *et al.*, 2006; Stojanovich and Marisavljevic, 2008).

At present, it is not possible to fully investigate the initiation and development of the disease by following infection with any of these agents. The tools presently available in this field are either *in vivo* animal models or monolayer cultures of cells, usually carcinoma cell lines derived from animals, mostly rats (Nelson, Manzella and Baker, 2013). However, the models are unable to replicate this multifactorial disease and have limitations in the extrapolation of results from animal to the human situation. While monolayer culture cells are well recognised as a useful laboratory tool, they do not faithfully replicate the complex cell structures seen *in vivo*. Thus, the development of *in vitro* models of human salivary glands will enable these experiments to be carried out.

1.3 SALIVARY GLANDS: NORMAL DEVELOPMENT

Salivary glands consist of three major paired glands: parotid, sublingual and submandibular glands as well as many minor salivary glands. The main function of these glands is to secrete saliva, which is highly dilute and consists of >99% water, electrolytes, proteins and peptides. Saliva also contains digestive enzymes, antimicrobial agents and growth factors. Important functions of saliva include protection of teeth, maintenance of oral health through clearing unwanted food and bacterial debris from the mouth, acting as a lubricant to protect the mucosa and aid speech, to enhance taste and to begin the digestion process (Jang *et al.*, 2015). Saliva also acts as an immunological barrier against microorganisms and has a high wound healing capacity (Kouznetsova *et al.*, 2010).

1.3.1 Anatomy of Salivary Glands

The parotid glands are the largest salivary glands and are situated below and in front of the ear on each side of the face. They are flat, well encapsulated and mainly associated with peripheral branches of the facial nerve. Ducts open into the oral

cavity opposite the second upper molar teeth on each side. Parotid glands are comprised only of serous cells (Amano *et al.*, 2012).

The sublingual glands are almond shaped and lie on the floor of the mouth between the frenulum of the tongue and the teeth. Short ducts open into the mouth near to, or with, submandibular ducts. They are predominantly composed of mucous cells.

The submandibular gland is ovoid in shape and located in the posterior part of the floor of the mouth, just below the mandible. Ducts open into the floor of the mouth by a small orifice lateral to the frenulum of the tongue. They are composed of both mucous and serous cells but predominantly serous cells (Amano *et al.*, 2012).

1.3.2 Histology of Salivary Glands

Human salivary glands contain primarily acinar and ductal cells. As mentioned above there are two types of acinar cells, serous and mucous cells, and it is from these secretory units that saliva is actively secreted (Tucker, 2007). Histologically, serous acini are round and have a small lumen. The nuclei of serous acinar cells are spherical and situated in the basal 1/3rd of the cell. The apical cytoplasm stains eosinophilic because of secretory granules. Mucous cells are characterized by tubular acini with large lumens and the nuclei are flat and pressed to the edge of the cell. The cytoplasm appears empty after haematoxylin and eosin staining because of the higher carbohydrate content (Amano *et al.*, 2012).

The secretory acini empty into intercalated ducts, which open into striated and then into excretory ducts. Histologically, intercalated ducts are lined by a single layer of low cuboidal epithelium with relatively clear cytoplasm and the nucleus is placed centrally. The intercalated ducts merge to form striated ducts, which are characterized by tall columnar epithelium, central nuclei and eosinophilic cytoplasm. They show a characteristic striated pattern due to the infoldings of the basal cytoplasm which contain the mitochondria needed for energy to actively alter the composition of the saliva (Pease, 1956). Intercalated ducts fuse to form the terminal excretory duct, which is lined by a non-striated pseudostratified epithelium. As the

duct approaches the oral cavity, it gradually changes into a stratified epithelium (Tucker, 2007; Amano *et al.*, 2012).

Aside from these two cell types, myoepithelial cells are found lying between the basal lamina and the acinar or ductal cells. The myoepithelial cells are closely related to the secretory acini and intercalated duct cells, and are innervated by the autonomic nervous system (Proctor and Carpenter, 2007; Ianez *et al.*, 2010; Amano *et al.*, 2012).

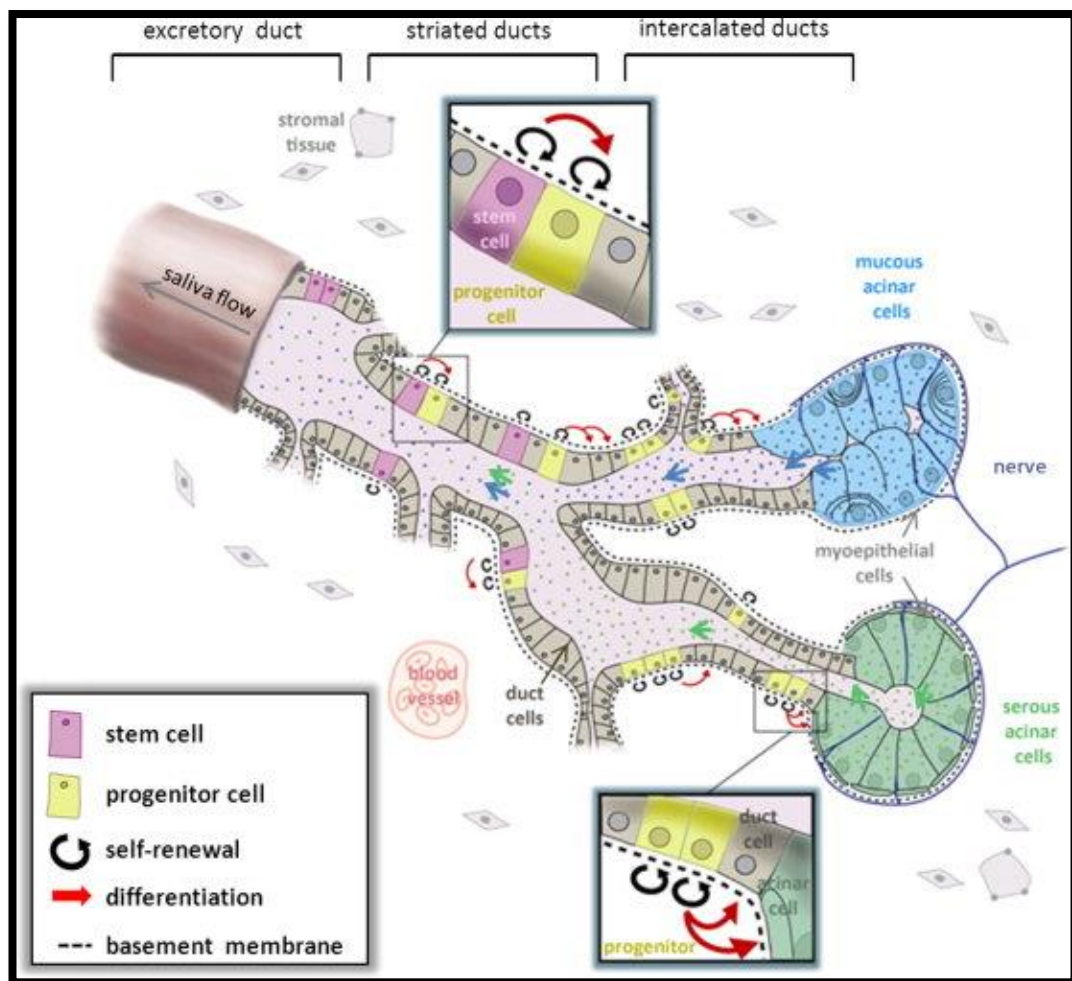


Figure 1.1 Schematic diagram shows component of cell types (serous and mucous acinar cells, duct cells and myoepithelial cells) of a salivary gland. Image reproduced from (Pringle, Van Os and Coppes, 2013).

1.3.3 Embryology of Salivary Glands

Salivary glands are generated by a branching morphogenesis during embryonic development. The submandibular gland is the first of the major salivary glands to develop followed by sublingual and parotid glands (Tucker, 2007). The first visible sign of salivary glands in the embryo is around E11.5 (embryonic day 11.5) in mouse, and week E8 in humans, and involves the thickening of the epithelium next to the tongue. This is known as the prebud stage. At E12.5 (mouse) or week E12 (human), the epithelium invaginates and forms a bud, linked to the oral surface by a duct which will later form the main duct of the salivary gland. The bud then undergoes branching morphogenesis with approximately 3 to 5 buds, called the pseudoglandular stage, at E13.5 (mouse) or week E13 (human). At the canalicular stage which is around E15.5 (mouse) or week E14 (human), the majority of the ducts develop lumen spaces by apoptosis of the cells located at their centre while the epithelial cells around the forming lumens are actively proliferating. The branches and the terminal buds form the excretory ducts and develop the secretory acini around E17.5 (mouse) or week E15 (human); known as the terminal bud stage. The development of salivary glands continues after birth with the final differentiation of granular tubules occurring at puberty. Formation of the final complex structure of salivary glands also involves coordinated development of endothelial and neuronal cells (Tucker, 2007; Patel and Hoffman, 2014).

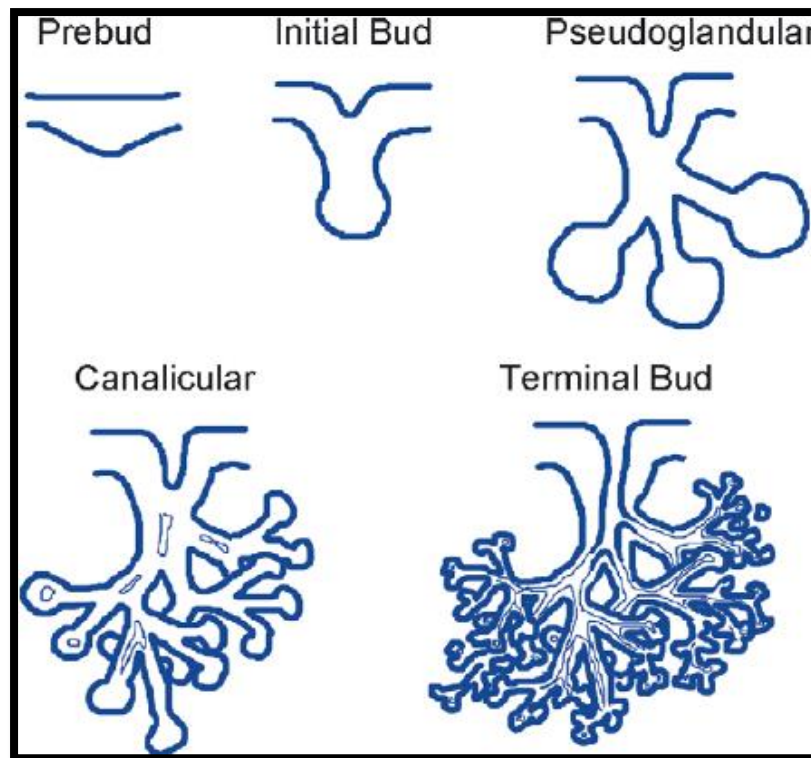


Figure 1.2 Schematic diagram shows stage of salivary gland development from prebud to terminal bud of mouse submandibular gland as a model. Image reproduced from (Tucker, 2007).

1.3.4 Physiology of Salivary Glands

Acinar cells are specialized for synthesis, storage and secretion of fluids. Acinar cells are water permeable and so allow fluid movement in the glands. The consistency of the secretions from acinar cells is either serous or mucous and this is based on whether it is watery or viscous. The product of serous acinar cells is watery, containing a large number of proteins such as amylase but there is a lack of mucins. Mucous acinar cells secrete mucins, large glycoproteins with carbohydrate chains, which add to the viscosity of the saliva (Tucker, 2007; Patel and Hoffman, 2014).

Ductal cells are water impermeable, are biochemically active and modify the concentration and content of saliva by reabsorption of electrolytes and secretion of proteins. They convey the saliva secreted by the secretory units to the oral cavity (Patel and Hoffman, 2014).

Myoepithelial cells have some features of smooth muscle cells and are contractile in nature. They function to facilitate secretion by contracting the acinar cells and causing the expulsion of stored saliva. The contraction of these cells results from stimulation by both the parasympathetic and sympathetic nervous systems (Proctor and Carpenter, 2007; Patel and Hoffman, 2014).

1.4 STEM CELLS

Basically, there are three stem cell types: adult stem cells, embryonic stem cells, and induced pluripotent stem cells. Generally, adult stem cells are organ restricted, either somatic or tissue-derived, and unipotent (a cell that can differentiate along only one lineage). They are able to proliferate for long periods of time which is referred as long-term self-renewal and can differentiate to produce all specialized cell types. Typically, they generate an intermediate cell type called a progenitor or precursor cell before they achieve their fully differentiated state. A progenitor cell in adult tissues is unspecialized or has partially differentiated cells that can be divided only a limited number of time and give rise to differentiate into its 'target cells'. While embryonic stem cells are derived from the undifferentiated inner mass cells of human embryo and pluripotent. Induced pluripotent stem cells which closely resemble embryonic stem cells are cells that have capacity to self-renew by dividing and developing onto the three primary germ cell layers (ectoderm, endoderm and mesoderm) and therefore into all cells of the adult body. Salivary gland adult stem cells are undifferentiated but reside between stem cells niche, similar with any other adult stem cell population. The primary role of the adult stem cells in humans is to maintain and repair of the tissue in which they are reside (Coppes and Stokman, 2011).

1.5 TISSUE ENGINEERING: GENERATING *IN VITRO* THREE-DIMENSIONAL (3D) MODELS OF HUMAN SALIVARY GLAND (hSG)

As outlined above salivary glands are complex 3D organs therefore it is sensible to consider using tissue engineered 3D models to study their function. Several studies have attempted to develop human salivary gland (hSG) 3D tissues and have been

tested as human cell-based models with translational potential. In 2007, Joraku *et al.* published a paper in which they described the reconstitution of 3D human salivary gland (hSG) tissue structures *in vitro*. They cultured human parotid gland cells in 3D matrix containing Collagen and Matrigel, in serum-free KGM with epidermal growth factor (EGF) and bovine pituitary extract (BPE) and showed the *in vitro* formation of functional and differentiated salivary units containing acinar and ductal-like structures. Furthermore, all structures maintained tight junctions, expression of the water channel protein aquaporin 5 (AQP5) and amylase production (Joraku *et al.*, 2007). Feng and colleagues (2009) demonstrated that hSG progenitor cells, when grown with Collagen type I in defined media (containing EGF and fibroblast growth factor 2 (FGF2)), developed into ductal structures and mucin-expressing acinar-like cells and demonstrated long-term self-renewal *in vitro*. Maria *et al* (2011) suggested that Matrigel provided a suitable microenvironment for morphological and improved functional properties of an hSG cell line. The hSG cells cultured in serum-free conditions on Matrigel-coated dishes, could be induced to differentiate into polarized secretory acinar like cells. Further study on developing hSG *in vitro* by Pradhan Bhatt *et al* (2013) indicated that a hyaluronic acid (HA)-hydrogel culture system could support salivary phenotypic features of hSG progenitors long-term, *in vitro*.

Jang *et al* (2015) showed that specific media components have an impact on growth and maintenance of specific acinar cell protein expression, cell polarity and secretory function. They found that high calcium concentrations (0.8 mM) in the medium promote the growth of AQP5 producing acinar-like cells, increased calcium mobilization, expression of the tight-junction protein zona occludin (ZO-1) with high transepithelial resistance and polarized amylase secretion after β -adrenergic receptor stimulation. Furthermore, the hSG cell cultures displayed the expression of the progenitor cell-type markers, keratin 5 and nanog, as well as the acinar cell-type markers, α -amylase, cystatin C, TMEM16A, and NKCC1.

Pringle (2016) presented promising findings of the therapeutic potential of hSG stem cells cultured from biopsy material for the treatment of radiation-induced

hyposalivation. The hSG primary cells were grown in Matrigel with serum-free media containing EGF and FGF which supported differentiation, self-renewal and growth as salispheres which were then injected into in a xenotransplantation model using mouse submandibular gland. Transplanted hSG cells (100,000 hSG cells per mouse) were capable of rescuing radiation-induced hyposalivation and enhanced salisphere formation two months after irradiation (Pringle *et al.*, 2016). Ono *et al* (2015) reported their findings of regenerating salivary glands using induced pluripotent stem (iPS) cells *in vivo* and *in vitro*. iPS cells transplanted into mouse salivary glands partially produced glandular tissues that closely resembled the adult salivary glands. Coculture of embryonic submandibular glands (SMG) cells and iPS cells *in vitro* had more developed epithelial structures than monoculture of embryonic SMG cells (Ono *et al.*, 2015).

To date an artificial salivary gland for therapeutic use in humans has still to be developed and intrinsic challenges arise from each protocol. Incompatible biomaterials for clinical translation as well as evaluation of salivary flow need to be addressed.

1.5 DEVELOPMENT OF *IN VITRO* 3D MODELS

Tissue engineering of salivary glands requires cells that retain specific gene and protein expression, extracellular matrix proteins that enable differentiation of the cells into functional structures, and a biocompatible scaffold as a surface that mimics the microenvironment of the salivary glands and allows cell growth (Pradhan-Bhatt *et al.*, 2014). Thus, one way to create an artificial salivary gland is by seeding cells onto biodegradable 3D scaffolds in optimal growth conditions to allow the cells to mimic as closely as possible those growing *in vivo*.

1.5.1 Primary Human Salivary Glands

The use of primary cells to create an artificial salivary gland is a recent technique and the critical problem in this field is the preparation (or harvesting) of adequate cells. When compared to cell lines, primary cells more closely resemble native tissue and

thus, are the best option for manipulation *in vitro* prior to transplantation into diseased or damaged organs. However, primary cells are difficult to isolate and culture. They are highly differentiated and this reduces their ability to form acinar structures *in vitro* (Nelson, Manzella and Baker, 2013; Pradhan-Bhatt *et al.*, 2014). New methods are therefore needed to improve cell differentiation, secretory function and to maintain cell viability in *in vitro* culture conditions.

1.5.2 Basement Membrane

Basement membrane is a continuous layer of extracellular matrix (ECM) that separates the epithelium from the surrounding mesenchyme. The ECM consists of two main classes of macromolecules; fibrous proteins and proteoglycans. The main fibrous ECM proteins are collagens, fibronectin, elastin and laminins. Proteoglycans are composed of glycosaminoglycans which are extremely hydrophilic, form as a hydrated gel and thus enable the matrices to endure high compressive forces. The ECM is represented as scaffolds on which the cells grow and also provide important biochemical elements that are required for controlling tissue development (Frantz, Stewart and Weaver, 2010).

Collagens are the most abundant fibrous protein within the interstitial ECM. They provide structural support, regulate cell adhesion and direct tissue development (Frantz, Stewart and Weaver, 2010; Yang *et al.*, 2010). For example, collagen type I accounts for 90% of the matrix protein of bone ECM and is involved in fibroblast and osteoblast differentiation and function (Kern *et al.*, 2001). Fibronectin is involved in mediating the cellular interactions of the interstitial ECM and plays a role in general cell attachment, migration, growth and development (Pankov, 2002; Frantz, Stewart and Weaver, 2010). Fibronectin has previously been shown to be a useful matrix protein for enhancing the seeding efficiency and growth of salivary epithelial cells (Tran *et al.*, 2005).

Matrigel is a complex protein mixture that has been used extensively, and has provided optimal growth conditions for cell cultures. Matrigel contains collagen IV,

laminin, fibronectin, entactin and a number of growth factors. It is a reconstituted basement membrane extracted from Engelbreth-Holm-Swarm (EHS) mouse tumour (Hughes, Postovit and Lajoie, 2010). It has been shown to promote cell differentiation, support cell growth and increase tumour growth (Kleinman and Martin, 2005). As mentioned previously, Matrigel has been seeded with human submandibular salivary gland cell lines and successfully facilitated the formation of acinar structures and the expression of acinar cell proteins, α -amylase and cystatin 3 (Maria *et al.*, 2011).

Hyaluronic acid (HA) hydrogel, as mentioned previously, has been used to demonstrate that isolated human salivary gland cells can be grown into spherical, organoid, acinar-like structures. These structures retained expression of salivary biomarkers such as tight junction proteins, ZO-1 and epithelial cadherin (E-cadherin), the water channel protein AQP5 and were able to secrete the salivary enzyme, α -amylase (Pradhan *et al.*, 2010). Polylactic-glycolic acid (PLGA) scaffolds have supported branching of foetal submandibular glands and self-assembly into branched gland-like structures (Sequeira *et al.*, 2012). In contrast, Chan (2011) demonstrated that human parotid gland acinar cells were able to grow spontaneously as either 3D or 2D clusters without the use of fabricated scaffolds. The protein expression pattern was different in the cells grown in these two cluster types. They found that cells cultured in 3D clusters expressed high levels of α -amylase, ZO-1, AQP3 and AQP5 compared to cells grown under 2D conditions (Chan *et al.*, 2011).

In my initial experiments (Chapter 3), I used collagen I, fibronectin, Matrigel and poly-L-lysine, a positively charged amino acid polymer widely used as a coating substrate to enhance cell attachment and growth of cells (Mazia, Schatten and Sale, 1975), as ECM to further investigate differences in cell growth and development.

Matrigel and collagen type I (derived from rat tail), both non-human in origin, are two of the most commonly used ECM mimicking matrices used to embed cells into 3D cultures. In addition, commercial ECM molecules such as fibronectin and poly-L-

lysine have also been used as ECM in multiple *in vitro* studies. All of these products have the same disadvantage for human studies as their composition differs from the native human tissue environment. Myogel is a gelatinous leiomyoma matrix which is derived from a benign human uterine leiomyoma, and has been recommended for *in vitro* human cell culture experiments since it closely mimics the human tumour microenvironment of solid cancers (Salo *et al.*, 2015). Thus, Myogel will be used in my study as an alternative ECM for the growth of SG cells *in vitro* and cell growth and differentiation will be compared to that on Matrigel (Chapter 4).

1.5.3 Culture Conditions

Culture conditions play a significant role in establishing functional acinar-like structures. Interestingly, most studies have commonly used a number of medium components such as EGF, insulin and dexamethasone or hydrocortisone. A number of studies have suggested that human salivary cells grow successfully with these added growth factors (Kruse *et al.*, 2004; Gorjup *et al.*, 2009; Pradhan *et al.*, 2010; Jang *et al.*, 2015). The addition of retinoic acid (RA) to the medium, appears to encourage cells to form a more keratinocyte-like phenotype (Maria *et al.*, 2011).

Chan *et al.* (2011) showed that low concentrations of calcium (0.09mM) in the medium affected cell proliferation, differentiation and led to an absence of tight-junction structures (Chan *et al.*, 2011). Similarly, Jang (2014) also found that low calcium concentrations in the medium resulted in a lack of cell-cell contact and junctional complex formation. However, and as mentioned previously, the number of acinar-like cells increased and displayed significant tight junction formation when the calcium concentration was high (0.8 mM) (Jang *et al.*, 2015). In my initial experiments (Chapter 3), KGM media was used without adding calcium as a supplement.

1.6 ORGANOID CULTURES

An organoid is basically defined as “resembling an organ,” which implies the presence of multiple specific cell types of the organ it models, displaying some specific

functions of the organ and structurally organized in a similar manner to the organ being modelled. Hence, an organoid is well-defined as a collection of specific-cell types that develop from stem cells or organ progenitors and self-organizes through cell sorting and spatially restricted lineage commitment (Lancaster and Knoblich, 2014). Organoid technology, therefore provides a useful tool for modelling human organ development and pathologies *in vitro*.

Several human organoids have been established from tissues such as kidney, gut, lung, retina and brain, all of which have reflected key structural and functional properties of the organs of origin (Lancaster and Knoblich, 2014; Clevers, 2016). Organoids can be cultured from two types of stem cells: (i) pluripotent stem cells, either embryonic stem (ES) cells or induced pluripotent stem (iPS) cells and (ii) organ-restricted adults stem cells (aSCs). Both approaches are dependent upon on the expansion and self-organization potential of cells whilst in culture. Growth factor cocktails that imitate the various organ stem cell niches in culture media will allow these stem cells to differentiate in a controlled manner, capable of self-organising into structures to which they are fated (Clevers, 2016). In addition, an important component in this culture system is a scaffold or 3D matrix, usually Matrigel, to support cell attachment and survival as well as to allow organoid formation (Lancaster and Knoblich, 2014; Clevers, 2016; Bredenoord, Clevers and Knoblich, 2017).

To date, only Coppes and colleagues have utilized organoid culture to differentiate single mouse salivary cells *in vitro* into definite lobular organoids consisting of a number of salivary gland lineages; CK7, CK18 and AQP5 (Nanduri *et al.*, 2014; Maimets *et al.*, 2016). I would like to further investigate the potential of this organoid system to develop a human salivary gland *in vitro*.

1.6.1 Defined Growth Factors

The Wnt pathway appears to be the key driver of epithelial adult stem cells (aSCs) (Clevers, Loh and Nusse, 2014). Wnt3a and R-spondin 1 are Wnt activators and have been shown to be vital components of many aSCs culture experiments (Clevers,

2016). For example, Sato *et al* (2009) described the culture conditions for unlimited *in vitro* expansion that allows the growth of small intestine epithelial organoids ('mini-guts') from single Lgr5+ stem cells. The Lgr5+ stem cells were embedded in Matrigel and cultured in serum-free media with R-spondin-1, EGF and noggin (BMP inhibitor). The mini-guts consisted of all cell types of the intestinal epithelium with crypt-like structures (Sato *et al.*, 2009). In contrast, Ootani *et al* (2009) demonstrated another approach by culturing neonatal mouse intestine consisting of epithelial and mesenchymal and organoids grown in collagen under air-liquid interface (ALI) with serum-containing medium without defined growth factors. Taken together, these studies provide important insights into stem cell *in vitro* culture systems with different approaches either by providing the specific growth factors (Wnt, R-spondin, EGF and noggin) (Sato *et al.*, 2009) or through the incorporation of stromal components (Ootani *et al.*, 2009).

FGF provided by the mesenchyme, is required for branching morphogenesis (Jaskoll *et al.*, 2005). Wells *et al* (2013) demonstrated that the epithelium leads initial salivary gland development which is later followed by bud development directed by FGF expression in the mesenchyme. Previous studies have suggested that epithelial progenitor cells can undergo branching morphogenesis without mesenchyme, by growing cells in a laminin-rich basement membrane together with growth factors (Steinberg *et al.*, 2005). In contrast, recent findings have demonstrated that FGF2 and laminin-111 stimulate the branching and pro-acinar differentiation of SG organoids in the presence of E16 salivary mesenchyme cells (Hosseini *et al.*, 2018). Patel *et al* (2011) suggested that FGF signalling is important for SG branching morphogenesis, but the onset of bud formation is still unclear. Thus, I aim to culture SG cells in Matrigel with or without Myogel at an ALI or traditionally by submerging in serum-free media containing defined growth factors such as Wnt3a, R-spondin-1, EGF and FGF2 (Chapter 4).

The addition of ROCK inhibitor (Y27632) to cell cultures has been shown to enhance basal cell expansion in airway epithelial cultures (Mou *et al.*, 2016). It has also been used to permit the survival of dissociated human embryonic stem cells (Watanabe *et*

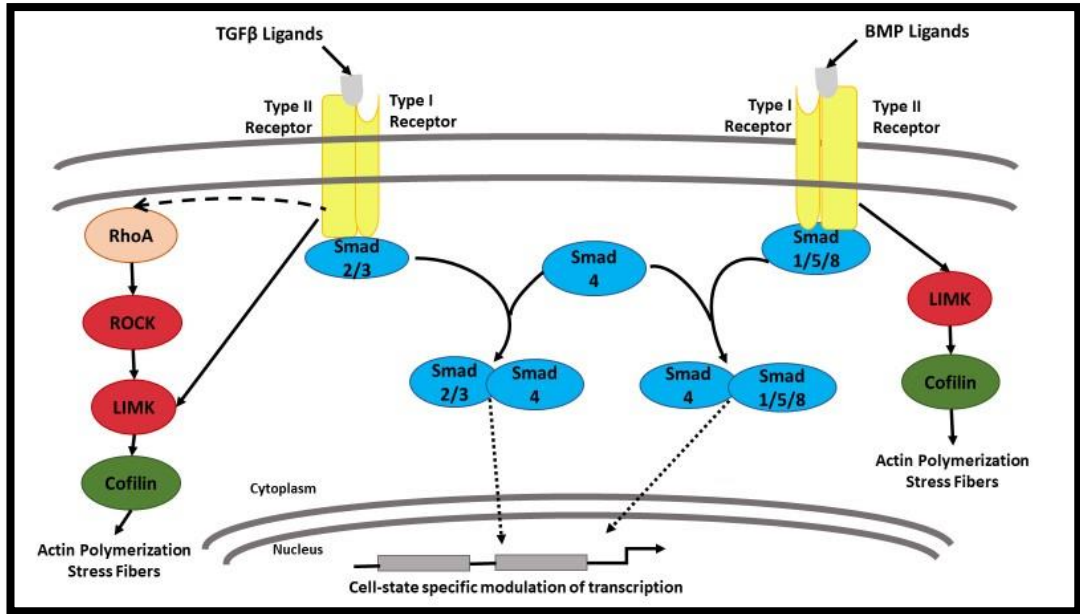
al., 2007). In contrast, Daley *et al* (2009) showed that Y-27632 inhibits branch formation by inhibiting myosin II activity in mouse salivary glands, even though shallow initial clefts still formed. In my study, Y-27632 will be included in the media in the initial stages to promote cell proliferation and expansion, and withdrawn from the media at the differentiation stage similar to the previous studies of Nanduri and Maimets (Nanduri *et al.*, 2014; Maimets *et al.*, 2016).

1.6.2 The Inhibitors in Enriched Media

Activation of signalling pathways can result in self-renewal and proliferation while preventing differentiation; this is required in order to maintain the stem/progenitor cell population during culture expansion (Gurung, Werkmeister and Gargett, 2015). Transforming growth factor- β (TGF β) and bone morphogenic protein (BMP) signalling have been recognized to encourage progenitor proliferation, migration and survival (Broutier *et al.*, 2016) while the LIM kinase (LIMK) pathway typically results in actin cytoskeletal reorganisation, morphogenesis and altered cell motility and invasion by phosphorylating and inactivating cofilin (Morin *et al.*, 2011).

Generally, signalling is initiated when ligands bind to serine/threonine receptor kinases, inducing oligomerization and leading to phosphorylation of the cytoplasmic signalling molecules Smad 1/5/8 for the BMP pathway or Smad 2/3 for the TGF β pathway (Refer Figure 1.3). Smad phosphorylation then activates the common signalling transducer Smad4 and leads to translocation to the nucleus (Schmierer and Hill, 2007; Horbelt, Denkis and Knaus, 2012). TGF β signalling also leads to activation of target proteins such as ROCK through the Rho GTPase (RhoA) pathway. ROCK kinase phosphorylation increases myosin ATPase activity, filamentous actin (F-actin) stabilisation and actin-myosin association. The LIMK pathway is activated downstream of the RhoA-ROCK pathway and inactivates cofilin resulting in actin polymerization. Even though ROCK and LIMK are located in a linear downstream pathway of RhoA, their functions in actin cytoskeleton regulation are dissimilar (Morin *et al.*, 2011).

Numerous small molecules targeting signalling pathways involved in preventing spontaneous differentiation and maintaining stem cell status for prolonged periods of time have been studied. Dorsomorphin (DM) has been described to mimic the function of noggin, the endogenous BMP inhibitor, which allows the formation of cardiomyocytes from mouse embryonic stem cells (Ao *et al.*, 2012). Whereas, DMH1, dorsomorphin homologue 1, a second-generation small molecule BMP inhibitor, has been shown to be a more selective inhibitor of BMP Type I receptors than DM. A8301 is a potent inhibitor of the TGF β type I receptor superfamily activin-like kinase, ALK5 and its relatives ALK4 and ALK7. It has no effect on BMP signalling, but inhibits epithelial-to-mesenchymal transition by transforming growth factor β and SMAD signalling. It has been used to maintain proliferation and self-renewal of mouse and human iPS cells in culture without feeder layers (Li *et al.*, 2009). Furthermore, it also prevented senescence and apoptosis of cultured human endometrial mesenchymal stem cells (MSC), and thus may have a role in spontaneous MSC differentiation during culture expansion (Gurung, Werkmeister and Gargett, 2015). Thus, DMH1 (as a BMP inhibitor) and A8301 (as a TGF β inhibitor) will be used in my study (Chapter 5) to determine their roles in maintaining growth and preventing the spontaneous differentiation of SG cells during culture expansion. In addition, SR7826, is a potent and selective LIM kinase inhibitor, which inhibits cofilin phosphorylation and suppresses migration and invasion of cells in vitro. Hence, the actions of SR7826 during the morphogenetic process in SG cell development will be investigated in my study (Chapter 5).



Pathway Diagram Keys:

- Receptor
- Transcription Factor
- Kinase
- GTPase
- Direct Stimulatory Modification
- Tentative Stimulatory Modification
- Translocation
- Joining of Subunits
- Transcriptional Stimulatory Modification

Figure 1.3 Schematic diagram show TGFβ/BMP Signalling Pathway. Image modified from (Horbelt, Denkis and Knaus, 2012).

1.7 CELL SPECIFIC MARKERS

Salivary units consist of well differentiated functional acinar and ductal structures. In order to develop three-dimensional models of *in vitro* human salivary glands, in which cells could form mature salivary gland tissues structures, the structures should maintain and demonstrate their functional activity. All structures of salivary units must be capable of establishing tight junctions and cell-cell adhesion, and competent to express and produce secretory proteins (Pradhan *et al.*, 2010).

Besides acinar and ductal cells, salivary glands are also composed of progenitor and myoepithelial cells. In my study, the cell specific markers to be studied were chosen based on those used in previous studies (Tran *et al.*, 2005; Ianez *et al.*, 2010; Nanduri *et al.*, 2013; Jang *et al.*, 2015). The four groups of cell specific markers that will be used in this study are for progenitor cells, acinar cells, ductal cells and myoepithelial cells, as I have outlined above, they are extremely important to salivary gland physiology and development.

Progenitor cells exist both in embryonic and adult salivary glands. Several markers of the nucleus, cytoplasm and the cell surface have been used to assess the status of progenitor cells. Nanog, keratin 5 (CK5) and cKIT are well-established as progenitor cells markers. Nanog is a transcription factor expressed in embryonic stem cells and is a key marker of self-renewal and in the maintenance of pluripotency (Gorjup *et al.*, 2009). Previous studies have detected the expression of nanog in embryonic salivary gland stem cells (Gorjup *et al.*, 2009) and also in the nucleus of primary human minor salivary gland cell cultures (Jang *et al.*, 2015).

CK5 is an epithelial progenitor mainly expressed in ductal cells. Shubin *et al.* (2017) demonstrated intense staining of CK5 in cells at the periphery of mice SMG cell spheres (Shubin *et al.*, 2017). Abundant CK5 has also been observed in single-cell-derived mice mini-glands and thus firmly established as a marker of progenitor cell in embryonic salivary glands (Maimets *et al.*, 2016). cKIT, also known as CD117, is a receptor tyrosine kinase expressed on the surface of hematopoietic stem cells as well

as a variety of normal human cell types, including breast epithelium, germ cells, melanocytes, immature myeloid cells and mast cells. The expression of cKIT indicates cell survival, and the ability of the cells to proliferate and differentiate. cKIT has been localised to the excretory duct and striated duct cells of mouse submandibular glands (Nanduri *et al.*, 2013) confirming that the major ducts of salivary glands contain progenitor-like cells.

Amylase, AQP5 and cystatin C (CST3) will be used as acinar cell markers in my study. Amylase, a secretory protein, is a typical marker of serous acinar cells (Kouznetsova *et al.*, 2010). The findings of Chan *et al.* (2011) strongly supported the clear expression of amylase in acinar cells, but not in ductal cells of human parotid glands. Significant expression of amylase has also been found in glandular cells of cultured human parotid gland cells (Joraku *et al.*, 2005). AQP5 is a water transportation-associated protein, also identified as an acinar cell marker (Jang *et al.*, 2015). The main function of AQP5 is to aid the secretion of saliva, tears and pulmonary secretions through the transport of water molecules across cell membranes. This function is carried out in association with cytoskeletal filaments. A recent study has detected the expression of AQP5 at the apical membrane of acinar cells of cultured cells (Joraku *et al.*, 2005; Chan *et al.*, 2010). Significant expression of AQP5 has also been found at the lobule-like structures of mice SG organoids (Nanduri *et al.*, 2014). Expression in this region of the cell suggested that the cultured cells were able to produce water channel proteins important in regulating volume changes and mediating the water permeability of acinar cells. CST3 is a non-glycosylated protein, found mainly in biological fluids such as saliva. It has been found in the cytoplasmic region of primary human minor salivary gland acinar-like cells (Jang *et al.*, 2015).

ZO-1 and claudin-1 are tight junction proteins involved in signal transduction at cell-cell junctions. Tight junctions play important roles in the secretion of fluids, salts and proteins by epithelial cells. The formation of tight junction is associated with the functional ability of fluid movement and with the correct apical-basal orientation (Tran *et al.*, 2005; Jang *et al.*, 2015). Both ZO-1 and claudin-1, have been detected at the cell boundary of cultured human parotid gland cells (Joraku *et al.*, 2005). The

expression of ZO-1 in the plasma membrane indicates the formation of mature cell-cell tight junctions (Jang *et al.*, 2015). Tran *et al.* (2005) suggested using transepithelial electrical resistance (TER) measurement to validate tight junction formation. They found that the cells grown as a monolayer expressed ZO-1, displayed tight junction formation and exhibited a high TER value in the apical-basal orientation. E-cadherin is found within the membrane that surrounds epithelial cells, and functions by helping neighboring cells stick to one another (cell adhesion) to form organized tissues. E-cadherin is involved in salivary gland epithelial cell self-organization, branching morphogenesis and also acinus formation (Hsu and Yamada, 2010). The expression of these tight junction proteins and cell adhesion proteins will indicate that our model contains cells that closely resemble those from the ductal regions of salivary glands.

Myoepithelial cells are important in assisting the expulsion of saliva. Alpha smooth muscle actin (α -SMA), CD10 and p63 are myoepithelial cell markers that have previously been used to investigate expression during salivary gland morphogenesis in human glands (Ianez *et al.*, 2010). They found that α -SMA and p63 were expressed in the myoepithelial cells from the earliest stages of salivary gland maturation. However, the presence of CD10 was found in stromal cells only. α -SMA is a contractile protein, surrounding the acinar cells to provide a contracting force in response to neurotransmitters (Chan *et al.*, 2010). The expression of this myoepithelial cell marker is more abundant around acinar lobules and at the end of intercalated ducts as salivary gland morphogenesis progresses (Ianez *et al.*, 2010). CD10 is a cell surface enzyme, endopeptidase and is present on either epithelial cells or stromal cells. It has been used as a cell surface marker of the stem cells in normal breast, lung, adipose and bone tissues (Maguer-Satta, Besançon and Bachelard-Cascales, 2011). CD10 expression was found restricted to myoepithelial cells of mammary gland (Atherton *et al.*, 1994). However, in a review of salivary gland pathology by Cheuk and Chan (2007) CD10, was described as a myoepithelial cell marker with low specificity (Cheuk and Chan, 2007). P63 has been reported as a marker of basal cells in skin and prostate, as well as a myoepithelial cell marker of mammary glands. In salivary glands, p63 expression has been shown in myoepithelial

and basal cells of the glandular structures of developing parotid and submandibular salivary glands (Ianez *et al.*, 2010). These myoepithelial cell-type specific markers might prove to be useful tools for the identification of myoepithelial cells during the differentiation of our *in vitro* salivary gland models.

Mucins are the chief glycoprotein components of saliva, characterized as gel-forming secretions and synthesized by epithelial cells (Teshima *et al.*, 2011). MUC5B is well known as a gel forming mucin in human saliva (Sonesson *et al.*, 2008). It is mainly expressed in the cytoplasm of mucous cells of the submandibular and sublingual glands and also the submucosal glands of the airways (Rousseau *et al.*, 2008; Piras *et al.*, 2010). In contrast, Teshima (2011) detected MUC5B in the luminal border of excretory ducts.

Mucin 7 (MUC7) is a low molecular weight mucin with antimicrobial activity and has been described as having interactions with salivary components such as amylase, histatin-1 and statherin. The presence of MUC7 has been reported in a subpopulation of mucous cells of submandibular glands and labial glands (Kouznetsova *et al.*, 2010). While, Piludu (2003) indicated that MUC7 was expressed in both serous and mucous components of the submandibular and sublingual gland with varying intensities (Piludu *et al.*, 2003).

BPIFA2 (SPLUNC2) is a member of the BPI-fold containing family of proteins which are expressed in the upper airways, nose and mouth. BPIFA2 is expressed predominantly in salivary glands with positive staining in serous acinar cells, negative staining in mucous acinar cells, and is secreted into saliva (Bingle *et al.*, 2009). These cell-type markers, MUC5B, MUC7 and BPIFA2, will be used to validate the serous and mucous acinar cell expression of our models.

HE4 (also known as WFDC2) is a 2 Whey Acidic Protein (WAP) domain containing protein that was initially described as a marker of human epididymis and is also known to be an ovarian tumour marker gene (Bingle, Singleton and Bingle, 2002; Bingle *et al.*, 2006; Moore *et al.*, 2014). In addition, previous studies have

demonstrated that HE4 expression appears in a number of normal human tissues outside of the male reproductive system including nasal and upper respiratory tract, as well as in a subset of lung tumour cell lines (Bingle, Singleton and Bingle, 2002). Further studies have shown that HE4 is also expressed in some epithelial cells as well as in mucous cells of submucosal glands of the upper airways, and the ducts of the major salivary glands (Bingle *et al.*, 2006). Thus, study of the expression of this marker in SG models may raise our understanding of HE4 as a novel, useful marker.

1.8 TISSUE ENGINEERING SCAFFOLD: POLYMERISED HIGH INTERNAL PHASE EMULSION (POLYHIPE) SCAFFOLDS

Culturing cells on a scaffold has been proposed as a solution for engineering a functional salivary gland. Previous studies have demonstrated attempts to culture salivary gland (SG) cells on scaffolds using both natural and synthetic materials. Shubin *et al* (2016) showed that encapsulation of primary SG cells in enzymatically degradable poly (ethylene glycol) hydrogel, a synthetic material, promoted acinar cell characteristics, but no functional secretion. SG cells have also been cultured in several types of ECM derived from natural material, such as the previously mentioned Matrigel, and these matrices are able to support the viability and proliferation of the cells and to stimulate apicobasal polarity (Maria *et al.*, 2011). This type of ECM is, however, impractical for *in vivo* implantation in humans. Cantara *et al* (2012) generated nanofiber, poly-lactic-co-glycolic acid (PLGA) scaffolds to mimic the fibrillar characteristics of the basement membrane and have demonstrated that while a SG ductal epithelial cell line attached and proliferated, they were not able to fully polarize.

Various polymers and natural materials have been engineered to create scaffolds that mimic structures in the natural environment. The synthetic polymers must be prepared with a porous microstructure as micro-porosity plays a vital role in increasing cell attachment, growth and also protein absorption. Thus, emulsion templating using high internal phase emulsions (HIPE), in which the continuous phase consists of monomer and crosslinker, and the internal phase (aqueous phase)

constitutes the majority of the total volume, is the best technique for introducing micro-porosity within a scaffold (Wang *et al.*, 2016). PolyHIPE scaffolds serve as an excellent material for tissue engineering as it is highly porous with interconnected porosity which enables the transportation of oxygen, nutrients and metabolic waste, as well as the migration and proliferation of the cells (Owen *et al.*, 2016; Wang *et al.*, 2016). Besides, the thickness of PolyHIPE monoliths also affect cell penetration. Thus, by using microstereolithography, the individual fibre's depth limit can be created specifically for cell ingrowth and plasma penetration (Akay, Birch and Bokhari, 2004; Owen *et al.*, 2016). My study uses emulsion templating in combination with microstereolithography to fabricate PolyHIPE scaffolds, which were seeded with human salivary gland cells. Our aim was to investigate the potential of PolyHIPE scaffolds as cell delivery vehicles for the SG model to be implanted *in vivo* and also for regeneration of functional salivary gland tissue.

1.9 ORGANOID AS MODEL FOR INFECTIOUS DISEASE: *STAPHYLOCOCCUS AUREUS*

Theoretically, organoids are suitable for infectious disease studies as unlike cell lines, they closely represent all cellular components of a given organ. A notable example of this has been the use of human stomach organoids grown from adult stem cells which it has been shown can be effectively infected by the gastric pathogen, *Helicobacter pylori* (Bartfeld and Clevers, 2015). This is further exemplified in studies using forebrain-specific organoids from human induced pluripotent stem cells (iPSCs) to investigate infection by Zika virus (ZIKV). The infected forebrain organoids with ZIKV resulted in productive infection of neural progenitors, increased cell death, decreased proliferation and reduced neuronal cell-layer volume, hence closely resembling microcephaly (Qian *et al.*, 2016). Furthermore, Qian *et al.* (2016) also described the development of brain-region-specific organoids using miniaturized spinning bioreactor as models for ZIKV exposure. Thus, organoid technology has significant potential as a tool for translational research.

Staphylococcus aureus is the most common cause of salivary gland infection, often referred to as Sialadenitis (Kukita *et al.*, 2013). The infection can be caused by reduced salivary flow due to blockage or inflammation of a salivary duct, Sjogren's syndrome or radiation therapy for head and neck cancer (O Lewis *et al.*, 1993). My study involved preliminary experiments to establish the potential of my SG organoids as a suitable model for the study of host-pathogen interactions.

1.10 AIMS AND HYPOTHESIS

The primary aim of this study is to develop an *in vitro* 3D culture system of human salivary glands through the optimisation of growth conditions that will allow salivary gland cells to grow and replicate *in vivo* in a similar manner to that *in vivo*. Another aim is to verify the phenotypic and functional characteristics of the cells in the cultures to ensure they resemble, as closely as possible, those growing *in vivo* by investigating the expression of cell specific markers using reverse-transcription polymerase chain reaction (RT-PCR), immunohistochemistry (IHC) and immunofluorescence confocal microscopy (IFC). A further aim is to investigate the potential of the SG model for *in vivo* transplantation using a biodegradable scaffold as a vehicle and a final aim is to utilise the SG model as a tool for the study of infectious disease.

The main objectives of this study are:

1. **Establishment of *in vitro* models of human salivary gland.** We will establish culture conditions using HTB41 cells and transfer the knowledge gained to the culture of normal human salivary gland cells. There are two specific objectives:
 - a. To determine the optimal culture conditions for the development of *in vitro* models of human salivary glands using HTB41 cells and to investigate the expression of specific cell markers by RT-PCR and immunohistochemistry.

- b. To determine the optimum method for the isolation of normal human salivary gland cells from major gland tissue, to establish 3D models with these cells and to investigate the expression of specific cell markers.
2. **Development of organoid models of human salivary gland.** We will use the data from objective 1 to develop and use human salivary organoids. Two specific objectives are:
 - a. To develop an organoid model of human salivary glands using normal sublingual gland cells.
 - b. To utilise the model for the study of the pathogenesis of infectious disease with *Staphylococcus aureus* as a model infectant.
3. **Human salivary gland organoid models cultured in different media.** We will adapt culture conditions through the addition of specific TGF β signalling pathway inhibitors to the culture media to investigate the effects of differentiation factors on the development of SG organoids.
4. **Polymerised High Internal Phase Emulsion (PolyHIPE) scaffolds.** We will culture SGs cell on biodegradable Polymerised High Internal Phase Emulsion (PolyHIPE) scaffolds with a long-term view of transplanting these *in vivo*.

Our hypothesis is that the salivary gland cells can be manipulated by culture conditions to mimic the *in vivo* situation.

1.11 SIGNIFICANCE OF THIS STUDY

This study describes the isolation of human SG cells, the establishment of culture conditions for growing SG organoids and its potential for translational study by infecting with a known pathogen. I will demonstrate the ability of human salivary gland derived cells to proliferate, differentiate and self-renew *in vitro* forming branching SG organoids that express cell specific markers when grown in defined culture media with essential niche factors that mimic the *in vivo* environment.

Furthermore, I will demonstrate our approach for future regenerative studies through the use of PolyHIPE scaffolds as a 'cell vehicle' for *in vivo* transplantation. This study will provide necessary and fundamental information for future applications in developing an artificial salivary gland, with the potential to act as a new treatment for salivary gland dysfunction.

CHAPTER 2

General Methodology

CHAPTER 2: GENERAL METHODOLOGY

2.1 MATERIALS

All chemicals used in this study were molecular biology or cell culture grade and purchased from Sigma-Aldrich, Gillingham, Dorset, UK, unless otherwise stated.

2.2 BASIC CELL CULTURE TECHNIQUE

All cell culture work was carried out in Class II laminar flow hoods (Walker Safety Cabinets, Glossop, Derbyshire, UK). Laminar flow hoods and equipment used within them were sterilised prior to use with either 70% (v/v) industrial methylated spirits (IMS) or autoclave sterilisation. All cells were incubated at 37°C in humidified incubators with 5% CO₂.

2.2.1 Cell Culture/Thawing Cells

A vial containing cells in cryopreservation medium was removed from the storage tank and the cells were thawed rapidly by placing immediately in a 37°C water bath. The vial was wiped with 70% IMS before opening. The vial contents were transferred into a 20 mL tube; 10 mL of fresh culture medium was added slowly in a drop wise manner before centrifuging at 1,500 rpm for 5 minutes. The supernatant was discarded. 12 mL of fresh culture medium was added to resuspend the cells, which were then transferred into a new T75 flask. The flask was examined under the microscope to check cell viability and incubated at 37°C in 5% CO₂ incubator.

2.2.2 Culture and Passage Cells

Cells are ready to passage at around 80% confluency. The old medium was removed and the cells were washed with 5 mL Ca/Mg free Dulbecco's phosphate buffered saline (PBS) before 5 mL trypsin-EDTA (0.05% trypsin/ 0.02% EDTA w/v) was added and the flask incubated for 2 minutes at 37°C. The flask was observed under a microscope to ensure detachment of cells and 10 mL of fresh medium was added into the flask to inhibit the action of trypsin. The mixture was pipetted several times to detach all the cells. A new T75 flask with 12 mL fresh culture medium was

prepared and 500 µL of cell suspension added. The cells were incubated at 37°C in 5% CO₂ incubator and fresh culture medium replaced every 2 to 3 days.

2.2.3 Counting Cells

When required, after trypsinization cells were transferred into 15 mL tubes and centrifuged at 1,500 rpm for 5 minutes. Supernatant was discarded; 10 mL of fresh culture medium was added and mixed well. Approximately 10 µL of cell suspension was transferred to a haemocytometer and observed under a microscope. All viable cells were counted in the four corner squares. The formula below was used to determine the number of cells per millilitre.

$$\text{Concentration (cells/ml)} = \frac{\text{Number of cells} \times \text{Dilution factor} \times 10^4}{4 \text{ (squares)}}$$

$$\text{Total number of cells} = \text{Concentration (cells/mL)} \times \text{Volume of sample (mL)}$$

2.2.4 Freezing Cells

Before freezing, the cells were in log phase. After trypsinizing and counting, the cells were mixed with cryopreservation medium (10% DMSO in cell growth medium), aliquoted into 1 mL cryovial, and placed in Mr Frosty at -80°C overnight for slow cooling. The cryovial was then put into vapour phase of liquid nitrogen for long-term storage.

2.3 PREPARATION OF CELL CULTURE MEDIUM

Adenine

330 mg adenine powder was mixed with 100 ml of 0.1 M hydrochloric acid (HCl) until the powder dissolved completely. The solution was filter sterilised, aliquoted into 5 mL with a concentration of 1.8×10^{-2} M and stored at -20°C.

Hydrocortisone

40 mg of hydrocortisone powder was added to 4 mL of 100% ethanol and mixed before 36 mL DMEM was added to make up 10X concentration which was filtered and stored in 5 mL aliquots at -20°C. One 10X concentrate aliquot was added to 45 mL DMEM resulting in a final concentration of 100 µg/mL and this was stored in 2 mL aliquots at -20°C.

Epidermal Growth Factor (Human Recombinant from *E. coli*)

200 µg of EGF was dissolved in 10 mL of DMEM containing 10% FCS. 0.5 mL aliquots, with a final concentration of 10 µg/mL, were stored at -20°C.

Cholera Toxin (extracted from *Vibrio cholera*)

0.5 mg was dissolved in 1.67 mL of sterile water and stored at 4°C. Half of this stock was diluted in 50 mL of sterile water to make a final concentration of 10⁻⁷ M.

HTB41

HTB41 cell line is derived from a submandibular mucoepidermoid tumour. HTB41 cells were cultured in McCoy's 5A modified media supplemented as shown in **Table 2.1**. 500 mL media were made at a time, stored at 4°C and used for up to one month.

Component	Volume and stock solution	Final concentration	Storage
McCoy's 5A medium modified	440 mL		4°C
Penicillin/Streptomycin	5 mL of 10,000 i.u./mL penicillin and 10,000 µg/mL streptomycin	100 i.u./mL penicillin and 100 µg/mL streptomycin	-20°C
Fetal Bovine Serum	50 mL	10%	-20°C
L-Glutamine	5 mL	2 mM	-20°C

Table 2.1 HTB41 cell culture medium

Primary Human Salivary Gland (HuSG) Cells

Primary HuSG cells were cultured in KGM medium. 500 mL media was made at a time (**Table 2.2**), stored at 4°C and used for up to one month.

Component	Volume and stock solution	Final concentration	Storage
Dulbecco's modified Eagle's Medium (DMEM)	335 mL	1:3	4°C
Nutrient Mixture F12 HAM	115 mL		4°C
Penicillin/Streptomycin	5 mL of 10,000 i.u./mL penicillin and 10,000 µg/mL streptomycin	100 i.u./mL penicillin and 100 µg/mL streptomycin	-20°C
Fetal Calf Serum	50 mL	10%	-20°C
L-Glutamine	5 mL	2 mM	-20°C
Adenine	5 mL	1.8x10 ⁻⁴ M	-20°C
Hydrocortisone	2 mL	0.5 µg/mL	-20°C
Epidermal Growth Factor	500 µL	10 ng/mL	-20°C
Cholera Toxin	500 µL	10 ⁻¹⁰ M	4°C
Insulin	250 µL	5 µg/mL	4°C

Table 2.2 KGM medium

2.4 REVERSE-TRANSCRIPTION POLYMERASE CHAIN REACTION

2.4.1 Sample Preparation

Total RNA was extracted from tissue and from cultured cells using TRI-reagent according to the manufacturer's instructions. Briefly, tissue samples were homogenized by mincing and 1 mL TRI-reagent added. The volume of the tissue did not exceed 10% of the volume of the TRI-reagent. Cultured cells, were collected by centrifuging at 15,000 rpm for 5 minutes at 10°C. The supernatant was removed and the pellet lysed in 1 mL TRI-reagent by repeated pipetting. After cells had been homogenized or lysed in TRI-reagent, the samples were stored at -20°C before RNA isolation.

2.4.2 RNA Isolation

Samples were thawed and equilibrated to room temperature (RT) by leaving to stand for 5 minutes to ensure complete dissociation of nucleoprotein complexes. 200 µL of chloroform was added to the sample and mixed vigorously by vortexing for 15 seconds. The samples were left to stand for 5 minutes at RT. The mixture was centrifuged at 12,000 rpm for 15 minutes at 8°C resulting in three phases: a colourless, upper aqueous phase containing RNA, an interphase containing DNA, and a lower red organic phase containing protein.

The RNA containing phase was transferred into a fresh tube, 500 µL of isopropanol for each 1 mL of TRI-reagent used was added to each sample and mixed well by vortexing. The samples were allowed to stand for 5 minutes at RT, and then centrifuged at 12,000 rpm for 10 minutes at 8°C. A pellet of RNA precipitate was formed on the side and bottom of the tube. The supernatant was removed and the RNA pellet washed by adding 1 mL of 75% ethanol. The samples were centrifuged at 7,500 rpm for 5 minutes at 8°C. All ethanol was removed and the RNA pellet left to air dry for 10 minutes. Finally, 20 µL of water was added to the RNA pellet and mixed by repeated pipetting to resuspend the RNA.

2.4.3 RNA Quantification using Nanodrop

NanoDrop™ 1000 Spectrophotometer (Thermo Fisher Scientific, Loughborough, UK) was used to quantify the RNA. An acceptable 260/280 ratio was >1.9.

2.4.4 Denaturing Formaldehyde Agarose Gel Electrophoresis

Formaldehyde agarose gel electrophoresis was carried out to visualise the RNA and determine its integrity. A 1% (w/v) agarose gel was prepared in MOPS/EDTA buffer with formaldehyde. This step was carried out in a fume hood. The gel mixture was poured onto the assembled gel-casting tray and allowed to set.

3 µL of each RNA sample was added to 3 µL of RNA loading buffer containing ethidium bromide (Thermo Scientific, R0641) and mixed gently. The RNA mixture was heated

to 70°C for 2 minutes and loaded into the well. The agarose gel was run in 1X MOPS/EDTA buffer at 70V for 30 minutes. Ethidium bromide staining of RNA in agarose gels visualized two distinct bands, corresponding to the 28S and 18S ribosomal bands (rRNA). The 28S rRNA band should have an intensity of approximately twice that of the 18S rRNA band. The band images were acquired using a Syngene Gel-Doc system with InGenius 3 GENESys software.

2.4.5 Reverse Transcription-Polymerase Chain Reaction (RT-PCR)

One microgram of total RNA was reverse transcribed with random primers and oligo(dT) primers, and the polymerase chain reaction (PCR) was performed using specific primers as shown in the following sequences below. Primers were designed using sequence information from Ensembl (www.ensembl.org) and primer3 Input (primer3.ut.ee). Primers were purchased from Sigma-Aldrich, Dorset, UK.

Briefly, the RT step involved incubation at 37°C for 60 minutes and 95°C for 5 minutes. The PCR amplification was conducted using Maxima Hotstart green PCR master mix (MMx) (Thermo Scientific, K1061). 35 cycles of 95°C for 1 minute, annealing at 60°C for 1 minute, and extension for 1 minute at 72°C was ended by a final extension step at 72°C for 7 minutes.

PCR products were visualized on 2% agarose gels in TE buffer stained with ethidium bromide. 10 µL of each sample was loaded into the well and run in 1X TE buffer at 80V for 60 minutes. A GeneRuler 100bp DNA ladder (Thermo Scientific, Cheshire, UK) was used as a marker. The band images were acquired using a Syngene Gel-Doc system with InGenius 3 GENESys software.

Following sequences were optimized:

i. Keratin 5

HuKRT5-F1	CCAGGAGCTCATGAACACCA
HuKRT5-R1	GCTTCCACTGCTACCTCCG
HuKRT5-F2	GAGATCGCCACTTACCGCAA
HuKRT5-R2	ACACTGAGCCCACCACCTA

ii. Nanog

HuNANOG-F1	TGTGTTCTCTCCACCCAGC
HuNANOG-R1	AAAGGCTGGGGTAGGTAGGT
HuNANOG-F2	CACCCAGCTGTGTGTACTCA
HuNANOG-R2	TGGGGTAGGTAGGTGCTGAG

iii. cKIT

HucKIT-F1	GAAGGCTTCCGGATGCTCAG
HucKIT-R1	GTCTACCACGGGCTTCTGTC
HucKIT-F2	GCCCTGAACACGCACCTG
HucKIT-R2	CCGACAGAATTGATCCGCAC

iv. Amylase

HuAMY1A-F1	ACTTGTGGCAATGACTGGGT
HuAMY1A-R1	TCTCCAGAAATGACATCACAGT
HuAMY1A-F2	GACTGGGTCTGTGAACATCGA
HuAMY1A-R2	TGAGCTTTGCCATCATCAGA

v. Cystatin C

HuCST3-F1	AACCACGTGTACCAAGACCC
HuCST3-R1	GGGGTAAACACTTCCCAGCA
HuCST3-F2	CCTTCATGACCAGCCACAT
HuCST3-R2	CCCAGTCAGAGAAGGCACAG

- vi. E-Cadherin**
- | | |
|-----------|----------------------|
| HuCDH1-F1 | GACACCCGGGACAACGTTTA |
| HuCDH1-R1 | GGGTCAGTATCAGCCGCTTT |
| HuCDH1-F2 | GAAGGAGGCGGAGAAGAGGA |
| HuCDH1-R2 | AGAATCATAAGGCGGGGCTG |
- vii. Zona Occludin 1**
- | | |
|----------|-----------------------|
| HuZO1-F1 | ACAACAGCATCCTTCCACCT |
| HuZO1-R1 | GGATCTCCGGGAAGACACTTG |
| HuZO1-F2 | CGAAGGAGTTGAGCAGGAAA |
| HuZO1-R2 | AACACAGTTTGCTCCAACGA |
- viii. Claudin 1**
- | | |
|------------|----------------------|
| HuCLDN1-F1 | AATCTTTGTGGCCACCGTTG |
| HuCLDN1-R1 | CCAGTGAAGAGAGCCTGACC |
| HuCLDN1-F2 | TGGAAGACGATGAGGTGCAG |
| HuCLDN1-R2 | AAGGCAGAGAGAAGCAGCAG |
- ix. Smooth Muscle Actin**
- | | |
|----------|----------------------|
| HuSMA-F1 | GGCAAGTGATCACCATCGGA |
| HuSMA-R1 | GGAGCCACCGATCCAGACA |
| HuSMA-F2 | CCTGTTCCAGCCATCCTTCA |
| HuSMA-R2 | GCCACCGATCCAGACAGAG |
- x. CD10**
- | | |
|-----------|-------------------------|
| HuCD10-F1 | AAATTA CTTCTGGACTTGACCT |
| HuCD10-R1 | GAAGATCACCAAACCCGGCA |
| HuCD10-F2 | TCCTGGACTTGACCTAAATCACA |
| HuCD10-R2 | CCCGGCACTTCTTTTCTGGA |

xi.	p63	
	HuP63-F1	CTCTCCATGCCATCCACCTC
	HuP63-R1	AGGAGAATTCGTGGAGCTGC
	HuP63-F2	CCCACAGATTGCAGCATTGT
	HuP63-R2	GCAGGAGATGAGAAGGGGAG
xii.	Mucin 7	
	hMUC7-F1	GGCTAAAAGCAAGCAACTGG
	hMUC7-R1	TTGGGTGATTGGTGATGATG
	hMUC7-F2	CTGCACCAGGAGACATCAGA
	hMUC7-R2	CAGCGTTTGTGCAGACATTT
xiii.	MUC5B	
	hMUC5B-F1	CAACAGCCATGTGGACAACT
	hMUC5B-R1	CTCGCAGAAGGTGATGTTGA
	hMUC5B-F2	CTGAGGGTGGAGTCCATTTG
	hMUC5B-R2	GGGCCTCTGCTGAGTACTTG
xiv.	Cystatin 1	
	hCST1-F1	ACTTCGCCATCAGCGAGTAT
	hCST1-R1	GAAGGCACAGGTGTCCAAGT
	hCST1-F2	CAAGGCCACCAAAGATGACT
	hCST1-R2	TTGACACCTGGATTCACCA
xv.	Cystatin 5	
	hCST5-F1	CTTTGCCATCAGCGAGTACA
	hCST5-R1	ATCCTCCCAGGGAAC TTCAT
	hCST5-F2	GAAGTTCGGT CGAACCACAT
	hCST5-R2	GTGGGAGTAGGAGGTGGTCA

xvi. Aquaporin 5

HuAQP5-F1	CATCTTCGCCTCCACTGACT
HuAQP5-R1	TGGGGAAGAGCAGGTAGAAGT
HuAQP5-F2	TCCATTGGCCTGTCTGTCAC
HuAQP5-R2	CTTTGATGATGGCCACACGC
HuAQP5-F3	GGTGGAGCTGATTCTGACCT
HuAQP5-R3	CTCAGGGAGTTGGGGAAGAG
HuAQP5-F4	TCTACTTCACTGGCTGCTCC
HuAQP5-R4	GGTCAGCTCCATGGTCTTCT
HuAQP5-F5	ATGGTGGTGGAGCTGATTCT
HuAQP5-R5	CCCTACCCAGAAAACCCAGT

xvii. HE4

HE4-VOF	CCGACAACCTCAAGTGCTG
HE4-VOR	CGAGCTGGGGAAAGTTAATG

xviii. hOAZ1

hOAZ1-F1	CCAACGACAAGACGAGGATT
hOAZ1-R1	AGCGAACTCCAGGAGAACTG
hOAZ1-F2	AAACGCATTA ACTGGCGAAC
hOAZ1-R2	CGGTTCTTGTGGAAGCAAAT

2.5 HISTOLOGICAL ANALYSIS OF 3D MODEL

2.5.1 Fixing and Processing 3D Model

The fixing process ensured samples were dehydrated, cleared and ready for paraffin wax embedding. Samples were washed in PBS twice and placed directly into 3.7% formaldehyde for at least 24 hours at room temperature prior to histological processing. Samples were processed overnight using a Leica TP1020 benchtop tissue processor as shown in **Table 2.3**.

Samples were then bisected and embedded in molten paraffin wax using a Leica EG1160 embedding station and were embedded perpendicular to the bottom surface of the mould so that they could be cut in the correct orientation.

Pot	Time	Vacuum
1. MISS	MISS	MISS
2. 70% ethanol	15 mins	No
3. 70% ethanol	15 mins	No
4. 70% ethanol	15 mins	No
5. 95% ethanol	15 mins	No
6. 95% ethanol	15 mins	No
7. 100% ethanol	15 mins	No
8. 100% ethanol	15 mins	No
9. Xylene	15 mins	No
10. Xylene	15 mins	No
11. WAX	15 mins	No
12. WAX	15 mins	Yes

Table 2.3 Short processing run

2.5.2 Sectioning Blocks of the 3D Model

Samples embedded in wax blocks were cooled on ice for at least 20 minutes prior to sectioning using a Leica RM2235 microtome. 5 µm sections were cut, mounted onto SuperFrost®Plus slides and left to air dry. Before staining, the slides were heated in an oven to ensure the section was fully adhered to the slide.

2.5.3 Haematoxylin and Eosin (H&E) Staining

Samples were stained with haematoxylin and eosin using a linear staining machine (see **Table 2.4**), mounted with DPX and imaged using an Olympus BX51 microscope with Cell^D software (Olympus soft imaging solutions, GmbH, Münster, Germany).

Process	Solution	Duration
To remove the wax from the section	Xylene	45 seconds
	Xylene	45 seconds
	Xylene	45 seconds
To gradually rehydrate the section	100% Ethanol	45 seconds
	100% Ethanol	45 seconds
	95% Ethanol	45 seconds
	95% Ethanol	45 seconds
To stain basophilic parts of the section (cell nuclei)	Haematoxylin	45 seconds
	Haematoxylin	45 seconds
To wash off excess Haematoxylin	Running tap water	45 seconds
To differentiate the sample	1% Acid Alcohol	45 seconds
To wash off acidic alcohol	Running tap water	45 seconds
To increase the “blueing up” of the haematoxylin stain	Scott’s tap water	45 seconds
To wash off salt from Scott’s tap water substitute	Running tap water	45 seconds
To stain eosinophilic parts of the section	Eosin	45 seconds
To wash off excess eosin stain	Running tap water	45 seconds
To gradually dehydrate the sample	95% Ethanol	45 seconds
	95% Ethanol	45 seconds
	100% Ethanol	45 seconds
	100% Ethanol	45 seconds
Clearing	Xylene	45 seconds
	Xylene	45 seconds
	Xylene	45 seconds

Table 2.4 Haematoxylin and eosin staining procedure

2.5.4 Immunohistochemistry

Immunohistochemistry was performed on 5 µm sections. The same method was used for all antibodies apart from the antibody dilution, antigen retrieval step and blocking serum used (see **Table 2.5**).

Primary Antibody	Supplier (Cat. No)	Dilution in Serum	Serum	Antigen Retrieval
Monoclonal Mouse Anti-AMY1A, clone 2D4	Sigma (WH0000276M4)	1:300	Horse	Yes
Polyclonal Rabbit Anti-AQP5	Atlas Antibodies (HPA065008)	1:500	Goat	Yes
Polyclonal Rabbit Anti-BPIFA2	Eurogentec, Belgium	1:500	Goat	No
Polyclonal Rabbit Anti-Human CD117, ckit	Dako (A4502)	1:100	Goat	Yes
Monoclonal Mouse Anti-Human Cytokeratin 5, Clone XM26	Vector (VP-C400)	1:100	Horse	Yes
Monoclonal Rabbit Anti-Cytokeratin 7, EPR17078	Abcam (ab181598)	1:500	Goat	Yes
Polyclonal Rabbit Anti-Mucin 5B	Santa Cruz (H-300)	1:500	Goat	Yes
Monoclonal Mouse Anti-Human MUC7, Clone 4D2-1D7	Novusbio (NBP2-50391)	1:500	Horse	Yes
Polyclonal Goat Anti-ZO1 tight junction protein antibody – C-terminal	Abcam (ab190085)	1:500	Rabbit	No
Monoclonal Rabbit Anti-E-Cadherin, EP700Y – Intercellular Junction Marker	Abcam (ab40772)	1:500	Goat	No
Monoclonal Mouse Anti-Human Smooth Muscle Actin, Clone 1A4	Dako (M0851)	1:50	Horse	Yes
Monoclonal Mouse Anti-Vimentin, Clone V9	Dako (M0725)	1:100	Horse	Yes

Table 2.5 Primary antibodies, suppliers, dilutions, serum, and antigen retrieval.

Slides were de-waxed twice for 5 minutes in xylene and rehydrated twice for 5 minutes in absolute ethanol. Endogenous peroxidase activity was neutralised with 3% hydrogen peroxide in methanol for 20 minutes. Slides were then rinsed briefly for 5 minutes in PBS. Antigen retrieval was performed at this point (if needed), using 0.01 M sodium citrate buffer. The slides were submerged in the buffer, microwaved on medium heat for 8 minutes and rinsed for 5 minutes in stirring PBS. The slides were blocked against non-specific binding with 100% normal serum for 30 minutes at room temperature. The normal serum used was dependent upon the animal used to raise the secondary antibody. The primary antibody was diluted in the same blocking serum (**Table 2.5**), and slides incubated overnight at 4°C.

The slides were washed twice for 5 minutes in PBS, and a Vectastain® Elite ABC kit (Vector labs, Peterborough, UK) used according to manufacturer's instructions. Following two 5 minutes washes in PBS, the DAB solution, made according to manufacturer's instructions (Vector Labs, Peterborough UK), was added to the slides and left for 10 minutes. Slides were washed for 5 minutes in distilled water and counter-stained with haematoxylin using a Leica ST4020 staining machine (see **Table 2.6**) before dehydrating, mounting with DPX and coverslipping. The slides were imaged using an Olympus BX51 microscope with Cell[^]D software (Olympus soft imaging solutions, GmbH, Münster, Germany).

Process	Solution	Duration
To stain basophilic parts of the section (cell nuclei)	Haematoxylin	30 seconds
	Haematoxylin	30 seconds
To wash off excess Haematoxylin	Running tap water	30 seconds
To differentiate the sample	1% Acid Alcohol	30 seconds
To wash off acidic alcohol	Running tap water	30 seconds
To increase the “blueing up” of the haematoxylin stain	Scott’s tap water	30 seconds
To wash off salt from Scott’s tap water substitute	Running tap water	30 seconds
To gradually dehydrate the sample	95% Ethanol	30 seconds
	95% Ethanol	30 seconds
	100% Ethanol	30 seconds
	100% Ethanol	30 seconds
Clearing	Xylene	30 seconds
	Xylene	30 seconds
	Xylene	30 seconds

Table 2.6 Haematoxylin staining procedure

2.6 IMMUNOFLUORESCENCE STAINING

2.6.1 Sample preparation

A specific serum, dependent on the animal used for secondary antibody production, was diluted 1:10 in PBS with 0.5% (v/v) Triton X100 and used for permeabilisation and blocking buffer. For dual immunocytochemistry, the primary antibody solution was prepared by adding both antibodies in permeabilisation/blocking buffer using dilutions given in the **Table 2.7**. Then, two secondary antibodies specific for either mouse or rabbit primary antibodies but both raised in Goat were used (see **Table 2.8**).

Primary antibody	Supplier (Cat. No)	Dilution	Serum for Buffer
Monoclonal Mouse Anti-Human Cytokeratin 5, Clone XM26	Vector (VP-C400)	1:100	Goat
Monoclonal Mouse Anti-AMY1A, clone 2D4	Sigma (WH0000276M4)	1:300	Goat
Polyclonal Rabbit Anti-AQP5	Atlas Antibodies (HPA065008)	1:500	Goat
Polyclonal Rabbit Anti-BPIFA2	Eurogentec, Belgium	1:500	Goat
Monoclonal Rabbit Anti-Cytokeratin 7, EPR17078	Abcam (ab181598)	1:500	Goat
Monoclonal Rabbit Anti-E-Cadherin, EP700Y – Intercellular Junction Marker	Abcam (ab40772)	1:500	Goat

Table 2.7 Preparation of primary antibodies

Secondary antibody	Dilution	Target primary antibody
Alexa Fluor 488 Goat anti-rabbit Ab. Cat No- A11011. (Green)	1:200	AQP5, CK7, BPIFA2, E-cadherin
Alexa Fluor 568 Goat anti-mouse Ab. Cat No- A11001. (Red)	1:200	CK5, AMY

Table 2.8 Preparation of secondary antibody.

2.6.2 Transwell Fixation

The medium from the basal compartment was aspirated and the apical surface of transwell membrane was washed with PBS three times. 500 μ L of 100% ice-cold methanol was added to the apical side and 1 mL to the basal compartment and left at 4°C for 20 minutes. The transwells were washed three times with PBS, 500 μ L of PBS added to the apical chamber and 1 mL to basal compartment before storing at 4°C prior to the next step, but for no longer than 1 week.

2.6.3 Immunostaining

PBS was aspirated from both compartments before adding 300 μ L of permeabilisation buffer to the apical surface. The plate was then placed on a shaker at 80 rpm for 1 hour at room temperature. The permeabilisation buffer was aspirated from the apical surface, which was washed once with PBS before adding 300 μ L of primary antibody solution. The plate was again placed on a shaker at 80 rpm at 4°C overnight. The primary antibody solution was aspirated from the apical surface, which was washed twice with PBS and 300 μ L of secondary antibody solution added. The plate was wrapped with aluminium foil and placed on a shaker at 80 rpm for 1 hour at room temperature. The secondary antibody solution was aspirated and the apical surface washed twice with PBS in the dark or low light. The membrane was cut from its plastic scaffold using a scalpel, held carefully with forceps and placed cell side up on a microscope slide. A drop of DAPI mounting medium (Vector, H-1200) was added and left for 2 minutes before covering with a glass coverslip, which was sealed with nail polish and left it at room temperature to harden. Slides were stored at 4°C prior to analysis using a confocal microscope (Nikon A1+, Surrey, UK).

2.7 CONFOCAL MICROSCOPY

Confocal microscope Nikon A1+ was used for imaging SG organoid samples. For start-up, all the power to the microscope (motorized stage, piezo Z stage, halogen lamp, mercury lamp, control box A, laser, and controller) were turned on. Then, the PC was started by switching the POWER button and NIS-Elements software was run.

The slide was placed on the microscope stage and sample was observed through the microscope starting with low magnification (x10 magnification lens).

Image acquisition conditions were determined by following steps:

- i. The 'Remove Interlock' button was clicked to reset blinking and enable laser oscillation with the software.
- ii. The laser and channel to be used (DAPI, Alexa 488 and Alexa 568) were selected.

- iii. The 'Scan' button was clicked and then laser power and HV (detector sensitivity) were adjusted while checking the image. Offset "0" was used as the standard setting and adjusted to balance the background image. The 'Pixel saturation indication' button on the Lookup Table (LUTs) tab was used during adjustment to control oversaturated or undersaturated pixels.
- iv. The number of pixels necessary for resolution was set (for example pixel dwell was 12.1, and size was 512 x 512). Pixel dwell indicates laser application time per pixel, thus the larger the value the brighter the image that can be acquired.
- v. Then, the 'Capture' button was clicked to acquire an image and the image was saved in nd2 file format.
- vi. For z-stack images, the Capture Z-Series tab was opened and the 'Defined top & bottom' button was clicked. Then, the 'Scan' button was clicked and the focus knob of the microscope was moved while checking the image, and then the 'Top' or 'Bottom' button was clicked to determine the position. The top position was determined when the focus knob was moved in the direction where the value of the plane in the cube increases, whilst opposite for bottom position. Next, the number of 'Step' required was determined and then 'Run now' button was clicked to acquire z-stack images. The images were saved in nd2 file format.

Fiji (ImageJ) software was used to analyse the z-stack images.

CHAPTER 3

Establishment of *In Vitro* Models of Human Salivary Gland

CHAPTER 3: ESTABLISHMENT OF IN VITRO MODELS OF HUMAN SALIVARY GLAND

3.1 INTRODUCTION

At present, without a reproducible, *in vitro* human, salivary gland, model, it is not possible to fully investigate the development of a number of salivary gland disorders such as tumour development, Sjogren's syndrome or viral-associated infections. Radiotherapy for head and neck cancer, and chemotherapy for non-oral cancers, can lead to salivary gland damage, reduced salivary flow, xerostomia and a worst-case scenario of severe, debilitating mucositis with potentially life-threatening systemic infections (Feng *et al.*, 2009; Chan *et al.*, 2011; Pradhan-Bhatt *et al.*, 2014; Jang *et al.*, 2015). Salivary epithelium is eventually replaced by non-secretory tissue and thus loses its secretory ability. This results in numerous clinical problems including infections of the mucosa and teeth, impaired speech, difficulty in swallowing, and so greatly impacts on the patient's quality of life (Feng *et al.*, 2009; Chan *et al.*, 2011). Around 300,000 to 500,000 patients worldwide develop xerostomia due to radiation therapy annually (Vokes *et al.*, 1993).

Currently, the administration of saliva substitutes and sialogogues is the only treatment available to these patients. However, such medications have only transient effects and must be frequently administered (Joraku *et al.*, 2005; Nelson, Manzella and Baker, 2013). Therefore, the introduction of tissue engineering to this field and the creation of an artificial salivary gland is the ultimate solution for such patients.

The tools presently available to try to elucidate the basis of disease, or to develop artificial, replacement glands, are either *in vivo* models or monolayer cultures of cells. However, there are limitations using these; one of the problems associated with the use of animal models in the study of human disease is the extrapolation of results from the animal to the human situation; while monolayer cultures of cells do not faithfully replicate the cell of origin. Thus, the use of primary cells represents the best option for the investigation of the disease process and also for the creation of an artificial salivary gland because they more closely resemble native tissue.

Salivary glands consist of three major glands the parotid, sublingual and submandibular gland (Patel and Hoffman, 2014). Salivary glands are exocrine organs which are responsible for the secretion of saliva, a fluid that contains digestive enzymes, growth factors, lubricating mucins and antimicrobial agents. This is critical for the maintenance of oral health, for mastication, the onset of the digestion process and swallowing, for speech and general comfort (Chan *et al.*, 2011). The main types of cells found in salivary glands are acinar, ductal and myoepithelial cells (Chan *et al.*, 2010) and specific cell markers for these cell types will be used in this study.

A previous study demonstrated that when the HSG submandibular salivary gland cells were cultured in Matrigel, they were able to produce 3D acinar-like cells (Maria *et al.*, 2011). Chan *et al.*, 2011 demonstrated that human parotid gland acinar cells will spontaneously grow as either 3D or 2D clusters and that the protein expression pattern between these two cell types is different. Studies using lung derived cells, indicated that the choice of basement membrane or matrix protein used as a surface for cell growth can have a dramatic impact on the phenotype and function of the cells as well as influencing the growth of spherical organoids with an acinar-like structure that mimics the minor mucosal glands (Finkbeiner *et al.*, 2010; Wu *et al.*, 2011).

The primary aim of this study was to develop an *in vitro* model of human salivary glands. In order to do this, we optimised the growth conditions necessary for salivary gland cells to grow and replicate *in vitro* in a similar manner to that *in vivo*. Furthermore, we wanted to verify the phenotypic and functional characteristics of the cultures to ensure they resembled as closely as possible the *in vivo* situation by investigating the expression of cell specific markers.

This chapter will describe our preliminary study investigating the culture conditions for the development of an *in vitro* model of human salivary glands using HTB41 cells. HTB41 is a mucoepidermoid carcinoma cell line originating from a human submandibular gland. The cells were grown as a 3D model in polyethylene

terephthalate (PET) transwell inserts and on Alvetex® Scaffold. The PET transwell inserts have previously been used, successfully, for a variety of applications including air-liquid interface models. The microporous, permeable membranes of the insert allow the diffusion of media components to both the apical and basolateral cell surfaces thus mimicking the *in vivo* situation, helping to promote differentiation of epithelial cells *in vitro*. The Alvetex® Scaffold is made from a highly porous polystyrene scaffold designed for 3D cell culture (Knight *et al.*, 2011). Cells grown in the scaffold retain their natural tissue-like structure and do not flatten as is seen in conventional 2D cell cultures. This enables them to maintain their *in vivo* morphology and physiology within an *in vitro* model system.

The scaffolds were either coated with extracellular matrices (ECM) such as collagen type 1, fibronectin, poly-L-Lysine, and Matrigel or were used as produced by the manufacturers. The cells were submerged in culture media (non-ALI) or grown at an air-liquid interface (ALI), and either placed on a shaker to mimic a dynamic condition or grown under static conditions. Immunohistochemistry and RT-PCR were used to determine the expression of specific cell markers.

The knowledge gained from our preliminary 3D culture studies using HTB-41 cells was transferred to optimise the growth of normal human salivary gland cells isolated from all three major salivary glands. As with the HTB41 cells, primary cells were characterized by RT-PCR and IHC but also through immunofluorescent confocal microscopy.

3.2 AIMS

Two specific objectives in this chapter are:

1. To determine the optimal culture conditions for the development of *in vitro* models of human salivary glands using HTB41 cells and to investigate the expression of specific cell markers by RT-PCR and immunohistochemistry.
2. To determine the optimum method for the isolation of normal human salivary gland cells from normal major gland tissue, to establish 3D models and to investigate the expression of specific cell-type markers.

3.3 MATERIALS AND METHODS

3.3.1 Cell culture

Cells were grown and maintained as previously described (**Refer 2.2**).

3.3.2 Preparation of Extracellular Matrices (ECM)

Rat-tail collagen I (BD Biosciences, 354236) was diluted to a concentration of 0.8 mg/mL using cell culture grade water and handled on ice using pre-chilled pipette tips to perform the dilution and subsequent application. Fibronectin (BD Biosciences, 356008) was reconstituted to a concentration of 0.5 mg/mL using PBS. Matrigel™ (BD Biosciences, 356234; pre-thawed overnight on ice) was diluted to a concentration of 0.8 mg/mL using appropriate cell culture media and handled on ice using pre-chilled pipette tips to perform the dilution and subsequent application. Poly-L-Lysine (Sigma-Aldrich, P4707) was used directly without prior dilution.

3.3.3 Coating Alvetex® Scaffold with ECM

The same method of coating Alvetex® Scaffold (Alvetex Regenerate, AVP005) was used for all four ECM.

Alvetex® Scaffold was pre-treated with 70% ethanol followed by two PBS washes before coating. The Alvetex® Scaffold was left in the second PBS wash until the ECM solutions were ready to be applied. Immediately after aspirating the second PBS wash 500 µL of ECM solution, prepared as described above, was carefully pipetted onto each disc in a 12-well plate. The plate was left to stand for 3 hours in the incubator at 37°C. Excess fluid was removed by gentle aspiration from the edge of the wells. 0.5×10^6 cells in 50 µL of the appropriate culture media were seeded directly onto each wet ECM-coated membrane. The cells were allowed to settle for 30 minutes in the incubator with 5% CO₂ at 37°C before flooding with 4 mL of media per disc.

3.3.4 Coating PET Transwells with ECM

The same method for all four ECM was used to coat PET transwells (BD Falcon, 353180). 500 µl of ECM solution was pipetted onto each transwell in a 12-well plate. The plate was left to stand for 3 hours in the incubator at 37°C. Excess ECM solution was aspirated from the edge of the transwell which was then allowed to air dry for at least 5 minutes. The transwell was washed twice with PBS and left to air dry before 0.5×10^6 cells in 50µl were seeded per transwell. The cells were allowed to settle for 30 minutes in the incubator with 5% CO₂ at 37°C before flooding with 600 µl of media on the top and 2 mL of media at the bottom of each well.

3.3.5 Human Primary Cell Isolation

3.3.5.1 Human salivary gland collection

Salivary gland tissue (HuSG) was obtained from consenting patients (with full ethical approval by the North of Scotland Research Ethics Committee 2, REC reference: 13/NS/0120) during routine surgery. Typically, a 20 to 30 mm² piece of tissue was collected in a sterile tube containing PBS supplemented with 100 i.u./mL penicillin and 100 µg/mL streptomycin and stored at 4°C before processing.

3.3.5.2 Human salivary gland processing

Under a dissecting microscope, HuSG tissue was placed in a small petri dish in PBS supplemented with 2% Penicillin/Streptomycin. The adherent tissues, blood vessels or debris were removed and cleaned from the tissue. This step was performed by grasping the proximal end of the tissue with small forceps and stripping off adherent tissues with a second pair of forceps. The cleaned HuSG was placed in a new petri dish and washed three times in PBS supplemented with 2% Penicillin/Streptomycin. A portion of the HuSG tissue was fixed in formalin for histology with a further portion being placed in TRI-reagent for RNA isolation; this provided a positive control for downstream experiments. In a tissue culture hood, the remaining HuSG was mechanically minced using sterile curved dissection scissors until it gave the appearance of a slurry or thick paste.

3.3.5.3 Tissue explant technique

A portion of minced tissue (cut into approximately 1mm sized fragments) was collected, plated into a T75 flask in KGM medium. The cells were incubated at 37°C in 5% CO₂.

3.3.5.4 Human salivary gland isolation using Pronase

A portion of minced tissue was collected into a 15 mL tube of freshly made 0.15% (w/v) pronase (3-5 mL), using a further 1 mL of pronase and a Pasteur pipette. The pronase solution completely covered all of the tissue. The tube was mixed gently and incubated at 4°C overnight (18-24h) in an upright position.

On the second day, the HuSG in pronase was gently inverted 10 times and left to warm at room temperature for 10 minutes. Warm FBS was added to a final concentration of 10% and the tube gently inverted 20 times. The solution was filtered through a 70 µm cell strainer into a 50 mL Falcon tube. HBBS buffer was used to wash any remaining cells which were then also filtered. The filtrate was transferred into 15 mL tubes and centrifuged at 15,000 rpm for 10 minutes. The supernatant was discarded and the cells resuspended in 2 mL of KGM medium.

The cells were counted with a haemocytometer and plated in 35 mm petri dish with seeding density 0.2×10^6 cells/dish, incubated at 37°C, 5% CO₂ overnight. The supernatant containing floating aggregates of cells was then transferred to a second petri dish. Media was changed every 2 to 3 days.

3.3.5.5 Human salivary gland isolation using 0.1% Trypsin

A portion of minced tissue was collected into 0.1% trypsin in F-12 medium and incubated in a water bath for 1 hour; shaken vigorously every 15 minutes. The cells were collected by centrifugation at 15,000 rpm for 5 minutes. Supernatant was discarded and the cells were resuspended in 10 mL of cold DMEM supplemented with 10% FBS. The cells were collected by centrifugation at 15,000 rpm for 5 minutes. Supernatant was discarded and the resulting cell pellet was resuspended in 10 mL of KGM medium.

The cell suspension was filtered through a 70 µm cell strainer placed over a 50 mL Falcon tube. The filtrate was transferred into 15 mL tubes and centrifuged at 15,000 rpm for 10 minutes. Supernatant was discarded and the cells were resuspended in 2 mL of KGM medium. The cells were counted with a haemocytometer and plated in 35 mm petri dish with seeding density 0.2×10^6 cells/dish, incubated at 37°C, 5% CO₂ overnight. The supernatant containing floating aggregates of cells was then transferred into a second petri dish and the media changed every 2 to 3 days.

3.3.6 Cell Characterisation of HuSG From Explant Tissues

Cell suspensions were prepared and diluted in culture media to a cell density of 1×10^5 cells/ml. The samples were kept on ice prior to preparing a cytospin with 100 µl of each sample. Each slide was examined under the microscope to ensure the cells had adhered properly and were lying flat on the slide. The samples were fixed with 100% ice-cold methanol for immunostaining.

3.3.7 Culturing 3D *in vitro* Model

HTB41 and HuSG cells, were cultured in four different ECM, coated onto two different scaffolds to investigate any phenotypic difference under these different three-dimensional culture conditions (see **Figure 3.1**). Three independent batches were carried out for each culture model.

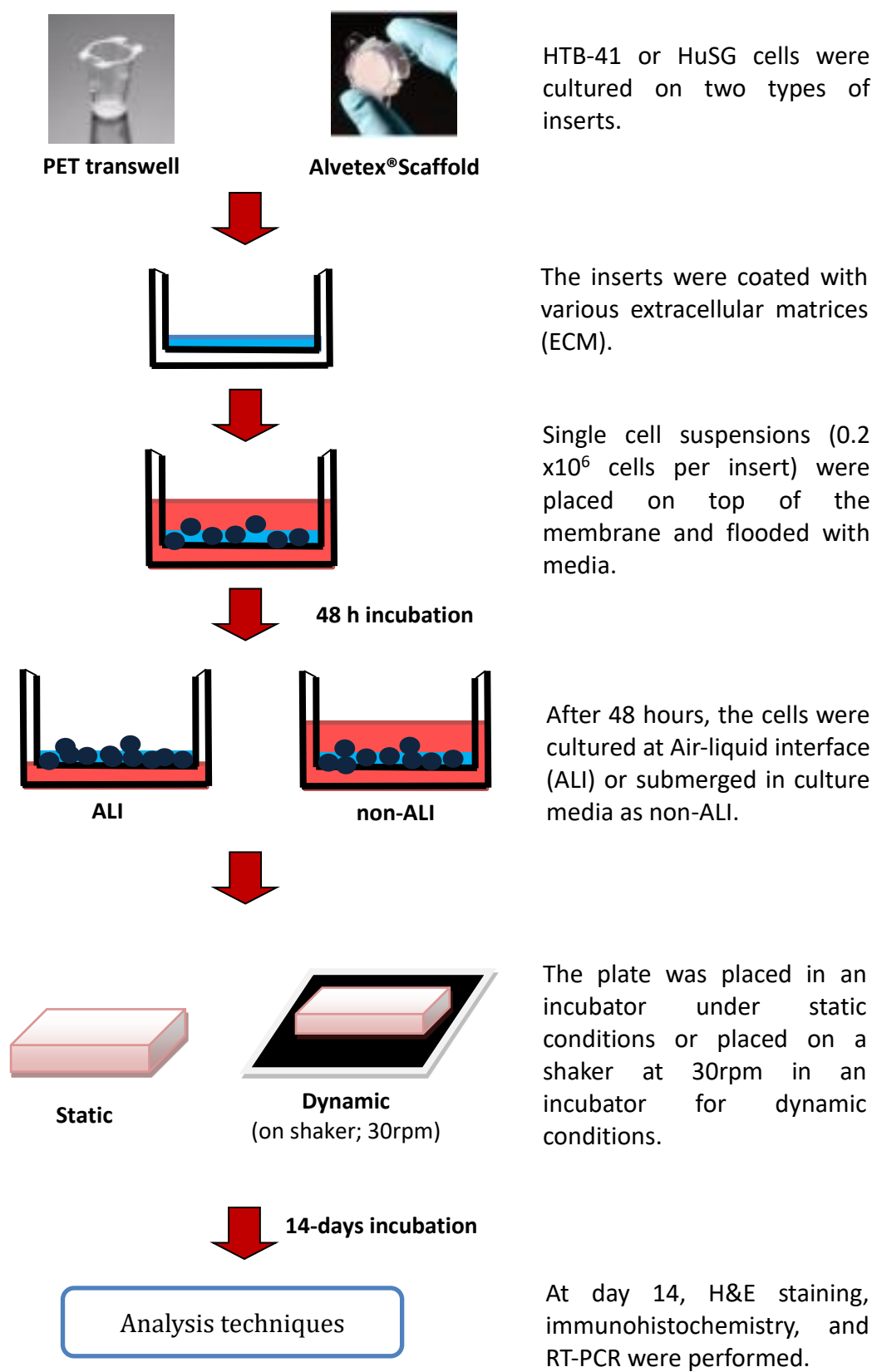
The PET transwell/Alvetex^(R)Scaffolds were divided into two 12-well plates with one plate of 4 PET transwell/Alvetex^(R)Scaffolds put on a shaker and another plate of 4 PET transwell/Alvetex^(R)Scaffolds put beside the shaker, both were in the same incubator. For each plate, 2 of the PET transwell/Alvetex^(R)Scaffolds were cultured at an air-liquid interface (ALI) and two submerged in culture medium (non-ALI).

After 48 hours, when the cells had reached confluence, PET transwell for ALI, had the media on the top of the transwell aspirated and 2 mL of fresh media added to the bottom. For non-ALI cultures, both the media at the top and the bottom of the transwell was replaced with fresh media (600 µL of media on the top and 2 mL of media at the bottom per well). For Alvetex^(R)Scaffolds, the media was aspirated and

replaced with 1.6 mL of fresh media for ALI scaffolds and 4 mL of fresh media for non-ALI scaffolds. The media was changed three times per week for 2 weeks. On day 14, one scaffold from each experiment was fixed for histology and one used for RNA isolation.

3.3.8 Analysis techniques

- H&E staining was performed on human salivary gland tissue and models sectioned for phenotypic assessment (**Refer 2.5**).
- Immunohistochemistry was performed on human salivary gland tissue and models sectioned to investigate protein expression of specific cell markers (**Refer 2.5.4**).
- RT-PCR was used for subjective analysis of mRNA expression (**Refer 2.4**). Eight primer pair sequences, previously optimised, were used to assess gene expression (**Refer Table 3.1**).
- Immunofluorescence staining was used for HuSG cell characterisation (**Refer 2.6**).



HTB-41 or HuSG cells were cultured on two types of inserts.

The inserts were coated with various extracellular matrices (ECM).

Single cell suspensions (0.2×10^6 cells per insert) were placed on top of the membrane and flooded with media.

After 48 hours, the cells were cultured at Air-liquid interface (ALI) or submerged in culture media as non-ALI.

The plate was placed in an incubator under static conditions or placed on a shaker at 30rpm in an incubator for dynamic conditions.

At day 14, H&E staining, immunohistochemistry, and RT-PCR were performed.

Figure 3. 1 Overview of culturing 3D *in vitro* model of human salivary glands by using HTB-41 cells

3.4 RESULTS

3.4.1 HTB41 Cell Line in 3D Culture Systems

Preliminary experiments were carried out using the mucoepidermoid carcinoma cell line, HTB41. This is a cell of submandibular gland origin. The cells were grown on different scaffold structures, including PET and Alvetex® Scaffold, coated with collagen, fibronectin, poly-L-lysine or Matrigel. These were either cultured at an air-liquid interface (ALI) or submerged in tissue culture medium (non-ALI), and both were either placed on a shaker (dynamic conditions) or directly in the same incubator (static conditions).

Haematoxylin and eosin stained sections showed significant variation in cellular organization and tissue development (**Figure 3.2**). After 14 days in culture, the cells grown on PET, either at an ALI or non-ALI, grew as multilayer cultures with different phenotypes. Cells grown at an ALI exhibited greater differences in the appearance of the cells, inferring greater differentiation and phenotypic differences, compared to those grown under non-ALI conditions, regardless of whether the PET was coated with ECM or not and regardless of the type of matrix used. Considering all culture conditions, it was apparent that growth was better (more marked) under dynamic rather than static conditions, although there was some difference between the different matrices used, and between ALI vs. non-ALI. Overall collagen-coated PET, at an ALI and with gentle agitation of the cultures (dynamic conditions) gave the greatest number of phenotypically distinct cell-types according to histological appearance (**Figure 3.2**).

The cells grown on Alvetex® Scaffolds were significantly different if grown at an ALI in comparison to those grown submerged in culture medium. The cells grew into the scaffold and formed structures at an ALI whilst non-ALI cultures did not appear to thrive. Comparing growth on the different matrices, the cells grew well on collagen-coated scaffolds at an ALI, however, unlike the cells growing on PET, they grew better and expanded more, under static rather than dynamic conditions (**Figure 3.3**).

For both scaffolds, collagen provided the best matrix for cell growth. Interestingly, the most effective growth condition for the PET inserts was at an ALI under dynamic conditions whilst the cells on Alvetex® Scaffolds, preferred to grow at an ALI under static conditions.

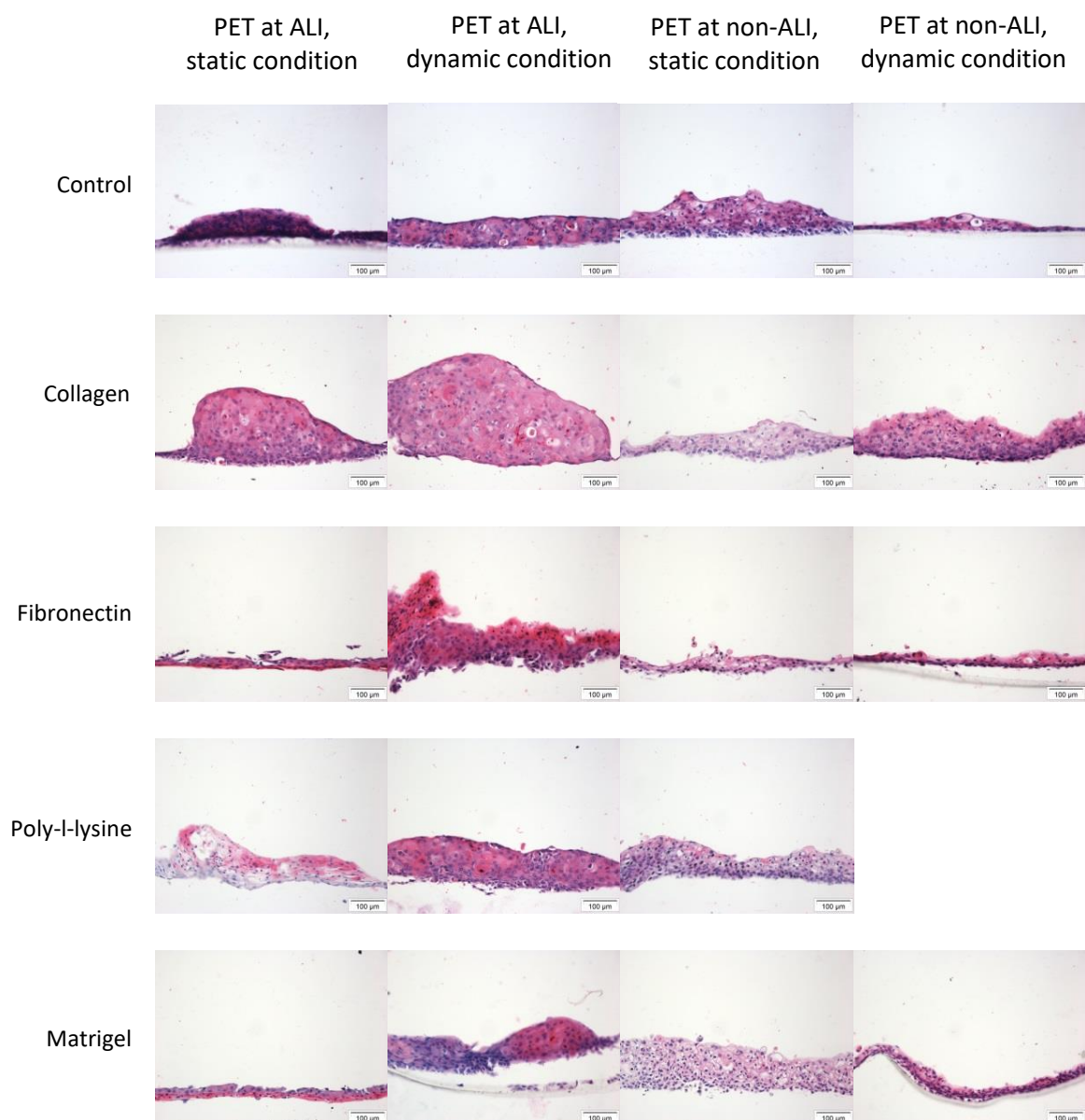


Figure 3. 2 Haematoxylin and eosin stained sections of 3D *in vitro* models of HTB41 cell line cultured on PET transwell with or without ECM coating, at ALI and non-ALI, under static or dynamic culture conditions at 14 days of culture show a number of different phenotypes present. Representation of three independent batches. Scale bar=100 μ m.

HE stained section of HTB41 cell line cultured on PET transwell with poly-l-lysine-coated at non-ALI under dynamic condition is missing.

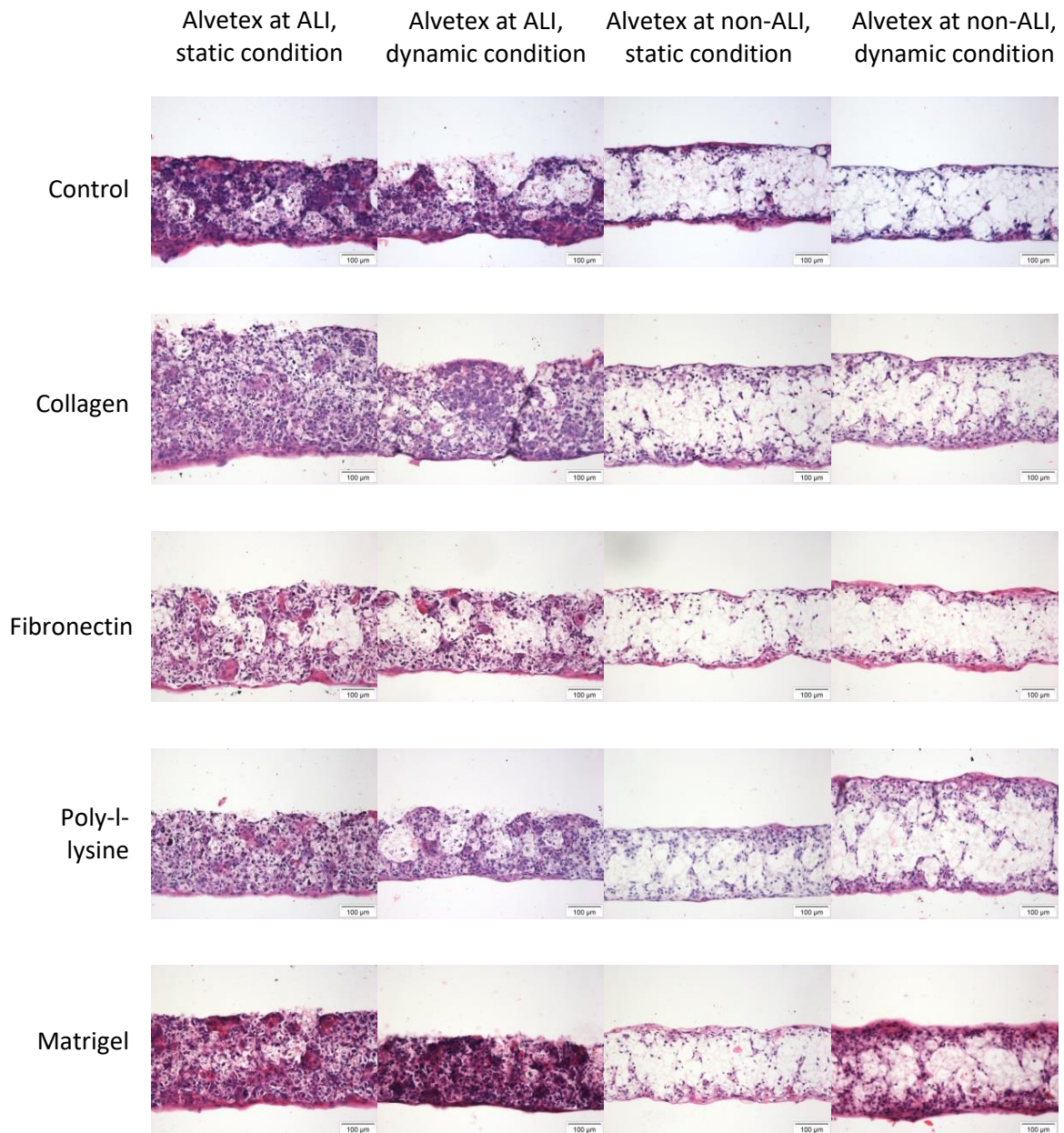


Figure 3. 3 Haematoxylin and eosin stained sections of 3D *in vitro* models of HTB41 cell line cultured on Alvetex® scaffold with or without ECM coating, at ALI and non-ALI, under static or dynamic culture conditions at 14 days of culture show a number of different phenotypes present. Representation of three independent batches. Scale bar=100 µm.

3.4.2 Immunohistochemistry of HTB41 Cultures

Four antibodies were used to identify cell type specific proteins by HTB41 cells under varying culture conditions. Amylase and BPIFA2 are serous, acinar cell markers, cKIT a progenitor cell marker and MUC5B a marker for mucous acinar cells.

Positive amylase staining was seen in only a very few cells cultured on collagen-coated PET inserts at ALI under dynamic conditions and also on Alvetex® Scaffolds at both ALI and non-ALI under dynamic conditions (**Figure 3.4**). This suggested that these cells showed some similarity to serous acinar cells, expressing cell-specific proteins.

Membranous cKIT staining (brown) was demonstrated on cells cultured on collagen-coated PET at ALI under static conditions, at non-ALI under dynamic conditions and also on Alvetex at ALI under dynamic conditions (**Figure 3.5**). Positive staining of cKIT also appeared in cells cultured on fibronectin-coated Alvetex at ALI under both static and dynamic conditions (**Figure 3.6**).

BPIFA2 was expressed in a small number of the cells cultured on static, fibronectin-coated PET at ALI and at non-ALI under dynamic conditions (**Figure 3.7**). Positive brown staining of BPIFA2 was also found on cells cultured on static matrigel-coated PET at ALI and non-ALI, and on Alvetex at ALI under static conditions (**Figure 3.8**). There was no evidence of any positive staining for MUC5B in any of the HTB-41 cultures.

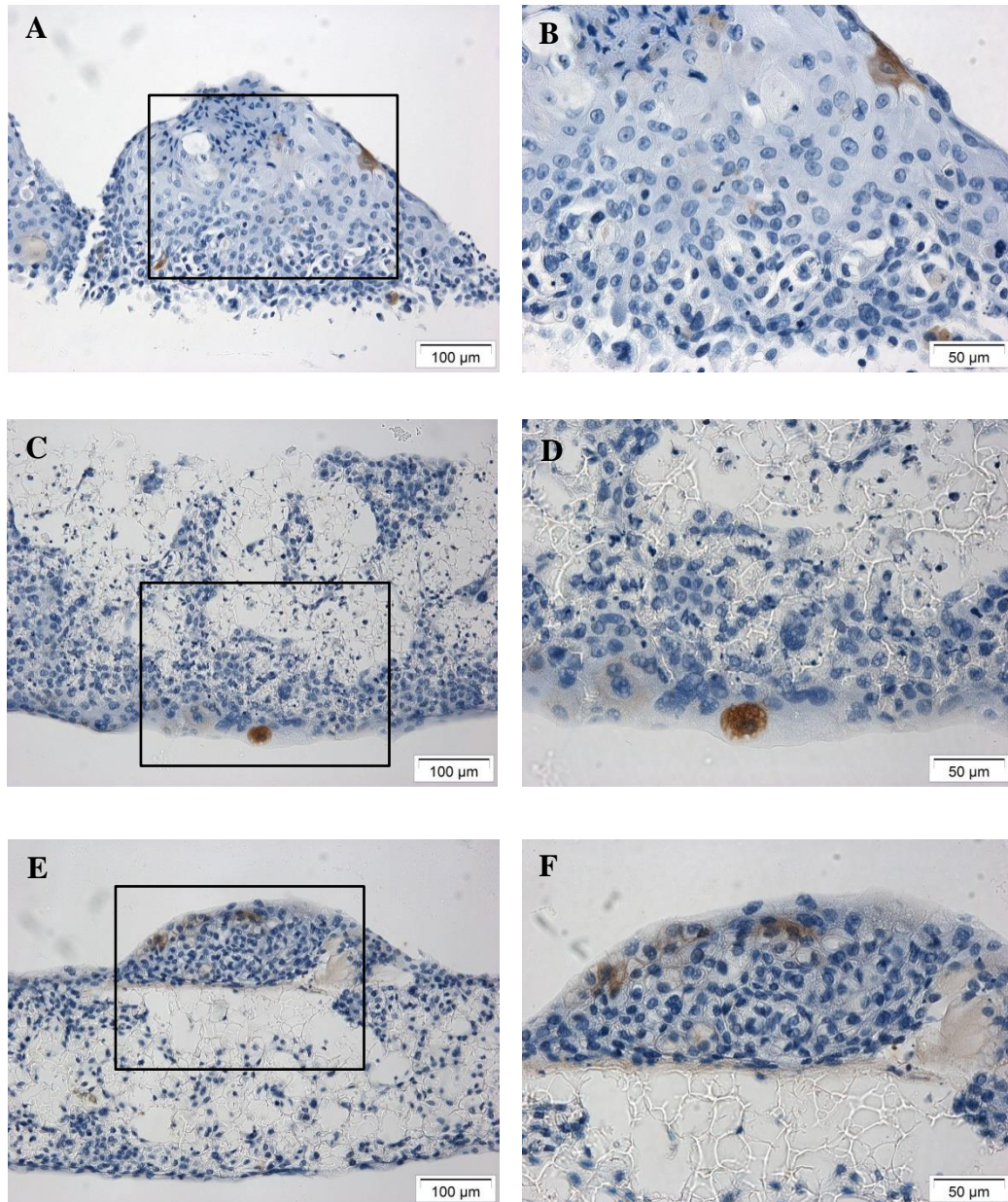


Figure 3.4 Positive immunohistochemistry staining of 3D *in vitro* models of HTB41 cells. (A, B) **amylose** staining on **collagen**-coated PET at ALI under dynamic conditions, (C, D) Alvetex at ALI under dynamic conditions, and (E, F) Alvetex at non-ALI under dynamic conditions. 20X and 40X magnification, 100 μ m and 50 μ m scale bars, respectively.

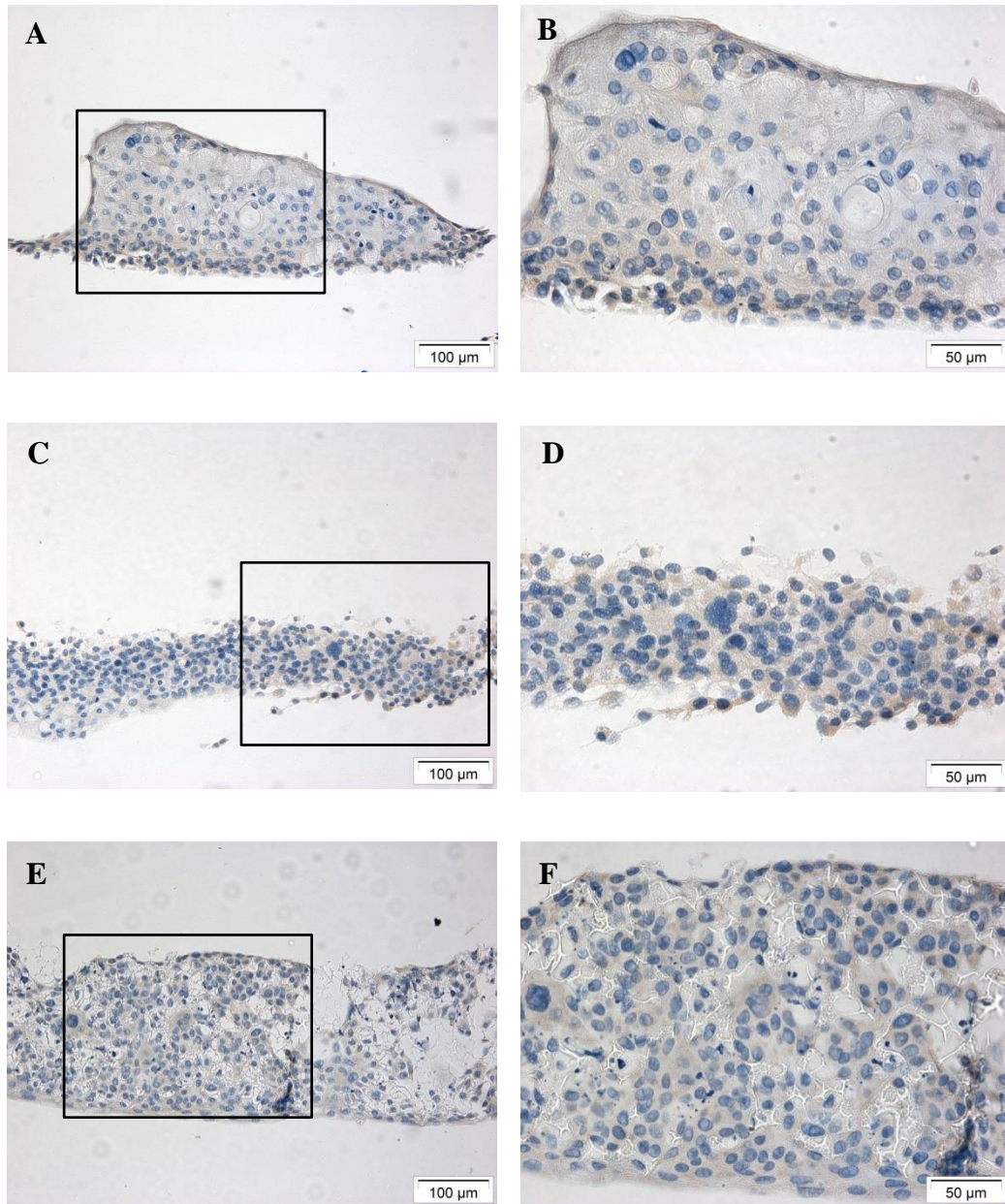


Figure 3.5 Positive immunohistochemistry staining of 3D *in vitro* models of HTB41 cells. (A, B) **cKIT** on **collagen**-coated PET at ALI under static conditions, (C, D) PET at non-ALI under dynamic conditions, and (E, F) Alvetex at ALI under dynamic conditions. 20X and 40X magnification, 100μm and 50μm scale bars, respectively.

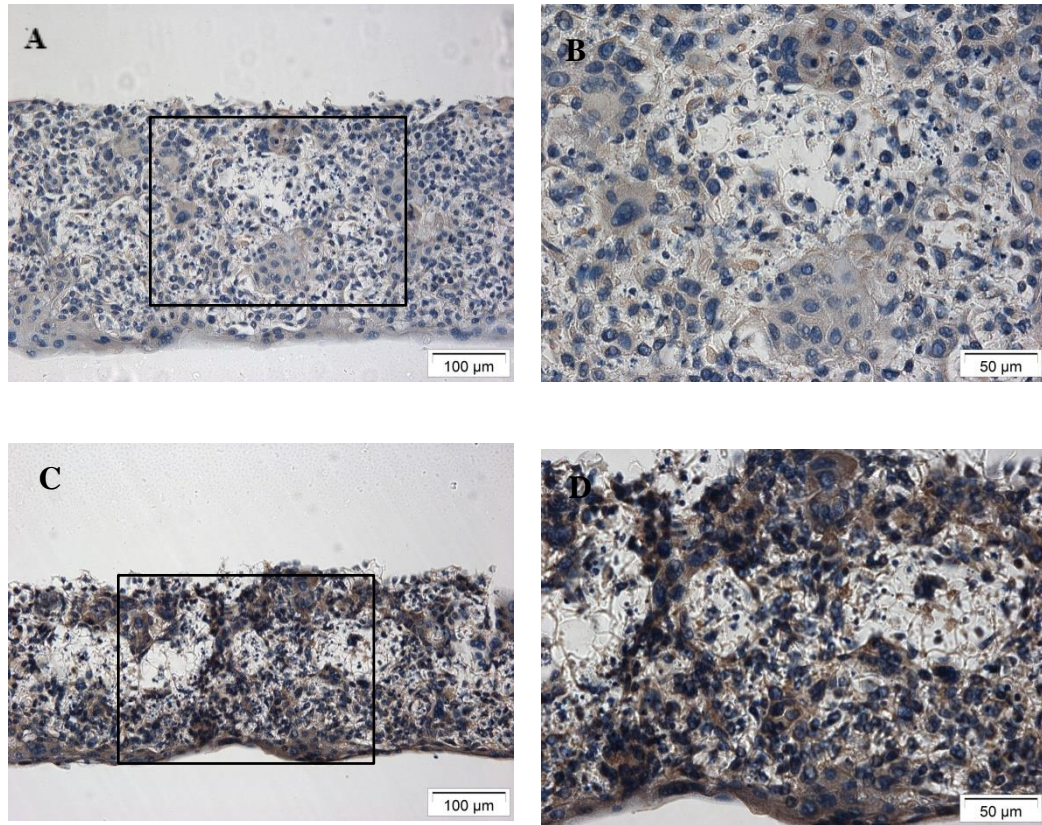


Figure 3. 6 Positive immunohistochemistry staining of 3D *in vitro* models of HTB41 cells. (A, B) **cKIT** on **fibronectin**-coated Alvetex at ALI under static conditions and (C, D) Alvetex at ALI under dynamic conditions. 20X and 40X magnification, 100μm and 50μm scale bars, respectively.

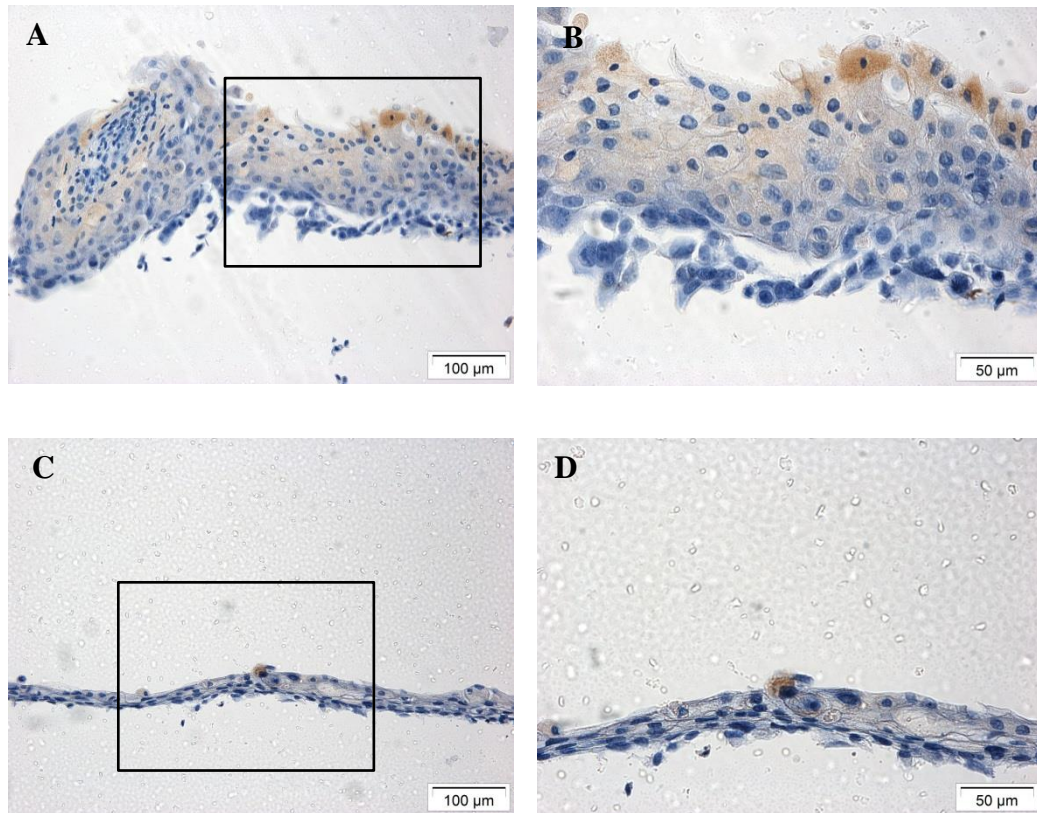


Figure 3. 7 Positive immunohistochemistry staining of 3D *in vitro* models of HTB41 cells. (A, B) **BPIFA2** on **fibronectin**-coated PET at ALI under static conditions and (C, D) PET at non-ALI under dynamic conditions. 20X and 40X magnification, 100μm and 50μm scale bars, respectively.

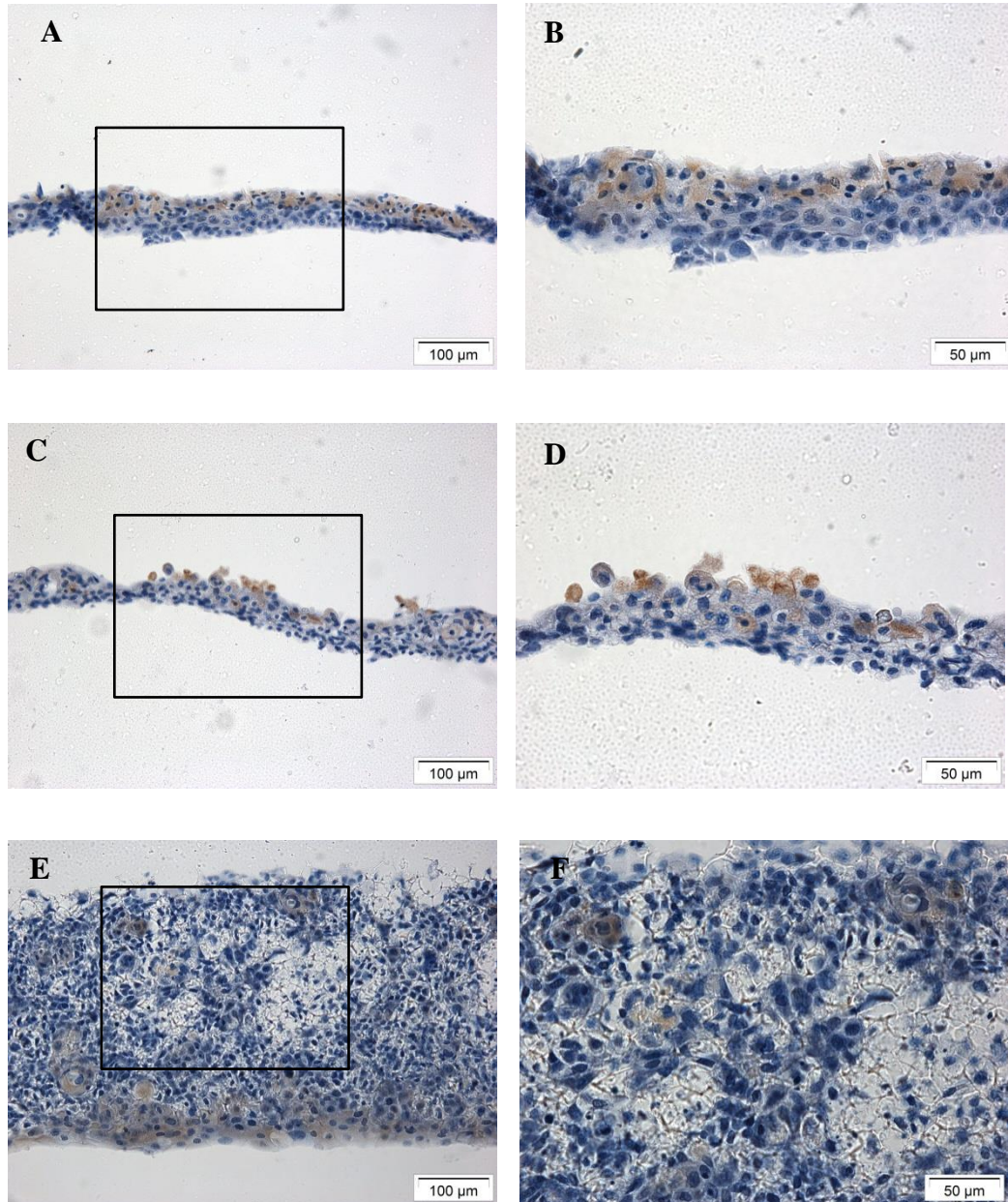


Figure 3. 8 Positive immunohistochemistry staining of 3D *in vitro* models of HTB41 cells. (A, B) **BPIFA2** on **matrigel**-coated PET at ALI under static conditions, (C, D) PET at non-ALI under static conditions and (E, F) Alvetex at ALI under static conditions. 20X and 40X magnification, 100μm and 50μm scale bars, respectively.

3.4.3 Reverse Transcription Polymerase Chain Reaction (RT-PCR) of HTB41 cultures

Specific primer pair sequences were designed to assess gene expression and were optimised with human sublingual gland tissue (see **Table 3.1**). RT-PCR was carried out to measure mRNA expression of the cell cultures at day 14. Cultures grown on all four ECM showed expression of Nanog (progenitor cell marker), amylase (acinar cell marker), E-cadherin, zona occludin1 and claudin-1 (tight junction markers) and also smooth muscle actin (myoepithelial marker). These results are in agreement with those for normal human salivary gland tissue (**Figure 3.9**). However, cKIT (progenitor cell marker), and CD-10 (myoepithelial cell marker) were not expressed by the cells.

Human Gene	Initial	Primer Sequence	Size bp
Nanog	HuNANOG-F2	CACCCAGCTGTGTGTAACA	221
	HuNANOG-R1	AAAGGCTGGGGTAGGTAGGT	
cKIT	HucKIT-F1	GAAGGCTCCGGATGCTCAG	204
	HucKIT-R1	GTCTACCACGGGCTTCTGTC	
Amylase	HuAMY1A-F1	ACTTGTGGCAATGACTGGGT	299
	HuAMY1A-R2	TGAGCTTTGCCATCATCAGA	
E-Cadherin	HuCDH1-F2	GAAGGAGGCGGAGAAGAGGA	293
	HuCDH1-R1	GGGTCAGTATCAGCCGCTTT	
Zona Occludin 1	HuZO1-F2	CGAAGGAGTTGAGCAGGAAA	204
	HuZO1-R1	GGATCTCCGGGAAGACACTTG	
Claudin 1	HuCLDN1-F2	TGGAAGACGATGAGGTGCAG	283
	HuCLDN1-R1	CCAGTGAAGAGAGCCTGACC	
Smooth Muscle Actin	HuSMA-F1	GGCAAGTGATCACCATCGGA	299
	HuSMA-R1	GGAGCCACCGATCCAGACA	
CD10	HuCD10-F1	AAATACTTCCTGGACTTGACCT	242
	HuCD10-R1	GAAGATCACCAAACCCGGCA	

Table 3. 1 Optimised primer pairs of human salivary gland expressed genes had been.

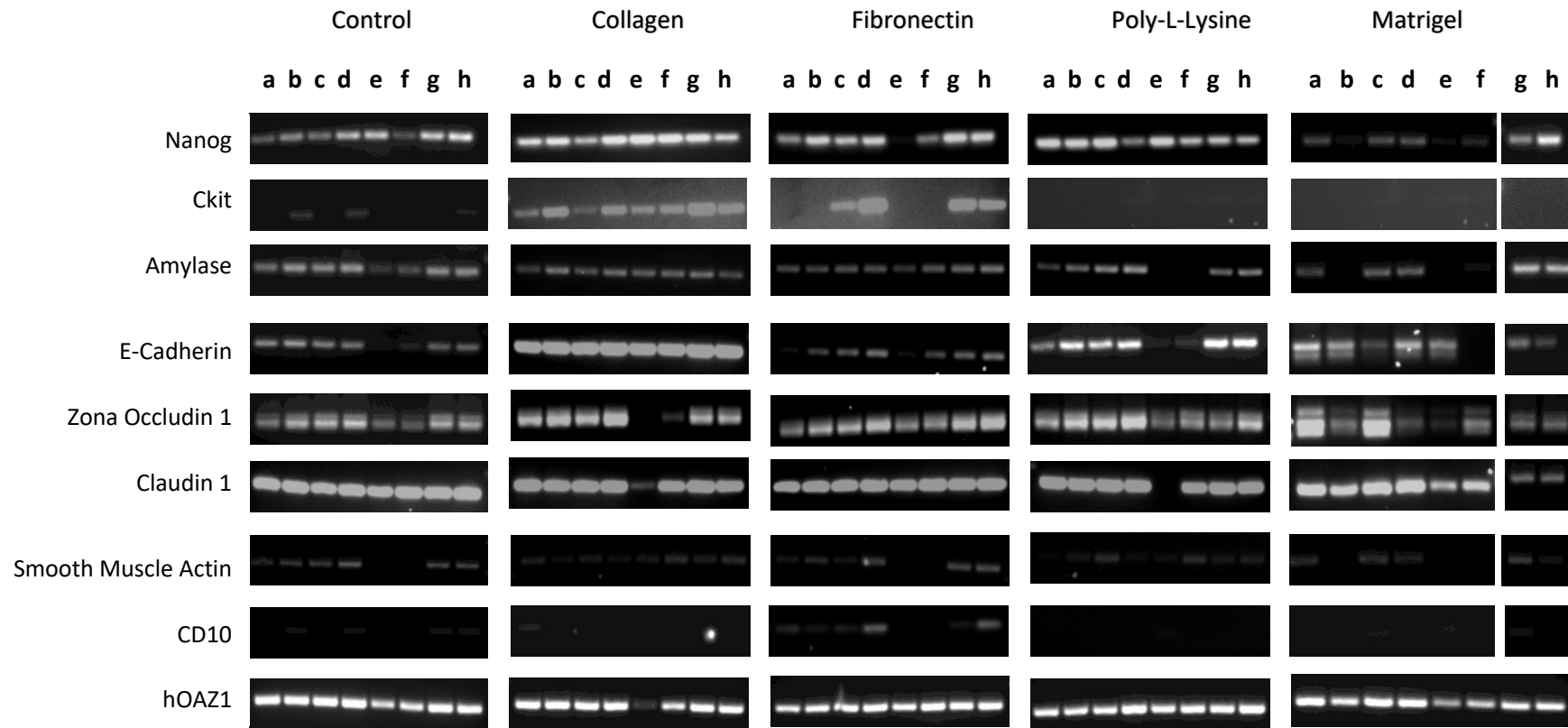


Figure 3. 9 RT-PCR of HTB41 cultures at day 14 on four types of ECM (collagen, fibronectin, poly-L-lysine, matrigel) showing mRNA expression under different growth conditions: **a**, PET at ALI, static; **b**, PET at ALI, dynamic; **c**, PET at non-ALI, static; **d**, PET at non-ALI, dynamic; **e**, Alvetex at ALI, static; **f**, Alvetex at ALI, dynamic; **g**, Alvetex at non-ALI, static; **h**, Alvetex at non-ALI, dynamic. hOAZ1 was used as an internal control.

3.4.4 Human Salivary Gland Tissue Isolation

Macroscopically, the tissues collected were fresh, well-perfused and typical of normal human salivary glands (**Figure 3.10**). The first biopsy collected was from a parotid gland as shown in **Figure 3.10A**. However, we did not successfully manage to isolate cells from this tissue, rather we found oily, fat floating in the tube even after washing numerous times. We assumed that the anonymised sample was from an older donor and the gland mostly replaced by fat tissue. We were able to isolate cells from both sublingual (**Figure 3.10B**) and submandibular glands (**Figure 3.10C**). All of my results in this study (**Chapter 3**) are from cells isolated from sublingual glands which are composed of mucous acini, serous acini and striated and excretory ducts (**Figure 3.12A**).

The tissue was digested mechanically and enzymatically using three different methods; tissue explant or digestion with pronase or 0.1 % trypsin. The wet weight of the specimen was on average 0.3 grams. The mean number of cells (N=3 glands) recovered following pronase digestion was $4.02 \times 10^5 \pm 0.18 \times 10^5$ cells/mL, and $1.38 \times 10^5 \pm 0.1 \times 10^5$ cells/mL from 0.1% trypsin digestion. The digested tissue initially consisted of floating clumps of cells which were re-plated after ~24 hours. Approximately 10% of the clumps attached to the first dish. Small islands of epithelial-like cells were observed from 5 to 7 days after plating. These islands spread and enlarged until they contacted each other to form an epithelial-like layer with round and polygonal cells. These cultures took approximately 2 to 3 weeks to reach 80% confluency. The cells were passaged for further experiments with trypsin-EDTA or stored in liquid nitrogen. The cells were grown in KGM medium as described in **Table 2.2**. The morphology of the human salivary gland (HuSG) cells did not change between passages 2 and 4 (**Figure 3.11B, 3.11C**).

Cells isolated from tissue explants (minced into ~1mm and seeded in a T75 flask) showed outgrowths within 7 days and required around 4 weeks to reach 80% confluency, approximately $3.48 \times 10^6 \pm 0.19 \times 10^6$ cells/T75 flask. Most of the cells displayed polygonal morphology (**Figure 3.11A**). Spindle shaped fibroblast-like cells were found in the initial growth of cultures and were treated with EDTA to separate

them from the epithelial cells. The cells were grown in KGM medium. After 3 to 4 weeks in culture, cell suspensions from the explant tissue were characterised using the cytopsin technique. As shown in **Figure 3.12B**, different cell types were present. Then, the cells were either passaged until passage 4 or cryopreserved for future use.



Figure 3. 10 Normal human salivary gland tissue. Images of tissue specimen showing (A) a fresh, well-perfused excised human parotid gland which is mostly covered by fat tissue; it is pre-fixation, (B) a fresh, well-perfused sublingual gland; it is pre-fixation, and (C) a fresh, well-perfused submandibular gland before processing and post-fixation with formalin.

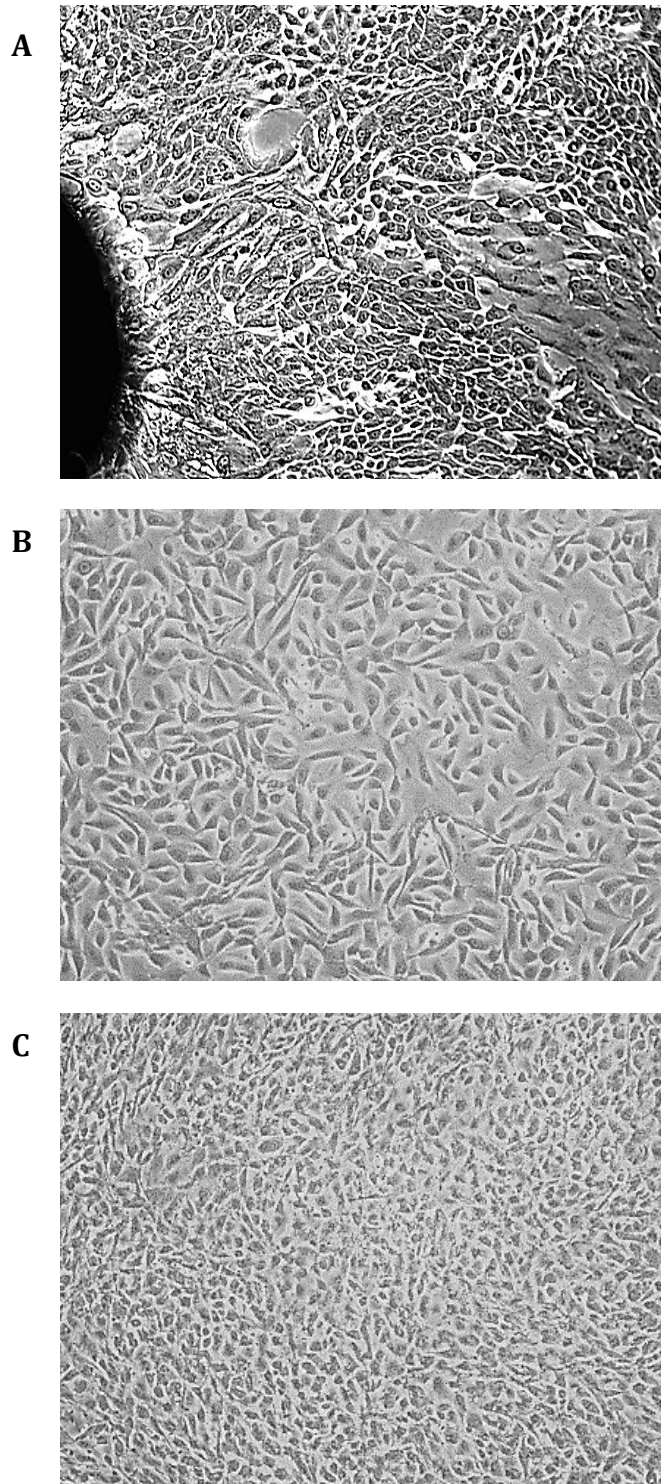


Figure 3. 11 Phase-contrast pictures showing the typical appearance of primary human salivary gland cell cultures, at passages 2-4, following 3 isolation methods; (A) tissue explant technique, (B) 0.1% Trypsin and (C) pronase. 10X magnification.

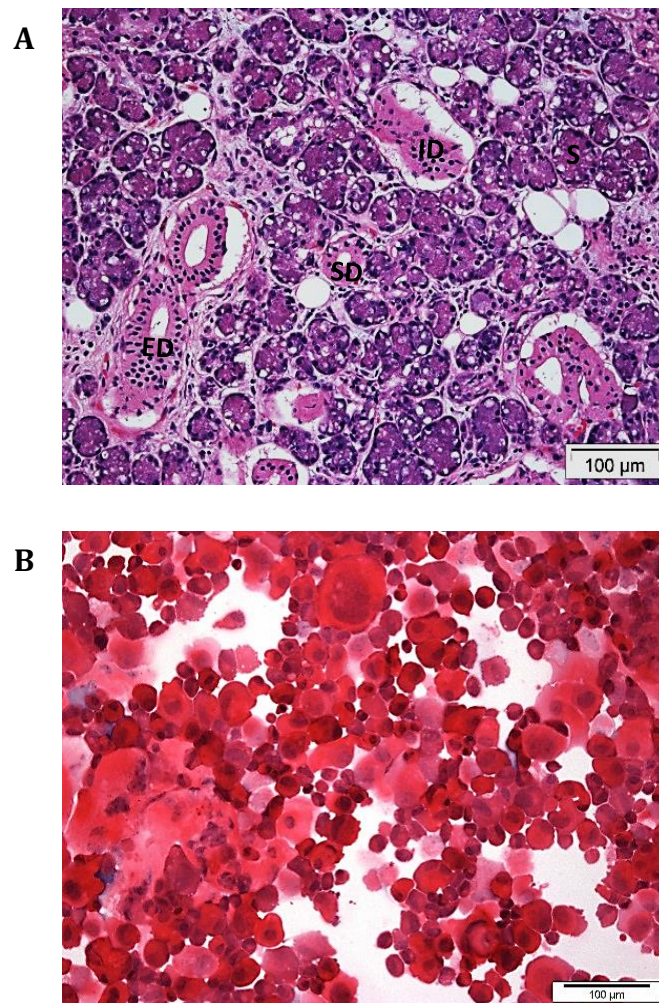


Figure 3. 12 Haematoxylin and eosin staining of (A) an excised human sublingual gland, and (B) single cells from explant culture using cytopsin. The excised gland demonstrates normal histological appearance: **S**, serous acini; **ID**, intercalated duct; **SD**, striated duct; **ED**, excretory duct. 20X magnification.

3.4.5 Cell characterisation of HuSG from explant tissues by using cytopins.

Salivary gland cell outgrowths from explant tissues were further characterised by immunofluorescence. Briefly, after 3 to 4 weeks in culture, cell suspensions from the explant tissue were characterised by using the cytopins technique. A number of cell-specific markers were expressed including cytokeratin 5 (CK5), α -SMA, MUC7, AQP5, mist1 and BPIFA2 (**Figure 3.13**).

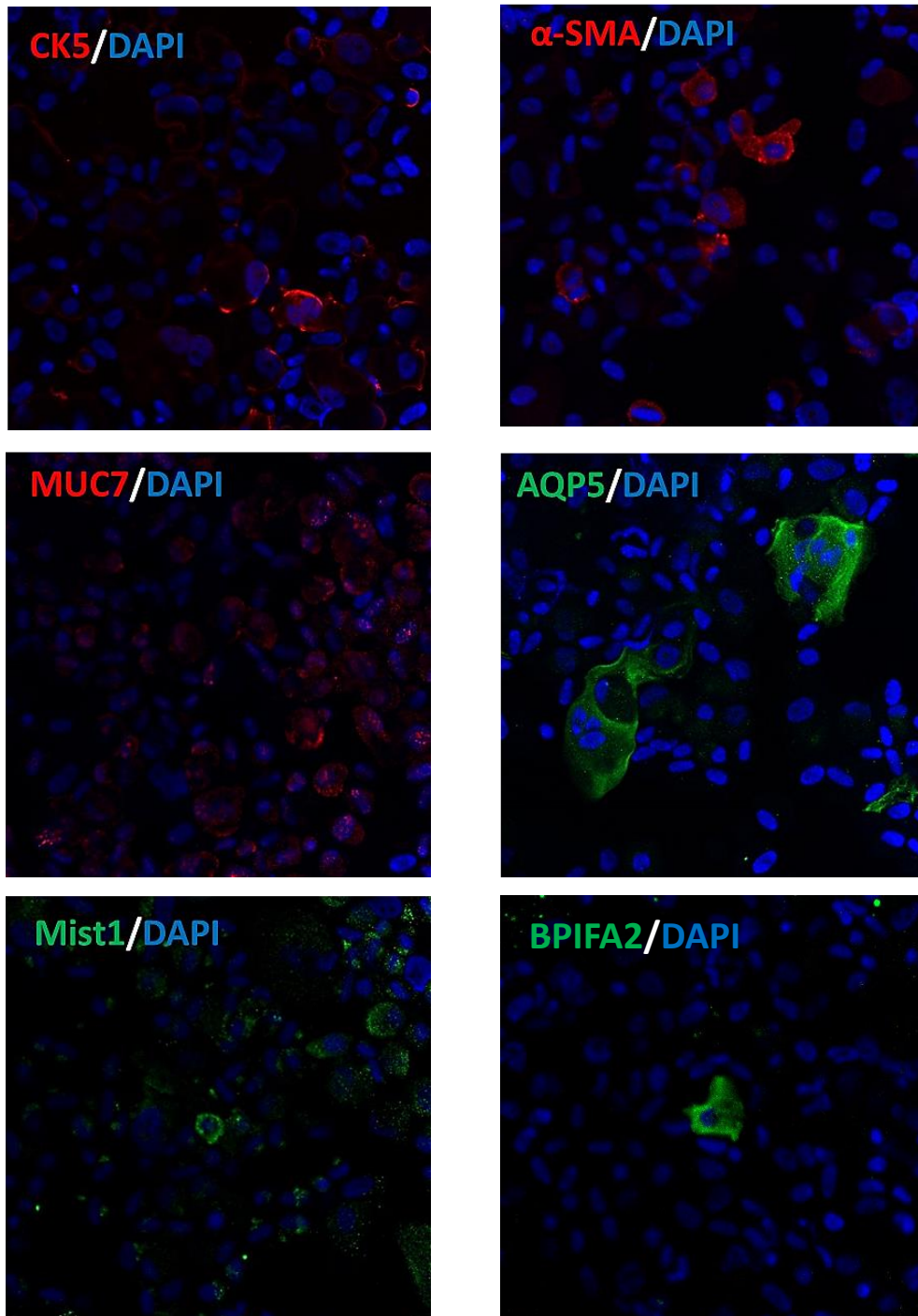


Figure 3.13 Cell characterisation of HuSG from explant tissues by using cytopins. Images (representative of three independent batches) of single cells derived from explant technique cultured in KGM media and characterised by using cytopins showing positive expression of CK5 (A), α-SMA (B), MUC7 (C), AQP5 (D), Mist1 (E), and BPIFA2(F). 20X magnification.

3.4.6 3D *in Vitro* Models of Human Sublingual Glands

A similar experimental design to that used with HTB41 cell cultures was performed with the primary human sublingual gland cells. They were cultured on the same four ECM with various culture conditions to determine differences in cellular organization and development. Haematoxylin and eosin stained sections showed significant variation in the morphology and development of the sublingual cell cultures (**Figure 3.14 and Figure 3.15**).

Figure 3.14 shows the appearance of different phenotypes of the cells after 14 days cultured on PET inserts under various culture conditions. Closer inspection of the images show that the cells mostly appeared to grow as a single layer on PET inserts under static conditions, both at ALI and non-ALI regardless of the ECM used to coat the insert. Interestingly, the cells were able to form multilayer structures when cultured on collagen under dynamic conditions, both at ALI and non-ALI and grew well on fibronectin under non-ALI, dynamic conditions. The cells did not grow well on poly-L-lysine nor on Matrigel under dynamic conditions. The HTB-41 cells (**Figure 3.2**) also grew well with multilayer structures on collagen under dynamic condition at both ALI and non-ALI but unlike the primary sublingual cells the HTB41 cells did not grow as well on fibronectin under non-ALI, dynamic condition.

The sublingual cells did not thrive on collagen-coated Alvetex®Scaffolds regardless of any other conditions (ALI/non-ALI and dynamic/static). The HTB-41 cells (**Figure 3.3**), grew best on collagen-coated Alvetex®Scaffold at an ALI under static conditions. The sublingual cells did grow as multilayer structures on fibronectin and Matrigel coated Alvetex®Scaffolds, at both ALI and non-ALI. The non-ALI cells expanded more than those grown at an ALI. We found that Matrigel-coated scaffolds at non-ALI under static conditions were the best culture conditions for primary sublingual cells on Alvetex®Scaffolds (**Figure 3.15**).

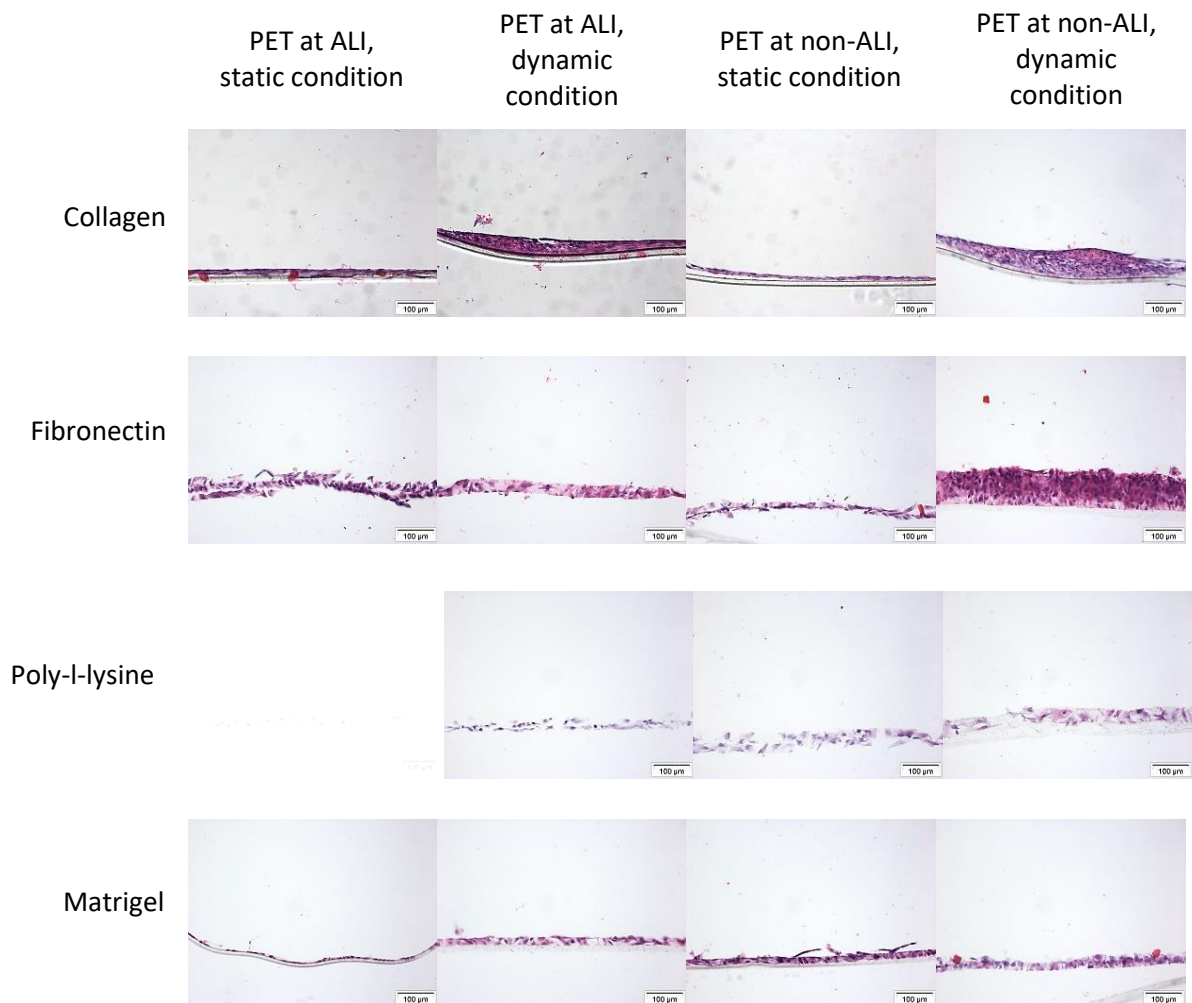


Figure 3. 14 Haematoxylin and eosin (HE) stained sections of 3D *in vitro* models of human salivary gland cells cultured on PET transwell with or without ECM coating, at ALI and non-ALI, under static or dynamic culture conditions at 14 days of culture show a number of different phenotypes present. Scale bar=100 μ m.

HE stained section of human salivary gland cells cultured on PET transwell with poly-l-lysine-coated at ALI under static condition is missing.

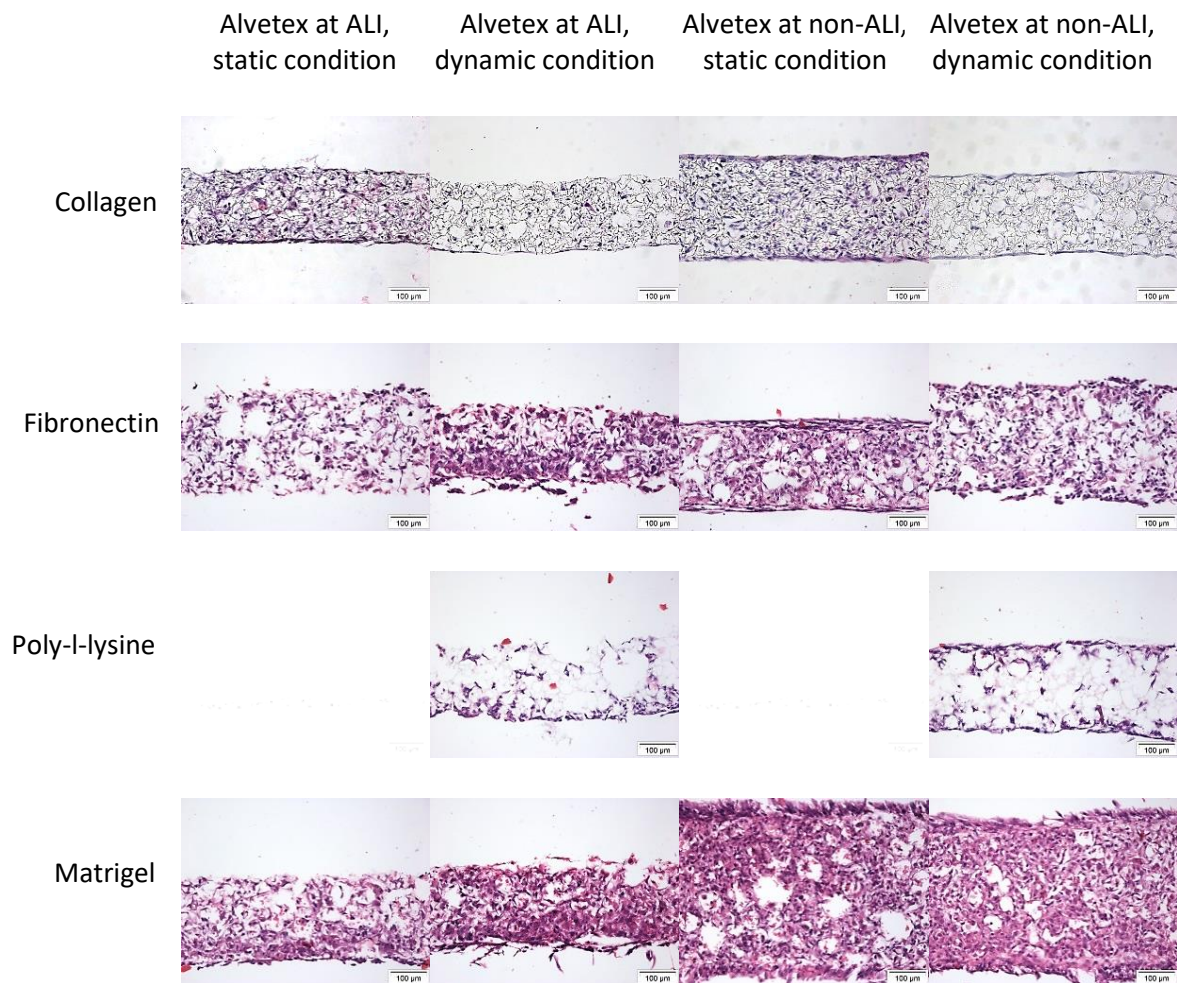


Figure 3. 15 Haematoxylin and eosin (HE) stained sections of 3D *in vitro* models of human salivary gland cells cultured on Alvetex scaffold with or without ECM coating, at ALI and non-ALI, under static or dynamic culture conditions at 14 days of culture show a number of different phenotypes present. Scale bar=100 μ m.

HE stained section of human salivary gland cells cultured on Alvetex scaffold with poly-l-lysine-coated both at ALI and non-ALI under static condition are missing.

3.4.7 Reverse transcription polymerase chain reaction (RT-PCR) of HuSG cultures

As can be seen from **Figure 3.16**, human sublingual cell cultures demonstrated expression of genes for nanog and cKIT (progenitor cell markers), amylase (acinar cell marker), zona occludin1 (tight junction marker) and also smooth muscle actin and CD10 (myoepithelial markers). It was apparent that the expression of nanog and amylase was more readily detected in the cells grown on PET inserts rather than Alvetex scaffolds, both collagen- and Matrigel-coated. In comparison, nanog and amylase was expressed in all culture conditions by the HTB-41 (**Figure 3.9**). Furthermore, ckit was expressed by HTB41 cells cultured on collagen but less so by cells cultured on fibronectin whilst most of the culture conditions allowed expression of ckit by sublingual cells.

Figure 3.9 also shows significant expression of three tight junction markers by HTB-41 cells whilst only ZO-1 was expressed by the sublingual cells. There was very limited expression of E-cadherin and claudin-1 by the primary cell cultures. CD10, a myoepithelial marker, showed extremely limited expression by the HTB-4 cells, really only in cells cultured on fibronectin. However, CD10 was highly expressed by the primary cells under most culture conditions. hOAZ1 was used as an internal control throughout.

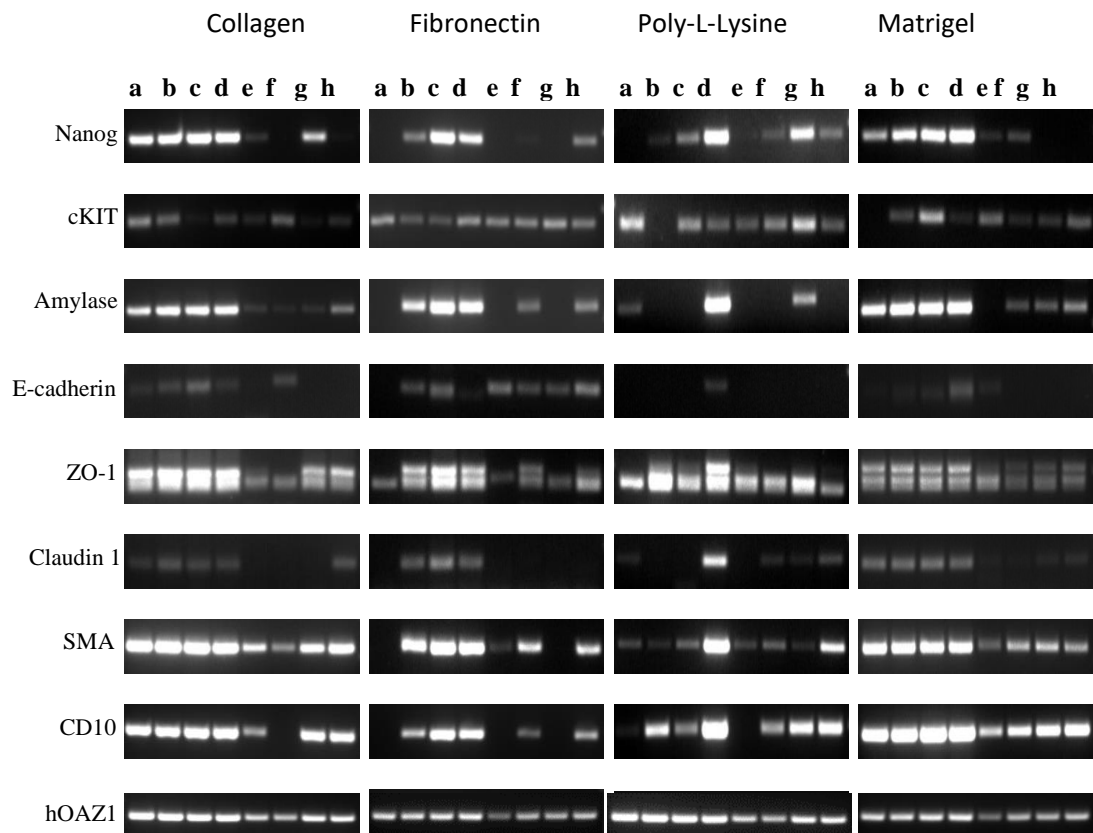


Figure 3. 16 RT-PCR showed mRNA expression of human sublingual cell cultures at day 14 on four types of ECM (collagen, fibronectin, poly-L-lysine, matrigel) under different growth conditions: **a**, PET at ALI, static; **b**, PET at ALI, dynamic; **c**, PET at non-ALI, static; **d**, PET at non-ALI, dynamic; **e**, Alvetex at ALI, static; **f**, Alvetex at ALI, dynamic; **g**, Alvetex at non-ALI, static; **h**, Alvetex at non-ALI, dynamic. hOAZ1 was used as an internal control.

3.5 DISCUSSION

Previous studies have tried to develop suitable conditions for the growth of human primary salivary gland cells *in vitro* (Tran *et al.*, 2005; Joraku *et al.*, 2007; Pradhan-Bhatt *et al.*, 2014; Jang *et al.*, 2015), however, no study to date has reported success in developing an artificial human salivary gland.

3.5.1 HTB41 Cultured as 3D Model

The aim of this chapter was to establish the optimal culture conditions for use in developing an artificial salivary gland by initially culturing HTB41 cells, a cell-line derived from a submandibular mucoepidermoid tumour. It has been stated in the literature that the choice of basement membrane or matrix protein used as a surface for cell growth can have a dramatic impact on the appearance and function of the cells (Finkbeiner *et al.*, 2010; Wu *et al.*, 2011). Four different ECM (collagen I, fibronectin, poly-L-lysine, Matrigel) were used in this study to serve as basement membrane, coated onto two types of scaffold, cultured as ALI or non-ALI, and either placed under static or dynamic conditions. Under these different culture conditions, histology was assessed with haematoxylin and eosin stained sections, gene expression was confirmed by RT-PCR analysis and proteins were localised by immunohistochemistry.

We found that HTB41 cells grew more effectively as multilayers under ALI conditions than when fully submerged. Interestingly the most effective growth conditions for cells grown on the PET inserts was ALI under dynamic conditions whilst ALI under static conditions was preferred by cells seeded onto Alvetex® Scaffolds, where the cells grow into the scaffold. Collagen I provided the best matrix for HTB41 cell growth. Our PCR results demonstrated that HTB41 cells expressed genes for a progenitor cell marker (nanog), an acinar-specific protein (amylase), and tight junction proteins (E-cadherin, ZO-1 and claudin-1) but not the myoepithelial cell markers (smooth muscle actin, CD10).

Immunohistochemistry was used to validate our *in vitro*, HTB41, 3D models by demonstrating similarities in protein staining between the models and normal human sublingual glands (refer to Appendix 7). The staining confirmed the presence of amylase, cKIT and BPIFA2 but as the cells were not structurally organised it was not possible to

compare structural similarities with normal tissue. This preliminary data indicates that the salivary gland cell phenotype *in vitro* is very much dependent upon the scaffold, the ECM and the culture conditions used. This data provided important information for further experiments involving the culture of primary acinar-like cells from normal, human salivary glands.

3.5.2 Human Sublingual Gland as 3D Model

Cells are one of the basic elements needed to engineer functional tissues. In order to successfully develop cell culture systems, we need to be able to collect cells from patients, grow them in culture and return them to the patient for functional restoration (Joraku *et al.*, 2005). In this study, we have attempted to isolate primary acinar cells from sublingual glands using a number of different isolation methods, as well as to develop optimal conditions for culturing acinar cells that retain their functionality.

Of the different methods used to isolate human salivary gland cells, the tissue explant technique has recently been used alongside enzyme digestion (Joraku *et al.*, 2007; Pradhan-Bhatt *et al.*, 2014; Jang *et al.*, 2015). Human parotid gland tissue has been dissociated by mincing into small pieces and suspending in Hepato-STIM medium (Pradhan-Bhatt *et al.*, 2014), in serum-free keratinocyte growth medium (Joraku *et al.*, 2007) and in KGM (Jang *et al.*, 2015) allowing cells to adhere and migrate out of the explants. Our results showed that enzymatic digestion with 0.1% Trypsin allowed the cells to grow more quickly (5 to 7 days to observe small islands of salivary epithelial-like cells) than the tissue explant technique (21 to 28 days to observe small islands of salivary epithelial-like cells). However, the number of cells surviving enzymatic digestion was lower than from tissue explants and the phenotype of the cells did not as closely resemble the normal cells as did those derived from explants (**refer 3.4.4**). Cells growing out of explants could be used to culture approximately 16 transwells of 12-well plate per T75 flask. This could, therefore, minimize the number of salivary gland tissue biopsies needed and thus tissue explants were used in my study aimed at determining optimal culture conditions.

It is also important to consider cell culture medium when engineering functional tissues. Many studies have reported that the cell culture medium affects the characteristic and functionality of the models. For example, a keratinocyte serum-free medium low in calcium (0.09 mM) was reported to encourage more acinar cell proliferation than differentiation and resulted in fewer tight junctions (Chan *et al.*, 2011). Furthermore, Jang *et al* (2015) demonstrated that cells grown in KGM with low calcium (0.05 mM) were scattered throughout the flask, whilst those grown in high calcium (0.8 mM) appeared smaller in size and aggregated together. The effects of different culture supplements were also observed by Jang *et al* (2015) when evaluating morphology and cell expression. They found that cells grown in KGM media containing 6 supplements (bovine pituitary extract (BPE), human epidermal growth factor (hEGF), insulin, hydrocortisone, epinephrine and transferrin) exhibited no apparent difference in morphology, rather they displayed a more uniform population compared to those in KGM media with 4 supplements (BPE, hEGF, insulin and hydrocortisone). However, no significant differences in the expression of cell type-specific markers were noted (Jang *et al.*, 2015). Chan *et al* (2010) tested three different types of medium to encourage the growth of different types of human salivary gland cells; acinar, myoepithelial and fibroblast cells. They had an 80% success rate in isolating and expanding the three different cells types; parotid gland acinar cells grew as a monolayer of polygonal shaped epithelioid cells in K-SFM (with BPE, EGF and insulin), parotid gland myoepithelial cells grew in M199S medium (with 10% FBS), and cells growing in M199 medium had a fibroblast morphology (Chan *et al.*, 2010).

The composition of a 3D *in vitro* models plays an important role in the formation of salivary gland tissue structures. Surrounding extracellular matrices and culture conditions significantly influence the development of salivary gland cells (Maria *et al.*, 2011; Pradhan-Bhatt *et al.*, 2014). A similar experimental design to that with the HTB41 cell cultures was performed in my study using primary sublingual gland cells isolated by the tissue explant technique. The normal salivary gland cells were cultured in DMEM/F12 supplemented with serum and growth factors (EGF, insulin, hydrocortisone, L-glutamine) as used by previous researchers and referred to as KGM media.

Our preliminary findings demonstrated that HTB41 cells preferred ALI conditions and grew well on collagen. In comparison, the normal sublingual cells preferred non-ALI, dynamic conditions on the PET inserts and non-ALI, static conditions in the Alvetex® Scaffolds. For both cell types, collagen provided the best matrix for cell growth on PET and interestingly whilst the HTB41 cells also preferred collagen-coating of Alvetex® Scaffolds, Matrigel was a better matrix in these scaffolds for the primary sublingual cells. Similarly, Maria *et al* (2011) reported that the human submandibular cell line (HSG) cultured on Matrigel (2 mg/ml) encouraged morphologic changes into polarized, secretory acinar like cells. Whereas, Joraku *et al* (2007) suggested that a mixture of 60% collagen and 40% Matrigel encouraged a well differentiated acinar morphology of human parotid gland cells (Joraku *et al.*, 2007).

RT-PCR was used to confirm the expression of cell specific markers. In comparison to the HTB41 cultures, the human sublingual cells expressed both progenitor cell markers, nanog and cKIT, whereas HTB41 cultures detected more expression of nanog than cKIT. Similarly, Gorjup *et al* (2009) demonstrated the mRNA expression of cKIT and nanog in submandibular gland stem cell cultures. They showed that nanog was expressed in embryonic stem cells but absent in differentiated cells (Gorjup *et al.*, 2009). We also showed the expression of both myoepithelial cell markers smooth muscle actin (SMA) and CD10 in human sublingual cells but the HTB41 cells had limited expression of SMA and extremely limited CD10 expression. SMA is the classical marker of myoepithelial cells and the protein was found in an increasing number of cells as salivary gland morphogenesis progressed. Ianez *et al* (2010) were not able to detect the presence of CD10 in glandular structures, it was only present in the walls of blood vessels while Cheuk and Chan (2007) considered CD10 to have low specificity as a myoepithelial cell marker. Thus, further investigations of CD10 expression should be carried out to firmly correlate expression in myoepithelial cells.

My study found that both normal salivary gland cells and those from a mucoepidermoid cell line, HTB-41, expressed high levels of the acinar cell marker, amylase but only one tight junction protein, ZO-1, was expressed in the human sublingual cells. These findings

demonstrate that, using the described culture conditions, normal salivary gland cells are able to retain, *in vitro*, many of the functional phenotypes of human sublingual cells.

Nevertheless, further research in this area could allow for further development of the model. Future studies should focus on developing culture conditions that would facilitate the formation of salivary gland structures in 3D *in vitro* models. Our sublingual cells cultures were not structurally organised and we have no real evidence of structural similarities to normal tissue. The study could also be improved by focusing on growing and expanding the cells at the same time as maintaining their normal cell phenotype and function. More specific cell markers should also be used to confirm the functionality of the model by immunohistochemistry and RT-PCR. Further study of all salivary gland cells should focus on determining amylase production through the collection of secretions and the use of amylase biochemical assays.

3.6 KEY EXPERIMENTAL CONCLUSIONS

- HTB41 cells preferred to grow under ALI conditions; for the PET inserts this was under dynamic conditions whilst on the Alvetex® Scaffold it was under static conditions. Collagen I provided the best matrix for HTB41 cell growth.
- Normal sublingual cells preferred to grow under non-ALI conditions; and as for the HTB-41 cells for PET inserts this was under dynamic conditions whilst on the Alvetex® Scaffolds it was under static conditions. Collagen I again provided the best matrix for cell growth on PTFE while Matrigel was a better for growth on Alvetex® Scaffolds.
- Normal sublingual cells cultures displayed significant expression of mRNA for cKIT, nanog, amylase, SMA, CD10 and ZO1, but lower expression of E-cadherin and claudin 1.
- Significant numbers of normal salivary gland cells were successfully isolated using the explant technique. These cells have been cryopreserved and thawed for future use.

This study has shown that generally, the HTB41 cells preferred to grow on Collagen I-coated under ALI conditions while normal sublingual cells preferred to grow on Matrigel-coated under non-ALI conditions. However, they were not structurally organised and unable to form glandular structure. Instead, they grew in layers and did not fully differentiate. The explant technique is the best method for the isolation of normal human salivary gland cells from normal major gland tissue. Taken together, these results suggest that using normal salivary gland cells isolated from explant technique, culturing them in an ECM rather than on a coated surface under both ALI and non-ALI conditions to encourage gland formation for further experiment. Moreover, addition of specific growth factors in the culture media should be considered in further experiment in order to facilitate the formation of salivary gland structures *in vitro*.

CHAPTER 4

Development of Organoid Models of Human Salivary Gland

CHAPTER 4: DEVELOPMENT OF ORGANOID MODELS OF HUMAN SALIVARY GLAND

4.1 INTRODUCTION

In chapter 3, I showed that normal human salivary gland cells preferred to grow on Matrigel at an Air-Liquid interface (ALI). However, the cells did not fully differentiate and grew in layers rather than as a glandular structure. To encourage gland formation by the isolated cells, I designed experiments to culture the normal salivary gland cells in an extracellular matrix (ECM) rather than on a coated surface.

Previous studies have successfully cultured intestine and gastric cells as organoids by growing them in Matrigel in a culture medium that mimicked the environment of intestinal stem cells through the presence of EGF, Noggin, R-spondin1 and WNT3a. Under these conditions the stem cells proliferated to form small structures containing intestinal crypts and villi, and the organoids were able to self-organize to mimic the *in vivo* situation (Van De Wetering *et al.*, 2015). Nanduri *et al.* (2014) demonstrated that single murine salivary gland cells could be expanded *in vitro* into distinct ductal/lobular organoids consisting of a number of salivary gland lineages when grown under culture condition dependent upon FGF, EGF and Matrigel. Further studies by this group showed that the addition of Wnt3A and R-spondin 1 activated the Wnt pathway and allowed long-term expansion of the organoids containing all differentiated salivary gland cell types (Maimets *et al.*, 2016). Addition of Rho-inhibitor Y-27632 in the media in the initial stages resulted in a more-rapid and pronounced expansion of cells and enhanced the secondary sphere-formation (Nanduri *et al.*, 2014).

The aim of this chapter is to develop human salivary gland organoids by adapting the culture technology described in the published mouse studies.

The SG cells were cultured in an ECM, either Matrigel, a mouse EHS sarcoma derived product used in my preliminary studies, or Myogel, derived from a benign, human uterine leiomyoma. Thus, we will investigate and compare the differential effects of Matrigel and Myogel on the growth of the normal human cells with the aim of

replacing a murine ECM by a human ECM and thus developing a model which will mimic the human *in vivo* situation.

The SG cells will be cultured, as described in **Figure 4.1**, in medium supplemented with EGF, FGF2, Wnt3a and R-spondin 1 both at an ALI and non-ALI. Cell specific markers will be used to confirm functionality of the model by immunohistochemistry and RT-PCR and immunofluorescent confocal microscopy will be used to determine the exact location of expression.

I have used my SG model as a tool for a preliminary study of infectious disease. Bacterial sialadenitis (infection of salivary gland) is well-recognised as being associated with xerostomia, especially in patients who have Sjogren's syndrome. In addition, hyposalivation permits microbial colonisation of the parotid duct, which leads to the development of acute or chronic suppurative infection (O Lewis *et al.*, 1993). Little is known about the initial stages of colonisation and pathogenesis of infectious disease due to the lack of a suitable model. My SG model will be infected with the salivary gland pathogen, *Staphylococcus aureus*, the most common cause of salivary gland infection and isolated, at increased levels, from the eyelid and conjunctiva of primary Sjogren's patients (Hori *et al.*, 2008; Kukita *et al.*, 2013). Briefly, the SG organoid model will be exposed to the bacteria and incubated for up to 72 hours post infection prior to analysis.

4.2 AIMS

This chapter addresses two major aims:

- 1) The first aim of this chapter was to develop an organoid model of human salivary glands using normal sublingual gland cells.
- 2) The second aim of this chapter was to use the model to study the early stages of infectious disease with *Staphylococcus. Aureus*.

4.3 MATERIALS AND METHODS

4.3.1 Cell culture

- SG cells were isolated from human sublingual gland tissue using the explant method (**Refer 3.3.5.3**) and maintained in KGM media as previously described (**Refer 2.2**).
- Cells were mixed with ECM (Matrigel and/or Myogel) prior to growth on transwells, both at ALI and non-ALI, and cultured in enriched media (later referred to as Nan media) to encourage cell differentiation and organoid growth.

4.3.2 Media preparation for organoid models

R-Spondin 1 conditioned media

HA-R-Spondin1-Fc 293T cells were bought from AMSBIO (cat.no. 3710-001-01). Cells were grown in DMEM with 10% FBS, 1% penicillin-streptomycin and 1% L-Glutamine. After the cells had attached to the plate (1-2 days), the medium was changed to OPTIMEM (Gibco, 31985070) with 1% penicillin-streptomycin for 7 days. Conditioned medium was collected and filtered through a 0.22 μm filter, and subsequently referred to as R-Spondin1 conditioned media.

WNT-3a conditioned media

L-Wnt3a clone 5.5, passage 7 was a generous gift from Dr Hans Clevers, Hubrecht Institute for Developmental Biology and Stem Cell Research, Netherlands. Cells were grown in DMEM with 10% FBS and 1% penicillin-streptomycin for 7 days. Conditioned medium was collected and filtered through a 0.22 μm filter, and subsequently referred to as Wnt3a conditioned media.

Dexamethasone (D4902)

1 mg dexamethasone was dissolved in 1 ml of absolute ethanol and 49 ml of DMEM added to make a final concentration of 20 $\mu\text{g}/\text{ml}$. 1 ml aliquots were stored at -20°C

Y-27632 (Y0503)

2 mg Y-27632 was dissolved in 624 µl of DMSO and incubated in a 37°C water bath for 5 minutes to dissolve any precipitate. 50 µl aliquots were stored at -20°C.

FGF2 (F5392)

1 µg of FGF2 was dissolved in 1 ml of sterile DMEM. 500 µl aliquots were stored at -20°C.

Epidermal Growth Factor (Human Recombinant from E. coli)

200 µg of EGF was dissolved in 10 ml of DMEM containing 10% FCS. 0.5ml aliquots (final concentration 10µg/ml) were stored at -20°C.

Component	Volume (V₂:50mL) and stock solution	Final concentration
Dulbecco's modified Eagle's Medium (DMEM)	13.5 ml	(3:1)
Nutrient Mixture F12 HAM	4.5 ml	
Penicillin/Streptomycin	500 µl of 10,000 i.u./ml penicillin and 10,000 µg/ml streptomycin	100 i.u./ml penicillin and 100µg/ml streptomycin
L-Glutamine	500 µl of 200 mM	2 mM
N-2 Supplement (Gibco, 17502048)	500 µl of 100X	1X
Epidermal Growth Factor	50 µl of 20 µg/ml	20 ng/ml
FGF2	50 µl of 10 µg/ml	10 ng/ml
Insulin (Sigma, I9278)	25 µl	10 µg/ml
Dexamethasone	1 ml of 20 µg/ml (5x10 ⁻⁵ M)	1 µM
Y-27632 (ROCKi)	50 µl of 10mM	10 µM
R-Spondin 1 conditioned media	5 mL	10%
Wnt3a conditioned media	25 mL	50%

Table 4. 1 Enriched Media

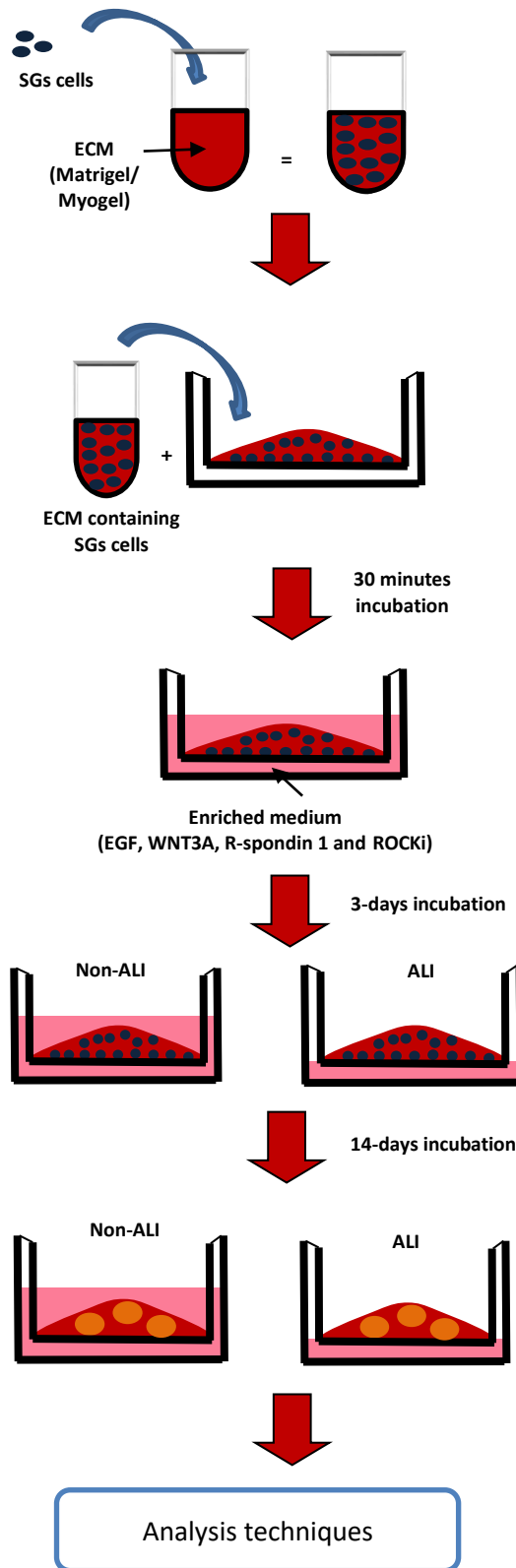
4.3.3 Organoid models of human salivary glands

The method used was adapted and modified from Nanduri *et al.* (2014) and Maimets *et al.* (2016). Briefly, a day before seeding, a 12-well culture plate was placed in a 37°C, 5% CO₂ incubator to ensure the plate was warm before seeding. ECM (Matrigel and Myogel) were kept ice-cold at all times, to ensure they remained in liquid form. 25 µl of a cell suspension (4 x 10⁶ cells/ml) was mixed with 50 µl of ECM and placed in the centre of a PET transwell. ECM was left to solidify for 30 minutes at 37°C, 5% CO₂. Following ECM polymerization, 500 µl of warm, enriched media was added to the top of the transwell without disturbing the ECM, and 1.5 ml media to the bottom. After 3 days, the media was changed to that without ROCKi (Nan media) either submerged (non-ALI) or at an air-liquid interface (ALI) for up to 14 days. ROCKi was added only directly after seeding of SG cells or after splitting (Bartfeld and Clevers, 2015). The medium was refreshed 3 times per week (**Figure 4.1**). For RNA isolation, Matrigel was dissolved by incubation with Dispase (1 mg/ml; Sigma) for 1 hour at 37°C. This was followed by a washing step with PBS and centrifuged at 13,000 rpm for 5 min. SG organoids released from the gels were lysed in Trizol reagent for further RNA analysis (**Refer 2.4**).

4.3.4 Organoid model analysis

- Diameter of organoids was measured using FIJI-ImageJ Win64 with an average of four readings per organoid being taken.
- Number of organoids formed was counted randomly. An average of three transwells of SG organoid cultures was counted per batch (N= 3 batches).
- Haematoxylin and eosin (HE) staining was performed on organoid sections for phenotypic assessment (**Refer 2.5**).
- Immunohistochemistry was performed on organoid sections to investigate protein expression of cell specific markers (**Refer 2.5.4**).
- RT-PCR was used for subjective analysis of mRNA expression (**Refer 2.4**). Primer pairs were designed to assess gene expression of mucin7, MUC5B, cystatin 1, cystatin 5, HE4 and aquaporin 5 (**Refer Table 2.3**).

- Immunofluorescent confocal microscopy was used to localize the expression of cell specific markers (**Refer 2.6**).



Single cell suspensions were prepared. 4×10^6 cells/ml were mixed with ice-cold ECM.

The ECM containing SG cells were placed in the centre of a PET transwell in a 12- well plate.

Following ECM polymerisation cells were submerged in enriched media.

After 3 days fresh media (without ROCKi) was added and cultured either submerged (non-ALI) or placed at an air-liquid interface (ALI).

After 14 days the SG cells had developed into organoids.

Analysis included diameter of organoids, H&E staining, immunohistochemistry and immunofluorescence.

Figure 4. 1 Overview of developing an organoid model of human salivary glands by using SG cells.

4.3.5 Culture of Bacteria

Bacteria

Bacteria (strain)	Antibiotic Resistance	Origin
<i>Staphylococcus aureus</i> (S235, a lab strain)	-	Lyophilised stocks within the School of Clinical Dentistry, Sheffield, UK

Media preparation

All growth media was prepared according to the manufacturer's instructions using distilled water and sterilised by autoclaving at 15 psi (120°C) for 20 minutes.

Blood Agar (BA)

7.8 grams of Columbia Blood Agar Base was added into 200 mL of distilled water. The mixture was swirled until all the powder was dispersed and freely suspended. The medium was autoclaved under standard conditions for liquid reagents (15 psi/120°C) for 20 minutes before placing in a 56°C water bath. This allowed the medium to cool sufficiently for the addition of blood and antibiotics without denaturing any activity but still being warm enough to prevent the agar from solidifying. 15 mL of Horse Blood Oxalated (~5 to 7% v/v), previously warmed to room temperature, was added and mixed gently until uniformly distributed. The medium was immediately dispensed into 100-mm petri dishes and any bubbles formed removed by flaming. The warm plates were allowed to cool at room temperature until the agar had set, placed in a plastic sleeve and stored at 4°C until needed.

Growth of *S. Aureus* on Solid Media

Using aseptic technique, a small amount of *S. Aureus* was streaked out from the frozen stock onto a small section of a BA plate (~1/4) by using a sterile wooden applicator. With a new sterile wooden applicator, a new quadrant of *S. Aureus* was streaked out by passing through the initial quadrant several times. This process was repeated 1 to 2 more times, passing a new sterile applicator through the most recently streaked quadrant. The plates were incubated for 16-24 hours at 37°C.

Growth of *S. Aureus* in Liquid Media

Using aseptic technique, a single colony of *S. Aureus* was transferred from the streak plate into the aliquoted broth by tilting the culture tube and rubbing the inoculating loop against the side of the tube at the liquid-air-interface. The bacteria were visible on the loop. The cultures were grown overnight (~16 to 18 hours) at 37°C at which point the culture is in stationary phase.

Preparation of *S. Aureus* Frozen Stocks

Using aseptic technique, 150 µl of sterile DMSO was added to one sterile cryotube. 850 µl of overnight culture was added to the same cryotube, again using sterile technique. The cryotube was mixed briefly by inversion and stored at -80°C.

Multiplicity of Infection (MOI)

Two parameters were considered when estimating the multiplicity of infection (MOI): the number of bacteria and the number of cells per organoid.

The overnight liquid culture was prepared and the bacterial density assessed using a Neubauer chamber and microscope and the bacterial concentration reported as colony forming units in 1 mL of PBS (cfu/mL). The formula below was used to determine the number of bacteria per millilitre.

Concentration (cfu/mL)	=	$\frac{\text{Total counted organism} \times \text{Dilution factor}}{\text{Area of squares counted} \times \text{Chamber depth}}$
	=	$\frac{N \times \text{Dilution Factor}}{(5 \times 0.04) \times 0.02}$

To estimate the number of cells per organoid the number of organoids in 1 well was counted, the organoids were dissociated into single cells using Dispase (**Refer 4.3.3**) and then counted using a haemocytometer (**Refer 2.2.3**).

Bacteria Preparation for FITC-Staining

The bacteria were cultured overnight in liquid media, counted and diluted with PBS to give a concentration of 1×10^9 bacteria/mL. 1 mL of bacterial suspension was centrifuged at 13,000 rpm for 2 mins and the supernatant discarded. The pellet was washed twice with 1 mL of PBS by centrifuging at 13,000 rpm for 2 mins. The pellet was then suspended in 1 mL PBS with 10 μ L of FITC solution (1 mg/mL of FITC in DMSO) and incubated in the dark for 15 mins at 4°C with gentle agitation. Finally, the pellet was washed four times with 1.5 mL PBS by centrifugation to remove excess FITC.

4.3.6 Infection of SG Organoid Model with *S. Aureus*

SG cells were cultured in Matrigel at ALI for 14 days as described previously (**Refer Figure 4.1**). The antibiotics were removed from the media for 48 hours prior to infection in order to dilute the antibiotics in the basement membrane. FITC-tagged *S. aureus* (S235) was prepared as described (**Refer 4.3.5**). An appropriate amount of bacterial culture, in antibiotic-free Nan media, to infect at a MOI of 1:100 (SG organoids: bacteria) was added to the apical chamber of ALI day 14 SG organoids. An equal volume of PBS was added to further organoid cultures to generate negative controls. Cultures were incubated for 1 hour and washed three times with sterile PBS to remove non-adherent bacteria. Antibiotic-free Nan media was added to the basal chamber and cultures incubated for 24, 28 and 72 hpi. At each time point SG organoids were fixed for IFC (**Refer 2.6**).

4.4 RESULTS

I established culture conditions for the development of an organoid model of normal human salivary glands. I performed a morphological analysis of the organoids and determined the expression of cell specific markers and compared this to normal human salivary gland tissue. I used the normal human salivary gland organoid model as a model of infection by co-culturing with the salivary gland pathogen, *S. aureus*.

4.4.1 Morphological analysis of SG organoids cultured in Matrigel

As described in section 3.3.5.3 and 3.4.4, primary human SG cells were successfully isolated from sublingual glands and expanded in culture. The average size of the tissue was 0.3 grams and it took approximately 28 days to isolate the SG cells from explant tissue with average number was $3.61 \pm 0.43 \times 10^6$ cells/T75 flask (n=3 SG batches).

Addition of ROCKi during the initial stages of culture (with all cells submerged) has been shown to facilitate the proliferation of cells (Lalitha S Y Nanduri *et al.*, 2014; Mulay *et al.*, 2016) allowing seeding at the lowest possible density. Hence, SG cells were initially seeded at a density of 1×10^5 cells/well in Matrigel and submerged in culture medium with ROCKi for 3 days. Fresh media used from this time point onwards did not include ROCKi and organoids were cultured either as non-ALI or at an ALI (as day 1).

I found that SG cells from single cell suspensions (day 1) were able to proliferate and differentiate to form small mini-gland like structures after 14-days. At ALI day 3, cells migrated towards each other, formed aggregates and the spherical-like structure of organoids could be observed by ALI day 7. At around ALI day 10, the spherical organoids were larger in size and by ALI day 14 small structures resembling SG organoids were visualised (**Figure 4.2**).

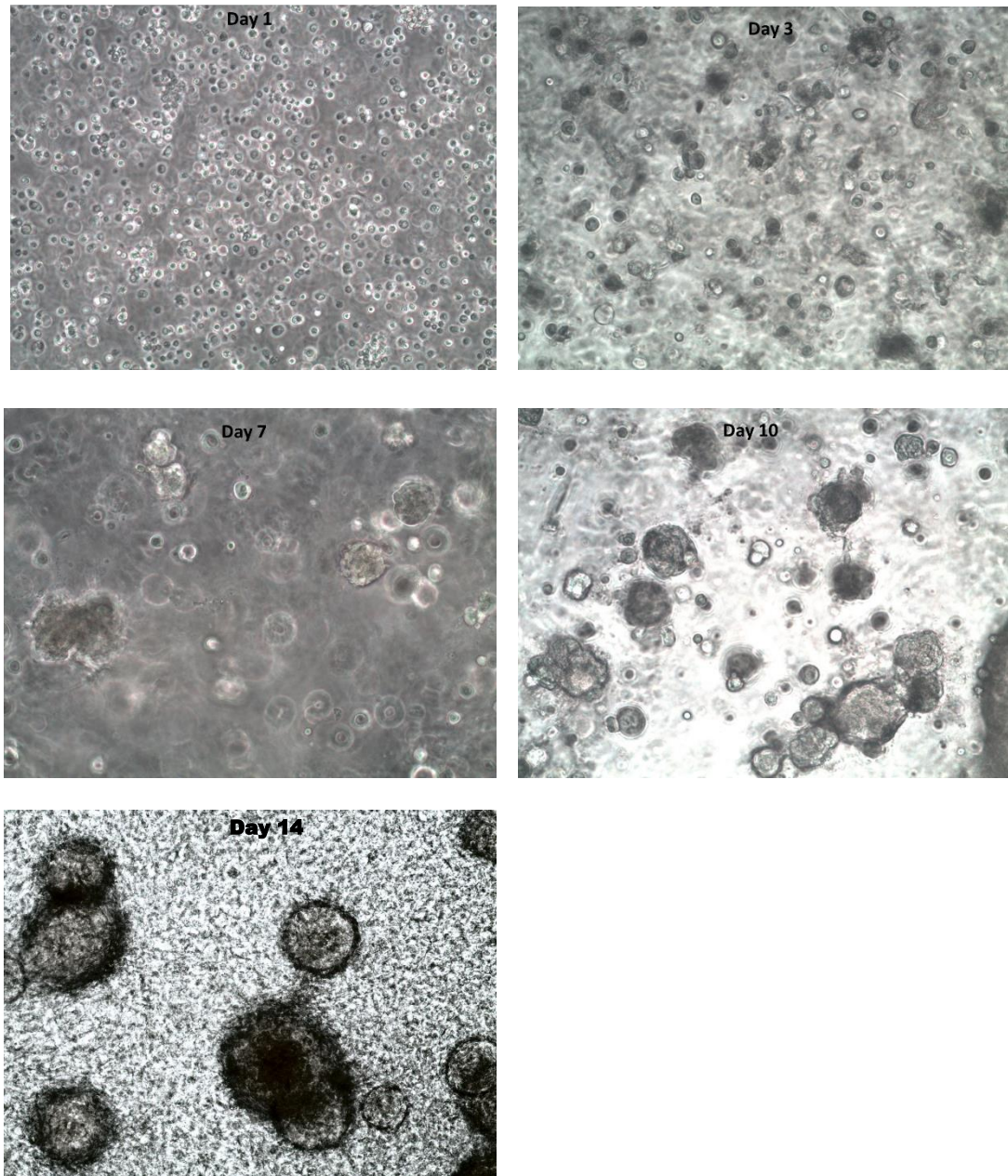


Figure 4. 2 Organoid models of human salivary glands cultured at an ALI. SG cells from single suspensions were able to proliferate and differentiate to form small structures resembling mini-glands for up to 14-days in culture. (10x magnification)

Haematoxylin and eosin stained sections of SG organoids showed uniformly compact, flat, polygonal cells with well-defined cell boundaries at the periphery and fewer cells towards the centre of the organoids. Compared to those grown at an ALI, non-ALI organoids were significantly smaller in size (**Figure 4.3**). Mean diameter of SG organoids cultured in Matrigel at ALI was $272.6 \pm 1.53 \mu\text{m}$, $p=0.0001$, significantly larger than those not at ALI ($101.4 \pm 3.99 \mu\text{m}$). The number of SG organoids formed was also significantly different between the two conditions with the mean number of SG organoids formed in Matrigel at ALI being 73.33 ± 5.24 , $p=0.001$ compared to 22.33 ± 1.76 SG organoids formed at non-ALI (**Figure 4.4**).

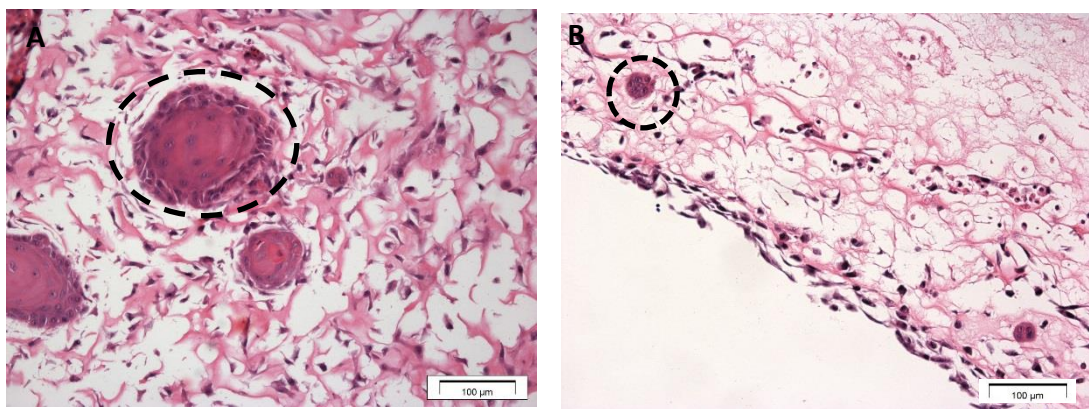


Figure 4.3 SG organoids cultured in Matrigel. Haematoxylin and eosin stained sections of SG organoids cultured in Matrigel at ALI (A) for up to 14-days were significantly larger than non-ALI (B) cultures. Scale bar=100 μm .

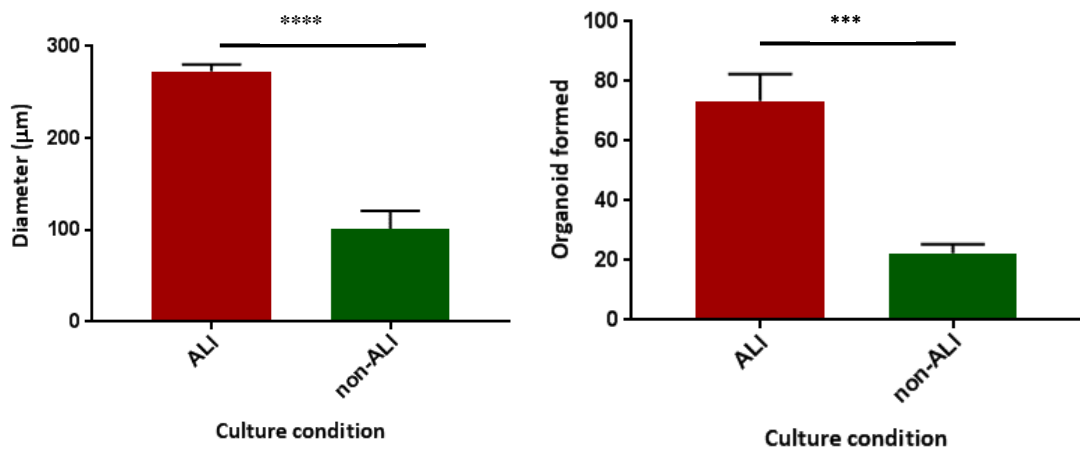


Figure 4.4 SG organoids cultured in Matrigel. Diameter of SG organoids (A), and number of SG organoids formed(B) cultured in Matrigel was compared between ALI and non-ALI cultures. N=3, ****p-value ≤ 0.0001 , ***p-value ≤ 0.001 .

4.4.2 Expression of cell specific markers in SGs organoids cultured in Matrigel

Expression of a selected panel of human salivary gland genes was analysed by RT-PCR with RNA from normal human salivary glands being compared to that isolated from 14-day organoid cultures (**Figure 4.5**). Expression of nanog (a progenitor cell marker) and CD10 and α -SMA (myoepithelial cell markers) were clearly seen under both ALI and non-ALI culture conditions. The expression of Amylase, AQP5 and MUC7 was only detected in organoids cultured at ALI. Expression of E-cadherin, ZO1 and claudin-1 were highly expressed in organoids cultured at ALI, with less expression in non-ALI cultures. Ckit and HE4 were also expressed under both culture conditions. Expression of CST1, CST5 or MUC5B was not detected in any cultures. Human OAZ1 (hOAZ1) was used as an internal control for all RT-PCR experiments.

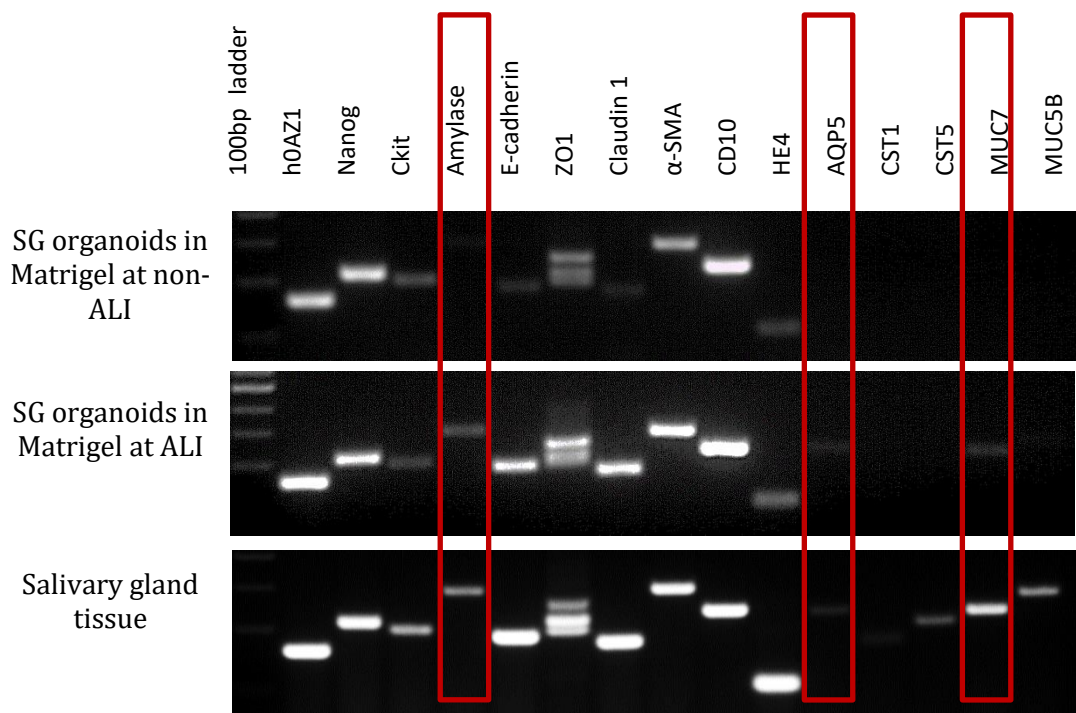


Figure 4.5 Expression of cell-type specific markers of SG organoids cultured in Matrigel. RT-PCR expression of a selected panel of salivary gland genes in organoids cultured in Matrigel for 14 days compared to normal salivary gland tissue. hOAZ1 was used as an internal control.

4.4.3 Localisation of epithelial markers in SG organoids cultured in Matrigel

Immunohistochemistry was used to study the localisation of the epithelial marker, CK5, and the myoepithelial marker, α -SMA, in SG organoids cultured in Matrigel at Day 14 (**Figure 4.6**). Positive staining of CK5 was found both at ALI and non-ALI, however, α -SMA was detected only at the periphery of ALI cultures with no positive staining in non-ALI cultures.

At this stage, I stained CK5 by immunofluorescence. Staining of nuclei with DAPI and Z-slice imaging using confocal microscopy demonstrated that the epithelial cells were uniformly compact around the periphery of the organoid (**Figure 4.7A and 4.7C**) with fewer cells towards the centre (**Figure 4.7B and 4.7D**). They also appeared to form, buds and branches from the mainly spherical structures.

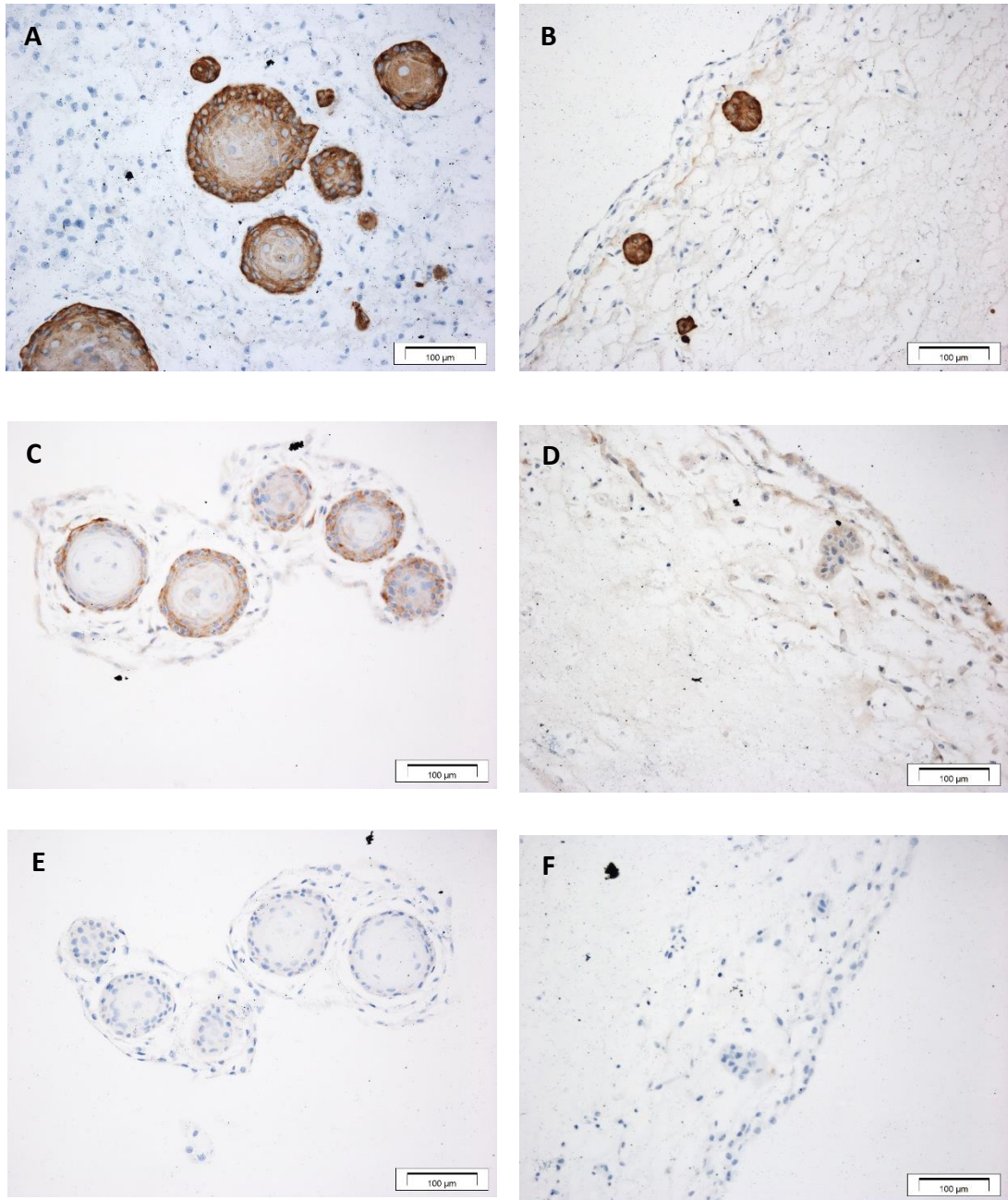


Figure 4.6 Immunohistochemistry of SG organoids cultured in Matrigel. Positive staining of CK5 in SG organoids cultured in Matrigel for 14-days at ALI (A) or non-ALI (B), α -SMA at ALI (C) or non-ALI (D), with negative controls at ALI (E) or non-ALI (F). Representation of three independent batches. Scale bars = 100 μ m.

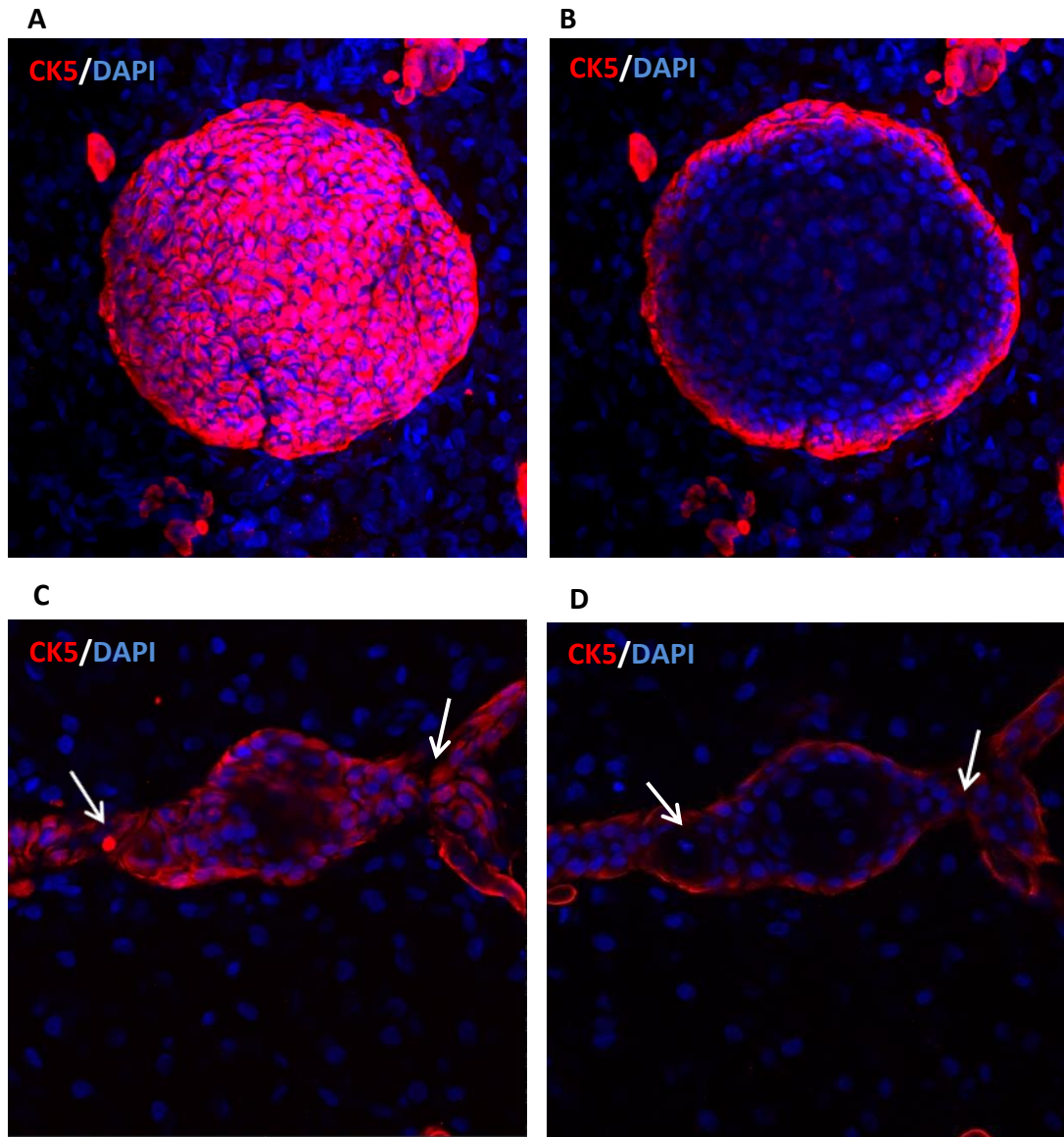


Figure 4. 7 Immunofluorescent confocal microscopy of SG organoids cultured in Matrigel. Confocal images (representative of three independent batches) of CK5 (red) and DAPI (blue) showing spherical (A-top, B-middle), and budding and branching (arrows)(C-top, D-middle) structures of SG organoids at 40x magnification.

4.4.4 Morphological analysis of SG organoids cultured in Myogel

Differentiated organoid structures resembling mini-glands developed when the cells were grown in Matrigel but this was less obvious when grown in Myogel. As Myogel is less solid than Matrigel, more gel-like, the SG cells tended to settle at the bottom and attach to the plate rather than remaining suspended in the matrix. Thus, the cells grew as a 2D model rather than forming 3D organoids (**Figure 4.8**).

The SG cells cultured in Myogel at ALI adhered to the membrane of the transwell and displayed small clumping islands of cells surrounded by flat, elongated cells (**Figure 4.8A**). Two distinct sub populations of cells could be observed in submerged cells (non-ALI); the majority were flat, polygonal, more compactly arranged cells, intersected by clusters of slightly elevated and elongated cells (**Figure 4.8B**).

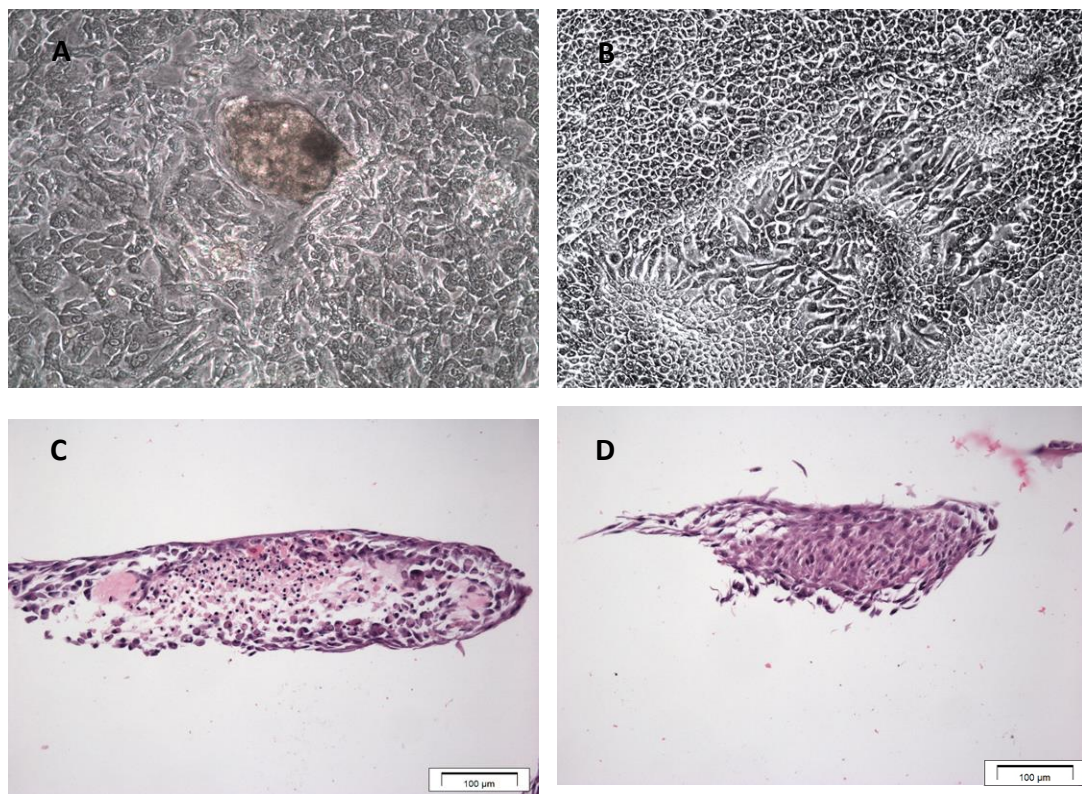


Figure 4.8 Salivary gland cells cultured in Myogel. SG cells grew as a 2D-model rather than forming organoids when cultured in Myogel at ALI (A), and non-ALI (B) (10x magnification). Haematoxylin and eosin stained sections of SG cells cultured in Myogel at ALI (C), and non-ALI (D) for up to 14-days. Scale bar=100 μm.

4.4.5 Morphological analysis of SG cells cultured in combinations of Matrigel and Myogel

Experiments were undertaken to further examine the potential role for Myogel as an ECM supporting the growth of SG organoids in which a combination of Matrigel and Myogel (1:1) was used. SG cells did not grow under non-ALI conditions, however, two different populations of cells, 2D and 3D organoids were seen in the ALI cultures. The organoid models appeared to form and differentiate in the Matrigel only as the two matrices separated from each other rather than remaining as a single suspension (Figure 4.9).

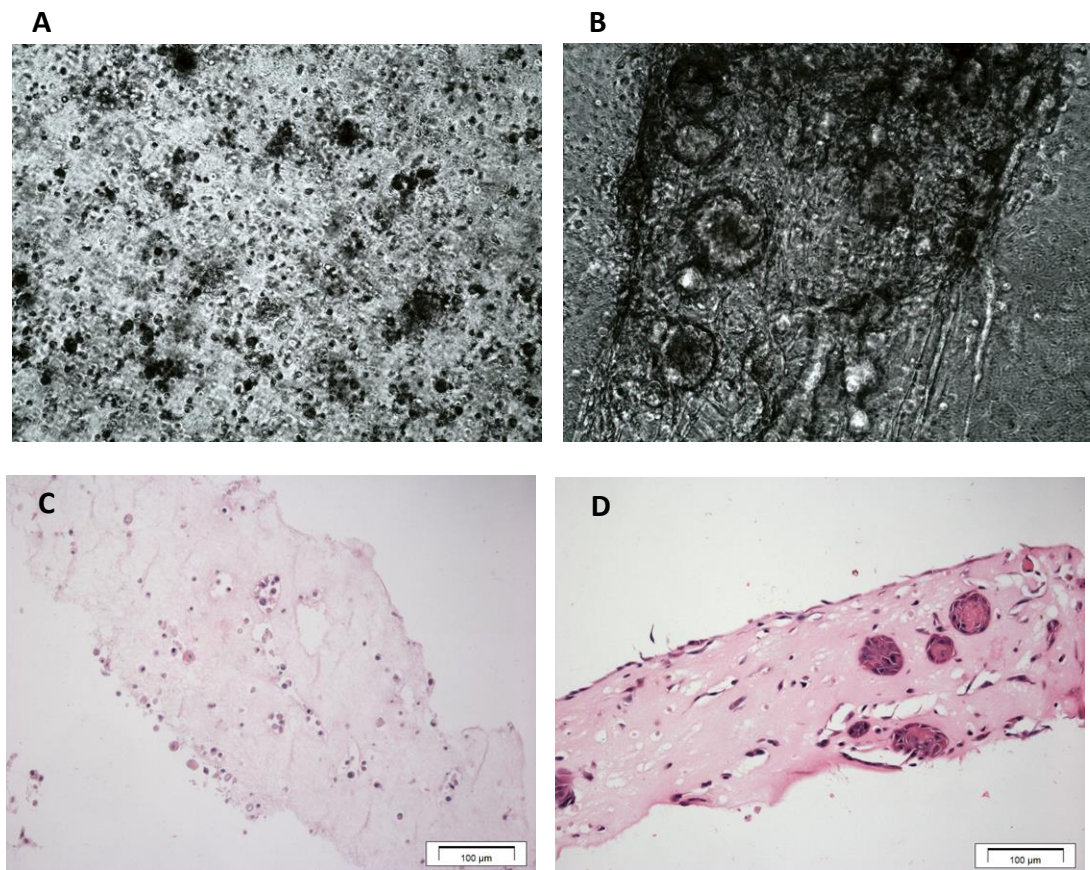


Figure 4.9 Salivary gland cells cultured in a mixture of Matrigel and Myogel (1:1). At non-ALI conditions, the cells did not grow (A), while they formed two populations at ALI conditions, 2D and 3D organoids (B) (10x magnification). Haematoxylin and eosin stained sections of SG cells cultured in Matrigel/Myogel mixture at ALI (C), and non-ALI (D) for 14-days. Scale bar=100 μ m.

4.4.6 Expression of cell specific markers in SG organoid models cultured in Myogel with and without Matrigel

Using RT-PCR, expression of cell specific markers identified in Figure 4.10 were compared between RNA from normal human salivary glands and that from four different cultures conditions; Myogel at ALI and non-ALI and a mixture of 1:1 Matrigel and Myogel, both at ALI and non-ALI. All cultures were grown for 14 days.

The SG cells cultured in Myogel were unable to form organoids, however, relatively high expression of amylase and AQP5 RNA were detected when cultured at an ALI, both with Myogel alone and also in the 1:1 mixture of Matrigel and Myogel. Interestingly, the SG cells in the mixture of Matrigel and Myogel also expressed the mucous cell markers, MUC7 and MUC5B. There was no noticeable difference in expression of any of the other genes analysed.

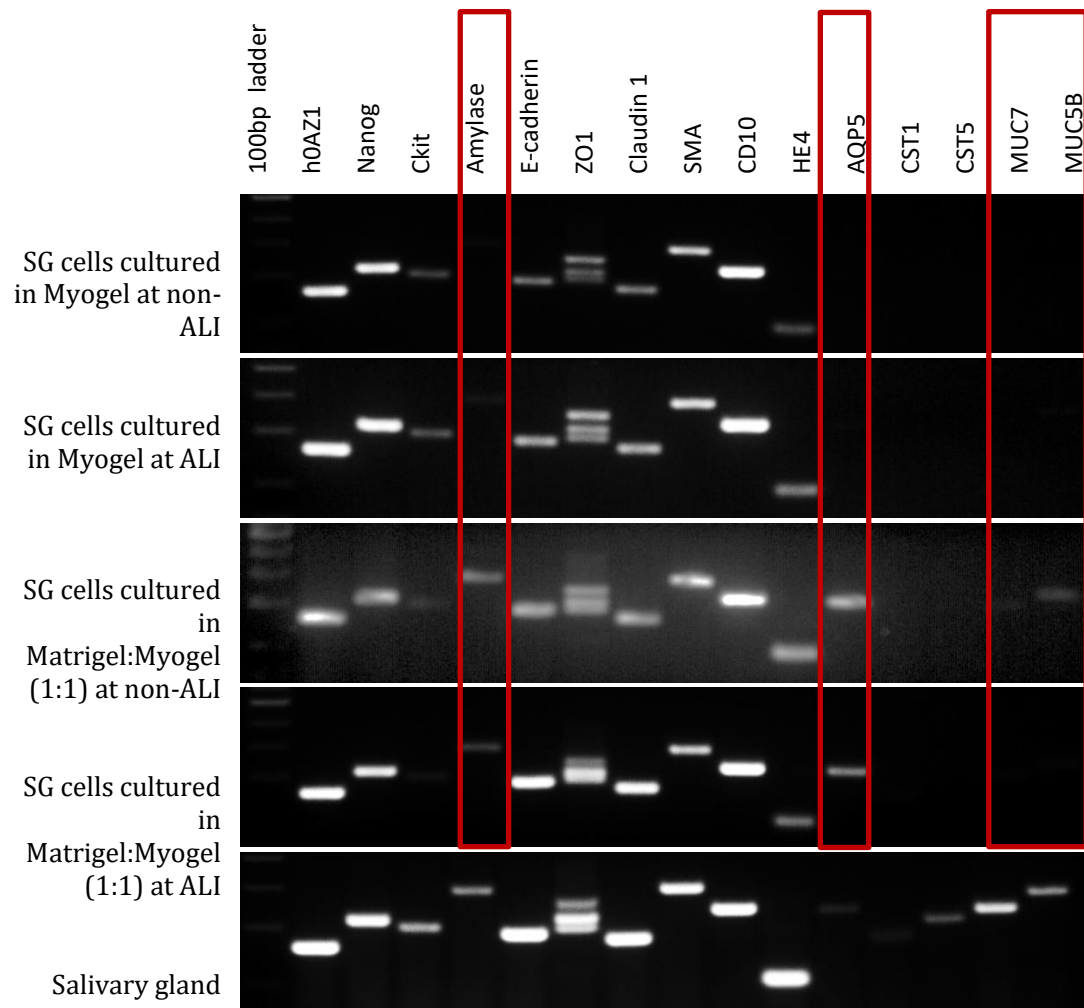


Figure 4. 10 Expression of cell specific markers of SG cells cultured in Myogel with and without Matrigel. RT-PCR expression of a selected panel of salivary gland genes in organoids cultured in Myogel with or without Matrigel for 14 days compared to normal salivary gland tissue. hOAZ1 was used as internal control.

4.4.7 Infection of SG Organoid cultured in Matrigel with *S. aureus*

Having successfully developed an SG organoid model in Matrigel under ALI conditions, we evaluated its utility as a model of salivary gland infection. We infected the SG organoids at day 14 with FITC-tagged *S. aureus*. IFC microscopy indicated that only a few bacteria were able to invade into the SG organoids, and some of them infected the SG cells at 24 hours post infection (hpi) as shown in Figure 4.11B. Figure 4.11C shows that at 48 hpi, a small number of bacteria had infected the inner cells of SG organoids as well as the outer cells. By 72 hpi, the bacteria had infected the majority of the peripheral cells of the organoids (Figure 4.11D) but did not appear to affect viability (not directly assessed).

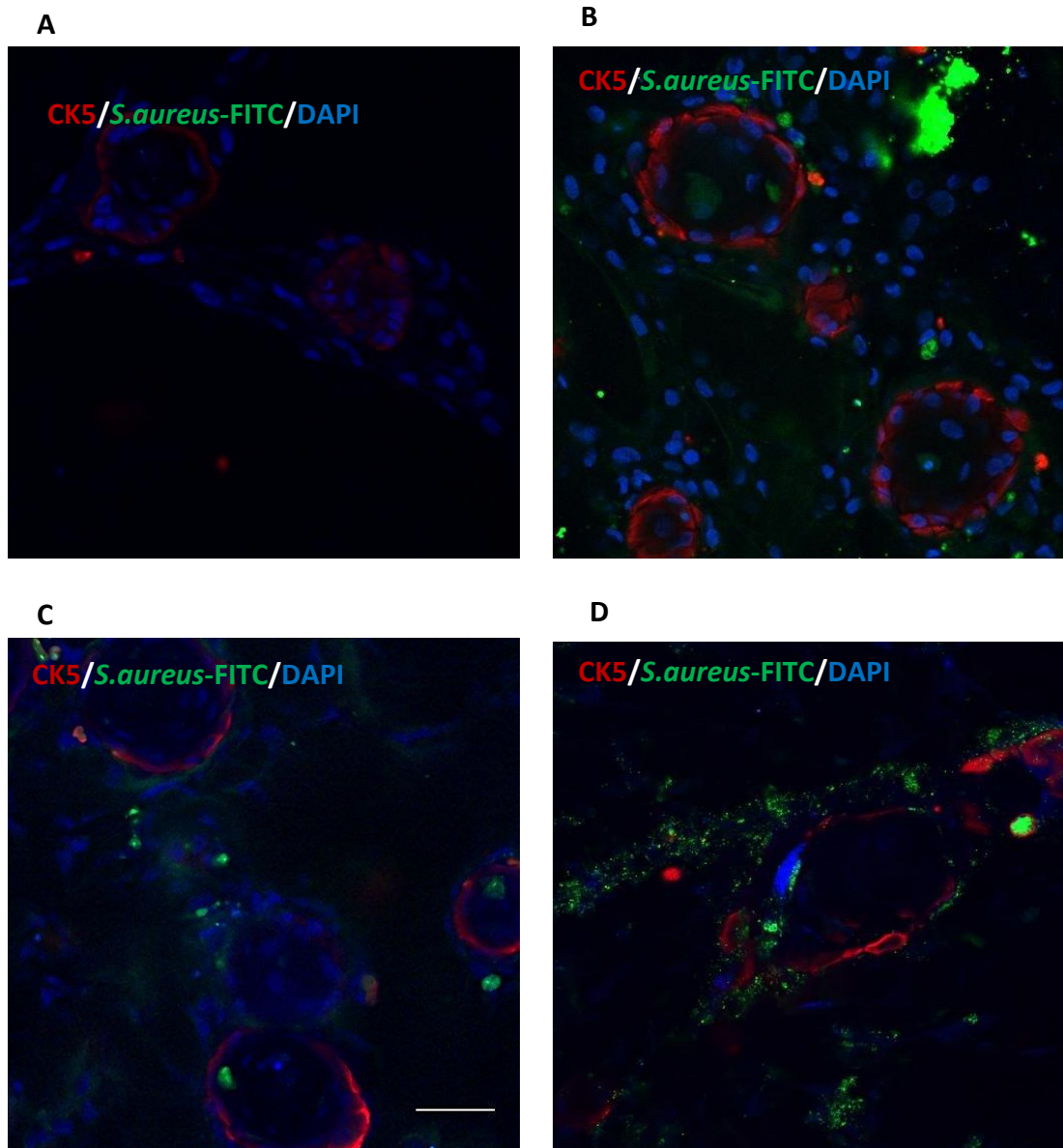


Figure 4. 11 SG Organoids as Model for Infectious Diseases: *S. Aureus*. Images (representative of three independent batches) of SG organoids infected with *S. aureus*-FITC (green), positive staining of CK5 (red) and DAPI (blue) at 24hpi (B), 48hpi (C) and 72hpi (D). SG organoids cultured without *S. aureus* was used as negative control for 72 hours (A). 40x magnification.

4.5 DISCUSSION

We have determined, for the first time, favourable conditions to isolate and grow 3-dimensional organoid cultures from primary human salivary gland cells, which will allow us to study regeneration of human salivary glands and the pathogenesis of disease. The SG cells, cultured in Matrigel with specific growth factors, differentiated into mini-glands with phenotypic expression of specific SG genes and proteins.

The culture method that I have established was adapted from those used to culture mouse salivary gland organoids (Nanduri *et al.*, 2014; Maimets *et al.*, 2016). The culture media was supplemented with a number of specific growth factors including, EGF which is important for mitogenesis of stem cells (Clevers, 2013). FGF signalling is essential for SG branching morphogenesis and cell survival, however, it's role remains unclear in the initiation of bud formation (Patel, Sharpe and Miletich, 2011). The addition of ROCKi to cell cultures has previously been shown to promote basal cell expansion in airway epithelial cultures (Mou *et al.*, 2016). Furthermore, previous studies have indicated that in using ROCKi, the number of transwell cultures could be maximised from a limited number of cells isolated from the middle ear epithelium, without altering differentiation (Mulay *et al.*, 2016). We did not formally investigate the difference in the presence/absence of ROCKi in the media at early stages of culture.

Wnt3a and R-spondin 1 have previously been shown to be vital for proliferation, differentiation and long-term culture of small intestine (Sato *et al.*, 2011), stomach (Bartfeld *et al.*, 2015) and liver (Huch *et al.*, 2015) 3D cultures or organoids. The Wnt pathway appears to be the main driver of epithelial adult stem cells (Clevers, 2016) constituting the key pathway in maintaining stem cell fate and driving proliferation of stem and daughter cells. Similarly, Maimets *et al.* (2016) identified Wnt signalling as a key driver of adult SG stem cells which allowed extensive *in vitro* expansion and enabled restoration of SG function upon transplantation of cells into the SMG of irradiated mice. R-spondin 1 is a Wnt signal amplifier, a vital factor to activate Wnt signalling (Sato *et al.*, 2011). Thus, the addition of these essential components to the

culture media is one of the keys to success in growing the SG organoids, as was observed in this study.

Matrigel is commonly used as an ECM in experimental studies, is known to stimulate and maintain differentiation of a number of cell types (Maria *et al.*, 2011) and allows remodelling of cell behaviour *in vitro*. In the present study, Matrigel was mixed with culture medium containing SG cells prior to seeding on a transwell insert. This technique provided a 3D framework rich in laminin and collagen to allow the cells to grow into organoids. The same protocol has previously been shown to allow the formation of more rigid neural-epithelial tissues (Eiraku *et al.*, 2008; Clevers, 2016). The cultures were then grown at either ALI or submerged in media (non-ALI). Interestingly, this study shows the SG cells grown in Matrigel differentiated to form mini-glands/organoids with budding and branching structures, particularly when grown at an ALI rather than under traditional conditions with cells fully submerged in culture medium. ALI culture conditions have not been previously described in studies attempting to culture mouse salivary organoids (Nanduri *et al.*, 2014; Maimets *et al.*, 2016). Although growth at an ALI does not exactly mimic the *in vivo* salivary gland, mammalian glandular cells are never fully submerged in fluid. Furthermore, the SG cells at ALI were not exposed to the air as they were somewhat protected by the Matrigel and secretions they themselves produced. The conditions we have proposed, may allow the Matrigel to become somewhat stiffer and thus provide further support for the growth not only of differentiated organoids but also those that more closely resemble the *in vivo* situation.

Matrigel, although a useful experimental tool, is derived from mouse sarcoma and thus could not be used in the development of clinical applications. In order to investigate alternative matrices SG cells were cultured in Myogel, an ECM derived from a benign human uterine leiomyoma (Salo *et al.*, 2015). However, we found that the SG cells were unable to form organoids, instead they grew as monolayers. This was due in part to the physical property of Myogel, which is less solid than Matrigel, and so the cells tended to drop through the Myogel and attach to the membrane

rather than remaining in suspension. We experimented by culturing the SG cells in combinations of ECM with 1:1 of Matrigel and Myogel. We found that the two different matrices did not mix but instead formed two suspensions and thus two different cell populations, 2D and 3D organoids. Future studies will involve the addition of collagen to Myogel (Salo *et al.*, 2015) to increase the rigidity of the supporting matrix. It might be possible to use human collagen Type I, the most abundant type of collagen in the human body and which serves as a major structural protein in ECM.

Epithelial tissues require interaction with each other, extracellular matrices, and also signals from their microenvironment, to polarize (Pradhan *et al.*, 2010). The expression of mRNA for the tight junction protein, ZO-1 and cell-cell adhesion proteins, E-cadherin and claudin, in SG organoids suggests an apical-basal polarity. It is interesting to note that the expression of amylase, AQP5 and MUC7 was detected in RNA from organoids grown at ALI in either Matrigel or Myogel alone, and in the mixture of the two matrices. This suggests some functionality for this 3D culture system as both amylase and AQP5 are acinar cell markers, while MUC7 is a mucous cell marker. However, these findings need to be further confirmed by studying the proteins.

The most important finding from this study was that the organoids were able to form buds and branching structures. Wang and colleagues (2018) stated that the core structure of all branched organs consists of tightly associated epithelial cells, which will actively interact, biochemically and biophysically, with ECM and other cell types such as smooth muscle cells, neurons and blood vessels during branching morphogenesis (Wang *et al.*, 2017). Consistent with the literature, our SG organoids demonstrated positive expression of CK5, an epithelial cell marker, and expressed smooth muscle cell markers at the periphery of the organoids. The budding and branching seen in my study might be due to the fact that our culture media include receptor tyrosine kinases, FGF and EGF, which are required for most branched organs (Wang *et al.*, 2017). Similarly, Shamir and Ewald (2014), stated that the epithelia

themselves are able to branch if certain growth factors (for examples FGFs, and VEGF) are provided (Shamir and Ewald, 2014). Further research is required to investigate the factors that contribute to *in vitro* budding and branching.

Despite these promising results, questions still remain. Does growing as an organoid create any problems? One of the problems that I noticed was the ability to visualize growth without terminating the experiment. Another issue that emerges from this study is the sampling and analysis of cell secretions. As the SG organoids are growing inside the Matrigel, it is not currently possible to collect cell secretions. As we have seen, the cells were loosely 'arranged' towards the centre of SG organoids and it is possible this would be a hypoxic region. It can therefore be assumed that the cells would have limited access to nutrients and oxygen. It is also possible, however, that this might represent the initiation of lumen formation. Further work is required to investigate these questions.

An issue that was not addressed in this study is there are no details of confirmation that Wnt3a and R-spondin 1 conditioned media contained the desired molecules. Further study should take this into consideration by performing a TopFlash assay, which is known as a luciferase reporter assay. It has been used to determine the concentration and activity of both Wnt3a and R-spondin 1 in the conditioned media (Zhao, 2014). This is important in understanding that both factors contribute into the development of SG organoids.

Infection of SG organoids using the human pathogen, *S. aureus*, demonstrated that our SG organoid model can be used for the study of host-pathogen interactions within human salivary glands. In this study, we showed that *S. aureus* initially infected a small number of SG cells in culture, invaded into the SG organoids and the infection spread from both directions, inside and outside of the organoids over time. Further analysis could be carried out to gain a better understanding of the interactions between salivary gland cells and pathogens and the pathogenesis of salivary gland diseases such as Sjogren syndrome.

4.6 KEY EXPERIMENTAL CONCLUSIONS

- I have developed a suitable culture system to isolate, maintain and proliferate primary epithelial cultures from human salivary gland tissue into 3D organoids.
- SG organoids cultured in Matrigel at ALI with enriched media displayed the optimal culture conditions and were able to express acinar cell-specific markers (amylase, AQP5 and MUC7), crucial markers for human salivary glands.
- The positive staining of CK5 suggests that most cells have some progenitor cell characteristics but this needs to be further investigated.
- SG organoids were able to form buds and begin to form branches.
- SG organoids can potentially be utilised to study the pathogenesis of infectious diseases.

The main goal of the present study was to develop an organoid model of human salivary glands using normal sublingual gland cells and then use the model to study the early stages of infectious disease with *S. aureus*. In this study, we have successfully developed SG organoids from SG cells that have been isolated from SG tissue by using explant technique, cultured in Matrigel at ALI with enriched media supplemented with Wnt3A, R-spondin 1, EGF and FGF2. Moreover, the SG organoids were able to form buds and displayed positive protein expression of CK5 as well as mRNA expression of amylase, AQP5 and MUC7. Besides, we have shown that the SG organoids model can be utilised for infectious diseases study. This would be a fruitful area for further work. Further experiments should be carried out to investigate other factors that may contribute and have effects on the development of SG organoids cultures.

CHAPTER 5

Human Salivary Gland Organoid Models Cultured in Different Media

CHAPTER 5: HUMAN SALIVARY GLAND ORGANOID MODELS CULTURED IN DIFFERENT MEDIA

5.1 INTRODUCTION

I have previously shown the successful development of human SG organoid models cultured in Matrigel under ALI culture conditions. Addition of Wnt3A and R-spondin-1 to other growth factors (EGF and FGF2) appears to allow indefinite growth of human SG organoids.

Transforming growth factor- β (TGF β) and bone morphogenic protein (BMP) signalling have been acknowledged to promote progenitor proliferation, migration and survival (Broutier *et al.*, 2016). BMP/TGF β signalling also balances stem cell proliferation, differentiation and reversible cell-cycle exit and regulates the maintenance of stem cells and their activity in response to tissue injury (Oshimori and Fuchs, 2012; Mou *et al.*, 2016). Furthermore, BMP/TGF β signalling inhibition has been used to prevent spontaneous differentiation of, and thus facilitate, mouse colon and tracheal organoid cultures (Barker *et al.*, 2010; Mou *et al.*, 2016).

A previous study has described the use of dorsomorphin (DM) to mimic the function of the endogenous BMP inhibitor, Noggin, to direct cardiomyocyte formation in mouse embryonic stem cells (Ao *et al.*, 2012). DMH1, dorsomorphin homologue 1, a second-generation small molecule BMP inhibitor, has been shown to be a more selective inhibitor of BMP Type I receptors than DM (Ao *et al.*, 2012) and has thus been selected for our study.

A8301 is a potent inhibitor of the TGF β type I receptor superfamily activin-like kinase, ALK5 and its relatives ALK4 and ALK7. It inhibits SMAD signalling and epithelial-to-mesenchymal transition by transforming growth factor β but has no effect on BMP signalling. It has been used to maintain self-renewal and proliferation of rat and human induced pluripotent stem cells in cultures without feeder layers (Li *et al.*, 2009). Furthermore, it also prevented senescence and apoptosis of cultured human endometrial mesenchymal stem cells (MSC), and thus may have a role in

spontaneous MSC differentiation during culture expansion (Gurung, Werkmeister and Gargett, 2015). Thus, I would like to determine whether A8301 can maintain growth and prevent the spontaneous differentiation of SG cells during culture expansion.

LIM kinases play crucial roles in various cell activities, including migration, division, and morphogenesis by phosphorylating and inactivating cofilin. They regulate both actin and microtubule organization which is contributed to salivary gland branching morphogenesis (Ray *et al.*, 2014). SR7826 is potent and selective LIM kinase inhibitor, which inhibits cofilin phosphorylation and suppresses migration and invasion of cells *in vitro*. Thus, we would like to investigate the responses of SR7826 during morphogenetic process in SG cells development.

This chapter outlines the effects of specific differentiation factors, DMH1 (BMP inhibitor), A8301 (TGF β inhibitor) and SR7826 (LIMK inhibitor) on the development, cell viability and morphology of SG organoids. Preliminary proliferation assays of SG monolayer cultures in enriched media with specific differentiation inhibitors allowed us to assess any detrimental effects of the inhibitors on cell growth prior to their use in organoids cultures.

Previously I demonstrated that the human SG organoids expressed CK5, an epithelial cell marker. Following the addition of the specific differentiation factors we included four new cell-type specific markers in order to assess the similarity of the cells within the organoids to native salivary gland tissue. These included acinar cell markers (BPIFA2, AQP5), a ductal cell marker (CK7), and the cell adhesion marker (E-cadherin). α -amylase, an important digestive enzyme, is produced only by salivary glands and thus in order to confirm the functionality of our SG organoids, we performed amylase activity assays.

5.2 AIM

To investigate the effects of differentiation factors on the development of SG organoid cultures.

5.3 MATERIALS AND METHODS

5.3.1 Media preparation with differentiation factors in enriched media

A8301 (Cat#: 2939, Tocris, Bristol, UK)

2.1 mg was added to 100 μ l of DMSO and mixed with gentle warming in water bath for a final concentration of 50 mM. The solution is made immediately prior to use.

DMH-1 (Cat#: 4126, Tocris, Bristol, UK)

1.5 mg was added to 200 μ l of DMSO (20 mM) followed by the addition of 800 μ l of absolute ethanol and mixed with gentle warming for a final concentration of 5 mM. 10 μ l aliquots were stored at -20°C.

SR7826 (Cat#: 5626, Tocris, Bristol, UK)

3.9 mg was added to 100 μ l of DMSO (100 mM) and then 1 mL of absolute ethanol was added prior to mixing with gentle warming for a final concentration of 10 mM. 5 μ l aliquots were stored at -20°C.

Media	Final concentration of differentiation factor	Volume (V ₂ :50mL) and stock solution
Enriched Media (Nan)	-	-
Nan with DMH1	1 μ M of DMH1	10 μ L of 5 mM DMH1
Nan with A8301	1 μ M of A8301	1 μ L of 50 mM A8301
Nan with SR7826	1 μ M of SR7826	5 μ L of 10 mM SR7826
Nan with ALL	1 μ M of DMH1, 1 μ M of A8301 and 1 μ M of SR7826	10 μ L of 5mM DMH1, 1 μ L of 50 mM A8301 and 5 μ L of 10 mM SR7826

Table 5. 1 Enriched media with differentiation factors

5.3.2 Cell culture

- HuSG cells were grown and maintained as previously described (**Refer 2.2**).
- HuSG cells were cultured on PET transwell as a monolayer for viability test with Alamar blue dye (**Refer 5.3.3**).
- HuSG cells were cultured as organoid models in Matrigel at ALL, as previously described (**Refer 4.3.3**). Five different media were used as in **Table 5.1**: enriched media (Nan), Nan with DMH1, Nan with A8301, Nan with SR7826, and Nan with ALL (DMH1, A8301 and SR7826).

5.3.3 AlamarBlue®

Principle: AlamarBlue® incorporates an oxidation-reduction (REDOX) indicator that both fluoresces and changes colour in response to the chemical reduction of growth media resulting from cell growth. Live cells maintain a reducing environment within the cytosol of the cell. Resazurin, the active ingredient of AlamarBlue®, is a non-toxic, cell permeable compound that is blue in colour and virtually non-fluorescent. Upon entering cells, Resazurin is reduced to Resorufin, which is red in colour and highly fluorescent. Viable cells continuously convert Resazurin to Resorufin, increasing the overall fluorescence and colour of the media surrounding the cells.

Procedure: A 10% AlamarBlue® (BUF012B, Bio-Rad, Oxford, UK) solution was made in culture media and 2 mL added to the cell cultures. The plate was covered with aluminium foil and incubated for 5 hours at 37°C in a cell culture incubator. 200 µl of the AlamarBlue solution from the cultures was transferred to a 96-well plate and the colour change, from blue to pink, was recorded by Magellan software using a fluorescence excitation wavelength of 560nm and emission wavelength of 590nm.

5.3.4 Amylase Activity Assay

Principle: Amylase activity is determined using a coupled enzymatic assay, which results in a colorimetric (405 nm) product, proportional to the amount of substrate, ethylidene-pNP-G7, cleaved by amylase. One unit is the amount of amylase that

cleaves sufficient ethylidene-pNP-G7 to generate 1.0 μ mole of *p*-nitrophenol per minute at 25°C.

Procedure: 0, 2, 4, 6, 8, 10 μ L of the 2 mM Nitrophenol standard was added to a 96-well plate to generate 0 (blank), 4, 6, 8, 12, 16 and 20 nmole/well standards. Distilled water was added to each well to bring the volume to 50 μ L. 5 μ L of the Amylase Positive Control solution was added to one well and adjusted to 50 μ L with Amylase Assay Buffer. For the negative control, 50 μ L of PBS was added to one well. 50 μ L of each sample was also added to the 96-well plate.

A Master Reaction Mix was prepared by adding 50 μ L of Amylase Assay Buffer to 50 μ L of Amylase Substrate Mix for each reaction (per well). 100 μ L of this was added to each sample, standard, positive and negative control wells and mixed using a horizontal shaker. After 2 to 3 minutes (T_{initial}), the initial absorbance at 405 nm ($A_{405})_{\text{initial}}$ was measured. The plate was incubated at 25°C and the absorbance (A_{405}) measured every 5 minutes until the value of the most active sample was greater than the value of the highest standard (20 nmole/well). At this time, the most active sample is near to, or exceeds the end of the linear range of the standard curve. This is the final absorbance measurement ($A_{405})_{\text{final}}$ and the time of the penultimate reading is T_{final} .

The change in absorbance from T_{initial} to T_{final} was calculated as below:

$$\Delta A_{405} = (A_{405})_{\text{final}} - (A_{405})_{\text{initial}}$$

For each sample, the ΔA_{405} was compared to the standard curve to determine the amount of Nitrophenol generated by the amylase between T_{initial} and T_{final} .

5.3.5 Organoid model analysis

- Diameter of organoids was measured using FIJI-ImageJ Win64.
- Number of organoids formed was counted randomly. An average of three transwells of SG organoid cultures was counted per batch (N= 3 batches).

- HE staining was performed on 4 μ M sections of formalin-fixed paraffin embedded organoids for phenotypic assessment (**Refer 2.5**).
- RT-PCR was used for subjective analysis of mRNA expression (**Refer 2.4**).
- Immunofluorescent confocal microscopy was used to localize the expression of cell specific markers (**Refer 2.6**).
- Amylase activity was assessed to determine the amount of amylase secreted into the media by SG organoids (**Refer 5.3.4**).

5.3.6 Statistical analysis

Two-way analysis of variance (ANOVA) was carried out to compare the difference among the groups using GraphPad Prism (version 7.04) software. Data were presented as mean \pm standard error of the mean (SEM). Differences of $P < 0.05$ were considered significant.

5.4 RESULTS

5.4.1 Viability and morphology of SG cells cultured in enriched media with differentiation factors

Human SG cells isolated from explant technique were cultured as a monolayer for up to 21 days in media containing differentiation factors in order to investigate any effects on cell viability and morphology. No significant differences were found in terms of cell proliferation but morphology of the SG cells was affected by the differentiation factors.

Figure 5.1 illustrates cell viability (based on fluorescence intensity) of SG cells cultured in five different media over the 21-day period. At day 1, all samples indicated a similar level of cell viability. Surprisingly, the cell viability following culture in enriched media (Nan) decreased at day 3 but increased sharply at day 7. In all other culture conditions, the cell viability increased steadily until a plateau was reached at day 10. The cell viability in "ALL" media remained stable up to 21 days, while the remainder appeared to decrease from day 14. A statistically significant difference in cell viability was seen on day 21 between the SG cells cultured in ALL media and Nan media ($p \leq 0.05$). However, the differences in cell viability amongst the other media groups were not statistically significant.

Haematoxylin and eosin stained sections of SG cells cultured as monolayers on transwell inserts demonstrated clear changes in morphology amongst the different media combinations used. The SG cells cultured in Nan media (Figure 5.2A) as well as in A8301-media (Figure 5.2C) grew as a single layer, while in DMH1-media (Figure 5.2B), the cells, although still a monolayer, appeared slightly thinner than those grown in Nan media. Interestingly, uniform multilayers of cuboidal cells were observed in SR7826-media (Figure 5.2D) and cells cultured in ALL-media (Figure 5.2E) showed multilayer cultures of varying phenotype.

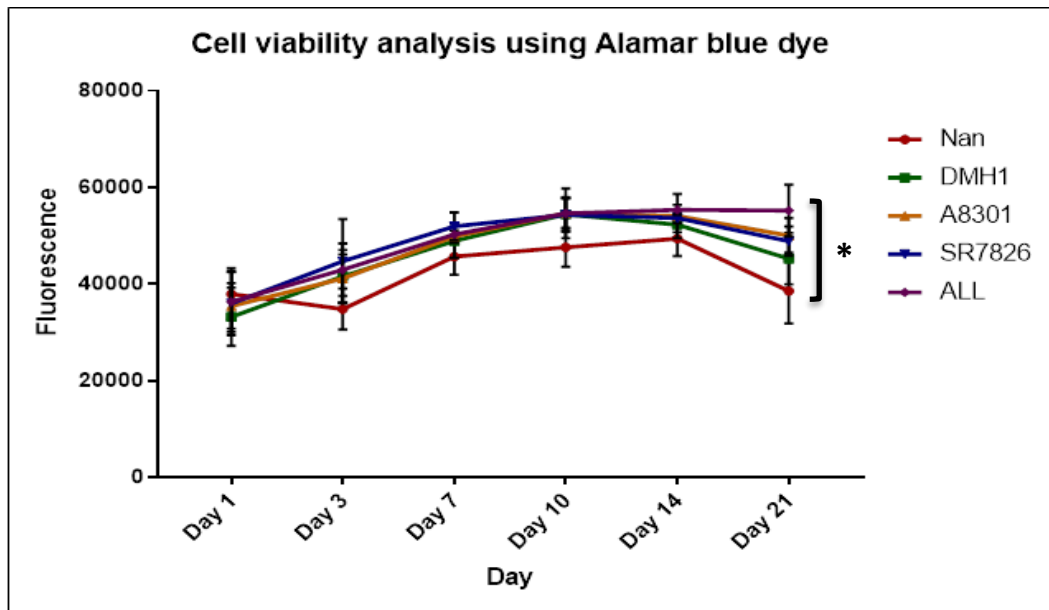


Figure 5. 1 Cell viability analysis of SG cells cultured as monolayer in different inhibitor media. Viability test of SG cells cultured as monolayer in Matrigel at ALL in Nan enriched media, Nan with DMH1, Nan with A8301, Nan with SR7826, and Nan with all inhibitors for 21-days by using AlamarBlue. N=3, *p-value ≤ 0.05 .

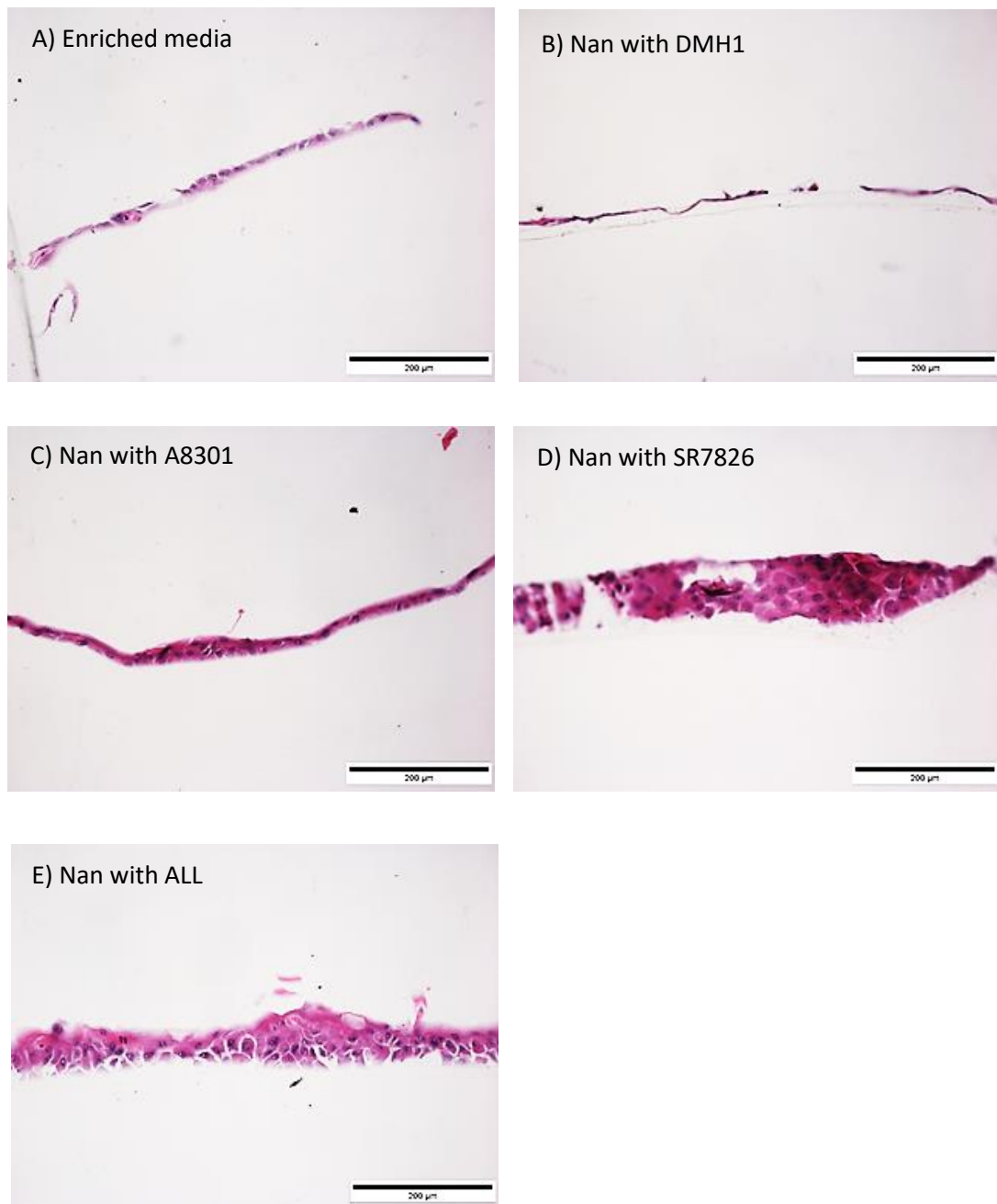


Figure 5.2 Haematoxylin and eosin stained sections of SG cells cultured as monolayer in different inhibitor media. Images show SG cells cultured in Matrigel at ALL in Nan enriched media (A), Nan with DMH1 (B), Nan with A8301 (C), Nan with SR7826 (D), and Nan with all inhibitors (E) for 14-days. Scale bars = 200µm. Images representative of three independent batches.

5.4.2 Morphological analysis of SGs organoids cultured in enriched media with differentiation inhibitors

Human SG cells isolated from explant technique were cultured as organoids in Matrigel at an ALI in media containing differentiation inhibitors for up to 14 days. At Day 14, the morphology of SG organoids was observed using a stereomicroscope prior to proceeding with histology (Figure 5.3). The number of organoids formed was counted and the diameter of the organoids measured using FIJI software (Figure 5.4).

As shown in Figure 5.3, the characteristics and morphology of SG organoids was affected by the inhibitors present in the culture media. They were more compact when cultured in media with A8301 (TGF β inhibitor; Figure 5.3C) and a significant increase was noted in the number of SG organoids formed was recorded (227.3 ± 6.26 , $p < 0.0001$; Figure 5.4A). Moreover, the number of SG organoids formed reduced significantly when grown in Nan with DMH1 as well as Nan with SR7826 media in comparison to the enriched media (Nan). However, the number increased significantly when all the three inhibitors were present (ALL media) when compared to Nan media (192.5 ± 11.24 , $p < 0.0001$).

Interestingly, the SG organoids cultured in Nan with ALL media were larger than in any of the other media (Figure 5.3E; Figure 5.4B). There was a statistically significant difference between the diameter of SG organoids grown in Nan with ALL media and Nan media ($145.4 \pm 10.33 \mu\text{m}$, $p < 0.01$). The mean diameter of SG organoids cultured in Nan with SR7826 media was significantly less than that in Nan media ($92.42 \pm 3.19 \mu\text{m}$, $p < 0.05$) but no statistically significant differences were found when cultured in Nan with DMH1 media and Nan with A8301.

Figure 5.5 illustrates very clearly the variation in morphology of the SG organoids following culture in the presence of the different inhibitors. A8301 allowed the growth of large organoids with compact multilayers of epithelial cells around the periphery but fewer cells towards the centre (Figure 5.5C), while small acinar-like structures could be seen following growth with DMH1 (Figure 5.5B). SG organoids

cultured in Nan with ALL media demonstrated acinar-like structures with stratified squamous cells (Figure 5.5E) whereas, simple cuboidal cells were seen at the periphery of organoids cultured in SR7826 media (Figure 5.5D).

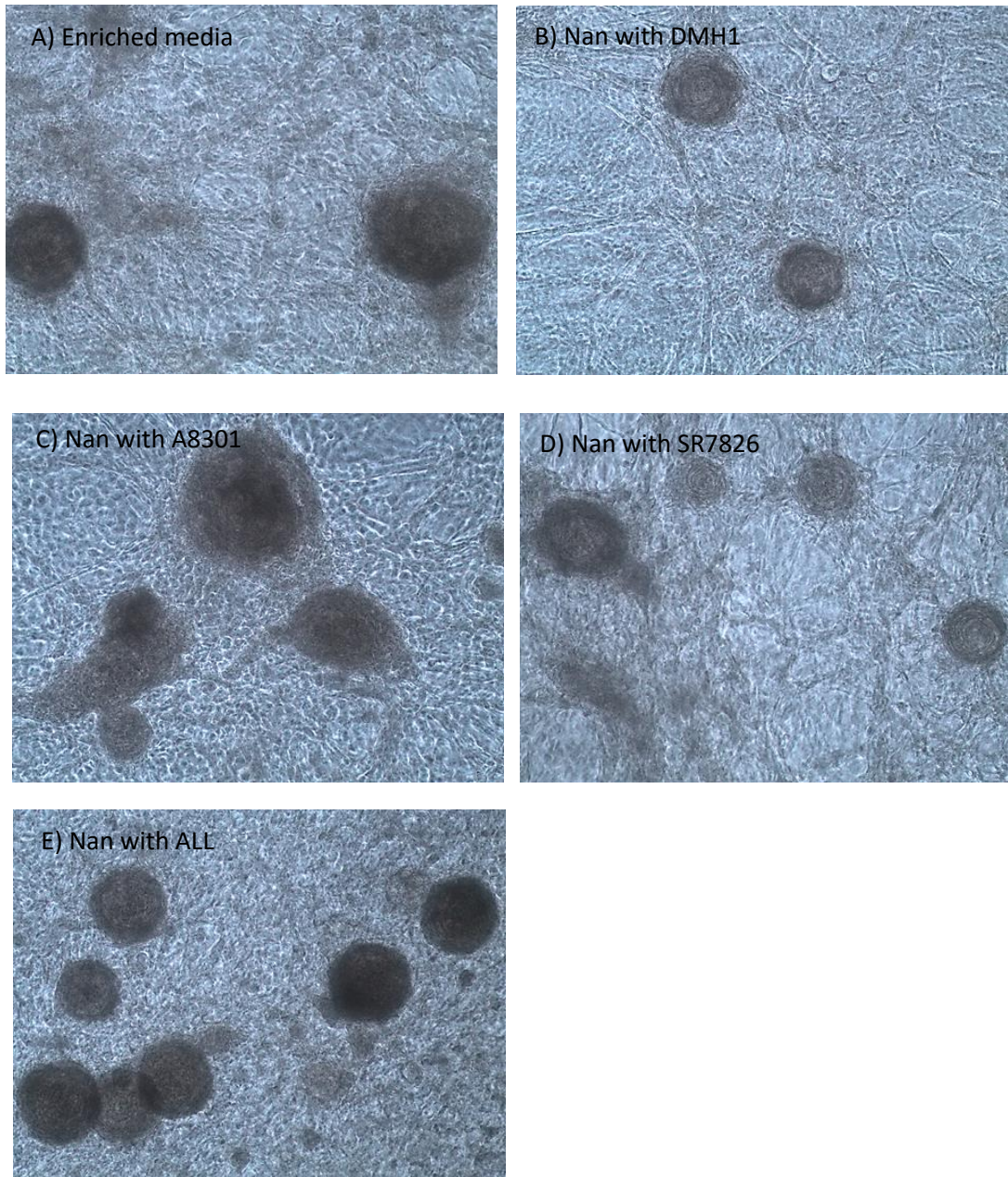


Figure 5.3 SG organoids cultured in different inhibitor media. Images (representative of three independent batches) showing SG organoids cultured in Matrigel in enriched Nan media (A), Nan with DMH1 (B), Nan with A8301 (C), Nan with SR7826 (D), and Nan with all inhibitors (E) for 14-days at ALI. Magnification at 10x.

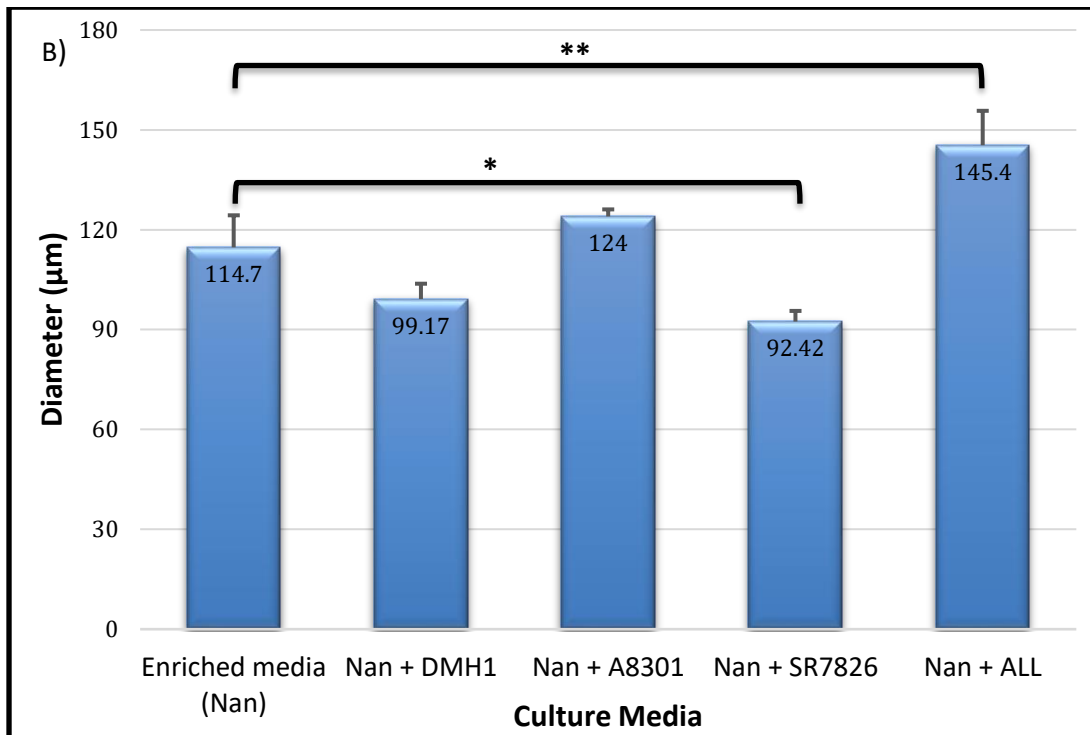
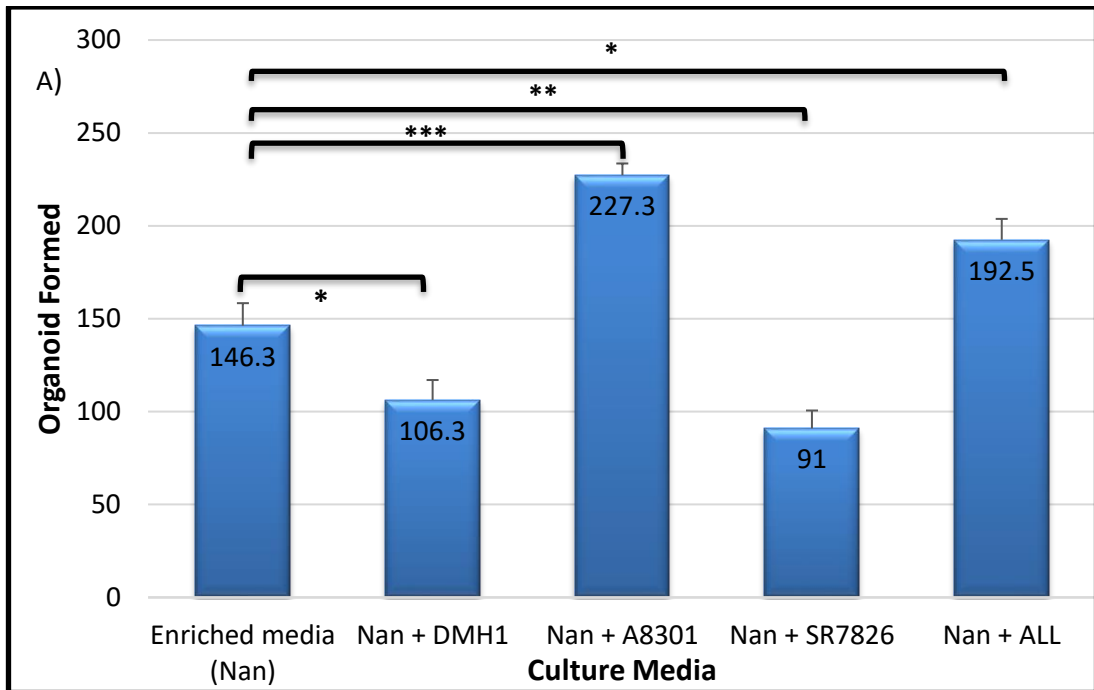


Figure 5.4 SG organoids cultured in Matrigel at ALI in different inhibitor media. Number of SG organoids formed (A), and diameter of SG organoids (B) cultured in Matrigel at ALI for 14-days was compared amongst culture media. N=3, ***p-value ≤ 0.001 , **p-value ≤ 0.01 , *p-value ≤ 0.05 .

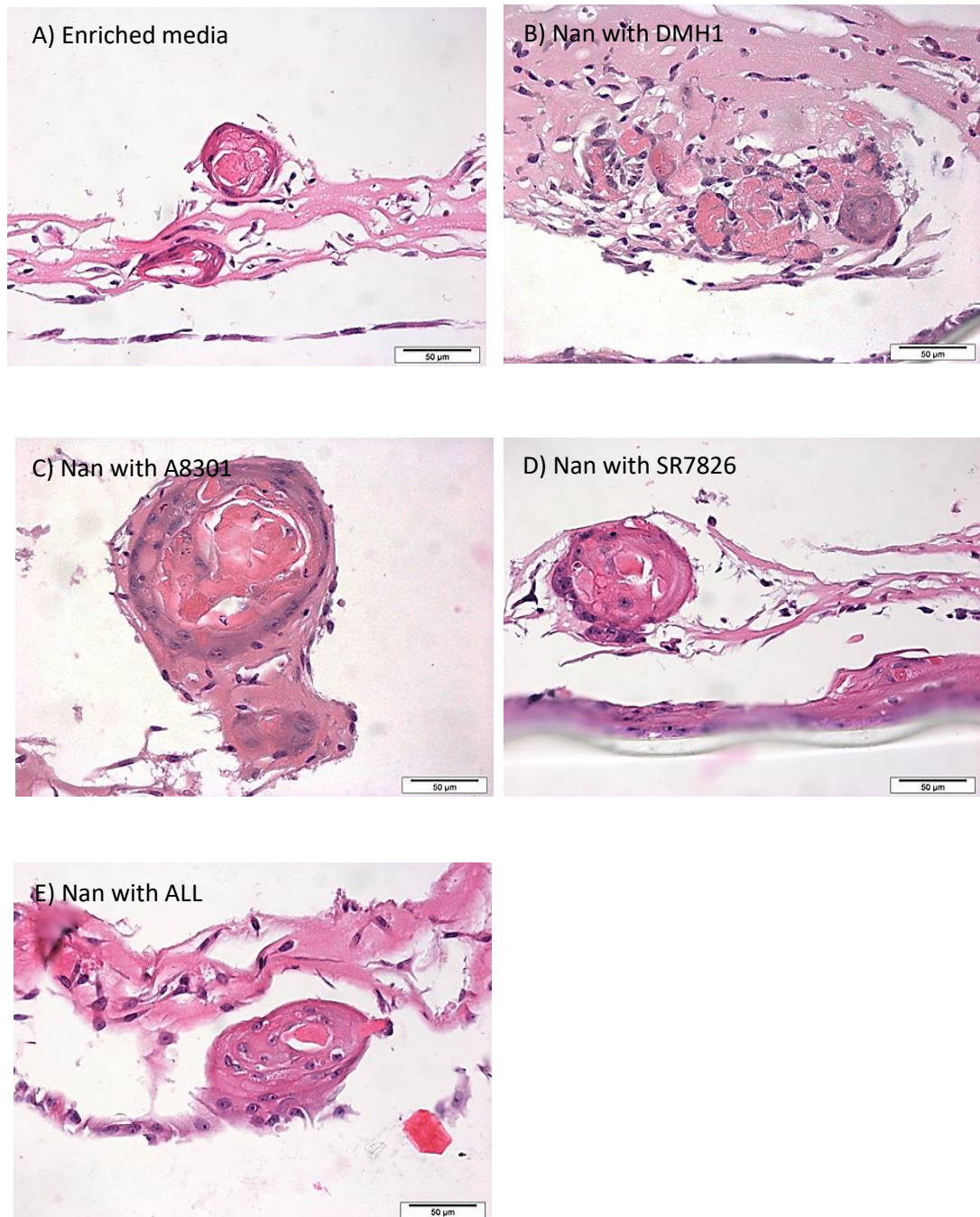


Figure 5.5 Haematoxylin and eosin stained sections of SG organoids cultured in different inhibitor media. Images show organoids cultured in Matrigel at ALI in enriched Nan media (A), Nan with DMH1 (B), Nan with A8301 (C), Nan with SR7826 (D), and Nan with all inhibitors (E) for 14-days at ALI. Scale bars = 50µm. Images representative of three independent batches.

5.4.3 RNA expression of cell specific markers in SG organoid models cultured in enriched media with differentiation inhibitors

To further characterize the SG organoids, we assessed the expression of progenitor, acinar, ductal and myoepithelial cell-specific markers. Expression of nanog (a progenitor cell marker), E-cadherin, ZO1 and claudin-1 (ductal cell markers), α -SMA and CD10 (myoepithelial cell markers) and HE4 was high following culture in all types of media. Amylase and AQP5 (acinar cell markers) were also detected in the cultures but low expression of AQP5 appeared in Nan with A8301 media. Interestingly, expression level of MUC7 (a mucous cell marker) and cKIT (a progenitor cell marker) were detected only in SG organoid models cultured in Nan with A8301 media. There was no expression of MUC5B in any of the cultures (**Figure 5.6**).

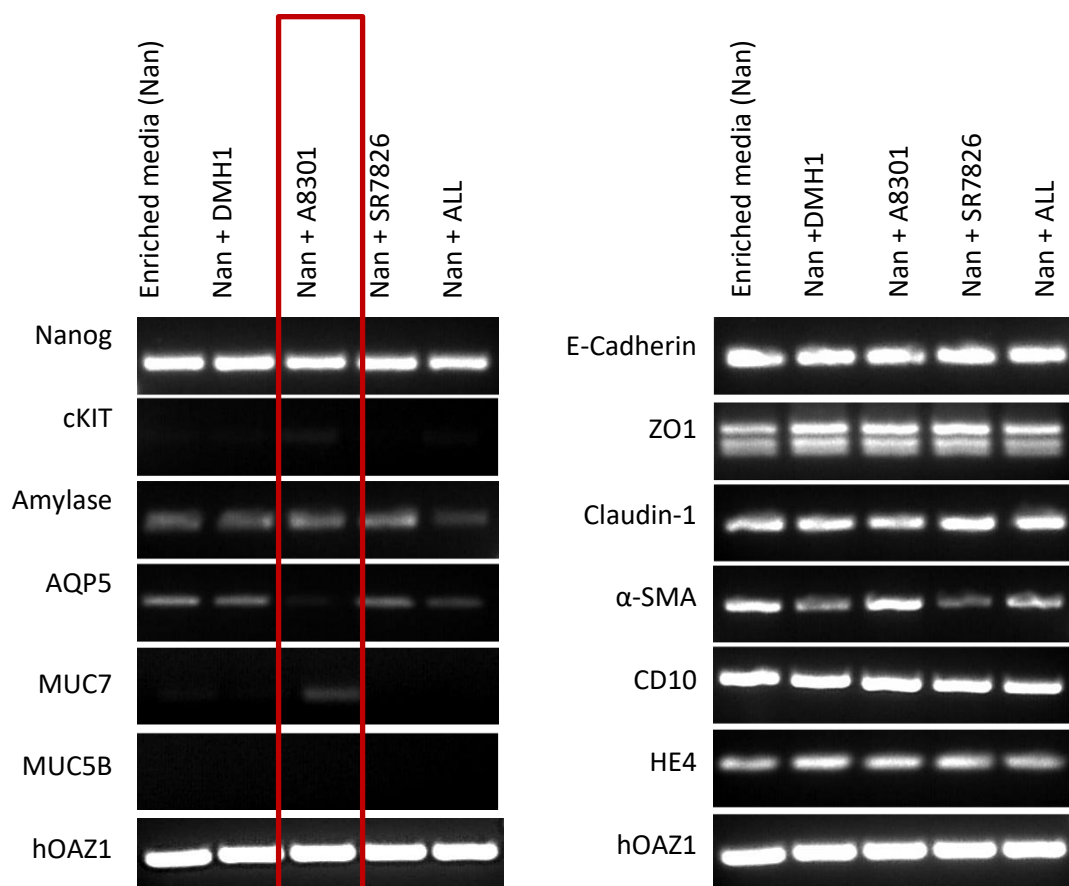


Figure 5.6 Expression of cell specific markers of SG organoids cultured in different inhibitor media. RT-PCR expression of a selected panel of salivary gland genes in organoids cultured in Matrigel at ALI in enriched Nan media, Nan with DMH1, Nan with A8301, Nan with SR7826, and Nan with all inhibitors for 14-days at ALI. hOAZ1 was used as an internal control.

5.4.4 Localisation of epithelial cell marker, CK5 and ductal cell marker, CK7 in SG organoid cultured in enriched media with differentiation factors

To confirm that our SG organoids represent native SG, we localised cell specific markers present in human salivary glands through immunofluorescent confocal microscopy. CK5 was used initially as it is a well-established epithelial cell marker, and its presence has been correlated with SG morphogenesis. CK5 was stained with Alexa-Fluor 568 (red). CK7 has previously been used to detect ductal cells present in SG cultures (Nanduri *et al.*, 2014). CK7 was detected with Alexa-Fluor 477 which displayed as green. In this study, co-localization of CK5 and CK7 would be observed as a yellow colour.

Figure 5.7 illustrates the distinct morphology of SG organoids cultured in different media as well as the staining of CK5 and CK7. CK5 was observed in all of the SG organoids cultured in each media, mostly at the periphery of the structures. Thus, CK5 was used as a guidance to detect the presence of SG organoids in the cultures.

As can be seen in Figure 5.7A, the SG organoids cultured in Nan media were differentiated from a spherical form into ductal-like structures with branches into a what looked like acinar-like structures. CK7 staining was seen near the junctions that formed the branching structures. Some of the small SG organoids showed co-localisation of CK5 and CK7. This finding is similar with the observation seen in SG organoids cultured in Nan with DMH1 media (Figure 5.7B). More CK7 was observed in the areas of ductal-like structures compared to spherical form.

The most striking results to appear from the data is the morphology of SG organoids cultured in Nan with A8301 (Figure 5.7C). The structures of these was very different when compared amongst other groups media. They formed two distinct structures with the basal organoids consists of simple squamous and cuboidal epithelial cells, and the projection of branching from the organoid consisted of what appeared to be squamous and columnar epithelial cells. Furthermore, CK5 was detected at the basal area of the organoid, whilst both CK5 and CK7 proteins were seen at the protrusion structure of the SG organoids.

In SG organoids cultured in Nan with SR7826 media, the cells also differentiated into spherical forms but clear structures of branching organoids were not seen. There was positive CK7 expression in a few areas (Figure 5.7D).

As shown in Figure 5.7E and Figure 5.7F (under 20x magnification), the structure of SG organoids cultured in Nan with ALL media had two distinct characteristics, the basal organoids with cuboidal epithelial cells and the protrusion organoids with columnar epithelial cells. Interestingly, CK7 was detected in the protrusion organoid structures only. SG organoids cultured in A8301-media and ALL-media formed two distinct structures with basal and protrusion organoids but differed in their expression CK7. Figure 5.7G shows an immunofluorescent staining negative control of SG organoids in enriched media.

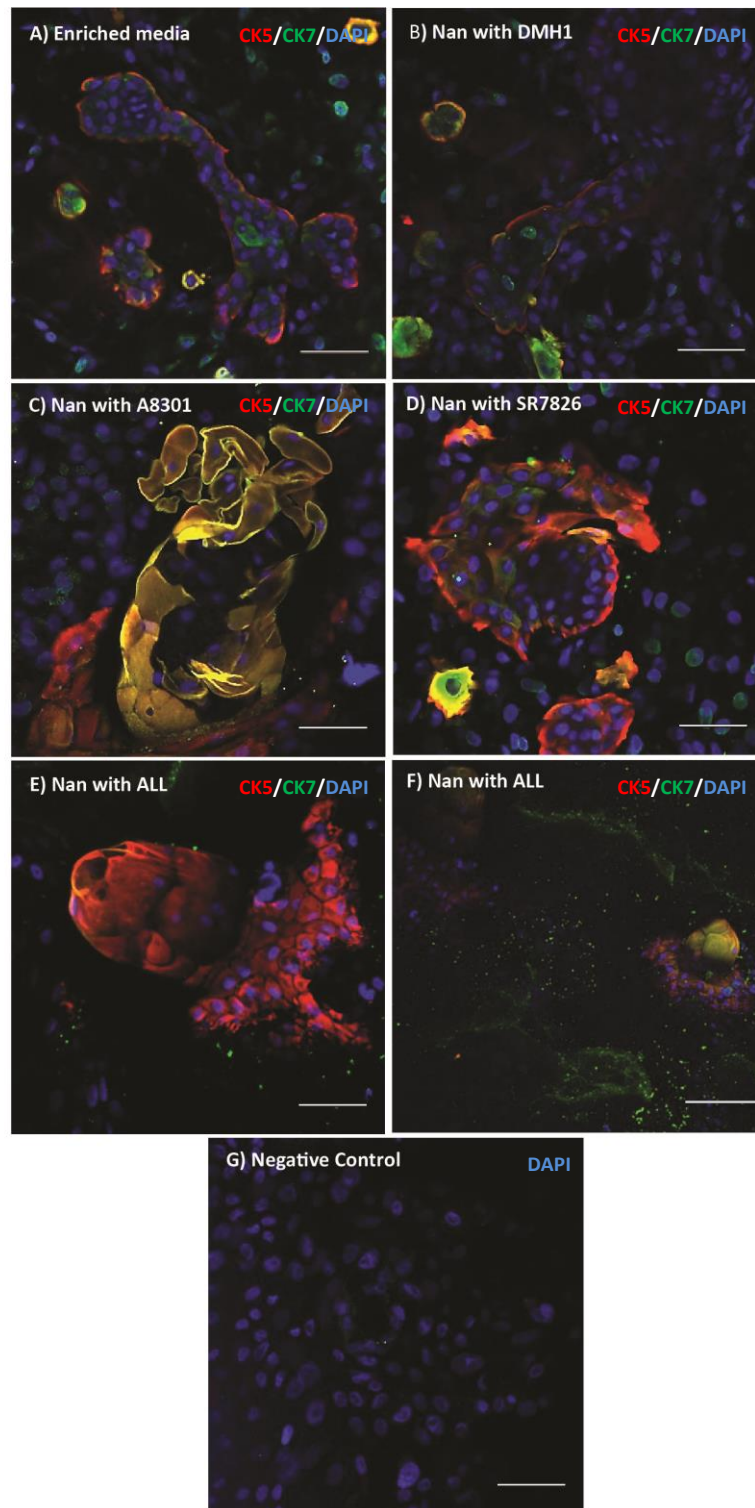


Figure 5. 7 Localisation of ductal cell marker, CK7 in SG organoids cultured in different inhibitor media. Images (representative of three independent batches of SG cells) show positive expression of CK5 (red), **CK7** (green) in SG organoids cultured in Matrigel in enriched Nan media (A), Nan with DMH1 (B), Nan with A8301 (C), Nan with SR7826 (D), Nan with all inhibitors (E), Nan with all inhibitors under 20x magnification(F) and negative control of SG organoids cultured in enriched media (G) for 14-days at ALI. Scale bars = 50µm.

5.4.5 Localisation of acinar cell marker, BPIFA2 in SG organoid cultured in enriched media with differentiation factors

BPIFA2 is expressed in both major and minor human salivary glands, specifically in serous cells (Bingle et al, 2009; da Silva *et al.*, 2011). Our findings demonstrated that BPIFA2 was detected in the SG organoids, mostly in cells in the middle area of the structure. This can be seen in SG organoids cultured in Nan media (Figure 5.8A). However, only a few cells stained for BPIFA2 in the cultures of Nan with DMH1 media. Interestingly, staining was observed not only inside the SG organoids but also in the cells nearby (Figure 5.8B).

Closer inspection of SG organoids cultured in Nan with A8301, shows the expression of BPIFA2 at the junction of branching structures (asterisk) and also towards the centre of the SG organoids (Figure 5.8C). In Nan with SR7826 media, BPIFA2 was seen in some of the SG organoids (Figure 5.8D). Figure 5.8E, shows that BPIFA2 was abundant in SG organoids cultured in Nan with ALL media.

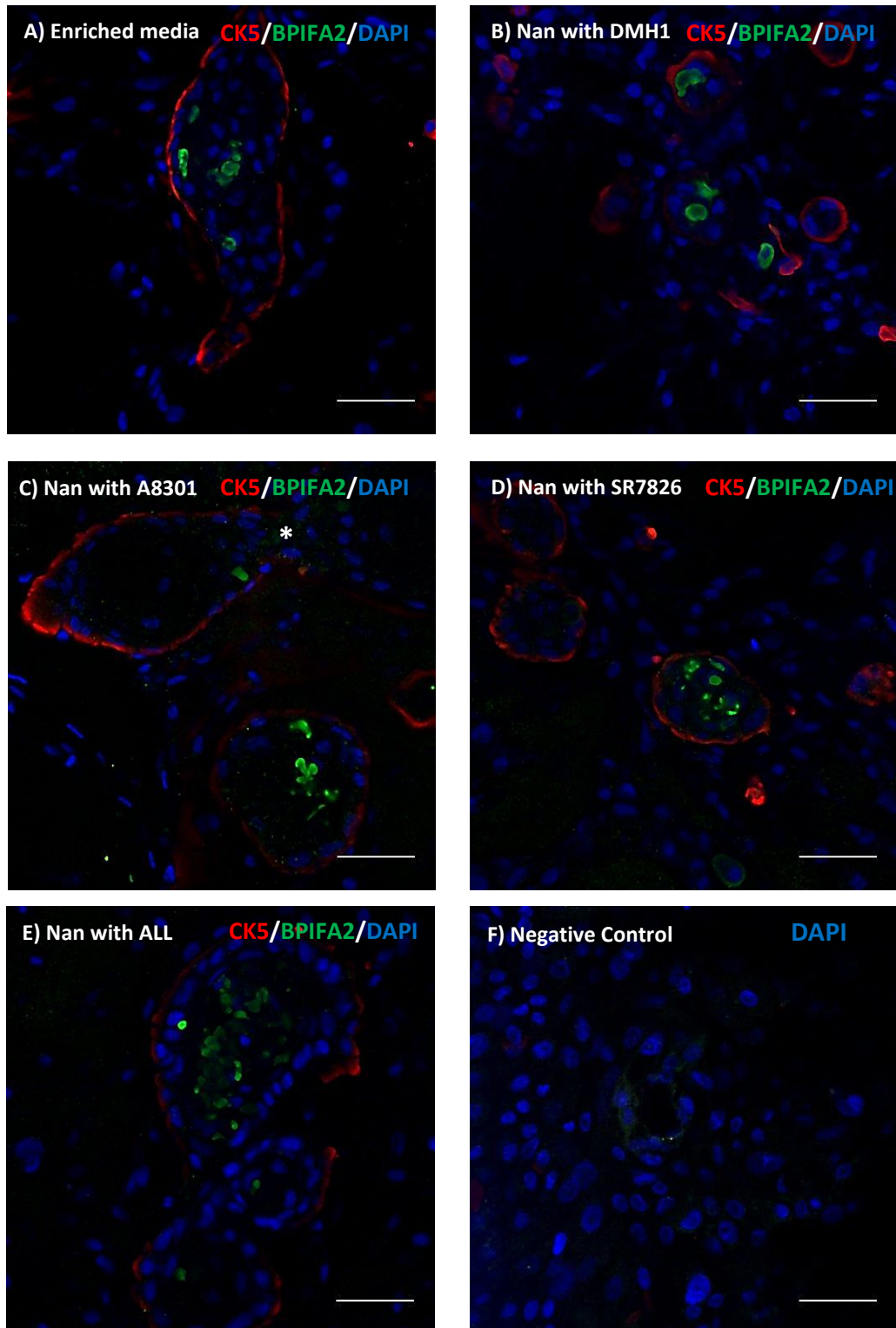


Figure 5.8 Localisation of acinar cell marker, BPIFA2 in SG organoids cultured in different inhibitor media. Images (representative of three independent batches of SG cells) showing positive expression of CK5 (red), **BPIFA2** (green) in SG organoids cultured in Matrigel in enriched Nan media (A), Nan with DMH1 (B), Nan with A8301 (C), Nan with SR7826 (D), Nan with all inhibitors (E), and negative control of SG organoids cultured in enriched media (F) for 14-days at ALI. Scale bars = 50µm.

5.4.6 Localisation of the acinar cell marker, AQP5 in SG organoids cultured in enriched media with differentiation factors

AQP5 is a water channel protein that plays a role in the generation of saliva secretion. AQP5 has exclusively been localized to the apical membrane of serous acini (Delporte, Bryla and Perret, 2016). Figure 5.9 shows that AQP5 was not detected in SG organoid cultures in enriched media (Nan), however, it was seen in the cultures as single large cells (Figure 5.9A).

As shown in Figure 5.9B, AQP5 was present inside the SG organoids cultured in Nan with DMH1 media. It appeared in a few cells inside small spherical SG organoids. Interestingly, AQP5 was more strongly expressed by SG organoids cultured in Nan with A8301 media. The distribution of the protein was scattered at the periphery (Figure 5.9C) and in the middle of the SG organoids (Figure 5.9D). A few cells were positive in SG organoids cultured in Nan with SR7826 media (Figure 5.9E). The most striking result to emerge from the data was that the expression of AQP5 proteins were found in SG organoids cultured in Nan with ALL media at the branching structures, protruding out from the base of organoids (Figure 5.9F).

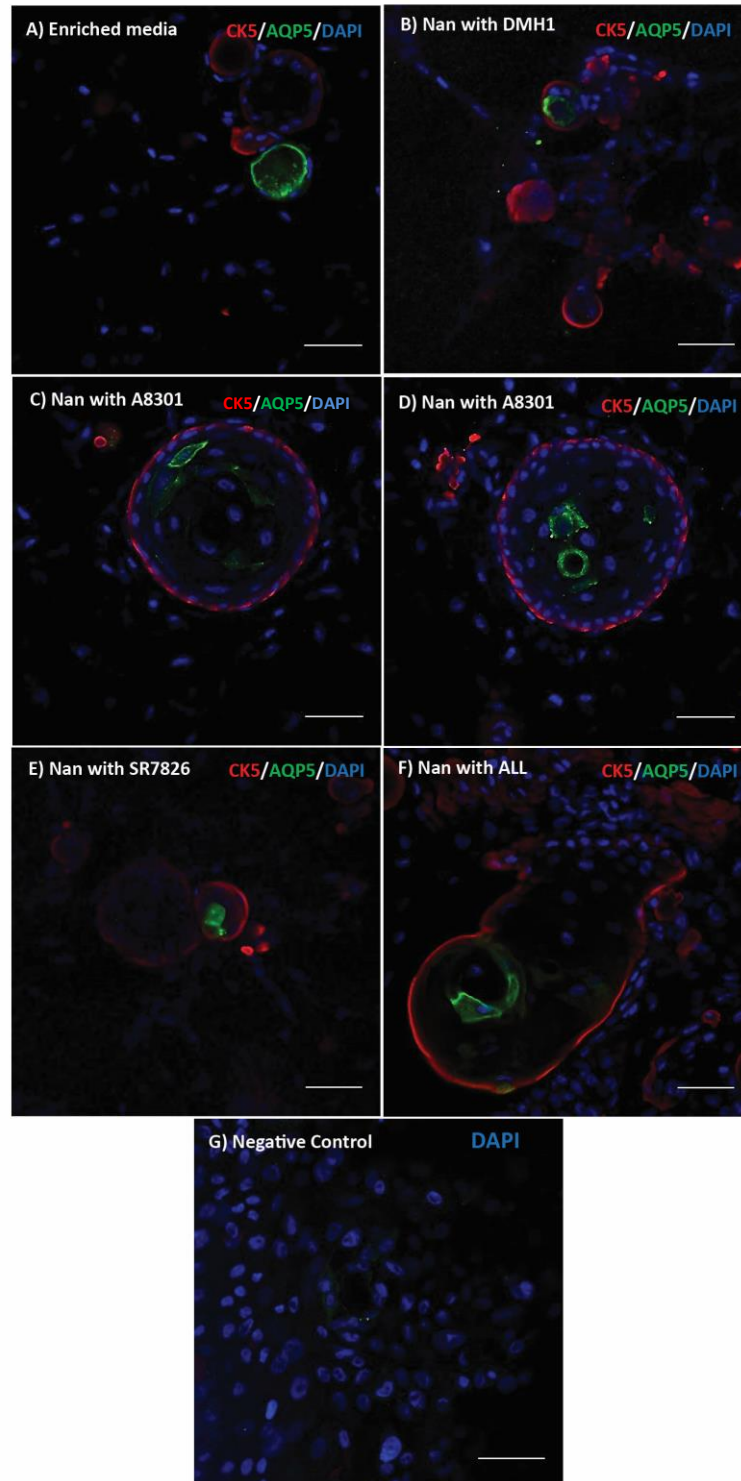


Figure 5.9 Localisation of acinar cell marker, AQP5 of SG organoids cultured in different inhibitor media. Images (representative of three independent batches of SG cells) showing positive expression of CK5 (red) and **AQP5** (green) in SG organoids cultured in Matrigel in enriched media (A), Nan with DMH1 (B), Nan with A8301 (C, D), Nan with SR7826 (E), Nan with all inhibitors (F), and negative control of SG organoids cultured in enriched media (G) for 14-days at ALI. Scale bars = 50μm.

5.4.7 Localisation of E-cadherin in SG organoid cultured in enriched media with differentiation factors

During salivary gland branching morphogenesis, the dramatic changes that occur in structure and cellular organization could be guided not only by mechanical forces but also by dynamic interactions between neighbouring cells. E-cadherin is known as a cell-cell adhesion protein playing a critical role during SMG development (Hsu and Yamada, 2010).

It is apparent that E-cadherin staining is very marked both between the cell junctions of the outer epithelial cells and also between the inner cells of the organoids. This was similar in all types of media (Figure 5.10).

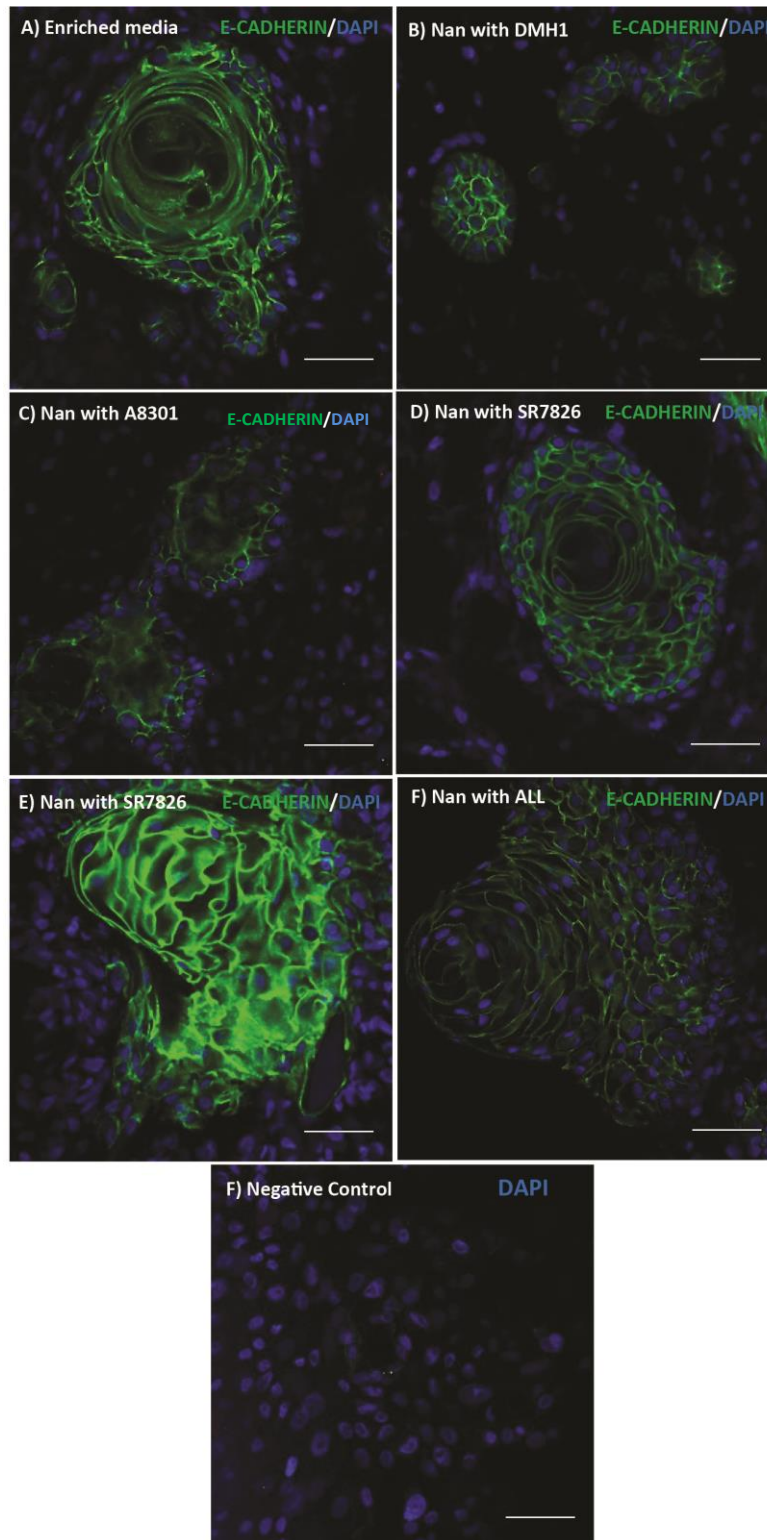


Figure 5. 10 Localisation of cell-cell adhesion marker, E-cadherin in SG organoids cultured in different inhibitor media. Images (representative of three independent batches of SG cells) showing positive expression of **E-cadherin** (green) in SG organoids cultured in Matrigel in enriched Nan media (A), Nan with DMH1 (B), Nan with A8301 (C), Nan with SR7826 (D, E), Nan with all inhibitors (F), and negative control of SG organoids cultured in enriched media (G) for 14-days at ALI. Scale bars = 50µm.

5.4.8 Amylase assay activity in SG organoids cultured in enriched media with differentiation factors

We investigated the capability of SG organoids to secrete amylase. An enzymatic assay with colorimetric detection was used to measure amylase activity in the culture media. The amount of amylase that cleaves sufficient ethylidene-pNP-G7 to generate 1.0 μ mole of *p*-nitrophenol per minute is known as one unit.

Figure 5.11 illustrates amylase activity in the different culture media. It can be seen from the data that the amylase activity (secretion) was increased in SG organoids cultured in three groups compared to Nan media: Nan with A8301, Nan with SR7826, and Nan with ALL media. Statistical tests showed that only the difference between SG organoids cultured in Nan with SR7826 and Nan media was significant.

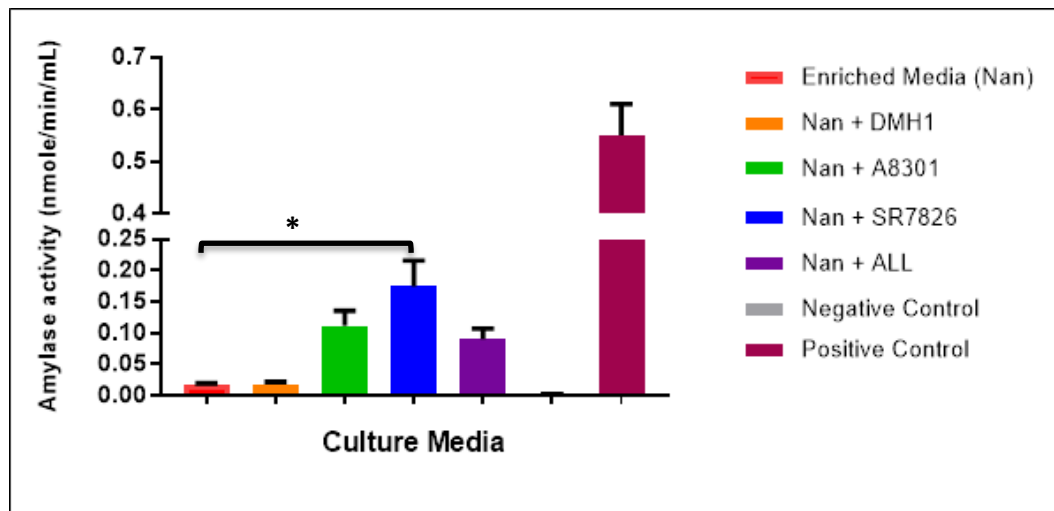


Figure 5. 11 Amylase assay activity in SG organoid cultured in different inhibitors media. The apical secretion was collected from each culture media at Day-14 and the amylase activity was determined. Negative control is PBS solution, and positive control is Amylase Positive Control solution. N=3, *p-value \leq 0.05.

5.5 DISCUSSION

The main findings from this study are the different effects in terms of the formation, size and gene and protein expression of SG organoids when cultured in media enriched with the differentiation factors. Although our preliminary study on 2D cultures demonstrated no significant differences in cell proliferation amongst the different media, the SG organoid morphology varied markedly.

In the previous chapter, I showed that we successfully developed a human SG organoid model in Matrigel at the ALL in enriched media (Nan) that showed staining of CK5. In this chapter, the cells at the junctions of SG organoids were shown to stain for CK7, which is consistently expressed in SG duct cells. This finding matches those observed in earlier studies on mice salivary gland organoids (Nanduri *et al.*, 2014). Furthermore, SG organoid cultures in enriched media also displayed positive staining for BPIFA2. This further supports the idea of BPIFA2 is present in serous acinar cells of human salivary glands (Bingle *et al.*, 2009; da Silva *et al.*, 2011).

I found that by blocking TGF β signalling, the number of organoids formed increased. These results corroborate the studies of Gurung *et al.*, (2015), who suggested that TGF β inhibition promoted cell proliferation and maintained cell fate. We also showed that the SG organoids cultured in the three-inhibitor combination (ALL-media) grew more effectively in terms of both number and size. Whereas the size and number of SG organoids cultured in SR7826-media was the lowest. A possible explanation for these results may be that the effect of dual SMAD (TGF β /BMP) signalling inhibition is more dominant in ALL-media. Thus, it indirectly affects the LIMK signalling inhibition and as a result generated the 'best' SG organoids.

The effect of dual SMAD (TGF β /BMP) signalling inhibition is known to promote epithelial basal cell expansion. Mou *et al.*, (2016) reported that dual SMAD (TGF β /BMP) signalling inhibition allows the expanded cells (esophagus, epididymis, larynx and mammary gland) to differentiate efficiently, and possess the same cellular architecture and marker expression as their corresponding tissue (Mou *et al.*, 2016).

This also accords with our earlier observations, which showed that the SG cells cultured in ALL-media produced SG organoids with branching forms contained simple columnar epithelium. This is consistent with previous research into this area which characterizes ductal cells as simple columnar cells (Delporte, Bryla and Perret, 2016). Specifically, the branches of our SG organoids may be differentiating towards striated ducts (consisting of simple columnar cells displaying longitudinal striations due to mitochondria at the base of cells) or excretory duct (simple columnar cells). Further investigations should be done to confirm this. We showed that the expanded SG epithelial cells efficiently generated organoids in Matrigel at the ALI. The SG organoids were also positive for markers found in the SG tissues. The most abundant staining of BPIFA2, as well as AQP5 (both serous acinar markers) was found in the SG organoids cultured in the combination of inhibitors media. This finding suggests that the effect of (TGF β /BMP/LIMK) signalling inhibitors promote cell differentiation into acinar and ductal cells of salivary glands

Another important finding was the effect of TGF β antagonist signalling on the production of SG organoids. Specifically, we showed that adding A8301, a small molecule TGF β inhibitor, in the media generated SG organoids with two distinct structures. We showed that the SG cells expanded and differentiated into simple cuboidal cells in spherical-form and simple columnar epithelia in branching-form. According to these data, we can infer that by blocking the TGF β pathway, the SG epithelial cells expanded and differentiated into ductal and acinar cells. These results are in line with those of previous studies that suggested TGF β inhibition acts to induce cell differentiation (Gurung, Werkmeister and Gargett, 2015; Broutier *et al.*, 2016). The SG organoids also showed positive staining for CK7, a ductal cell marker, specifically in the branching-forms. BPIFA2 positive cells were also abundant. It is somewhat surprising that expression of AQP5 was low by PCR, but abundant AQP5 protein was present in the SG organoids cultured in A8301-media. This inconsistency between RNA and protein expression may be due to post-transcriptional or post-translational regulation, for example by RNA degradation and proteolytic processing (Burghartz *et al.*, 2017). mRNA expression of MUC7, a mucous acinar cell marker was

only detected in this culture. Further work with a greater focus on identifying gene expression in similar cultures is therefore suggested.

In this study, DMH1 (BMP inhibitor) was found to produce SG organoids with more ductal-like structures than spherical forms. Positive expression of CK7 was observed mainly in the junctional areas that formed the branching structures. Less abundant acinar cell-type markers were seen in this SG organoid culture system. These results suggested that inhibiting BMP signalling causes cells to differentiate towards a more ductal phenotype. This finding was also reported by Clevers (2013) who suggested that BMP signalling has been acknowledged to be active in the villus compartment of gut cells, and their inhibition (by Noggin) is crucial to create a crypt-permissive environment of small intestine epithelium (Clevers, 2013).

LIM kinase signalling has been described as controlling embryonic salivary gland cleft formation during branching morphogenesis. Ray *et al* (2014) showed that LIMK regulates the early stages of cleft formation via establishment of actin stability. In my study, SR7826 (LIMK inhibitor) produced SG organoids with no clear branching structures and limited expression of CK7 (ductal cell marker). Thus, our findings suggested the involvement of LIMK pathway in salivary gland development, by up regulation.

AQP5 and α -AMY have been described as acinar markers (Burghartz *et al.*, 2017). Expression of both acinar markers was detected in SG organoids in media containing all differentiation factors. I was unable to detect the amylase protein by IF microscopy in any of the SG organoids cultures (data not shown). Thus, further work might explore culturing SG organoids for a longer-term to encourage the organoid differentiate into functional acinar. Previous research reported positive staining of AQP5 in mouse salivary gland organoids (Nanduri *et al.*, 2014; Maimets *et al.*, 2016). To confirm protein secretion, an amylase activity assay was conducted on SG organoid conditioned media and found to be significantly higher in SG organoids grown in SR7826-media compared to enriched media. This novel finding is consistent with data by Burghartz *et al* (2016) that showed that α -AMY enzyme activity was

significantly higher under 3D conditions for human salivary gland epithelial cells (Burghartz *et al.*, 2017).

As has been discussed in the previous chapter, the presence of the tight junction protein, ZO-1 and cell-cell adhesion proteins, E-cadherin and claudin, in SG organoid RNA suggests a level of apical-basal polarity in our cultures. This was further confirmed with the positive protein expression of E-cadherin in our SG organoids. The location of E-cadherin was noticeable between cell junctions of epithelial cells. It can be speculated that E-cadherin mediated adhesive cell-cell interactions with neighbouring cells in the organoids. Thus, it helps the cells to self-organize, aggregate and then undergo branching morphogenesis to form structural features of tissues. This corroborates the ideas of Davis and Reynolds (2006), who suggested that E-cadherin plays an important role in regulating the SMG epithelial self-organization, branching and acinus formation.

Another interesting finding from the study is the mRNA expression of HE4 (human epididymis 4) in all of our SG organoids cultures. Little is known about the function of this protein but its localization supports previous observations that HE4 is readily detectable in multiple tissues from the oral cavity, nasopharynx and respiratory tract (Bingle, Singleton and Bingle, 2002; Bingle *et al.*, 2006).

Overall our culture media experiments showed that we were able to produce human SG organoids that closely mimic native SG glands with positive expression of a number of cell-types specific markers. However, several questions remain unanswered. It is necessary to recognize that organoid culture still has limitations. It is unfortunate that there are fibroblasts surrounding the organoids that could be affecting the model. Further investigation and experimentation into minimizing the present of fibroblasts in the culture is strongly recommended. Previous studies showed by doing serial passaging and self-renewal assay could solve this issue (Nanduri *et al.*, 2014; Maimets *et al.*, 2016) Besides, additional validation of the cultures is required using perhaps the serous acinar marker, α -AMY and the mucous

acinar marker, MUC7. In future investigations, it might be possible to use a dual combination of inhibitors in the media, for example TGF β /BMP, TGF β /SR7826, BMP/SR7826 to determine their effectiveness in modulating SG organoid cultures. Transmission electron microscopy could also be used to enhance the visualization of many features of the organoids.

5.6 KEY EXPERIMENTAL CONCLUSIONS

- I have showed that inhibition of TGF β , BMP and LIMK signalling promoted cell proliferation and induced cell differentiation.
- SG organoids cultured in Matrigel at ALI in A8301-media and ALL-media displayed distinct characteristics that closely mimics native glands shown by expression of acinar cell markers (BPIFA2 and AQP5), the ductal cell marker, CK7 and E-cadherin.
- SG organoids cultured in Matrigel at ALI under DMH1-media demonstrated ductal-like structures.
- α -AMY enzyme activity was significantly higher in SG organoids under SR7826-media.
- HE4 gene expression was detected in SG organoid cultures.

In this study, the aim was to investigate the effects of differentiation factors on the development of SG organoid cultures. This study has shown that the addition of TGF β inhibitor and all the inhibitors (TGF β , BMP and LIMK) to the culture media affected SG organoid development by displaying distinct characteristics that closely resemble native glands and expressed specific cell-type markers; BPIFA2, AQP5, CK5 and E-cadherin. The inhibition of BMP signalling promoted cell proliferation and differentiation of SG organoids more into ductal like structures and expressed ductal cell marker, CK7. While, the inhibition of LIM kinase signalling demonstrated SG organoids with no clear branching structures and showed significantly higher of amylase activity assay. One source of weakness in this study which could affected the differentiation factors signalling in the SG organoids cultures was the present of

fibroblast surrounding the SG organoids. Further works need to be carried out in order to validate the effect of fibroblast in the culture. In spite of its limitations, the study certainly offers valuable insight into determining the optimal culture conditions for developing human SG organoids.

CHAPTER 6

Cultures on Polymerised High Internal Phase Emulsions (PolyHIPE) Scaffold

CHAPTER 6: CULTURES ON POLYMERISED HIGH INTERNAL PHASE EMULSIONS (POLYHIPE) SCAFFOLD

6.1 INTRODUCTION

Previously, I have demonstrated the growth of salivary gland cells, isolated from normal human tissue, on Alvetex®Scaffolds and PET inserts, with and without ECM coating, and either submerged in culture medium or at an ALI. I have shown that Alvetex®Scaffold does not provide a good scaffold for salivary gland cell growth and also that whilst the cells did grow on PET they did not fully differentiate. I subsequently demonstrated that Matrigel provides a better extracellular membrane support for the cells than does Myogel, both submerged in an enriched media culture medium and at an ALI. My results suggested that the best conditions to allow differentiation of SG cells was to mix the cells with Matrigel and after a short period of time culture the cells at an ALI; this allowed organoids to contain multiple cell types of varying differentiation status. The impact of adding specific differentiation factors, inhibitors of the BMP/TGF/LIMK signalling pathway, on the development, cell viability and morphology of SG organoids was also investigated. This resulted in significant differences in the growth and differentiation status (as demonstrated by specific protein expression) of the cell cultures. The most successful methods investigated to date, in terms of cell growth and differentiation status, have involved growth of organoids, enclosed in extracellular matrix. This does however, raise issues surrounding access of cells to oxygen and nutrients, access for researchers to collect “saliva” secretions, and the potential to use the SG organoids for implantation *in vivo* and replacement of damaged or diseased glands.

Polymerised High Internal Phase Emulsion (PolyHIPE) scaffolds are manufactured via emulsion templating and display a highly interconnected porosity which is an ideal candidate for tissue engineering. The interconnected porous structures enable cellular migration and proliferation, and the transport of oxygen, nutrients and metabolic waste (Wang *et al.*, 2016). PolyHIPE scaffolds have successfully been used as thin membranes for 3D cell culture in which they demonstrated biocompatibility

with human embryonic stem-cell derived mesenchymal progenitors (Owen *et al.*, 2015).

In this study I attempted to culture SG cells on a biodegradable PolyHIPE scaffolds with a microporous structure which would accommodate a large number of cells and promote nutrient diffusion. In addition, scaffolds were treated with plasma to increase cell attachment. Lasers were used to produce such biomaterials which should allow the cells to grow more effectively, proliferate and differentiate into acinar and ductal structures. We designed a laser cut with long tubes that had the potential to mimic a ductal structure with a connected circular structure to induce acinar development.

Briefly, in our initial experiment, SG cells were mixed with Matrigel and seeded into the PolyHIPE scaffold in enriched media (Nan) for 14 days. In a follow-on experiment, SG cells were mixed with Matrigel and seeded onto the PolyHIPE scaffold in Nan media containing the BMP/TGF/LIMK inhibitors for up to 14 days. Finally, the PolyHIPE scaffolds were coated with Matrigel prior to seeding with the SG cells which were then cultured in Nan media with the BMP/TGF/LIMK inhibitors for 14 days. Immunofluorescent confocal microscopy was performed for imaging and analysis.

6.2 AIMS

To culture SG cells on Polymerised High Internal Phase Emulsion (PolyHIPE) scaffolds.

6.3 MATERIALS AND METHODS

6.3.1 PolyHIPE scaffold

PolyHIPE scaffolds were made in the laboratory of Dr F Claeysens, Tissue Engineering Group, Kroto Institute, University of Sheffield. Briefly, photocurable monomers were made from the following materials:

- 10.45 gram of 2-Ethylhexyl acrylate (EHA, Sigma Aldrich, Poole, UK).
- 1 gram of isobornyl acrylate (IBOA, Sigma Aldrich, Poole, UK).

- 2.89 gram of trimethylolpropane triacrylate (TMPTA, Sigma Aldrich, Poole, UK).
- 10% (w/w) of surfactant Hypermer B246-SO (MV, kindly donated by Croda, UK) was added relative to total monomers used. Thus, 1 gram of monomer contains 0.1 gram of surfactant.
- 5% (w/w) of photoinitiator (2,4,6-trimethylbenzoyl)-phosphine oxide/2-hydroxy-2-methylpropiophenone, 50/50) was added relative to the monomers used.

2 grams of the prepolymer liquid solution (EHA, IBOA, TMPTA, surfactant and initiator) was weighed into a 50 ml glass beaker and the solution mixed at 300 rpm using an overhead paddle stirrer (Pro40, SciQuip). Water was added slowly dropwise creating a white mayonnaise like consistency with a volume ratio of 1:9, monomer to water. High internal phase emulsions (HIPE) have a high-volume ratio of water which following polymerisation results in a porous foam or polymerised high internal phase emulsion (PolyHIPE).

The PolyHIPE was poured into a glass petri dish until the total height was approximately 2 mm and irradiated with UV light (Omniculture S1000) for 2 minutes on both sides; with the glass petri dish being turned upside-down to ensure the bottom part was also sufficiently cross-linked. Finally, the PolyHIPE was washed with acetone and then methanol and dried under vacuum at room temperature.

To create the etched features, the PolyHIPE was laser cut with a 40 W CO₂ laser tube source (9-11 μm wavelength) within an Epilog Laser system. The laser was set to raster scan with 7% power and 10% speed to produce the respective grid design on the PolyHIPE.

6.3.2 SG cells cultured on PolyHIPE scaffold

Scaffolds were sterilised by soaking in 70% (v/v) ethanol for 2 hours before washing three times in sterile PBS. The scaffolds were then placed in a PET transwell in a 12-

well culture plate format and seeded either with a mixture of SG cells and Matrigel as previously described (**Refer 4.2.3**) or coated with Matrigel for 30 minutes before seeding with SG cells. After ECM polymerization, 500 μ l of warm media (**Refer Table 5.1**) was added to the top of the transwell without disturbing the scaffold, and 1.5 ml media to the bottom. After 3 days, media without ROCKi was added to the bottom of the transwells so that the scaffolds were essentially at an ALI for 14 days. The medium was refreshed 3 times per week.

6.3.3 Immunofluorescent confocal microscopy of SG cells on PolyHIPE scaffolds

To stain the SG cells, the media was removed and the scaffolds washed twice with PBS. They were then fixed with 1 ml of 100% ice-cold methanol and left at 4°C for 20 minutes before being washed with PBS a further two times. Immunofluorescence staining was carried out as described previously (**Refer 2.6**). Briefly, 300 μ L of permeabilization buffer was added to the scaffolds which were then left on a shaker at 80 rpm for 1 hour at room temperature. The buffer was removed and scaffolds washed once with PBS before adding 300 μ L of CK5 (1:100) and/or CK7 (1:500) and/or E-cadherin (1:500) antibody. Scaffolds were left on a shaker at 80 rpm, 4°C overnight, after which the primary antibody was aspirated, the scaffold washed twice with PBS and then 300 μ L of secondary antibody, Alexa Fluor 488 (Cat No. A11011, 1:200) and/or Alexa Fluor 568 (Cat No. A11001, 1:200), was added and left wrapped in foil for 1 hour at room temperature. The secondary antibody solution was removed, the scaffold washed twice with PBS in the dark or low light, and then 1 ml of DAPI working solution (0.1% DAPI in PBS) was added and left wrapped in foil for 10 min. The DAPI working solution was removed and the scaffolds washed once in PBS. Finally, samples were submerged in PBS, wrapped in foil and refrigerated until use for confocal microscopy (Nikon A1+, Surrey, UK).

Optical clearing was carried out before imaging to make the polymer transparent and enable us to view deeper into the material. Optical clearing involves submerging the sample in a solvent or liquid with the same refractive index as the polymer. Briefly,

the sample was washed in 20%, 40%, 60%, 80% and 100% ethanol for 5 minutes each to gradually displace the water and finally in xylene for 30 minutes.

6.4 RESULTS

6.4.1 PolyHIPE scaffold

Figure 6.1 shows SEM images of the PolyHIPE scaffolds formed using the direct-write UV stereolithography technique. Pore sizes over 50 μm are suitable for tissue engineering applications. The microporous structure of the PolyHIPE was retained after structuring.

Figure 6.2 shows two laser cutting designs of the PolyHIPE scaffold. The aim was to design a laser cut that would closely mimic salivary gland structures. Figure 6.2A shows tube-like structures with “holes” at the end to mimic branches of duct with acinar-like structures. Figure 6.2B shows a grid line design with “holes” in between.

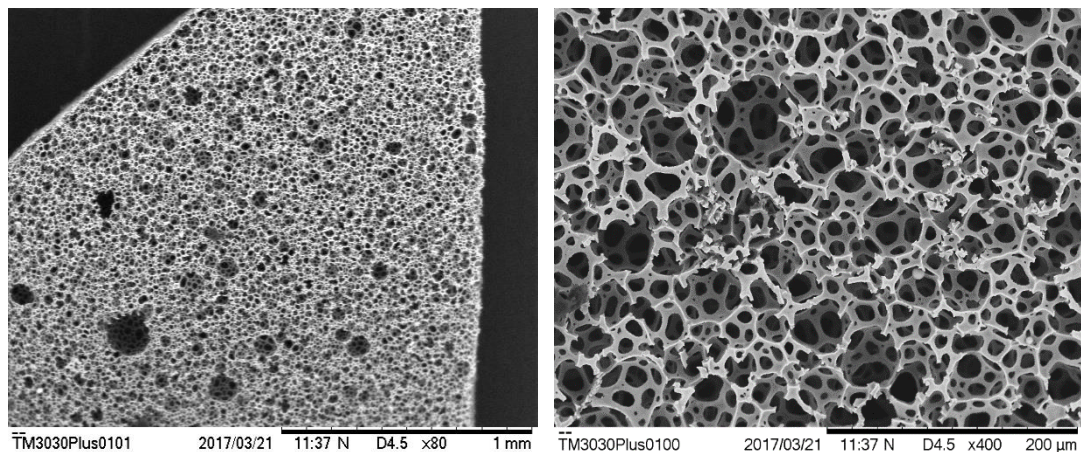
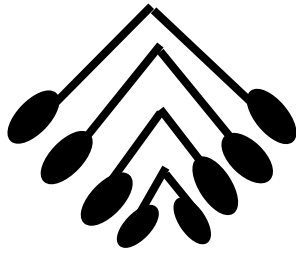


Figure 6. 1 SEM images of a PolyHIPE scaffold. Magnification of the same point from 80x to 400x, showing the macroscopic and microscopic porosity of the structure. Scale bars A: 1mm and B: 200 μm

(A)



(B)

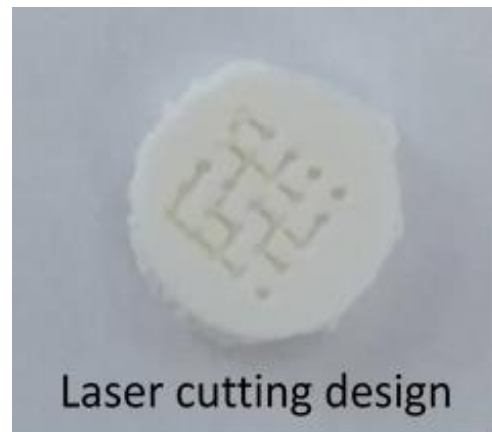
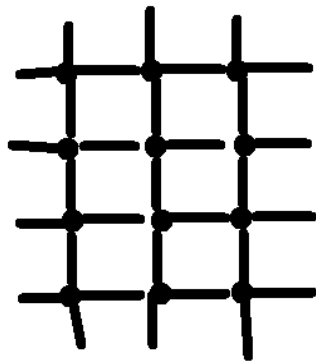


Figure 6. 2 Laser cutting design of PolyHIPE scaffold.

6.4.2 SG organoids cultured in enriched media on PolyHIPE scaffold (design A), seeded with a mixture of SG cells and Matrigel.

Confocal images were taken of SG organoids cultured on PolyHIPE scaffolds for 14 days. From the image (Figure 6.3A), it can be seen that the SG cells appeared to adhere and proliferate mostly on the top layers indicating that the mixture of cells and Matrigel did not drop to the bottom of scaffold. Some cells were seen adhered along the laser cut area (asterisk). Figure 6.3B shows that SG cells were able to grow as small organoids inside the laser cut area. Figure 6.3C, demonstrates that cells were able to grow up the scaffold fibres, penetrate the fibres and bridge the gaps between the fibres, eventually forming SG organoids. However, they grew on the scaffold layer but not along the laser cut area as we had expected.

Figure 6.4A shows positive expression of CK5 and E-cadherin in SG organoids cultured on the scaffold. However, the cell-cell-adhesion was not as great as was seen in the organoids cultured without scaffolds (**Refer Figure 5.11**). Figure 6.4B, demonstrates expression of CK7 on the upper layer of the scaffold and only trace amounts of E-cadherin were detected in the cultures.

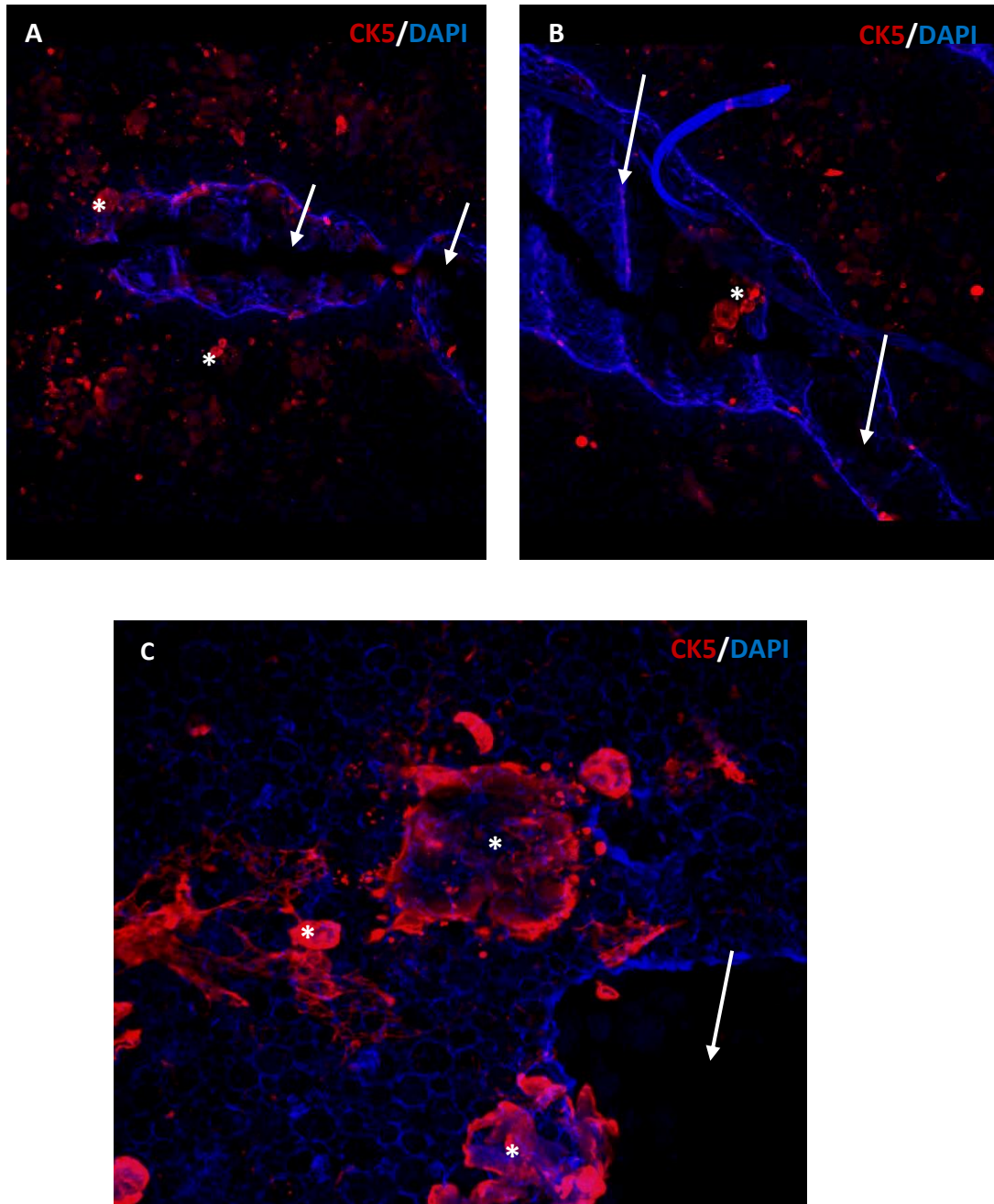


Figure 6.3 SG organoid model cultured on PolyHIPE scaffold (design A) in enriched media. Images (representative of three independent batches of SG cells) showing positive expression of CK5 (red) in SG organoids cultured in Matrigel at ALI for 14 days. An overview of SG organoids on PolyHIPE scaffold at low magnification (A), SG organoids inside the laser cutting area of PolyHIPE scaffold (B), and SG organoids on/in the PolyHIPE scaffold. Scale bars = 50 μ m
SG organoids (asterisk); laser cutting area (arrow).

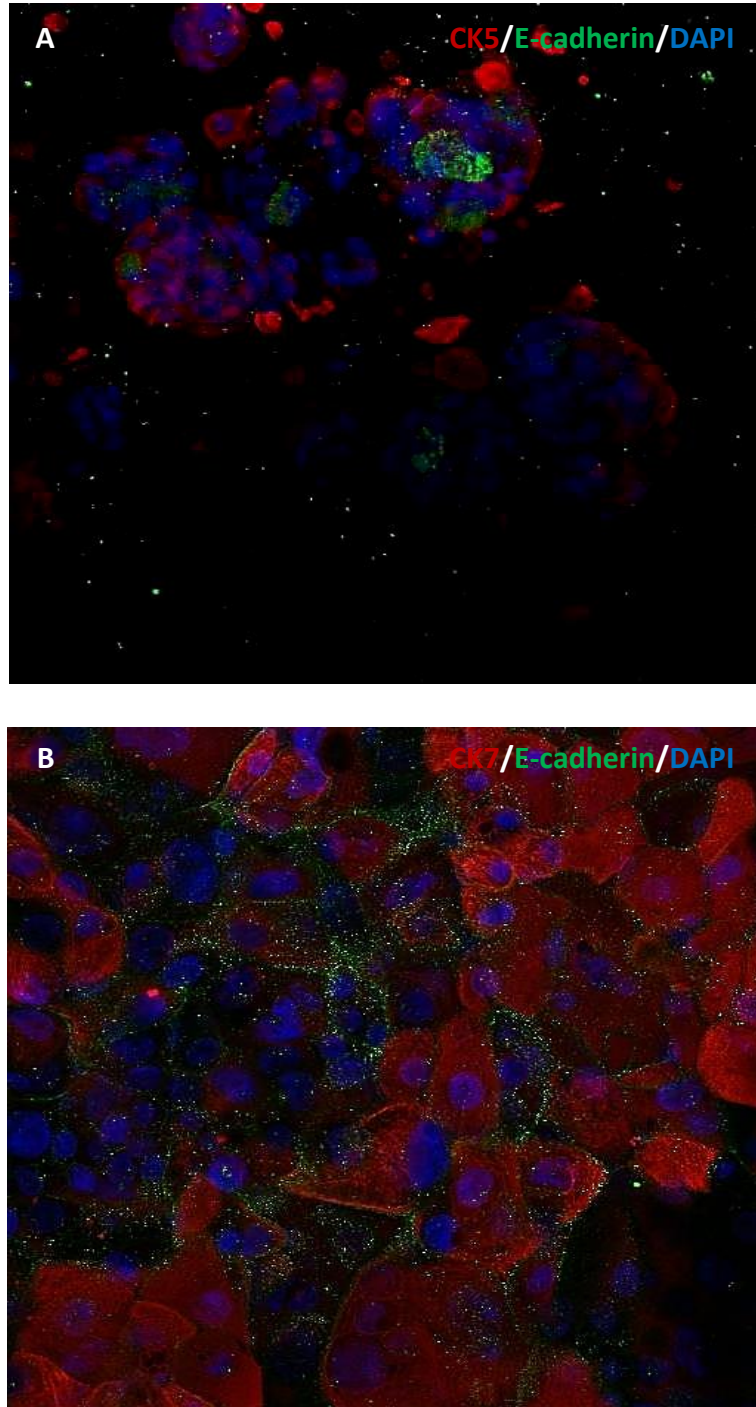


Figure 6.4 SG organoid model cultured on PolyHIPE scaffold (design A) in enriched media. Images (representative of two independent batches of SG cells) showing positive expression of CK5 (red in A), CK7 (red in B), and E-cadherin (green) in SG organoids cultured in Matrigel at ALI for 14 days. Scale bars = 50 μ m

6.4.3 SG organoids cultured on PolyHIPE scaffold (design A), seeded with a mixture of SG cells and Matrigel, in different inhibitors media.

CK5 was produced by SG cells grown on PolyHIPE scaffolds in the presence of BMP/TGF/LIMK inhibitors. The structure of the organoids differed dramatically dependent upon the inhibitor present. As shown in Figure 6.5B, the SG organoids cultured in Nan media with DMH1 (BMP inhibitor) grew on the scaffold fibres at the edge of the laser cut. No branches were clearly visible. In Nan media with A8301 (TGF β inhibitor), very small, elongated SG organoids were observed (Figure 6.5C). Figure 6.5D shows that in the presence of SR7826 (LIMK inhibitor), spheroid organoids formed with further small spheroids surrounding. The most striking structures were seen in the presence of all inhibitors, figure 6.5E, suggesting that all of the distinctive structures seen with the individual inhibitors again formed when all inhibitors were added. However, no real ductal or acinar structures formed along the laser cuts as we had expected.

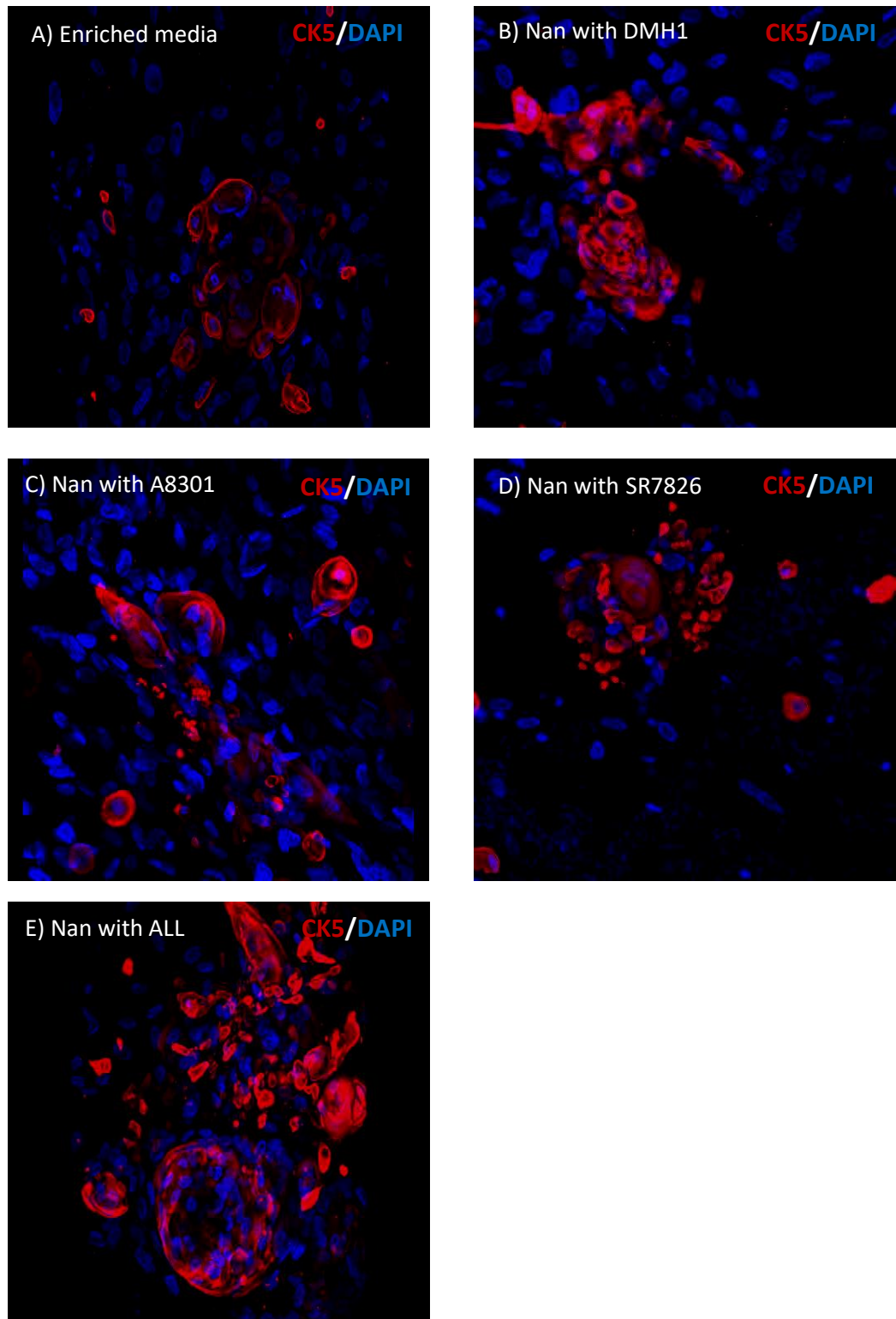


Figure 6.5 SG organoid model cultured on PolyHIPE scaffold (design A) in different inhibitor media. Images (representative of two independent batches of SG cells) showing positive expression of CK5 (red) in SG organoids cultured in Matrigel in enriched media (A), Nan with DMH1 (B), Nan with A8301 (C), Nan with SR7826 (D), and Nan with all inhibitors (E) for 14 days at ALI. Scale bars = 50 μ m

6.4.4 SG organoids cultured on PolyHIPE scaffold (design B), coated with Matrigel before seeding SG cells

In order to encourage the cells to grow and differentiate into the scaffolds, and as we thought that access might have been limited due to the cells being seeded after mixing with Matrigel, an experiment was designed whereby the scaffold was coated with Matrigel before seeding with the cells. Somewhat disappointingly cells did not grow as organoids on the coated surface of the scaffold (Figure 6.6). Small spheroids, with positive staining of CK5, were seen when the cells were grown in Nan media (6.6A), Nan with DMH1 (Figure 6.6B), and Nan with ALL inhibitors (Figure 6.6E). The SG cells cultured in Nan with A8301 (Figure 6.6C) and Nan with SR7826 (Figure 6.6D) were positive for CK7.

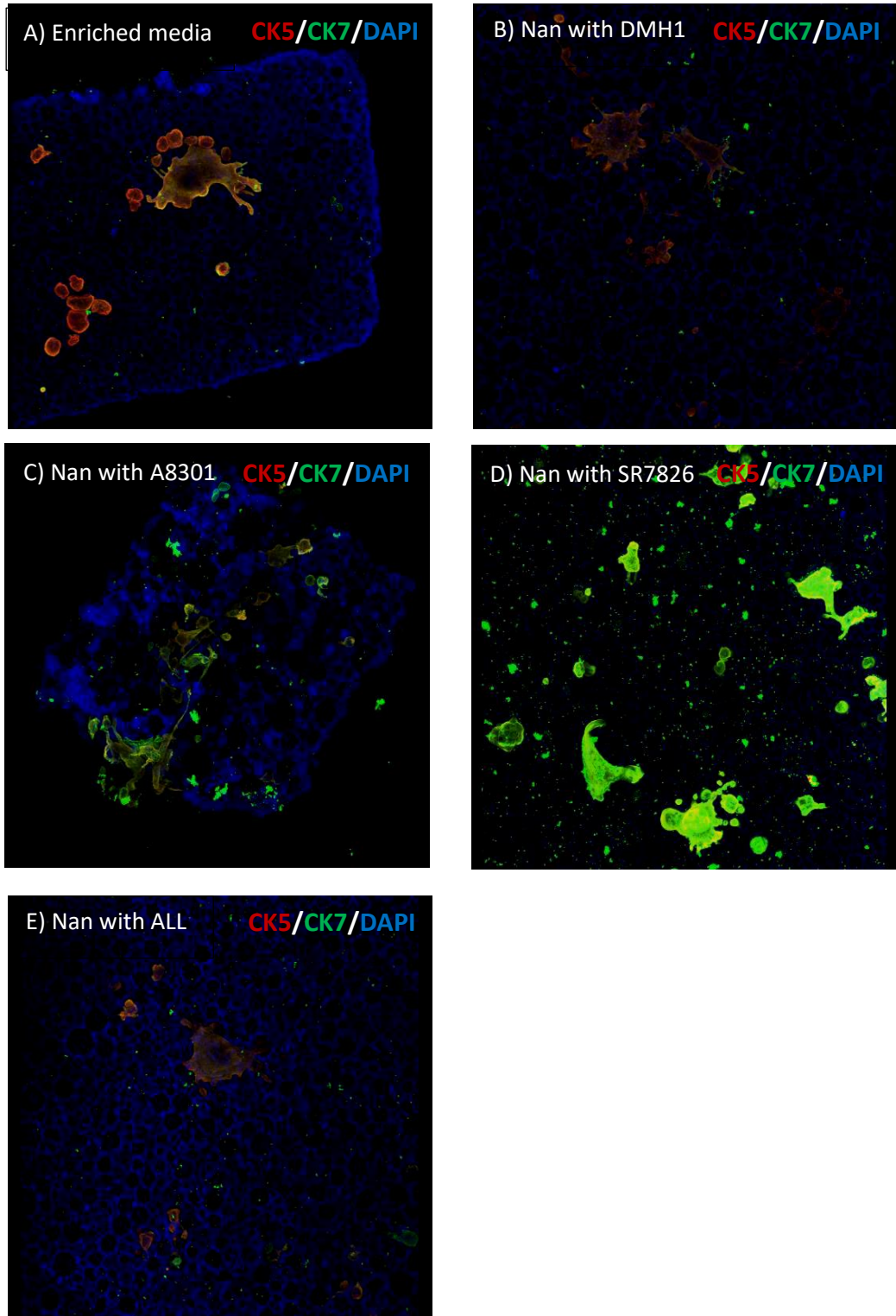


Figure 6.6 SG organoid model cultured on PolyHIPE scaffold (design B) in different inhibitor media. Images (representative of two independent batches of SG cells) showing positive expression of CK5 (red), and CK7 (green) in SG organoids cultured on PolyHIPE with Matrigel coating in enriched media (A), Nan with DMH1 (B), Nan with A8301 (C), Nan with SR7826 (D), and Nan with all inhibitors (E) for 14 days at ALI. Scale bars = 50µm

6.5 DISCUSSION

This study aimed to grow SG cells on PolyHIPE scaffolds where they would be able to freely access oxygen and nutrients, and we would more easily be able to analyse any cell secretions. The scaffolds are biodegradable and could have formed the basis of a regenerative model for introduction to damaged or diseased human glands. To our knowledge, this is the first time PolyHIPE scaffolds have been used to culture normal salivary gland cells and our study showed promising initial findings.

In the adult salivary gland, most epithelial cells have a basement membrane located on the basal side and a lumen on the apical side. Thus, scaffolds have been used as a tool to provide signals to cells from the basal side. The ultimate aim of this study was to develop a salivary gland model which could be used to replace, or initiate regeneration of diseased or damaged glands. Whilst acknowledging that Matrigel is not the perfect ECM for this, due to its origins being murine, we continued to use this ECM in the PolyHIPEs scaffold studies in the absence of a readily available human alternative; as our attempt at replacing Matrigel with Myogel (human derived ECM) demonstrated that the Myogel did not have the physical structure needed to support organoid growth. Furthermore, we also felt that growth of the cells solely on the scaffold would not encourage cell growth or polarity, thus a basement membrane would be needed for this. Therefore, our initial studies described here, continue with the use of Matrigel, caveats acknowledged.

Previously, in Chapter 5, we demonstrated that culturing SG cells in Matrigel stimulates apical-basal polarity in SG organoids with the expression of E-cadherin (**Refer 5.4.7**). However, the SG cells grown in Matrigel on PolyHIPE scaffolds had reduced staining of the cell-cell adhesion marker, E-cadherin. This could be attributed to the consistency of Matrigel on the PolyHIPE scaffold. A previous study, in which an immortalized salivary gland cell line was cultured on poly-lactic-co-glycolic acid (PLGA) scaffolds with laminin-111 showed that the cells attached, proliferated and exhibited cell polarity (Cantara *et al.*, 2012). Matrigel consists of 70%

laminin and so it would be interesting to investigate the treatment of PolyHIPE scaffolds with 100% laminin prior to seeding with normal salivary gland cells.

Whilst E-cadherin positivity may have decreased following culture on PolyHIPE scaffolds the SG cells were able to attach, proliferate, differentiate and were also shown to be positive for CK5 and CK7. These findings are in agreement with Owen et al (2015) who had tested the scaffold with mesenchymal progenitor cells and showed that they were able to support and enhance osteogenic differentiation. Previously it has been shown that the porous architecture of a scaffold can affect cell proliferation, however, conventional techniques are limited in their ability to produce porous scaffolds and are also time consuming (Paterson *et al.*, 2018). PolyHIPE scaffolds have been shown to solve these problems as their porosity is formed from emulsion templating using microstereolithography and have demonstrated increases in cell attachment and cell migration (Akay, Birch and Bokhari, 2004; Owen *et al.*, 2015).

The design used to laser-cut the scaffold included a hole to mimic an acinar-like structure and a tube which could allow the SG cells to grow and differentiate into ductal structures. The aim was to enhance effective cell growth, however, we found that the cells preferred to grow, proliferate and differentiate into SG organoids on the non-laser cut area, the upper layer of the scaffolds. A possible explanation for this might be that very few SG cells were able to reach and attach the laser-cut area, hence fewer SG organoids could be formed here.

An interesting finding from this study was the distinctive nature of the SG organoid structures, seeded onto PolyHIPE scaffolds after coating with Matrigel (thus mimicking the SG organoids in Matrigel, on Transwells at an ALI, **Refer 4.2.3**) cultured in media containing various combinations of TGF/BMP/LIMK inhibitor. Even though, ductal and acinar structure formation was not prominent when the cells were cultured on the scaffold, they did form structures which closely resembled those seen when the cells were grown in Matrigel on inserts at an ALI (**Refer Figure 5.8**). Thus,

it is clear that we have been able to establish culture conditions that allow the growth and development of ductal and acinar structures and to transfer this to cells cultured on the PolyHIPE scaffolds. Our data suggests that Nan media containing ALL of the TGF/BMP/LIMK inhibitors provided the optimal growth medium.

This study also highlighted the fact that SG cells do not grow as well on Matrigel-coated PolyHIPE scaffold. This is in agreement with our earlier observations (Chapter 3), that the SG cells did not grow well and did not fully differentiate on ECM-coated Alvetex scaffolds or PTFE transwells. This suggests that the SG cells prefer the support of the ECM, growing inside a gel rather than on the surface.

A number of problems, continue to prevent the growth, differentiation and downstream analysis of *in vitro* models of normal human salivary glands. These include the problem of visualising the cells whilst they are growing on the scaffold and also of collecting secretions from the cells both during *in vitro* growth and at the end of each experiment. These issues will need to be further investigated in order to fully realise the potential of PolyHIPE scaffolds as cell delivery vehicles such that engineered SG organoids can be implanted *in vivo* and provide a novel supply of saliva.

6.6 KEY EXPERIMENTAL CONCLUSIONS

- SG cells were able to attach, proliferate and differentiate on PolyHIPE scaffolds, and formed SG organoids.
- Less polarity was seen in SG organoids cultured in Matrigel on PolyHIPE scaffolds compared to those cultured in Matrigel only.
- SG organoids prefer to grow on the non-laser cut part of the PolyHIPE scaffold.
- SG organoids do not like to grow on Matrigel-coated PolyHIPE scaffolds.

The present study was designed to determine the potential of using SG organoids for implantation *in vivo* and replacement of damaged glands. This study has shown that SG organoids were able to grow in Matrigel on PolyHIPE scaffolds at ALI with Nan media containing all inhibitors as the optimal growth medium. Even though, the structural and polarity were less compared to those SG organoids cultured in Matrigel without PolyHIPE scaffolds, these findings suggested that the PolyHIPE scaffolds have a potential as cell delivery vehicles for *in vivo* implantation as well as for collecting saliva-cell secretions.

CHAPTER 7

General Discussion & Conclusion

CHAPTER 7: GENERAL DISCUSSION & CONCLUSION

7.1 GENERAL DISCUSSION

The purpose of the current study was to develop an *in vitro* model of human salivary glands. This study has found that in general human salivary gland cells can be manipulated when grown in defined culture systems *in vitro* to resemble their native *in vivo* situation. The evidence from this study suggests that SG cells embedded in Matrigel, grown at an ALI with enriched media supplemented Wnt3a, R-spondin-1, EGF, and FGF2 developed into SG organoids exhibiting budding and branching. These displayed functional characteristic of SGs with expression of cell specific markers. Furthermore, addition of inhibitor molecules targeting TGF β , BMP and/or LIMK in the culture media, enhanced SG organoid proliferation and differentiation.

In Chapter 3, I showed that SG cells grown on ECM-coated transwells with KGM media expressed mRNA for cell specific markers, but were not as structurally organised as in a 3D model and thus did not display structural similarities to native tissue. These results were in agreement with a previous study, which involved the use of a human SG cell line cultured on Matrigel-coated inserts, that demonstrated the induction of morphologic changes and cytodifferentiation into acinar-like structures but without ductal connections (Maria *et al.*, 2011). Further, previous studies have demonstrated various approaches in culturing SG cells growing them either in Matrigel (Maria *et al.*, 2011; Pringle *et al.*, 2016), collagen (Feng *et al.*, 2009) or a hydrogel (Pradhan-Bhatt *et al.*, 2013) with defined serum-free media. None of these studies reported the development of a fully functional artificial salivary gland.

Based upon my initial findings, I improved the culture system by focusing on growing and expanding the cells in the culture and at the same time maintaining their normal cell phenotype and function. In Chapter 4, I modified the culture conditions by replacing KGM media with an enriched media supplemented with specific growth factors (Wnt3a, R-spondin-1, EGF, and FGF2). I embedded the SG cells inside the ECM (Matrigel/Myogel) rather than growing them on ECM-coated vessels and subjected the cultures to both ALI or non-ALI conditions for comparison. I showed, the first

significant findings of this study when human salivary glands were grown in Matrigel at ALI, SG organoids developed in which buds and branches formed and the cells expressed crucial, specific markers (amylase, AQP5, and MUC7). These results indicated that embedding the cells in a laminin-rich matrix drives the cells to grow into organoids with the Matrigel further serving as a 3D framework. Growth of cells at an ALI also served as a key in promoting organoid formation, similar to results seen by Ootani et al (2009) who initiated an organoid culture system for intestinal epithelial cells using an ALI technique. In contrast, Coppes and colleagues did not use the ALI technique in their mouse salivary gland organoid culture system (Nanduri *et al.*, 2014; Maimets *et al.*, 2016). My findings contribute to the existing knowledge by providing another approach to growing human SG organoids. Even though, the ALI culture system does not precisely mimic the *in vivo* salivary gland, the SG cells appear protected by the Matrigel. It is also possible that the structure of the Matrigel is altered by exposure to the air and this may further favour the growth of the organoids.

Understanding the mechanism of branching morphogenesis of salivary glands during embryonic development may uncover novel approaches to regenerating functional artificial salivary gland. The mouse submandibular gland shows a classic branching morphogenesis and has been used as a model of organ culture *in vitro* for over 50 years (Tucker, 2007). The mechanical forces generated by the extracellular matrix, dynamic cell-cell interactions as well as growth factors are cues in the process of branching morphogenesis (Hsu and Yamada, 2010). My study indicates that the ECM protein laminin (from Matrigel), and signalling pathways of the growth factors FGF2 and EGF have roles in SG organoid branching development and are in agreement with previous studies of the promotion of branching morphogenesis by laminin-rich membranes and FGF2 and EGF growth factors (Jaskoll *et al.*, 2005; Steinberg *et al.*, 2005; Patel, Sharpe and Miletich, 2011; Patel and Hoffman, 2014). Moreover, Patel and Hoffman (2014) suggested that rapid cell proliferation was required during the process of clefting in SG organoid development. Thus, Wnt signalling known to be important in signalling for proliferation, cell migration and differentiation (Sato *et al.*, 2011; Bartfeld *et al.*, 2015; Huch *et al.*, 2015) was also shown to be important in

enhancing SG organoid development in my study. The abundant positive staining of CK5 protein in my cultures strongly suggests that our SG organoids consists of epithelial progenitor cells which are essential in SG development. Dynamic cell-cell interactions are also vital for SG organoid development, and E-cadherin (a cell-cell adhesion protein) has previously been shown to play a role in salivary gland branching morphogenesis (Davis and Reynolds, 2006). In my study, the SG organoids displayed positive gene expression of the tight junction proteins, ZO-1 and claudin as well as protein expression of E-cadherin.

In Chapter 5, I showed that the addition of TGF β , BMP and LIMK inhibitors to the culture media significantly affected SG organoid development through the promotion of cell proliferation and the induction of cell differentiation. Interestingly, SG organoids cultured in Matrigel at an ALI in A8301-media (TGF β inhibitor) and in ALL-media (with all inhibitors) demonstrated distinct characteristics that closely resembled native glands including the expression of acinar cell markers (BPIFA2 and AQP5), the ductal cell marker, CK7 and also E-cadherin. SG organoids cultured in the presence of DMH1 (BMP inhibitors) displayed ductal-like structures. Taken together, my study strengthens previous findings from murine studies that TGF β inhibition induces cell differentiation (Gurung, Werkmeister and Gargett, 2015; Broutier *et al.*, 2016), whereas inhibition of BMP signalling causes cells to differentiate more towards ductal formation (Clevers, 2013). SR7826 (LIMK inhibitor) resulted in the development of SG organoids with no clear branching structures and limited expression of the ductal cell marker, CK7 supporting the idea that the LIMK pathway is involved in cytoskeletal reorganisation and SG branching morphogenesis (Morin *et al.*, 2011; Ray *et al.*, 2014). Surprisingly, α -AMY enzyme activity was significantly higher in SG organoids in the presence of SR7826. Another interesting finding was the expression of the HE4 gene (WFDC2), previously described in the oral cavity, nasopharynx and respiratory tract (Bingle, Singleton and Bingle, 2002; Bingle *et al.*, 2006) in all SG organoid cultures.

PolyHIPE has been shown to be an excellent material for 3D cell cultures (Akay, Birch and Bokhari, 2004; Owen *et al.*, 2016), and has been exemplified by the Alvetex, a polystyrene-based PolyHIPE scaffold (Knight *et al.*, 2011). My aim was to assess the potential of a PolyHIPE scaffold as a cell delivery vehicle for *in vivo* implantation as well as for collecting saliva-cell secretions. I identified that PolyHIPE scaffolds allow the growth of SG organoids, but with reduced cell polarity compared to those cultured in Matrigel alone. Furthermore, I found that SG cells prefer to grow inside an ECM (Matrigel) rather than on ECM-coating in agreement with our earlier study (Chapter 3) where SG cells were cultured either on Alvetex scaffolds or PTFE transwells. These are novel findings and suggest the potential of PolyHIPE scaffolds as cell delivery vehicles for regenerative studies and may provide a novel supply of saliva although further investigations are required to fully determine the significance of my findings.

Although my study has focussed mainly on the development of a 3D salivary gland model, I also undertook a preliminary study into the potential use of the model to investigate the pathogenesis of salivary gland disease from initiation or upon bacterial or viral infection. In order to do this, I infected the model with a very relevant pathogen, *S. aureus*, and found that, up to 72hpi, the SG cells and the bacteria were both still viable. This study needs to be significantly expanded to determine any effect of the bacteria on the SG cells, or vice versa, but importantly demonstrates that my SG organoid model is a viable tool for the study of infectious disease.

7.2 CONCLUSION

In conclusion, I have provided clear evidence that human salivary gland cells isolated from a sublingual gland biopsy sample can proliferate and differentiate into SG organoids under a defined culture system. I determined that the essential components needed are (i) a laminin-rich extracellular matrix, (Matrigel) (ii) a potent source of Wnt (Wnt3a and R-spondin-1), (iii), a potent activator of tyrosine kinase receptor signalling (EGF, FGF2), and (iv) inhibition of BMP/TGF β signalling. I have also

shown that my model system has the potential as a tool for the study of infectious disease and that PolyHIPE scaffolds should be further investigated as for *in vivo* transplantation. Taken together, this study provides an efficient *in vitro* culture system for improving and implementing further studies on human SG development and pathophysiology as well as regeneration of diseased or damaged glands.

7.3 FUTURE STUDIES

Our findings addressed several research questions in order to further understand the development of human salivary glands. Additionally, we have determined the important niche factors required for successful human SG organoid culture, however, there still remain a number of areas for further study:

1) Extracellular matrix (ECM)

Matrigel is without doubt an excellent ECM for SG organoid development, however, as it derived from non-human in origin, the model cannot be further utilised for human studies using this source of ECM. Thus, human or non-allergenic ECM should be further investigated particularly those rich in laminin. Myogel, with the addition of laminin or collagen may provide such a matrix, but a number of alternatives have recently become available and warrant closer study.

2) Factors that contribute in branching morphogenesis

Aside from tyrosine kinase receptor signalling of FGF2 and EGF, there are other growth factor receptor-mediated signal transduction pathways involved in SG branching development. Platelet-derived growth factor (PDGF) signalling has also been shown to be involved in SG branching morphogenesis through the up-regulation of FGF expression (Yamamoto *et al.*, 2008). Thus, it would be useful to further determine regulation of these signalling pathways, their impact on interactions between ECM and cells and also cell-cell interactions, and how this might affect the formation of functional salivary glands. Morin *et al* (2011) suggested that the role of the

LIMK and ROCK pathways are not identical in the regulation of the actin cytoskeleton, cell motility or resulting morphological changes although they are in a linear pathway. Thus, the role of these pathways in SG branching development definitely warrants further investigation.

3) Addition of specific inhibitors molecules

In my study, TGF, BMP and LIMK inhibitors enabled the production of human SG organoids that closely mimicked native SG glands with positive expression of cell specific markers. In future studies, dual combinations of inhibitors in the media, for example TGF β /BMP, TGF β /SR7826, BMP/SR7826, would allow further investigation into the effects of each inhibitor on differentiating SG cells and may suggest novel, more effective culture conditions allowing truly representative organoids to develop. It is likely that other pathways may also be involved in SG and organoid growth. These could also be systematically studied.

4) Protein secretion from SG organoid models.

Another issue arising from this study is the sampling and analysis of cell secretions. The SG organoids preferentially grew inside the Matrigel, but this makes it almost impossible to collect cell secretions. Novel methods for sampling from the centre of the organoids, without causing disruption to growth so that sampling can be done at regular time intervals, need to be developed.

5) Immunofluorescence confocal (IFC) microscopy on cell specific markers

Further investigations into the production of the serous acinar marker, α -AMY and the mucous acinar marker, MUC7 in SG organoids needs to be carried out as both are vital constituents of normal saliva. CK14, which has been indicated as a multipotent epithelial progenitor cell in salivary glands, may provide further information on the potency of cells within the cultures and could suggest novel pathways for inducing further cell differentiation (Lombaert *et*

al., 2013). In addition, determination of the presence of apoptotic cells, by live/dead staining, in the organoids could indicate lumen formation and this warrants further investigation.

6) PolyHIPE scaffolds for future regeneration studies

PolyHIPE scaffolds are a promising platform to further study and investigate their potential for regeneration of functional salivary gland tissue. The main weakness of this study was the paucity of visualising the cells during growth on the scaffold and also of collecting secretions from the cells both during *in vitro* growth and at the end of each experiment. I also found that the cells did not grow into the laser cut, rather along the cut, and whilst we investigated the growth of cells previously coated with Matrigel, or after coating the scaffold with Matrigel, we did not investigate growth of cells in the absence of Matrigel. Results from point 1 above could also inform future studies with the PolyHIPE scaffolds.

7) Infectious study of SG organoids model

A challenge in modelling infectious study is the accessibility of the SG organoid lumen. Injecting the pathogens directly into the lumen of the organoid, instead of adding them to the culture medium may be a better approach, as in some respects this more closely mimics the *in vivo* situation. However, it should be acknowledged that infections may be blood borne and thus may arrive into the gland through blood vessels rather than the ductal system. As part of this study I attempted to microinject bacteria (*S. aureus*) into the organoids, but a number of limitations, which due to time constraints couldn't be addressed, were highlighted. These included i) visualising the organoids during the microinjection process, ii) it was technically difficult to reach the SG organoids with the glass needle. A previous study by Bartfeld and Clevers (2015) suggests some novel modifications and ideas for technical troubleshooting. Furthermore, whilst we were able to demonstrate co-culture of the bacteria and the epithelial cells 72hours post infection I did not

fully investigate the impact of the bacteria on the epithelial cells nor vice versa. However, we have shown that our SG organoid model has the potential to provide a valuable tool for infection biology and elucidating the pathogenesis of salivary gland infection.

8) Advanced microscopy

The use of scanning electron microscopy (SEM) would allow further investigation of cell-cell and cell-matrix contacts. It would also allow us to fully investigate the structures found within the “lumen” of the organoids and thus provide further information on the true structure of our cultures.

REFERENCES

- Akay, G., Birch, M. A. and Bokhari, M. A. (2004) 'Microcellular polyHIPE polymer supports osteoblast growth and bone formation in vitro', *Biomaterials*. doi: 10.1016/j.biomaterials.2003.10.086.
- Amano, O. *et al.* (2012) 'Advance Publication Review Anatomy and Histology of Rodent and Human Major Salivary Glands-Overview of the Japan Salivary Gland Society-Sponsored Workshop', *Acta Histochem. Cytochem*, 45(5), pp. 241–250. doi: 10.1267/ahc.12013.
- Ao, A. *et al.* (2012) 'DMH1, a novel BMP small molecule inhibitor, increases cardiomyocyte progenitors and promotes cardiac differentiation in mouse embryonic stem cells', *PLoS ONE*. doi: 10.1371/journal.pone.0041627.
- Atherton, A. J. *et al.* (1994) 'Immunolocalisation of cell surface peptidases in the developing human breast', *Differentiation*. doi: 10.1046/j.1432-0436.1994.56120101.x.
- Barker, N. *et al.* (2010) 'Lgr5+ve Stem Cells Drive Self-Renewal in the Stomach and Build Long-Lived Gastric Units In Vitro', *Cell Stem Cell*. doi: 10.1016/j.stem.2009.11.013.
- Bartfeld, S. *et al.* (2015) 'In vitro expansion of human gastric epithelial stem cells and their responses to bacterial infection', *Gastroenterology*. doi: 10.1053/j.gastro.2014.09.042.
- Bartfeld, S. and Clevers, H. (2015) 'Organoids as Model for Infectious Diseases: Culture of Human and Murine Stomach Organoids and Microinjection of Helicobacter Pylori', *Journal of Visualized Experiments*. doi: 10.3791/53359.
- Baum, B. J. *et al.* (2010) 'Development of a gene transfer-based treatment for radiation-induced salivary hypofunction', *Oral Oncology*. doi: 10.1016/j.oraloncology.2009.09.004.
- Bayetto, K. and Logan, R. (2010) 'Sjögren's syndrome: a review of aetiology, pathogenesis, diagnosis and management', *Australian Dental Journal*, 55(1), pp. 39–47. doi: 10.1111/j.1834-7819.2010.01197.x.
- Bingle, L. *et al.* (2006) 'WFDC2 (HE4): A potential role in the innate immunity of the oral cavity and respiratory tract and the development of adenocarcinomas of

the lung', *Respiratory Research*. doi: 10.1186/1465-9921-7-61.

Bingle, L. *et al.* (2009) 'Characterisation and expression of SPLUNC2, the human orthologue of rodent parotid secretory protein', *Histochemistry and Cell Biology*. doi: 10.1007/s00418-009-0610-4.

Bingle, L., Singleton, V. and Bingle, C. D. (2002) 'The putative ovarian tumour marker gene HE4 (WFDC2), is expressed in normal tissues and undergoes complex alternative splicing to yield multiple protein isoforms', *Oncogene*. doi: 10.1038/sj.onc.1205363.

Bredenoord, A. L., Clevers, H. and Knoblich, J. A. (2017) 'Human tissues in a dish: The research and ethical implications of organoid technology', *Science*, 355(6322). Available at: <http://science.sciencemag.org/content/355/6322/eaaf9414.abstract>.

Broutier, L. *et al.* (2016) 'Culture and establishment of self-renewing human and mouse adult liver and pancreas 3D organoids and their genetic manipulation', *Nature protocols*. doi: 10.1038/nprot.2016.097.

Burghartz, M. *et al.* (2017) 'Development of Human Salivary Gland-Like Tissue *In Vitro*', *Tissue Engineering Part A*. doi: 10.1089/ten.tea.2016.0466.

Cantara, S. I. *et al.* (2012) 'Selective functionalization of nanofiber scaffolds to regulate salivary gland epithelial cell proliferation and polarity', *Biomaterials*. doi: 10.1016/j.biomaterials.2012.08.021.

Chan, Y.-H. *et al.* (2010) 'Selective culture of different types of human parotid gland cells', *Head & Neck*. doi: 10.1002/hed.21465.

Chan, Y. H. *et al.* (2011) 'Human salivary gland acinar cells spontaneously form three-dimensional structures and change the protein expression patterns', *Journal of Cellular Physiology*. doi: 10.1002/jcp.22664.

Cheuk, W. and Chan, J. K. C. (2007) 'Advances in salivary gland pathology', *Histopathology*. doi: 10.1111/j.1365-2559.2007.02719.x.

Clevers, H. (2013) 'The intestinal crypt, a prototype stem cell compartment', *Cell*. doi: 10.1016/j.cell.2013.07.004.

Clevers, H. (2016) 'Modeling Development and Disease with Organoids', *Cell*. doi:

10.1016/j.cell.2016.05.082.

Clevers, H., Loh, K. M. and Nusse, R. (2014) 'An integral program for tissue renewal and regeneration: Wnt signaling and stem cell control', *Science*, 346(6205). Available at: <http://science.sciencemag.org/content/346/6205/1248012.abstract>.

Coppes, R. P. and Stokman, M. A. (2011) 'Stem cells and the repair of radiation-induced salivary gland damage', *Oral Diseases*. doi: 10.1111/j.1601-0825.2010.01723.x.

Davis, M. A. and Reynolds, A. B. (2006) 'Blocked acinar development, E-cadherin reduction, and intraepithelial neoplasia upon ablation of p120-catenin in the mouse salivary gland', *Developmental Cell*. doi: 10.1016/j.devcel.2005.12.004.

Delporte, C., Bryla, A. and Perret, J. (2016) 'Aquaporins in salivary glands: From basic research to clinical applications', *International Journal of Molecular Sciences*. doi: 10.3390/ijms17020166.

Eiraku, M. *et al.* (2008) 'Self-Organized Formation of Polarized Cortical Tissues from ESCs and Its Active Manipulation by Extrinsic Signals', *Cell Stem Cell*. doi: 10.1016/j.stem.2008.09.002.

Feng, J. *et al.* (2009) 'Isolation and characterization of human salivary gland cells for stem cell transplantation to reduce radiation-induced hyposalivation', *Radiotherapy and Oncology*. doi: 10.1016/j.radonc.2009.06.023.

Finkbeiner, W. E. *et al.* (2010) 'Cultures of human tracheal gland cells of mucous or serous phenotype', *In Vitro Cellular and Developmental Biology - Animal*. doi: 10.1007/s11626-009-9262-x.

Frantz, C., Stewart, K. M. and Weaver, V. M. (2010) 'The extracellular matrix at a glance', *Journal of Cell Science*, 123123, pp. 4195–4200. doi: 10.1242/jcs.023820.

Gatta, G. *et al.* (2015) 'Prognoses and improvement for head and neck cancers diagnosed in Europe in early 2000s: The EURO CARE-5 population-based study', *European Journal of Cancer*. doi: 10.1016/j.ejca.2015.07.043.

Gorjup, E. *et al.* (2009) 'Glandular tissue from human pancreas and salivary gland yields similar stem cell populations', *European Journal of Cell Biology*. doi:

10.1016/j.ejcb.2009.02.187.

Gurung, S., Werkmeister, J. A. and Gargett, C. E. (2015) 'Inhibition of Transforming Growth Factor- β Receptor signaling promotes culture expansion of undifferentiated human Endometrial Mesenchymal Stem/stromal Cells', *Scientific Reports*. doi: 10.1038/srep15042.

Horbelt, D., Denkis, A. and Knaus, P. (2012) 'A portrait of Transforming Growth Factor β superfamily signalling: Background matters', *The International Journal of Biochemistry & Cell Biology*, 44(3), pp. 469–474. doi: <https://doi.org/10.1016/j.biocel.2011.12.013>.

Hori, Y. *et al.* (2008) 'Bacteriologic Profile of the Conjunctiva in the Patients with Dry Eye', *American Journal of Ophthalmology*. doi: 10.1016/j.ajo.2008.06.003.

Hosseini, Z. F. *et al.* (2018) 'FGF2-Dependent Mesenchyme and Laminin-111 are Niche Factors in Salivary Gland Organoids'. Available at: <http://www.albany.edu/biology/faculty/mlarsen>.

Hsu, J. C. and Yamada, K. M. (2010) 'Salivary Gland Branching Morphogenesis — Recent Progress and Future Opportunities', *International Journal of Oral Science*. doi: 10.4248/IJOS10042.

Huch, M. *et al.* (2015) 'Long-term culture of genome-stable bipotent stem cells from adult human liver', *Cell*. doi: 10.1016/j.cell.2014.11.050.

Hughes, C. S., Postovit, L. M. and Lajoie, G. A. (2010) 'Matrigel: a complex protein mixture required for optimal growth of cell culture.', *Proteomics*. doi: 10.1002/pmic.200900758.

Ianez, R. F. *et al.* (2010) 'Human salivary gland morphogenesis: Myoepithelial cell maturation assessed by immunohistochemical markers', *Histopathology*. doi: 10.1111/j.1365-2559.2010.03645.x.

Jang, S. I. *et al.* (2015) 'Establishment of functional acinar-like cultures from human salivary glands', *Journal of Dental Research*. doi: 10.1177/0022034514559251.

Jaskoll, T. *et al.* (2005) 'FGF10/FGFR2b signaling plays essential roles during in vivo embryonic submandibular salivary gland morphogenesis'. doi: 10.1186/1471-213X-5-11.

- Joraku, A. *et al.* (2005) 'Tissue Engineering of Functional Salivary Gland Tissue', *Laryngoscope*, 115, pp. 244–248. doi: 10.1097/01.mlg.0000154726.77915.cc.
- Joraku, A. *et al.* (2007) 'In-vitro reconstitution of three-dimensional human salivary gland tissue structures', *Differentiation*. doi: 10.1111/j.1432-0436.2006.00138.x.
- Kern, B. *et al.* (2001) 'Cbfa1 Contributes to the Osteoblast-specific Expression of type I collagen Genes', *Journal of Biological Chemistry*. doi: 10.1074/jbc.M006215200.
- Kleinman, H. K. and Martin, G. R. (2005) 'Matrigel: Basement membrane matrix with biological activity', *Seminars in Cancer Biology*. doi: 10.1016/j.semcancer.2005.05.004.
- Knight, E. *et al.* (2011) 'Alvetex®: polystyrene scaffold technology for routine three dimensional cell culture.', *Methods in molecular biology (Clifton, N.J.)*, 695, pp. 323–340.
- Kouznetsova, I. *et al.* (2010) 'Expression Analysis of Human Salivary Glands by Laser Microdissection: Differences Between Submandibular and Labial Glands', *Cellular Physiology and Biochemistry*, 26(3), pp. 375–382. Available at: <https://www.karger.com/DOI/10.1159/000320561>.
- Kruse, C. *et al.* (2004) 'Pluripotency of adult stem cells derived from human and rat pancreas', *Applied Physics A: Materials Science & Processing*. doi: 10.1007/s00339-004-2816-6.
- Kukita, K. *et al.* (2013) 'Staphylococcus aureus SasA is responsible for binding to the salivary agglutinin gp340, derived from human saliva', *Infection and Immunity*. doi: 10.1128/IAI.00011-13.
- Lancaster, M. A. and Knoblich, J. A. (2014) 'Organogenesis in a dish: Modeling development and disease using organoid technologies', *Science*, 345(6194). Available at: <http://science.sciencemag.org/content/345/6194/1247125.abstract>.
- Li, W. *et al.* (2009) 'Generation of Rat and Human Induced Pluripotent Stem Cells by Combining Genetic Reprogramming and Chemical Inhibitors (DOI:10.1016/j.stem.2008.11.014)', *Cell Stem Cell*. doi: 10.1016/j.stem.2009.03.002.

- Lombaert, I. M. A. *et al.* (2013) 'Combined KIT and FGFR2b signaling regulates epithelial progenitor expansion during organogenesis', *Stem Cell Reports*. doi: 10.1016/j.stemcr.2013.10.013.
- Maguer-Satta, V., Besançon, R. and Bachelard-Cascales, E. (2011) 'Concise review: Neutral endopeptidase (CD10): A multifaceted environment actor in stem cells, physiological mechanisms, and cancer', *Stem Cells*. doi: 10.1002/stem.592.
- Maimets, M., Rocchi, C., Bron, R., Pringle, S., Kuipers, J., Giepmans, B. N. G., *et al.* (2016) 'Long-Term in Vitro Expansion of Salivary Gland Stem Cells Driven by Wnt Signals', *Stem Cell Reports*. doi: 10.1016/j.stemcr.2015.11.009.
- Maria, O. M. *et al.* (2011) 'Matrigel improves functional properties of human submandibular salivary gland cell line', *The International Journal of Biochemistry & Cell Biology*, 43, pp. 622–631. doi: 10.1016/j.biocel.2011.01.001.
- Mavragani, C. P. and Moutsopoulos, H. M. (2014) 'Sjögren's Syndrome', *Annual Review of Pathology: Mechanisms of Disease*. Annual Reviews, 9(1), pp. 273–285. doi: 10.1146/annurev-pathol-012513-104728.
- Mazia, D., Schatten, G. and Sale, W. (1975) 'Adhesion of cells to surfaces coated with polylysine. Applications to electron microscopy.', *The Journal of Cell Biology*, 66(1), p. 198 LP-200. Available at: <http://jcb.rupress.org/content/66/1/198.abstract>.
- Melnick, M., Deluca, K. A. and Jaskoll, T. (2014) 'CMV-induced pathology: Pathway and gene-gene interaction analysis', *Experimental and Molecular Pathology*. doi: 10.1016/j.yexmp.2014.06.011.
- Moore, R. G. *et al.* (2014) 'HE4 (WFDC2) gene overexpression promotes ovarian tumor growth', *Scientific Reports*. doi: 10.1038/srep03574.
- Morin, P. *et al.* (2011) 'Differing contributions of LIMK and ROCK to TGFβ-induced transcription, motility and invasion', *European Journal of Cell Biology*. doi: 10.1016/j.ejcb.2010.09.009.
- Mou, H. *et al.* (2016) 'Dual SMAD Signaling Inhibition Enables Long-Term Expansion of Diverse Epithelial Basal Cells', *Cell Stem Cell*. doi: 10.1016/j.stem.2016.05.012.

- Mulay, A. *et al.* (2016) 'An *in vitro* model of murine middle ear epithelium', *Disease Models & Mechanisms*. doi: 10.1242/dmm.026658.
- Nanduri, L. S. Y. *et al.* (2013) 'Salisphere derived c-Kit⁺ cell transplantation restores tissue homeostasis in irradiated salivary gland', *Radiotherapy and Oncology*. doi: 10.1016/j.radonc.2013.05.020.
- Nanduri, L. S. Y. *et al.* (2014) 'Purification and Ex vivo expansion of fully functional salivary gland stem cells', *Stem Cell Reports*. doi: 10.1016/j.stemcr.2014.09.015.
- Nelson, J., Manzella, K. and Baker, O. J. (2013) 'Current cell models for bioengineering a salivary gland: A mini-review of emerging technologies', *Oral Diseases*. doi: 10.1111/j.1601-0825.2012.01958.x.
- Nieder Korn, J. Y. *et al.* (2006) 'Desiccating Stress Induces T Cell-Mediated Sjogren's Syndrome-Like Lacrimal Keratoconjunctivitis', *The Journal of Immunology*. doi: 10.4049/jimmunol.176.7.3950.
- O Lewis, M. A. *et al.* (1993) 'Quantitative Bacteriology of the Parotid Salivary Gland in Health and Sjögren's Syndrome', *Microbial Ecology in Health and Disease*, 6(1), pp. 29–34. doi: 10.3109/08910609309141559.
- Ono, H. *et al.* (2015) 'Regenerating Salivary Glands in the Microenvironment of Induced Pluripotent Stem Cells', *BioMed Research International*. doi: 10.1155/2015/293570.
- Ootani, A. *et al.* (2009) 'Sustained *in vitro* intestinal epithelial culture within a Wnt-dependent stem cell niche', *Nature Medicine*. doi: 10.1038/nm.1951.
- Oshimori, N. and Fuchs, E. (2012) 'Paracrine TGF- β signaling counterbalances BMP-mediated repression in hair follicle stem cell activation', *Cell Stem Cell*. doi: 10.1016/j.stem.2011.11.005.
- Owen, R. *et al.* (2015) 'Data for the analysis of PolyHIPE scaffolds with tunable mechanical properties for bone tissue engineering'.
- Owen, R. *et al.* (2016) 'Emulsion templated scaffolds with tunable mechanical properties for bone tissue engineering', *Journal of the Mechanical Behavior of Biomedical Materials*. doi: 10.1016/j.jmbbm.2015.09.019.

- Pankov, R. (2002) 'Fibronectin at a glance', *Journal of Cell Science*. doi: 10.1242/jcs.00059.
- Patel, N., Sharpe, P. T. and Miletich, I. (2011) 'Coordination of epithelial branching and salivary gland lumen formation by Wnt and FGF signals', *Developmental Biology*. doi: 10.1016/j.ydbio.2011.07.023.
- Patel, V. N. and Hoffman, M. P. (2014) 'Salivary gland development: A template for regeneration', *Seminars in Cell and Developmental Biology*. doi: 10.1016/j.semcdb.2013.12.001.
- Paterson, T. E. *et al.* (2018) 'Porous microspheres support mesenchymal progenitor cell ingrowth and stimulate angiogenesis', *Citation: APL Bioengineering*, 2, p. 26103. doi: 10.1063/1.5008556.
- Pease, D. C. (1956) 'INFOLDED BASAL PLASMA MEMBRANES FOUND IN EPITHELIA NOTED FOR THEIR WATER TRANSPORT', *The Journal of Biophysical and Biochemical Cytology*, 2(4), p. 203 LP-208. Available at: <http://jcb.rupress.org/content/2/4/203.abstract>.
- Piludu, M. *et al.* (2003) 'Electron microscopic immunogold localization of salivary mucins MG1 and MG2 in human submandibular and sublingual glands', *Journal of Histochemistry and Cytochemistry*. doi: 10.1177/002215540305100109.
- Piras, M. *et al.* (2010) 'Ultrastructural localization of salivary mucins MUC5B and MUC7 in human labial glands', *European Journal of Oral Sciences*. doi: 10.1111/j.1600-0722.2009.00700.x.
- Pradhan-Bhatt, S. *et al.* (2013) 'Implantable Three-Dimensional Salivary Spheroid Assemblies Demonstrate Fluid and Protein Secretory Responses to Neurotransmitters', *Tissue Engineering Part A*. doi: 10.1089/ten.tea.2012.0301.
- Pradhan-Bhatt, S. *et al.* (2014) 'A novel in vivo model for evaluating functional restoration of a tissue-engineered salivary gland', *Laryngoscope*. doi: 10.1002/lary.24297.
- Pradhan, S. *et al.* (2010) 'Lumen formation in three-dimensional cultures of salivary acinar cells', *Otolaryngology - Head and Neck Surgery*. doi: 10.1016/j.otohns.2009.10.039.

- Pringle, S., Maimets, M., Van Der Zwaag, M., Stokman, M. A., Van Gosliga, D., Zwart, E., Witjes, M. J. H., *et al.* (2016) 'Human salivary gland stem cells functionally restore radiation damaged salivary glands', *Stem Cells*. doi: 10.1002/stem.2278.
- Pringle, S., Van Os, R. and Coppes, R. P. (2013) 'Concise review: Adult salivary gland stem cells and a potential therapy for xerostomia', *Stem Cells*. doi: 10.1002/stem.1327.
- Proctor, G. B. and Carpenter, G. H. (2007) 'Regulation of salivary gland function by autonomic nerves', *Autonomic Neuroscience: Basic and Clinical*. doi: 10.1016/j.autneu.2006.10.006.
- Qian, X. *et al.* (2016) 'Brain-Region-Specific Organoids Using Mini-bioreactors for Modeling ZIKV Exposure', *Cell*. doi: 10.1016/j.cell.2016.04.032.
- Ramos-Casals, M., Muñoz, S. and Zerón, P. B. (2008) 'Hepatitis C Virus and Sjögren's Syndrome: Trigger or Mimic?', *Rheumatic Disease Clinics*. Elsevier, 34(4), pp. 869–884. doi: 10.1016/j.rdc.2008.08.007.
- Ray, S. *et al.* (2014) 'LIM kinase regulation of cytoskeletal dynamics is required for salivary gland branching morphogenesis', *Molecular Biology of the Cell*. doi: 10.1091/mbc.E14-02-0705.
- Rousseau, K. *et al.* (2008) 'Proteomic analysis of polymeric salivary mucins: no evidence for MUC19 in human saliva', *Biochemical Journal*, 413(3), p. 545 LP-552. Available at: <http://www.biochemj.org/content/413/3/545.abstract>.
- Salo, T. *et al.* (2015) 'A novel human leiomyoma tissue derived matrix for cell culture studies', *BMC Cancer*. doi: 10.1186/s12885-015-1944-z.
- Sato, T. *et al.* (2009) 'Single Lgr5 stem cells build crypt-villus structures in vitro without a mesenchymal niche', *Nature*. doi: 10.1038/nature07935.
- Sato, T., Stange, D. E., Ferrante, M., Vries, R. G. J., *et al.* (2011) 'Long-term expansion of epithelial organoids from human colon, adenoma, adenocarcinoma, and Barrett's epithelium', *Gastroenterology*. doi: 10.1053/j.gastro.2011.07.050.
- Sato, T., Stange, D. E., Ferrante, M., Vries, R. G. J., *et al.* (2011) 'Long-term Expansion of Epithelial Organoids From Human Colon, Adenoma, Adenocarcinoma, and

- Barrett's Epithelium', *Gastroenterology*, 141(5), pp. 1762–1772. doi: 10.1053/j.gastro.2011.07.050.
- Schmierer, B. and Hill, C. S. (2007) 'TGF β –SMAD signal transduction: molecular specificity and functional flexibility', *Nature Reviews Molecular Cell Biology*. Nature Publishing Group, 8, p. 970. Available at: <http://dx.doi.org/10.1038/nrm2297>.
- Sequeira, S. J. *et al.* (2012) 'The regulation of focal adhesion complex formation and salivary gland epithelial cell organization by nanofibrous PLGA scaffolds', *Biomaterials*. doi: 10.1016/j.biomaterials.2012.01.010.
- Shamir, E. R. and Ewald, A. J. (2014) 'Three-dimensional organotypic culture: Experimental models of mammalian biology and disease', *Nature Reviews Molecular Cell Biology*. doi: 10.1038/nrm3873.
- Shubin, A. D. *et al.* (2017) 'Encapsulation of primary salivary gland cells in enzymatically degradable poly(ethylene glycol) hydrogels promotes acinar cell characteristics', *Acta Biomaterialia*. doi: 10.1016/j.actbio.2016.12.049.
- da Silva, A. A. *et al.* (2011) 'PLUNC protein expression in major salivary glands of HIV-infected patients', *Oral Diseases*. doi: 10.1111/j.1601-0825.2010.01733.x.
- Sipsas, N. V., Gamaletsou, M. N. and Moutsopoulos, H. M. (2011) 'Is Sjögren's syndrome a retroviral disease?', *Arthritis Research and Therapy*. doi: 10.1186/ar3262.
- Sonesson, M. *et al.* (2008) 'Mucins MUC5B and MUC7 in minor salivary gland secretion of children and adults', *Archives of Oral Biology*, 53(6), pp. 523–527. doi: <https://doi.org/10.1016/j.archoralbio.2008.01.002>.
- Steinberg, Z. *et al.* (2005) 'FGFR2b signaling regulates ex vivo submandibular gland epithelial cell proliferation and branching morphogenesis', *Development*, 132(6), p. 1223 LP-1234. Available at: <http://dev.biologists.org/content/132/6/1223.abstract>.
- Stojanovich, L. and Marisavljevich, D. (2008) 'Stress as a trigger of autoimmune disease', *Autoimmunity Reviews*. doi: 10.1016/j.autrev.2007.11.007.
- Taiym, S., Haghghat, N. and Al-Hashimi, I. (2004) 'Oral Surg Oral Med Oral Pathol Oral Radiol Endod', 97, pp. 579–83. doi: 10.1016/j.tripleo.2003.10.033.

- Teshima, T. H. N. *et al.* (2011) 'Development of human minor salivary glands: Expression of mucins according to stage of morphogenesis', *Journal of Anatomy*. doi: 10.1111/j.1469-7580.2011.01405.x.
- Tran, S. D. *et al.* (2005) 'Primary Culture of Polarized Human Salivary Epithelial Cells for Use in Developing an Artificial Salivary Gland', *Tissue Engineering*. Mary Ann Liebert, Inc., publishers, 11(1–2), pp. 172–181. doi: 10.1089/ten.2005.11.172.
- Tucker, A. S. (2007) 'Salivary gland development', *Seminars in Cell & Developmental Biology*, 18(2), pp. 237–244. doi: <https://doi.org/10.1016/j.semcd.2007.01.006>.
- Wang, A. *et al.* (2016) 'Photocurable high internal phase emulsions (HIPEs) containing hydroxyapatite for additive manufacture of tissue engineering scaffolds with multi-scale porosity', *Materials Science and Engineering: C*, 67, pp. 51–58. doi: <https://doi.org/10.1016/j.msec.2016.04.087>.
- Wang, S. *et al.* (2017) 'Patterned cell and matrix dynamics in branching morphogenesis', *The Journal of cell biology*. doi: 10.1083/jcb.201610048.
- Watanabe, K. *et al.* (2007) 'A ROCK inhibitor permits survival of dissociated human embryonic stem cells', *Nature Biotechnology*. doi: 10.1038/nbt1310.
- Van De Wetering, M. *et al.* (2015) 'Prospective derivation of a living organoid biobank of colorectal cancer patients', *Cell*, 161(4). doi: 10.1016/j.cell.2015.03.053.
- Wu, X. *et al.* (2011) 'Human bronchial epithelial cells differentiate to 3D glandular acini on basement membrane matrix', *American Journal of Respiratory Cell and Molecular Biology*. doi: 10.1165/rcmb.2009-0329OC.
- Yamamoto, S. *et al.* (2008) 'Platelet-derived growth factor receptor regulates salivary gland morphogenesis via fibroblast growth factor expression', *Journal of Biological Chemistry*. doi: 10.1074/jbc.M710308200.
- Yang, T. L. *et al.* (2010) 'Biomaterial mediated epithelial-mesenchymal interaction of salivary tissue under serum free condition', *Biomaterials*. doi: 10.1016/j.biomaterials.2009.09.052.
- Zhao, C. (2014) 'Wnt Reporter Activity Assay', *Bio-protocol*, 4(14), pp. 1–4.

APPENDICES

APPENDIX 1: List of reagents

List of Reagent	Catalogue #; Manufacturer details
100bp DNA ladder	Cat#: 15628019; Thermo Scientific, Cheshire, UK
A8301	Cat#: 2939; Tocris, Bristol, UK
Adenine	Cat#: A8626; Sigma-Aldrich, Dorset, UK
AlamarBlue®	Cat#: BUF012B; Bio-Rad, Oxford, UK
Amylase Activity Assay	Cat#: MAK009; Sigma-Aldrich, Dorset, UK
Cholera toxin	Cat#: C8052; Sigma-Aldrich, Dorset, UK
Columbia Blood Agar Base	Cat#: CM0331T; Thermo Scientific, Cheshire, UK
Corning® Dispase	Cat#: 354235; Thermo Scientific, Cheshire, UK
DAPI mounting medium	Cat#: H1200; Vector Laboratories Ltd, Peterborough, UK
Dexamethasone	Cat#: D4902; Sigma-Aldrich, Dorset, UK
Dimethyl sulfoxide	Cat#: D8418; Sigma-Aldrich, Dorset, UK
DMH-1	Cat#: 4126; Tocris, Bristol, UK
Dulbecco's Modified Eagle Media (DMEM)	Cat#: D5546; Sigma-Aldrich, Dorset, UK
FGF2	Cat#: F5392; Sigma-Aldrich, Dorset, UK
Fibronectin	Cat#: 356008; BD Biosciences, UK Thermo Scientific, Cheshire, UK
Fluorescein-5-isothiocyanate (FITC)	Cat#: F7250; Sigma-Aldrich, Dorset, UK
Foetal Bovine Serum (FBS)	Cat#: F9665, Sigma-Aldrich, Dorset, UK
Gibco Opti-MEM Reduced Serum Media	Cat#: 31985070; Thermo Scientific, Cheshire, UK
Goat anti-Mouse IgG (H+L) Secondary Antibody, Alexa Fluor 488	Cat#: A11001; Thermo Scientific, Cheshire, UK
Goat anti-Rabbit IgG (H+L) Secondary Antibody, Alexa Fluor 568	Cat#: A11011; Thermo Scientific, Cheshire, UK
Goat serum donor herd	Cat#: G6767; Sigma-Aldrich, Dorset, UK
Ham's F-12 Nutrient Mixture	Cat#: 11765054; Thermo Scientific, Cheshire, UK

HBBS Hank's Balanced Salt Solution	Cat#: 14025076; Thermo Scientific, Cheshire, UK
hEGF (Human Recombinant from E.coli)	Cat#: E9644; Sigma-Aldrich, Dorset, UK
Horse Blood Oxalated	Cat#: SR0049; Thermo Scientific, Cheshire, UK
Horse serum donor herd	Cat#:H1270; Sigma-Aldrich, Dorset, UK
Human epidermal growth factor (hEGF)	Cat#: E9644; Sigma-Aldrich, Dorset, UK
Hydrocortisone	Cat#: H4001; Sigma-Aldrich, Dorset, UK
Insulin	Cat#: 91077C; Sigma-Aldrich, Dorset, UK
Isopropanol	Cat#: 10674732; Fisher Chemical, Loughborough, UK
L-Glutamine	Cat#: G7513; Sigma-Aldrich, Dorset, UK
Matrigel Basement Membrane Matrix	Cat#: 356234; BD Biosciences, UK Thermo Scientific, Cheshire, UK
Matrigel Growth Factor Reduced	Cat#: 354230; Thermo Scientific, Cheshire, UK
Methanol	Cat#: 10598240; Fisher Chemical, Loughborough, UK
N-2 Supplement	Cat#: 17502048; Thermo Scientific, Cheshire, UK
Nuclease-free water	Cat#:AM9914G; Life Technologies, Paisley, UK
Penicillin-Streptomycin	Cat#: P4333; Sigma-Aldrich, Dorset, UK
Phosphate Buffered Saline (PBS)	Cat#: D8537; Sigma-Aldrich, Dorset, UK
Poly-L-Lysine	Cat#: P4707; Sigma-Aldrich, Dorset, UK
Pronase from <i>Streptomyces griseus</i>	Cat#: PRON-RO Roche; Sigma-Aldrich, Dorset, UK
Propan-2-ol	Cat#: 11428782; Fisher Chemical, Loughborough, UK
Rat-tail collagen I	Cat#: 354236; Thermo Scientific, Cheshire, UK
SR7826	Cat#: 5626; Tocris, Bristol, UK
TRI Reagent	Cat#: 93289; Sigma-Aldrich, Dorset, UK
Triton X100	Cat#: T8787; Sigma-Aldrich, Dorset, UK
Trypsin	Cat#: T4799; Sigma-Aldrich, Dorset, UK
Trypsin-EDTA solution	Cat#: T3924; Sigma-Aldrich, Dorset, UK
VECTASTAIN® Elite® ABC-HRP kit (peroxidase, Mouse IgM)	Cat#: PK-6102; Vector Laboratories Ltd, Peterborough, UK

VECTASTAIN® Elite® ABC-HRP kit (peroxidase, Rabbit IgG)	Cat#: PK-6101; Vector Laboratories Ltd, Peterborough, UK
VECTOR DAB peroxidase (HRP) substrate kit (with Nickel)	Cat#: SK-4100; Vector Laboratories Ltd, Peterborough, UK
Xylene, Extra Pure, SLR	Cat#: 10784001; Fisher Chemical, Loughborough, UK
Y-27632	Cat#: Y0503; Sigma-Aldrich, Dorset, UK

APPENDIX 2: List of equipment

List of Equipment	Details
Class 2 MSC Walker Safety Cabinets	Scientific-Lab Supplies, UK
DNA Engine Dyad® Peltier Thermal Cycler	Bio-Rad Laboratories Ltd., Hertfordshire, UK
Fridge/Freezer	Proline, UK
Galaxy R CO ₂ Incubator	Scientific-Lab Supplies, UK
Infinite® M200 Pro Series	Tecan UK Ltd, Reading, UK
JB series water bath	Scientific-Lab Supplies, UK
Leica EG1160 embedding station	Leica Biosystems, Milton Keynes, UK
Leica RM2235 microtome	Leica Biosystems, Milton Keynes, UK
Leica ST4020 staining machine	Leica Biosystems, Milton Keynes, UK
Leica TP1020 benchtop tissue processor	Leica Biosystems, Milton Keynes, UK
Nikon A1+ Confocal microscope	Surrey, UK
Nikon Eclipse TS100 inverted microscope	Nikon, Japan
Olympus BX51-P polarising microscope	KeyMed Ltd., Essex, UK
Spectrafuge™ 24D Digital Microcentrifuge	Labnet International Inc., NJ, USA
Thermal Cycler PCR machine (GeneAmp PCR System 9700)	Applied Biosystems, USA
Thermo Scientific NanoDrop™ 1000 Spectrophotometer	Thermo Fisher Scientific, Loughborough, UK

APPENDIX 3: List of miscellaneous

List of Miscellaneous	Catalogue #; Manufacturer details
96 well PCR plate, Semi-Skirted	Cat#: 1402-9700; STARLAB (UK) Ltd, Milton Keynes, UK
SuperFrost® Plus microscope slide	Cat#: 4951PLUS4, Thermo Fisher Scientific, Paisley, UK
T25 suspension culture flask with filter cap	Cat#: 658190; Greiner Bio-One Ltd, UK
T75 suspension culture flask with filter cap	Cat#: 690195; Greiner Bio-One Ltd, UK
Alvetex® Scaffolds	Cat#: AVP005, ReproCELL Europe Ltd, Glasgow, UK
Falcon® Transparent PET Membrane Inserts for 12-well plates	Cat#:353180, Thermo Fisher Scientific, Paisley, UK
12 well plate	Cat#: CC7682-7512; STARLAB (UK) Ltd, Milton Keynes, UK
35 mm petri dish	Cat#: P5112; Sigma-Aldrich, Dorset, UK
100 mm petri dish	Cat#: P5856; Sigma-Aldrich, Dorset, UK
Corning®Cell strainer, size 70 µm	Cat#: CLS431751; Sigma-Aldrich, Dorset, UK
0.22 µm Syringe filters	Cat#: E4780-1221; STARLAB (UK) Ltd, Milton Keynes, UK

APPENDIX 4: Solutions used for IHC

Solution	Constituents	Amount
Phosphate Buffered Saline (PBS) pH 7.5	NaCl (Sigma)	42.4 g
	Sodium phosphate (Fischer Scientific)	7.12 g
	Potassium phosphate (Sigma)	1.25 g
	Distilled water	5 L
0.01M Sodium Citrate	Sodium citrate (Sigma)	1.18 g
	Distilled water	400 mL
Biotinylated Secondary antibody	PBS	10 mL
	Concentrated biotinylated secondary antibody	50 µL
VECTASTAIN Elite ABC Reagent	PBS	10 mL
	Reagent A	100 µL
	Reagent B	100 µL
VECTOR DAB	Distilled water	5 mL
	Buffer Stock Solution	80 µL
	DAB Stock Solution	100 µL
	Hydrogen Peroxide Solution	80 µL

APPENDIX 5: Step in determining image acquisition conditions and acquire images by using Confocal Microscopy Nikon A1+

1) Resetting interlock

2) Selecting resolution

3) Selecting a laser

4) Adjusting laser power, HV and Offset

Starting scanning

Checking the settings

Detailed description: This screenshot shows the 'A1 Compact GUI' with various control panels. A 'Scan' button is highlighted in red. A table of resolution settings is also highlighted, showing values like 2.2, 4.8, 12.1, 27.2, 57.2, 87.8, and 117. A settings gear icon is highlighted. A laser selection panel is highlighted, showing 'Alexa 488' and '488.0 nm' with sliders for HV, Offset, and power.

5) Pixel saturation indication

6) Capture Z-Series tab

7) Saving image in nd2 file format

LUTs tab

Defined top & bottom

Top button

Bottom button

The value of the plane in the cube

Determine Step

Run now button to acquire Z series images

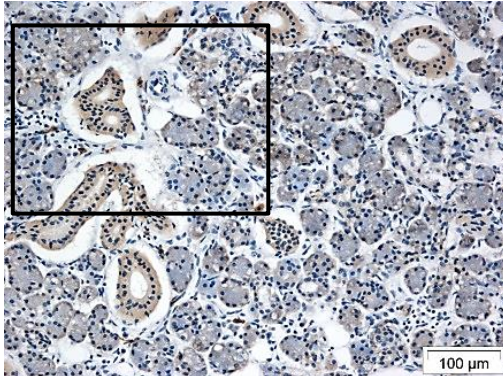
Detailed description: This screenshot shows the 'Capture Z-Series' dialog box. A 'Save to File' section is highlighted with a path and filename. A 'LUTs' tab is shown with a saturation graph. The 'Z-Series' section has 'Steps' set to 11 and 'Range' set to 2.35. A 'Run now' button is highlighted at the bottom right.

APPENDIX 6: List of Human Salivary Gland Tissue Biopsy

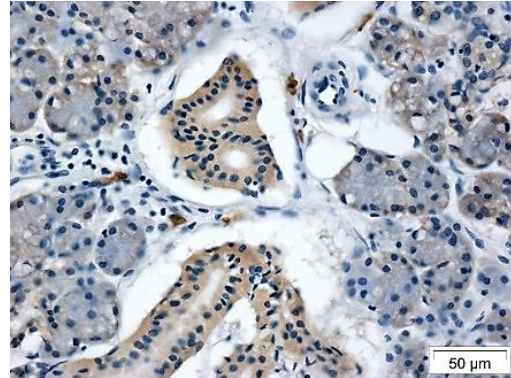
Date of Sample Collection	Sample	Remarks
04-06-2015	Parotid Gland	Anonymous
09-06-2015	Sublingual Gland	DOB: 04-05-1952 Storey Patricia
10-06-2015	Sublingual Gland	DOB: 19-04-1957 Barrass Brian
18-06-2015	Sublingual Gland	DOB: 19-10-1952 Bird Eileen
11-08-2015	Sublingual Gland	Anonymous
22-10-2015	Sublingual Gland	Anonymous
31.05.2016	Submandibular Gland	Anonymous
20.07.2016	Submandibular Gland	Anonymous
27.07.2016	Submandibular Gland	Anonymous
20.09.2016	Submandibular Gland	Anonymous
15.03.2017	Submandibular Gland	Anonymous
29-03-2017	Submandibular Gland	Anonymous

APPENDIX 7: Immunohistochemistry of Normal Human Sublingual Glands

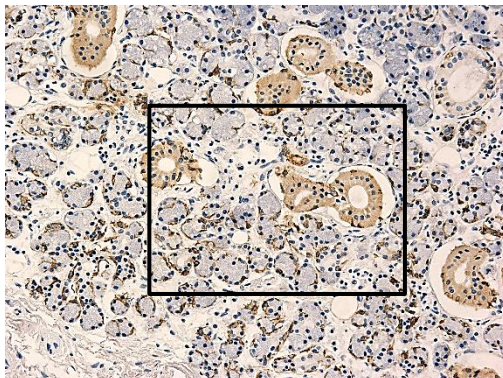
cKIT (20x magnification)



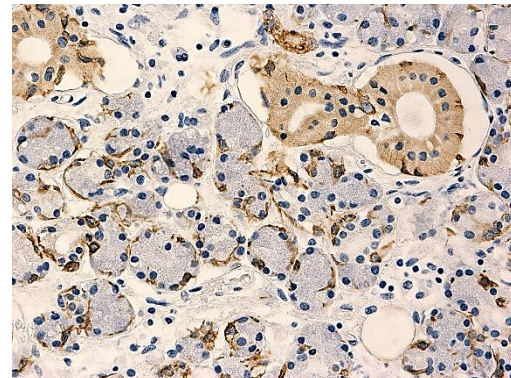
cKIT (40x magnification)



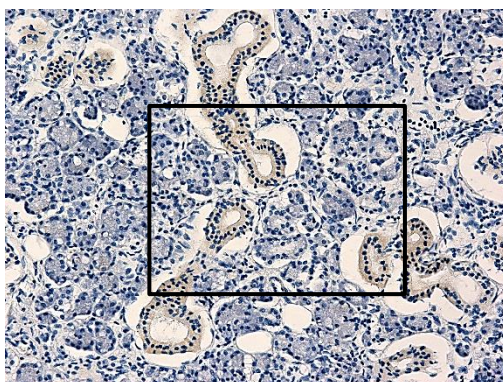
CK5 (20x magnification)



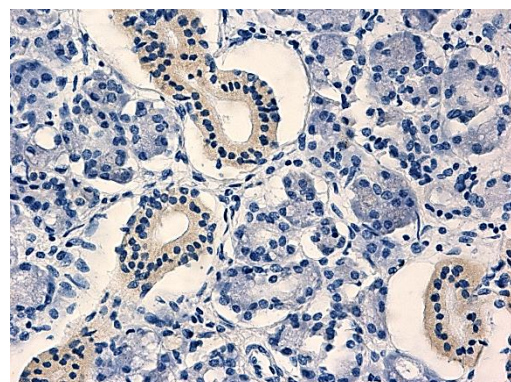
CK5 (40x magnification)



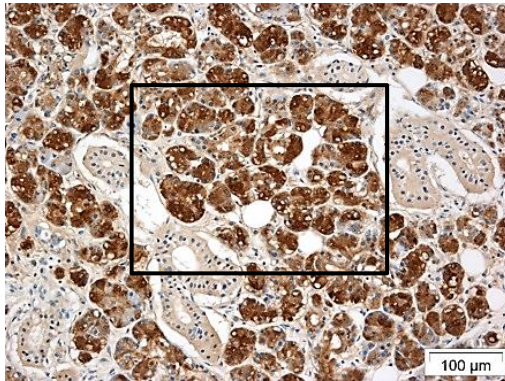
CK7 (20x magnification)



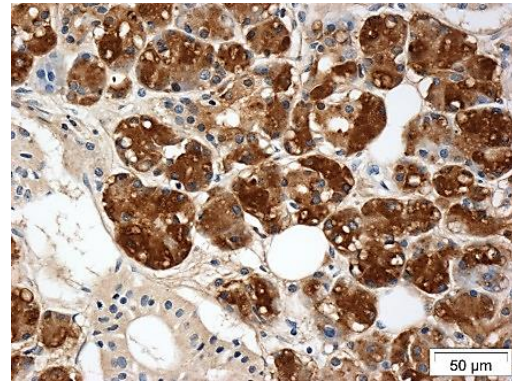
CK7 (40x magnification)



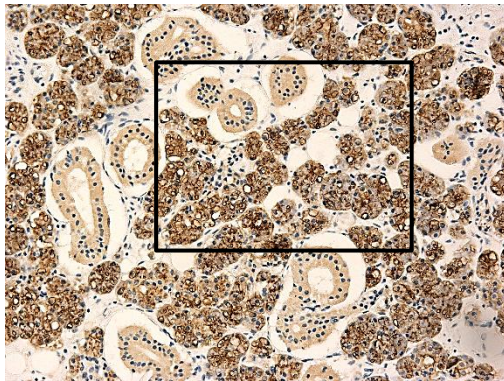
α -Amylase (20x magnification)



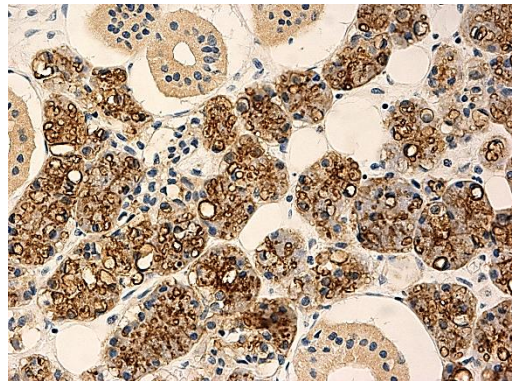
α -Amylase (40x magnification)



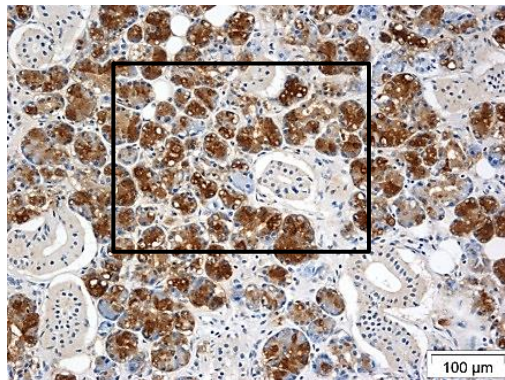
AQP5 (20x magnification)



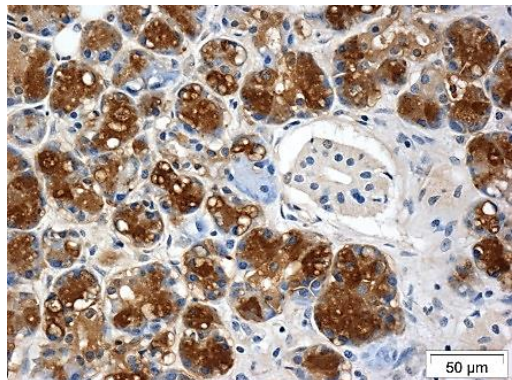
AQP5 (40x magnification)



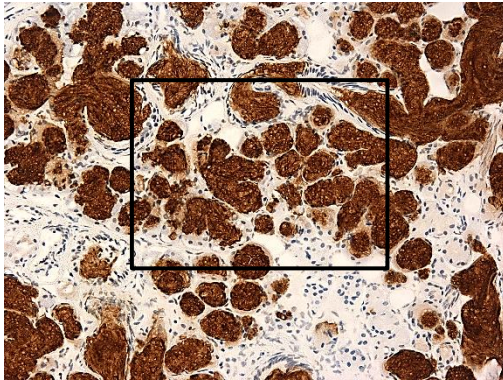
BPIFA2 (20x magnification)



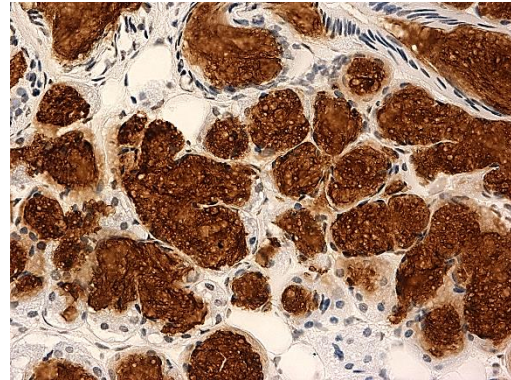
BPIFA2 (40x magnification)



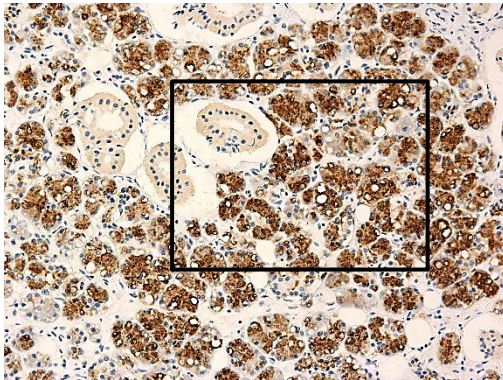
MUC5B (20x magnification)



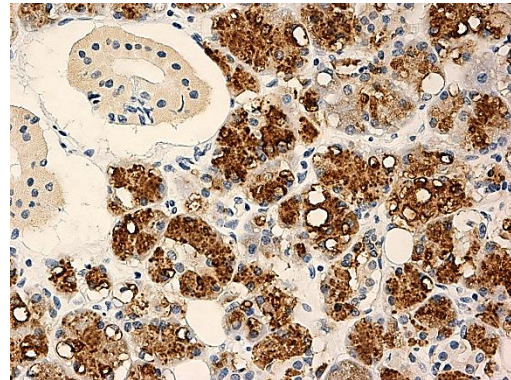
MUC5B (40x magnification)



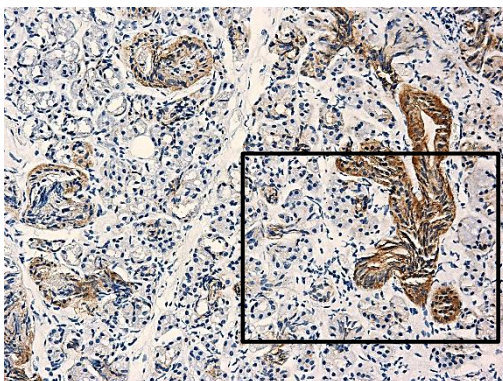
MUC7 (20x magnification)



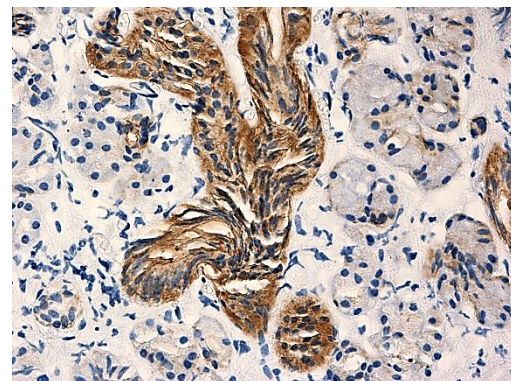
MUC7 (40x magnification)



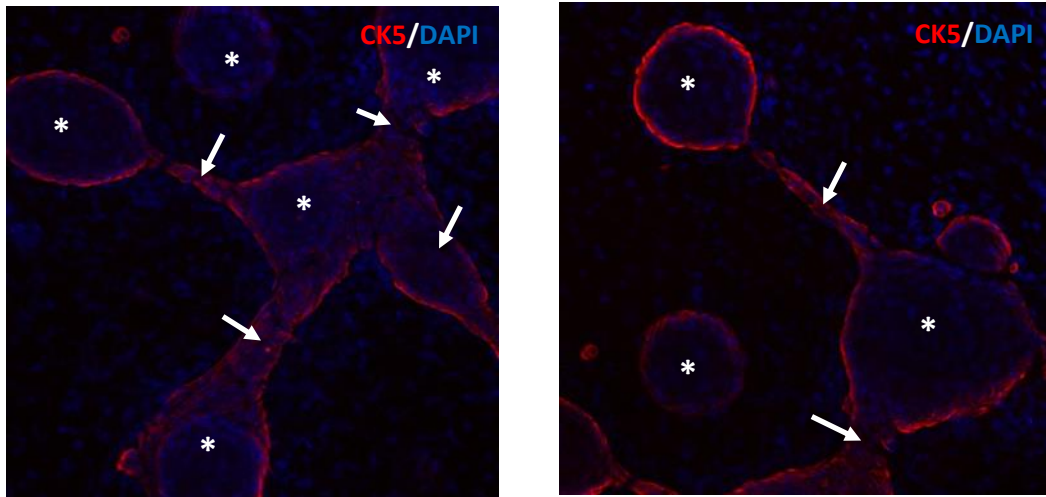
E-CADHERIN (20x magnification)



E-CADHERIN (40x magnification)



APPENDIX 8: Confocal Images of SG organoids showing spherical (asterisk) and branching (arrow) structure



Enriched media, 20x magnification